PHYSICOCHEMICAL CHARACTERIZATION OF NATIVE, MODIFIED AND NANO STARCHES OF SELECTED TUBERS AND SEEDS

OLADEBEYE Abraham Olasupo
(CHE/00/7994)

A Thesis written in the Department of Chemistry and submitted to the School of Postgraduate Studies in partial fulfillment of the requirement for the award of Doctor of Philosophy (Ph.D) in Analytical Chemistry of The Federal University of Technology, Akure, Ondo State, Nigeria.

July, 2014

CERTIFICATION

a) **By the Student**

This work has not been presented elsewhere for the award of a degree or any other purpose.

Candidate's Name: **OLADEBEYE Abraham Olasupo**

Signature:………………………………… Date:……………………………….

b) **By the Supervisors**

We certify that this work has been carried out by **Mr. Oladebeye Abraham Olasupo** in the Department of Chemistry, The Federal University of Technology, Akure, Nigeria.

Major Supervisor's Name: **Professor A.A. Oshodi**

Signature:…………………………………... Date:……………………………

Co-Supervisor's Name: **Professor I.A. Amoo**

Signature:…………………………………... Date:……………………………

DEDICATION

This project work is dedicated to the Almighty God, the Alpha and Omega of my success, and to my wife, Ronke and children – Ayomikun, Ayomiposi and Ayooluwatomiwa.

ACKNOWLEDGEMENT

I give glory to the Almighty God for His unfailing and unquantifiable love towards me and my family throughout the period of this programme.

I appreciate the distinctive academic tutelage and guidance of my major supervisor, Professor A.A.Oshodi and co-supervisor, Professor I.A. Amoo, which sailed this research work to a haven of success. Their patience and understanding are highly appreciated.

I wish to acknowledge the Head, Chemistry Department, the Federal University of Technology, Akure, Professor A.F. Ayesanmi, the Postgraduate Coordinator, Dr. A.E. Okoronkwo, Seminar Coordinator, Dr. B.J. Owolabi and other members of staff for their resourceful ideas, contributions and constructive criticisms that gave this research work a huge success.

My gratitude goes to Tertiary Education Trust Fund (TETFUND) of the Federal Republic of Nigeria for financial grant, through Auchi Polytechnic, Auchi that assisted this research work.

I am very grateful for the approval of non-exchange studentship granted at Universiti Sains Malaysia (USM), Malaysia for part of my benchwork, which was facilitated by Professor Alias Abd. Karim, Food Biopolymer Science Research Group, School of Industrial Technology, USM. Instrumental analyses involving RVA, flow behaviours, gel properties, XRD, SEM and TEM were parts of the benchwork done in Malaysia. I appreciate the Laboratory Technicians of the various labs (Physics, Biology and Food Technology) for their assistance.

My reserved appreciation goes to my big friend and tutor, Dr. Isiaka Bakare, who initiated the idea and link of going to USM, Malaysia for benchwork. The part you played is written with golden pen. Also, I appreciate Dr. Biola Oladoja for his moral support both at home and when we met in Malaysia.

Thanks to the Management of International Institute of Tropical Agriculture (IITA), Ibadan, especially, Mr. Ilo Emeka and cohorts in Food Technology unit for

ABSTRACT

The native starches of white and red cocoyam (*Colocasia esculenta*), white yam (*Dioscorea rotundata*) and yellow yam (*Dioscorea cayenensis*), and seeds of pigeon pea (*Cajanus cajan*), lima bean (*Phaseolus lunatus*) and jack bean (*Canavalia ensiformis*) were isolated and modified to obtain their hydroxypropyl and ozone-oxidized derivatives. The nanocrystals of the starches were prepared by mild acid hydrolysis at $40^{o}C$ with continuous stirring for five (5) days. The native starches were evaluated for proximate and mineral compositions and selected physicochemical properties. Molar substitution (MS) and degree of substitution (DS) of the hydroxypropylated starches were determined. The amount of reacted ozone, carbonyl and carboxyl contents of the ozone-oxidized starches were determined at 5, 10 and 15 min ozone generation time (OGTs). Comparative studies of the native and modified starches were carried out in terms of their functional properties, rheological properties, thermal properties, X-ray diffraction patterns, molar mass distribution and Fourier Transform Infrared (FTIR) spectroscopy. In addition, the starch nanocrystals were characterised for X-ray patterns, solubility and their morphologies, obtained by Transmission Electron Microscopy (TEM) were compared with those of the native starches obtained by Scanning Electron Microscopy (SEM). The yields for the native starches were 31.70% (white cocoyam starch, WCS), 31.68% (red cocoyam starch, RCS), 42.66% (white yam starch, WYS), 41.72% (yellow yam starch, YYS), 20.57% (pigeon pea starch, PPS), 20.36% (lima bean starch, LBS) and 20.26% (jack bean starch, JBS) while nanocrystals were 6.67% (WCS), 5.68% (RCS), 6.22% (WYS), 6.67% (YYS), 10.54% (PPS), 10.81% (LBS) and 13.51% (JBS) after five (5) days of acid hydrolysis. The results showed that JBS was richest in protein content (7.02±0.02%), LBS richest in crude fat (1.16±0.01%) and ash content (1.26±0.01%), PPS richest in crude fibre (1.77±0.01%) and YYS had peak carbohydrate by difference (84.28±0.02%). While potassium was the most abundant

mineral in all the native starches, the heavy metals, such as lead (Pb), nickel (Ni), cadmium (Cd) and mercury (Hg), were not detected. The native starches had peak values of LGCs, WAC and OAC as 8.00%, 96.23±0.01% and 4.77±0.01% respectively. The amounts of reacted ozone, carbonyl and carboxyl contents of the oxidized starches increased as OGT increased. MS of the hydroxypropylated starches ranged from 0.23 to 0.67 and DS from 0.02 to 0.04. Hydroxypropylation improved the swelling power and solubility of the native starches. All the oxidized starches exhibited lower tendency to retrograde than the native. Ozonation and hydroxypropylation enhanced the cohesiveness and resilience of the native starch gels. The data obtained from flow measurements showed that the native and modified starches exhibited non–Newtonian behaviour, which was evident by flow behaviour index, $n<1$. The retrogradation profiles of the starch samples were lower in value than their gelatinization profiles. ATR-FTIR spectroscopy revealed peaks of hydroxyl group, CH_2 asymmetric stretching, C–H stretch of alkyl groups and C–H deformation, which became broader upon modification. All the native starches exhibited C_B-type X-ray patterns, which remained unchanged upon modification whereas V-type patterns were observed for the nanocrystals. The morphological studies of the starches revealed that the granular sizes of the native starches were in the range 11.54–26.23 μm, having mixture of oval, ellipsoidal, irregular polygon, bean-like and spherical shapes. The TEM micrographs of the starch nanocrystals showed that they appeared as platelets. None of the nanocrystals was soluble in the solvents used, but LBS nanocrystals were sparingly soluble in acetic acid, ethanol and deionized (DI) water. Evidences of the nanocrystals of these starches were a step towards meeting the quest for nanotechnology in all fields. Therefore, the native starches used in this study showed extensive uses in food and non-food applications upon modification through ozone-oxidation and hydroxypropylation processes. Their nanocrystals could be potential fillers in nanocomposites.

TABLE OF CONTENTS

Chapter Two

Chapter Three

Chapter Four

Chapter Five

Chapter Six

LIST OF ABBREVIATIONS

In this thesis, the following abbreviations, whose meanings are given below:

WCS – White cocoyam starch

RCS – Red cocoyam starch

WYS – White yam starch

YYS – Yellow yam starch

PPS – Pigeon pea starch

LBS – Lima bean starch

JBS – Jack bean starch

AM – Amylose

AP – Amylopectin

DP_n – Number average degree of polymerization

DP_w – Weight average degree of polymerization

DS – Degree of substitution

DSC – Differential scanning calorimeter

LGC – Least gelation concentration

M_n – Number average

MS – Molar substitution

M_w – Weight average

OAC – Oil absorption capacity

OGT – Ozone generation time

PHI – Peak height index

ppm – parts per million

RVU – Rapid visco unit

T_c – Conclusion temperature

T_o – Onset temperature

T_p – Peak temperature

WAC – Water absorption capacity

XRD – X-ray Diffraction

ΔH_{gel} – Gelatinization enthalpy

ΔH_{ret} – Retrogradation enthalpy

LIST OF FIGURES

LIST OF PLATES

LIST OF TABLES

CHAPTER ONE

1.0   INTRODUCTION

Starch, the food reserve homopolysaccharide of plants (Malcolm, 1990), is a biocompatible, biodegradable, nontoxic polymer (Welsen and Welsen, 2002), which occurs widely in nature and commonly used (Whistler and Paschall, 1965 and 1967). Starch is one of the most important products to man. The major botanical and commercial sources of starch are cereals, roots and tubers, and pulses (Karim *et al.*, 2000). Other sources, classified as minor, are legumes.

Starch is an essential component of food providing a large proportion of daily calorie intake for both humans and livestock. Starch alone accounts for 60–70% of calorie intake of humans (Lawton, 2004). Besides, the nutritive value, there are non–food applications that have promoted the preferential use of starch in industries to other polysaccharides. These include adhesives, agrochemicals, cosmetics and toiletries, detergents, paper making additives, pharmaceuticals, paints, textiles, water purification, biodegradable plastics, super–adsorbent materials, sugar market and so on. This is partly because of the wide range of functional properties it can provide in its various natural and modified forms, and partly because of its low cost relative to alternatives (Sanderson, 1981).

These applications (food and non-food) depend on the functional properties of the starches such as gelatinization, pasting, retrogradation, water absorption capacity, swelling power, and solubility which vary considerably from one botanical source to another (Yuan *et al*., 2007), and with variety and environmental conditions (Chen *et al*., 2003). The functional properties are also dependent on composition and structures of the starches, which include amylose/amylopectin ratio, crystalline structure, granular size, molecular weight of the starches and chain length distribution of amylopectin (Lu *et al*., 2005). Therefore, unravelling the potential of starches for use in the food and non-food industries calls for a

better understanding of their unique physicochemical, functional and structural properties.

Modification processes have been adopted in extending the scope of usage of native starches in the industries. Attempts have been made on modifications of native (unmodified) starches from different sources, which include heat-moisture treatment of Babarra groundnut (Adebowale and Lawal, 2002), heat-moisture treatment of white and yellow yam (Oladebeye *et al.*, 2011), heat-moisture treatment of rice (Lai, 2001), annealing of red sorghum (Adebowale *et al.*, 2005), pregelatinization of jackfruits (Kittipongpatana and Kittipongpatana, 2011), acetylation of jack bean (Lawal and Adebowale, 2005), hydroxypropylation of pigeon pea (Lawal, 2011), dual modification-enzyme-hydrolyzed hydroxyl-propylation of corn and mung bean (Karim *et al.*, 2008), oxidation of waxy corn, using hypochlorite (Wang and Wang, 2003). In addition, in an attempt to address the issues of safety and environmental friendliness, hypochlorite oxidation of starches has been reportedly replaced by ozone-oxidation (Kesselmans and Bleeker, 1997; Chan *et al.*, 2009 and 2011).

The quest for nanotechnology in all fields of study is the new trend of interest of both scientists and industries with the view to processing polymeric composite materials filled with rigid particles at least one dimension in nanometer range. Nanoparticles of native starch called nano starch or starch nanocrystals can be obtained by acid hydrolysis (Angellier *et al.*, 2005a).

This research work is imperative, because underutilized crops such as cocoyam cultivars, yam cultivars, pigeon pea, lima bean and jack bean are investigated for their proximate, functional, thermal, crystalline and molecular properties with the view to increasing their competitiveness in the starch market. Up to now, scanty information exist on the possible use of these starches in applications other than food. Reports have been made on nanocrystals of waxy

maize starch (LeCorre *et al.*, 2011; Angellier *et al.*, 2006a; Li *et al.*, 2007), but none exists on nanocrystals of these underutilized crops. These, if maximally harnessed, will not only solve the imminent challenges of ever-increasing demand for starch, but also provide a stable socio-economic system.

1.1 ROOTS AND TUBERS

Tropical tuber and root crops, of which cocoyam and yam are examples, are the main staple food for many people in the world's hot and humid regions. These crops are highly adapted to the tropical agro-climatic environment and can grow in great abundance with little or no artificial input. Many of the developing world's poorest farmers and food insecure people are highly dependent on root and tuber crops as a contributing, if not the principal, source of food, nutrition, and cash income (Scott *et al.*, 2000).

1.1.1 Cocoyam (*Colocasia esculenta*)

Colocasia esculenta is an ancient tuber of the *Araceae* family (Plucknett 1983; Cable, 1984), which originated from South-East Asia, possibly, India (Onwueme, 1978; Wang, 1983), where it has been cultivated for more than 2000 years. It has both red and white varieties.

Colocasia esculenta is an herbaceous bush of 1–2m high that is built by leaves originating from a starchy corm (the edible portion). The leave lamina is up to 1 m in length and has the shape of a heart, resembling elephant ears. As a crop of the tropical rainforest, *Colocasia esculenta* prefers very high precipitation of 2500 mm per year and a temperature of 25–27°C. The crop is mature after a cultivation period of 8–10 months.

Cocoyam (*Colocasia esculenta)* can be processed into several food and feeds products and industrial inputs, similar to that of potatoes in Western world.

The processes include boiling, roasting, frying in oil, pasting, milling and conversion into 'fufu', soup thickeners, flour for baking, chips, beverages powder, porridge and specialty food for gastro-intestinal disorders (Onwueme, 1978; Hussain *et al.*, 1984; Ihekoronye and Ngoddy, 1985).

The present research work is based on two cultivars of cocoyam–white and red, among other underutilized roots and tubers, for comparative and possible food and non-food applications.

1.1.2 Yam (*Dioscorea spp.*)

Yam is a common name for some species in the genus *Dioscorea* (family, *Dioscoreacea*). Yams are the edible tubers of various species of the genus Dioscorea and are important staple foods of many tropical countries including Cộte d'Ivoire, Ghana, Togo, Burkina Faso and Nigeria (Kouakou *et al.*, 2010; Amanze *et al.*, 2011). It is a major contributor to food security in West Africa (Zannou *et al.*, 2009), but out of the over 600 known yam species, only seven are mostly consumed (Jayakody *et al.*, 2007). These include *Dioscorea rotundata Poir* (white yam), *Dioscorea cayenensis* (yellow yam), *Dioscorea alata* (water yam), *Dioscorea bulbifera* (Aerial yam), *Dioscorea esculenta*, *Dioscorea praehensalis* (bush yam) and *Dioscorea dumetorum* (bitter yam).

Yam tubers can grow up to 1.5 meters (4.9 feet) in length and weigh up to 70 kilograms (154 lb) and 3 to 6 inches high. They are large plants; the vines can be as long as 10 to 12 meters (33 to 39 ft). The tubers most often weigh about 2.5 to 5 kilograms (5.5 to 11 lb) each, but can weigh as much as 25 kilograms (55 lb). After 7 to 12 months growth the tubers are harvested (Kay, 1987).

1.2   LEGUMES

Legumes belong to the family *Fabaceae* (or *Leguminosae*). In the tropics, they are the next important food crop after cereals (Uzeochina, 2009), having low–cost dietary vegetable proteins and minerals, when compared with animal products such as meat, fish and egg (Apata and Ologhobo, 1997).

1.2.1 Pigeon Pea (*Cajanus cajan*)

Pigeon pea (*Cajanus cajan L.*) belongs to the genus *Cajanus,* subtribe *Cajaninae,* tribe *Phaseoleae*, and family *Abaceae*. It is also known as redgram, tur, arhar, gandul (Spanish) and pois d'Angole (Sharma and Green, 1980), congo bean (English), pois de Congo (French), and ervilba de Congo in Angola (Baldev, 1988). *Cajanus* is derived from a Malay word 'katschang' or 'katjang', meaning pod or bean. Many species of the closely related genus *Atylosia* successfully cross with pigeonpea (Van der Maesen, 1980). Its center of origin was reported to be India while Africa was the secondary center of origin of pigeon pea (Van der Maesen, 1980).

The stem of pigeon pea plant is woody, leaves are trifoliate, and compound. It possesses a strong taproot system. The plants grow into woody shrubs, 1–2 m tall, when annually harvested. It may attain a height of 3–4 m, when grown as a perennial plant in fence rows or agroforestry plots. Pods are of various color; green, purple, dark purple, or mixed green and purple. Pods with deep constrictions in shape are beaded, while others are somewhat flat. The seeds per pod range from two to seven, and sometimes, up to nine (Rao and Rao, 1974). There is little or no shattering of mature pods in the field.

1.2.2 Lima Bean (*Phaseolus lunatus*)

Lima bean (*Phaseolus lunatus L.*) is a perennial American legume species with annual cultivars. It is widely distributed in Latin America, the southern United States and Canada, and many other regions worldwide. The seeds are a rich source of protein (24%) and starch (63%) (Chel-Guerrero *et al.*, 2002). They are used for food and for the production of new materials (Betancur-Ancona, 2003). Seeds of this species are composed of the testa with the hilum, and the embryo with large cotyledons, the plumule, epicotyl, hypocotyl and radicle recognisable. The testa, in particular, is very diverse structurally and can also vary in color, according to genotype, from white to green, grey and yellow to brown, red, purple, and black (Bailey, 1963; Baudoin, 1988).

The pod of the lima bean is flat, oblong and slightly curved, averaging about three inches in length. Within the pod are the two to four flat kidney-shaped seeds that we call lima beans. The seeds are generally cream or green in color, although certain varieties feature colors such as white, red, purple, brown or black.

Genetic manipulation in breeding new lima bean cultivars may produce wide variation in the contents of these antinutrients, their chemical composition and protein quality. The chemical composition and protein quality of lima beans and other legumes have been shown to vary according to cultivar (Giami, 2006).

1.2.3 Jack Bean (*Canavalia ensiformis*)

Jackbean (*Canavalia ensiformis*) belongs to the family of the *Leguminosae*. It is native to the West Indies and Central America, but is now found scattered throughout the tropics and sub–tropics (Kay, 1979), having different native names. It is called jack bean in Southern Africaand Zimbabwe; sword bean in Australia, One eye bean in West Indies and Feijaode porco in Brazil (Odetokun, 2000).

It is a tropical climber producing long pendant green beans of 3.3 ft. in height. It has deep roots, which makes it drought resistant. It tolerates a wide range of rainfall (650–2000mm) evenly distributed throughout the year. The climber tolerates droughts, survives salinity and water logging. It grows best at altitude, up to 1800m, temperature of 15–30°C, soil pH of 4.5–8.0, and tolerates a wide range of soils. The plant can spread via long runners, producing flowers of pink–purple colour (Eke *et al.*, 2007).

As a legume, it fixes nitrogen in the soil and so needs artificial nitrogen. Agronomically, it is sown as an annual cover crop. If grown as a perennial intercrop, the plant needs such strong durable support as cocoa, coffee, sugar cane, maize, millet or sorghum.

Jack bean seed is white in colour and nearly oblong in shape and its coat is not to be eaten. Young pods and beans of Jack bean are eaten as vegetable, but only after much preparation and cooking as they contain mild poison in the form of anti–nutritional factors such as protease inhibitors, lectins, saponins and tannins (Eke *et al.*, 2007).

Presently in Nigeria, there are no farms where the Jack bean is commercially cultivated. People plant Jack bean as a flower around their homes while some grow wild.

1.3   AIM AND OBJECTIVES

The aims of this research work are to source for alternatives to conventional starches and unveil the latent potentials of starches from underutilized sources.

The specific objectives are to:

(a) determine the effect of hydroxypropylation and ozone-oxidation processes on the functional, pasting, textural, flow and thermal properties of white and red cocoyam (*Colocasia esculenta*) cultivars, white yam

(*Dioscorea rotundata*), yellow yam (*Dioscorea cayenensis*), lima beans (*Phaseolus lunatus*), pigeon peas (*Cajanus cajan*) and jack beans (*Canavalia ensiformis*);

(b) determine the molar mass distribution, FTIR spectroscopy and X-ray patterns of the native starches and their modified derivatives;

(c) examine the morphologies of the native starches and starch nanocrystals; and

(d) examine the X-ray patterns and solubilities of the starch nanocrystals

This research is expected to:

(a) develop modified and nano starches that could serve as viable alternatives to existing starch useful in pharmaceuticals, confectionery, bakery, polymer and paper industries.

CHAPTER TWO

2.0   LITERATURE REVIEW

2.1   STARCH

Starch is a naturally occurring polymer of α–D glucose. It is the main energy reservoir of higher plants, and also a major source of dietary energy for humans and animals. Starch is found in leaves of all green plants, in seeds, fruits, stems, roots and tubers of most plants. Starch granules are formed in amyloplasts of higher plants. They are also formed in chloroplasts where they serve as temporary store of energy and carbon (Robyt, 2008; Lawton, 2004; Sivak and Preiss, 1997). Besides its nutritive value, starch is a very useful raw material with a wide range of applications in both the food and non-food industries.

Starch application in industrial related products dates back to ancient times. Around 4000 B.C., Egyptians used wheat starch to body papyrus, the earliest writing material, and increase its ability to hold ink. The Chinese started using starch for similar purpose around 100 A.D. The Romans used starch to whiten cloth and powder hair as early as 100 B.C., and around 300 A.D., starch was used to stiffen cloth and was mixed with dyes to colour cloth (Robyt, 2008). Since then, the applications of starch in industries have rapidly increased, increasing its commercial value. Today, some of starch uses include food additive to control consistency and texture of sauces and soups, to resist the breakdown of gel during processing and increase shelf-life of an end product in the food industry, laundry sizing of fine fabrics and skin cosmetics in the textile and cosmetic industry, enhancing paper strength and printing properties in the paper industry, tablet fillers in pharmaceutical industry, and binders in the packaging industry.

The most common sources of starch for the food and non-food industry worldwide are maize, potato, wheat and to some extent tapioca (Vaclavik and Christian, 2008; Robyt, 2008; Lawton, 2004; Jobling, 2004; FAO, 1998; Ellis *et*

9

al., 1998). With increasing industrial demand for starches, there is need to explore new and alternative sources of starch. Tropical root and tuber crops could offer this opportunity as these crops are rich in starch (Wickramasinghe, 2009; Hoover, 2001). However, for long, their role has mostly been that of staple food for the world's hot and humid regions, the tropics and food security crops in the developing countries (Scott *et al.*, 2000; FAO, 1998).

The use of starch in various products and manufacturing processes is determined by its functional properties such as gelatinization, pasting, retrogradation, viscosity, swelling and solubility which vary considerably from crop to crop and with ecological and agronomic influences (Yuan *et al.*, 2007; Peroni *et al.*, 2006; Pérez *et al.*, 2005). The starch functional properties are dependent on composition and molecular structures of the starches, which include amylose/amylopectin ratio, molecular weight of the starches and chain length distribution of amylopectin (Sasaki and Matsuki, 1998; Lu *et al.*, 2005; Shibanuma *et al.*, 1996; Jane and Chen, 1992; Tian *et al.*, 1991).

Therefore, a comparative characterization of native and modified starches, for their physicochemical, functional, thermal and structural properties is essential in order to unravel their potentials for use in the food and non-food industries. The possibility of preparing nanocrystals of starches would be an added advantage in expanding the application of starches in food and non-food industries.

2.1.1 CHEMICAL COMPOSITION OF STARCH

Starch is mainly composed of two carbohydrates: amylose and amylopectin. Amylose has traditionally been considered to be a linear polymer composed of glucopyranose units linked through α–D–(1→4) glycosidic linkages (Fig. 2.1). Although there is now evidence that amylose is not completely linear (Curá *et al.*, 1995), its behavior approximates that of a linear polymer with less than 1% α–D–

(1→6) branching (Buléon *et al.*, 2007). Amylopectin is a branched polymer with one of the highest molecular weights known among naturally occurring polymers. It is composed of glucopyranose units linked by α–D–(1→6) glycosidic linkages (Fig. 2.2). For approximately every 20–30 glucopyranose residues, a branch point occurs, where a chain of α–D–(1→4)–glucopyranosyl units is linked to the C–6 hydroxymethyl position of a glucose residue through an α–D–(1→6) glycosidic linkage. Thus, about 4% of the glucopyranose residues in amylopectin are involved in branch points.

Amylose and amylopectin do not exist free in nature, but as components of discrete, semi crystalline aggregates called starch granules or blocklets. The size, shape, and structure of these granules vary substantially among botanical sources (Thomas and Atwell, 1999). Starch, from any source, exits in the form of white granules of varied size and form; these granules are organized structures, although their existence in relation to that of the cell is transitory (Thomas and Atwell, 1999).

Amylose has a molecular mass of approximately 10^5–10^6 Da, a degree of polymerization (DP) by number of (DP_n) 324–4920 with around 9–20 branching points equivalent to 3–11 chains per molecule. Each chain contains approximately 200–700 glucose residues equivalent to a molecular weight of 32400–113400 Da. The size and structure of amylose molecules vary considerably depending on the botanical source of the starch (Hoover, 2001).
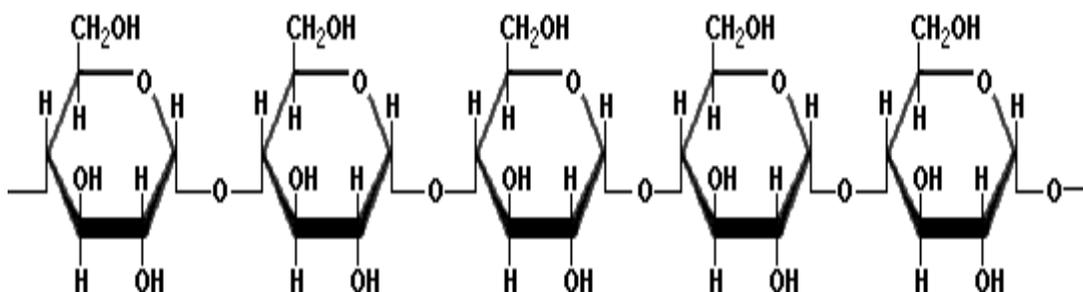
Figure 2.1: Amylose Structure
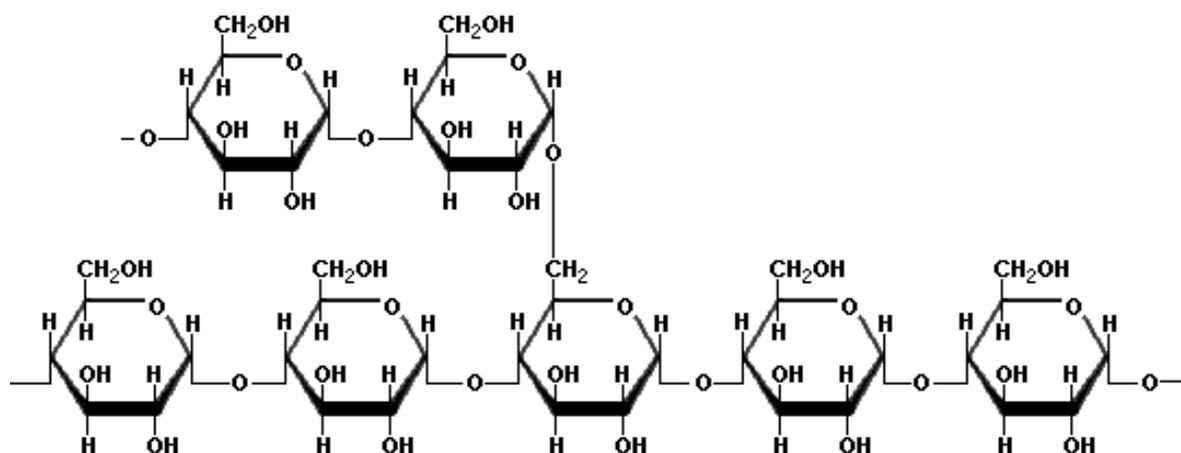
Figure 2.2: Amylopectin Structure

Amylopectin comprises 70–80% of starch and is a much larger molecule with a molecular mass ranging from 106 to 108 Da. Amylopectin has a heavily branched structure built from about 95% (1→4)–α– and 5% (1→6)–α– linkages (Robyt, 2008; Jobling, 2004). Amylopectin chains are relatively short compared to amylose; usually about 18–25 units long on average, and have a broad distribution profile. The presence of branching points allows the short linear chains to pack together efficiently as parallel left-handed double helices, giving rise to the crystalline nature of a starch granule. The DP_n of an amylopectin molecule is within the range 9600–15000 but has three major categories having a DP_n ranging from 13400–26500, 4400–8400, and 700–2100. There are three broad categories of

amylopectin chains; A, B and C. The A chains are the shortest, and B chains the longest. The A chains are chains whose reducing ends attach to other B or C chains but do not carry any other chain. The B chains have their reducing ends attached to other B or C chains, and also carry other A or B chains while the C chain is the only chain of the molecule carrying a reducing end. The B chains have different chain lengths and are subdivided into B1-3 groups with B3 group containing the longest chains. Like amylose, the molecular size, shape, structure and polydispersity varies with botanical origin (Tester *et al.*, 2004; Jobling, 2004; Jane, 2003; Hoover, 2001; Wang *et al.*, 1998; Ellis *et al.*, 1998).

The structural differences between these amylose and amylopectin contribute to significant differences in the starch properties and functionality (Radley, 1968 and 1976; Takahata, *et al.*, 1995; Thomas and Atwell, 1999; and Whistler and Paschall, 1967). The starch properties depend upon their amylose and amylopectin contents (Peterson and Johnson, 1978). Amylose holds the starch granules intact as they swell and gelatinize. Crystalline areas of the starch are partially dependent on the amylose, which reinforces the granule network (Numfor *et al.*, 1995).

Starch molecular weight is often influenced by botanical source, starch isolation procedures, amylose and amylopectin separation methods, and especially the technique used to determine polymer molecular weight (Mua and Jackson, 1997). Gel permeation chromatography, coupled on line to a multi-angle laser light scattering detector (GPC-MALLS), is currently the best available technique for the absolute determination of polysaccharide molecular weights and their distribution (Al-Assaf *et al.*, 2005). Multi-angle laser light scattering (MALLS) utilizes the principle that the intensity of light scattered elastically by a molecule (Raleigh scattering) is directly proportional to the product of the weight average molecular weight and concentration of the polymer. Macromolecular features of starches

13

from various botanical sources such as corn, wheat, potato and sago have been analyzed using GPC-MALLS (Bello-Pérez *et al.* 1998; Othman *et al.*, 2010).

In addition to amylose and amylopectin, starch granules also contain minor non–carbohydrate components: ash (minerals and salts) up to 0.5%; lipids from 0.01 to 0.80%, and proteins, from 0.10 to 0.40%. The most common minerals found in starches are calcium, magnesium, phosphorus, potassium and sodium. These minerals are found in relatively small quantities (<0.4%) and most of these are of little functional significance except phosphorus (Tester *et al.*, 2004). Phosphorus is found in three major forms: phosphate monoesters, phospholipids and inorganic phosphates. Root and tuber starches contain phosphorus in the form of mono phosphate esters covalently bonded to starch while phospholipids are predominant in cereal starches. Phosphorus affects starch functional properties as paste clarity, viscosity consistency and paste stability (Jane *et al.*, 1999). Higher swelling power and stability of starches observed in potato starches is attributed to higher levels of phosphates (Karim *et al.*, 2007).

2.1.2 CRYSTALLINITY OF STARCH GRANULE

Starch has a definite crystalline nature, which is attributed to the well-ordered structure of the amylopectin granules inside the granules. Starch molecules exist as helices and these helices can have different packing arrangements giving rise to different crystalline patterns. X-ray diffraction shows the regularly repeating nature of double helices of molecular structures, but it does not detect irregularly packed structures (Karim *et al.*, 2000). The position of the diffraction peaks defines the crystalline patterns while levels of crystallinity can be obtained by separating and integrating the areas under the diffraction peaks (Zobel, 1988a).

The two principal crystalline patterns of native starches based on the X-ray diffraction patterns have been classified as A or B. The A-type starches are mainly

found in cereals while B-type starches are found mainly in tubers and high amylose starches. The A-type crystallinity contains more abundant and shorter A and B1 chains, and has a ratio of short to long chains of 9–13:1 in molar terms (Hanashiro *et al.*, 2002; Tang *et al.*, 2001a, b; Tang *et al.*, 2002), while the B-type crystallinity has more abundant connecting B chains (B2 and B3) and longer A and B1 chains, and a ratio of short to long chains of 2–7:1 (Hanashiro *et al.*, 2002).

A third type of crystalline pattern has been classified as C-type and this pattern is proposed to be a mixture of both A and B types. The C-type pattern is further divided into C_A and C_B. The C_A pattern is type C which is closer or near A while C_B is type C pattern that is closer to B. The C-type starches are mainly found in legumes (Lopez-Rubio *et al.*, 2008).

A-type starches contain shorter average branch-chain lengths than the C- and B-type starches (Hizukuri, 1985). Native starch granules have absolute crystallinity ranging from 15 to 45%. Type A starches have higher levels of crystallinity (33-44%) and gelatinization temperatures than B, which shows levels ranging from 15-28% and lower gelatinization temperatures (Tian *et al.*, 1991). Furthermore, molecular modeling has shown that the organized molecular structure of glucans with α-(1,4) linkages, having the lowest energy, is based on double helices, regardless of the allomorphic type (A or B) (Imberty *et al.*, 1988). The differences between the two allomorphs relate to the packing of double helices in the crystal unit cell and the quantity of water molecules stabilizing these double helices (Imberty *et al.*, 1987; Imberty *et al*., 1988). Although the local structures of the amylopectin molecule, such as the 2D arrangement of the branched chains, the proportion of long chains to short chains, and the 3D arrangement of the double helix chains have been elucidated, a general 3D image of the amylopectin molecule has not yet been stated clearly (Tang *et al.*, 2006).

Starches from different botanical sources exhibit different crystalline patterns (Stevenson *et al.*, 2006; Singh *et al.*, 2006; Millan-Testa *et al.*, 2005; McPherson and Jane, 1999; Hoover *et al.*, 1995). Cereal grain starches, such as maize, wheat, and rice usually show typical A-patterns while most root and tuber starches exhibit B-patterns. A-type starches show peaks at 15°, 17°, 18° and 22° 2θ angles while B-type has four main reflection intensities at 5.5^o, 17°, 22° and 24° 2θ angles. The B-type X-ray pattern of starch is usually characterized by the position and relative peak intensity in the range of $2\theta = 5$–6°, while the absence of the peak of $2\theta = 5$–6° is characteristic of A-type starch. The C-type X-ray pattern reflects at 5.5^o, 17.0^o, 18.0^o, 20.0^o and 23.5^o 2θ, which is believed to be a superposition of the A– and B–type patterns (Zobel *et al.*, 1988). Cassava starch possesses A, C, or a mixed pattern with three major peaks at $2\theta = 15.3^o$, 17.1^o and 23.5^o. The C_A–type X-ray pattern is exhibited by yam starch, which changes to A-type pattern after acid hydrolysis for 12 days (McPherson and Jane, 1999). Since C-polymorph is a combination of the A- and B-polymorphs, it, therefore, suggests that the B-polymorph of the starches is preferentially hydrolyzed with obvious retention of more birefringence at the periphery of acid-treated starch granules.

Variations in crystalline nature of starches from the same crops have been attributed to variety, sample preparation, growth conditions and maturity of the plant at the time of harvest (Noda *et al.*, 1995; Sugimoto *et al.*, 1987).

In addition, amylose is known to form V-type crystalline inclusion complexes with small molecules such as lipids, alcohols, or flavours present during thermal treatments of starch (Bulèon and Colonna, 2007). The crystallization behaviour of such compounds also has a strong impact on the texture of starchy products (anti-staling effect of monoglycerides, for example) and the retention and the controlled release of guest molecules. Processed starches can be semi-crystalline depending on the conditions used for processing and the aging history.

A crystalline B-type similar to that of native starch can form during cooling or aging of molten starch. However, the V-type structure that occurs in the presence of a complexing agent is not encountered at the crystalline state in the native granule (Bulèon *et al.*, 2007).

2.1.3 MORPHOLOGY OF STARCH GRANULE

Granule size and size distribution of starch are unique properties of starch that have an influence on the functionality of the starches. For example, rice starches are used for laundry sizing of fine fabrics and for skin cosmetics for their small granule size. Cocoyam starches are used as fillers in biodegradable plastics, and in aerosols because of their small size as well (FAO, 2000). Smaller granules are reported to have higher solubility and water absorption capacity (Tian *et al.*, 1991). Smaller granule size is associated with lower RVA peak viscosity temperature while increase in granule size increases higher peak viscosity, breakdown and setback e.g. potato starch (Zaidul *et al.*, 2007a, b).

Microscopic analysis, light and scanning electron microscopy, has been used to study the morphological characteristics of the starch granule. Light microscopy is used for identifying type of starch, and general size and shape of granules from different sources can be observed. Scanning electron microscopy allows the shape and surface of starch granules to be viewed in three dimensions (Thomas and Atwell, 1999). The size and shape of starch granules vary considerably with botanical source. Mishra and Rai (2006) studied the morphology of commercial native corn, potato and tapioca starches, using light and scanning electron microscopy. Granule sizes ranged from 14.3–53.6 μm, 3.6–14.3 μm, and 7.1–25.0 μm for potato, tapioca and corn starches, respectively. Potato starch granules were oval/flattened and ellipsoid in shape, while those of corn were polyhedral and those of tapioca were spherical and truncated. Bello-Pérez *et al.* (2005) reported mostly

lenticular shapes for banana starch granules with an average size of 39 μm. Peruvian carrot starch exhibited spherical and truncated-egg shaped granules with size ranging between 4 and 26 μm (Pérez *et al.*, 1999).

Most morphological studies of starches from root and tuber crops have reported cassava starches to be round with a flat surface on one side containing a conical pit, which extends to a well-defined eccentric hilum, truncated, cylindrical, oval, and spherical or compound with granule size ranging from 4 to 43 μm. Sweet potato starch granules usually exhibit round, polygonal, oval, and bell shapes, and their average granule size ranges from 2 to 72 μm. Cocoyam starch has smaller granule size compared to cassava and sweet potato starches ranging from 1-10 μm. The granules are usually round in shape though polygonal and irregular shapes have also been reported. The surfaces of granules when observed under scanning electron microscopy appear to be smooth (Wickramasinghe *et al.*, 2009; Nwokocha *et al.*, 2009; Aboubakar *et al.*, 2008; Chen *et al.*, 2003; Moorthy, 2002; Hoover, 2001; Noda *et al.*, 1995). However, size and distribution of starch granules also vary with variety. Goering and DeHaas (1972) observed two distinctly different size ranges of granule size in different varieties of *Colocasia esculenta* starches.

The granular morphologies of legume starches such as pigeon pea, mucuna bean, jack bean have been studied, using scanning electron microscope (Lawal, 2011; Adebowale and Lawal, 2002; Lawal and Adebowale, 2005). The pigeon pea starch granules appeared oval or elliptical in shape ranging from 7–40 μm in width and 10–30 μm in length, appearing smooth with very minimal damage. Hydroxypropylation was found by Lawal (2011) not altering the shape of the starch granules in a pronounced way. This compares favourably with the observation made by Chuenkamol *et al.* (2007) for the granules of canna starches. However, traces of degradation were observed on some starch granules after

modification. Changes in appearance of starch granules after hydroxypropylation have been reported for potato starches (Kim *et al.*, 1992) and cassava starch (Jyothi *et al.*, 2007). Granular size has been adduced as a factor for starch granule damage after modification. Smaller granules have low tendency of damage, after modification, via acetylation, than large granules of cassava and wheat (Segura *et al.*, 2003, Hung and Morita, 2005).

2.1.4 STARCH GRANULAR ARCHITECHURE

The conventional model for the inner structure of starch is that it is formed from two regions–crystalline and amorphous lamellae, which together form the crystalline and amorphous growth rings (Jenkins *et al.*, 1994), with dimensions that range from 1 to 100 μm and properties that strongly depend on their crystalline ultrastructure (Buléon *et al.*, 1998a). When the starch granules are observed under polarized light, a characteristic Maltese cross (centred at the hilum) can be seen, which has led to the granules being considered as distorted spherocrystals. The sign of birefringence is positive with respect to the spherocrystal radius, which indicates that, theoretically, the average orientation of the polymer chains is radial (Buléon *et al.*, 1998b). In addition, the intrinsic structure of starch investigated by various measurements such as nuclear magnetic resonance (NMR) spectroscopy (Paris *et al.*, 1999), X-ray microfocus diffraction (Waigh *et al.*, 1997), and small angle X-ray microfocus scattering (Waigh *et al.*, 1999; Suzuki *et al.*, 1998), and it was shown that native starch granules possessed an annular structure of alternate crystalline and semi-crystalline layers.

The growth rings, amorphous (single chain) and ordered (double helix) components (Gidley and Bociek, 1985), are arranged alternately and encircle the point of initiation of the granule, called the hilum. The inner architecture of native starch granules is characterized by 'growth rings' that correspond to concentric

semi-crystalline 120–400 nm thick shells separated by amorphous regions (Figure 2.3).

However, thickness of the growth rings may depend on other factors. New evidence now shows that a structure level, termed the 'blocklet' exists between the macromolecules and the organization of starch granules (Baker *et al.*, 2001; Gallant *et al.*, 1997; Ridout *et al.*, 2003; Szymonska and Krok, 2003)(See Fig. 2.4).

The blocklet has a very much asymmetric structure according to atomic force microscopy (AFM), and an axial ratio of 2 or 3:1, with a maximum length of about 130–250 nm for pea starch granules (Ridout *et al.*, 2003), 20–50 nm for potato starch granules (Szymoska and Krok, 2003), and 10–30 nm for corn starch granules (Baker *et al.*, 2001).

Tang *et al.* (2006) have highlighted the intrinsic characteristics of blocklet as follows:

1. Blocklet structure is similar in shape but differs in size with the plant;
2. In the same plant, most of the blocklets are similar in size, although in different ranges;
3. The blocklet is continuous throughout the granule;
4. The blocklet sizes may not relate to their granular sizes and the thickness of growth or amorphous rings;
5. The blocklet production may have 'defects' in the amorphous rings, and is assembled loosely;
6. An interconnecting matrix surrounding groups of blocklets (blocklet complex) exists and
7. The growth rings and amorphous rings are not always continuous structures.
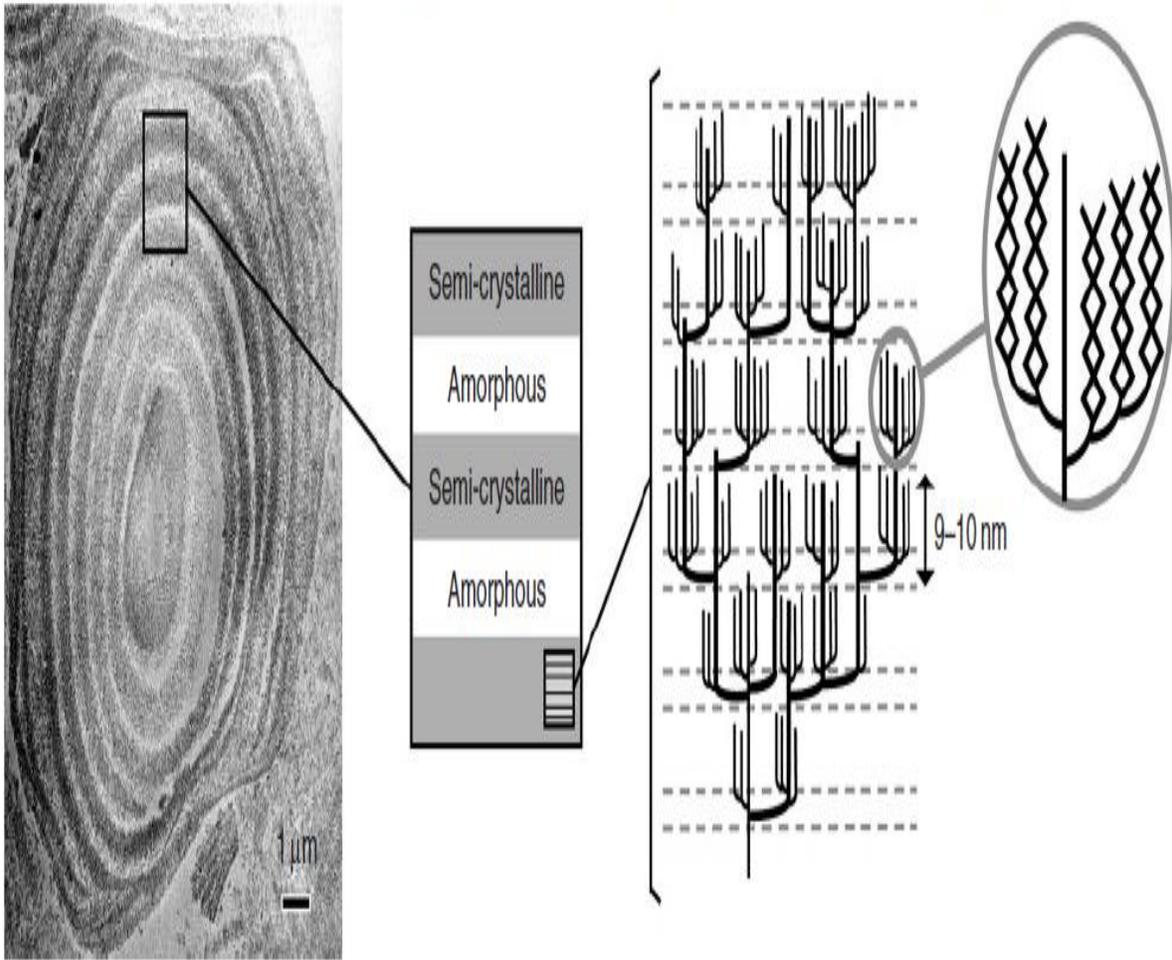
Figure 2.3: Schematic illustration of starch granule ultrastructure
Source: Buléon et al. (2007)
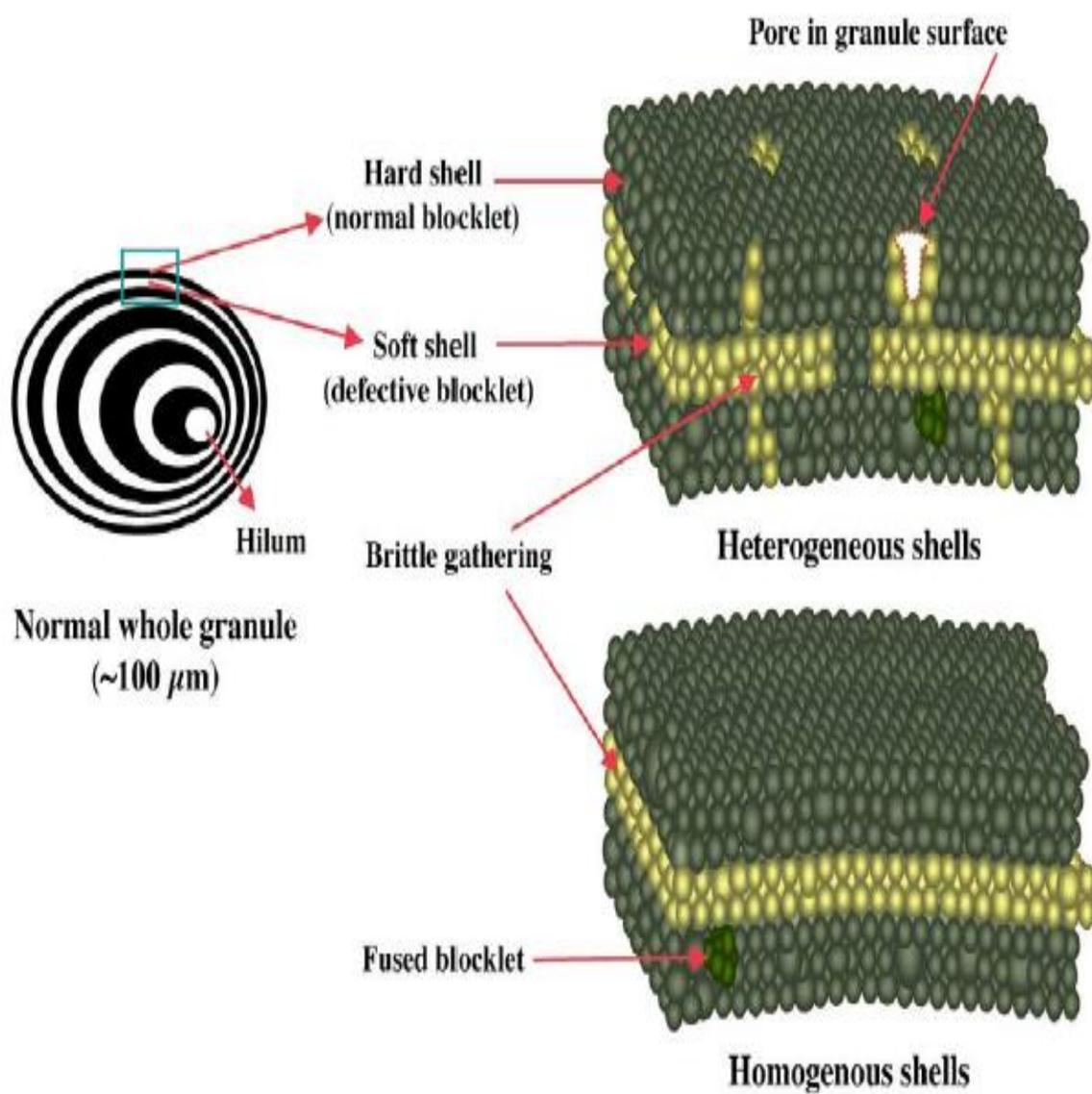
Figure 2.4: Starch Blocklet Structure
(Gallant et al. (1992))

According to the size and distribution of blocklets within starch granules, and the proportion and structural characteristics of the amylopectin molecule, the blocklet is believed to be majorly organized by the crystalline and amorphous lamellae from the amylopectin (Gallant *et al.*, 1997).

Amylopectin differs greatly with the plant source, and ranges around 4000–40,000 residues for the number-average degrees of polymerization (DP_n), and 180–1800 chains for the average number of chains per molecule (NC) (Takeda, 1993; Tang *et al*., 2002; Tang *et al*., 2004).

The semi-crystalline blocklets have generally two types, 'normal' and 'defect' in the same starch, and are basic units that construct starch granules. The normal blocklets construct the hard shells, while the defective blocklets construct the soft shells. The reducing terminal side for all the blocklets is toward the hilum of the granules. It is believed that the surface layer of starch granules consists of the hard shell. However, the starch granules with the heterogeneous shell may be general in nature (Gallant *et al.*, 1992; Tang *et al.*, 2002).

2.2   STARCH MODIFICATION

Native starches have many disadvantages for industrial applications such as insolubility in cold water, loss of viscosity, and thickening power after cooking. In addition, retrogradation occurs after loss of ordered structure on starch gelatinization, which results in syneresis or water separation in starchy food systems. However, these shortcomings of native starch could be overcome, for example, by introducing small amounts of ionic or hydrophobic groups onto the molecules. The modifications alter the properties of starch, including solution viscosity, association behavior, and shelf-life stability in final products. The functionality of starch can be modified through physical, chemical, and biotechnological means. Another purpose of starch modification is to stabilize

starch granules during processing and make starch suitable for many food and industrial applications.

Starch can be physically modified to improve water solubility and to change particle size. The physical modification methods involve the treatment of native starch granules under different temperature/moisture combinations, pressure, shear, and irradiation. Physical modification also includes mechanical attrition to alter the physical size of starch granules.

Starch is widely modified by chemical methods. The most common chemical modification processes are acid treatment, cross-linking, oxidation, and substitution, including esterification and etherification. The development of biotechnology provides another means for starch modification during the growth of the plant. Different amylose levels, amylopectin structure, and phosphorus contents from various plant sources can be produced using anti-sense reduction of enzyme activity of single or multiple enzymes (Jobling *et al.*, 1999). New starch functionalities can also be identified in naturally occurring mutants, which have been widely employed in food industry, because of their natural and specific functional properties.

2.2.1 PHYSICAL MODIFICATION

Physical modification of starch can be applied alone or with chemical reactions to change the granular structure and convert native starch into cold water soluble starch or into small crystallite starch. Small granular starches (diameter < 5 μm) have been used as a good fat substitute. Small particle starch can be made by a combination of acid hydrolysis and mechanical attrition of the native starch (Trubiano and Marotta, 1971).

2.2.1.1　　　Pregelatinization

Pregelatinized starch can be produced by spray cooking, drum drying, solvent-based processing, and extrusion. During a spray cooking process, starch slurry enters through one special nozzle and is atomized (fine spray) in a chamber (Pitchon *et al.*, 1981). At the same time, hot steam is injected into the chamber through a second nozzle to cook out the starch. This method is particularly useful in producing a uniformly gelatinized starch with minimum shear and heat damage. Pregelatinized starch can be made by the drum drying method, in which a cooked starch sheet is produced from a starch slurry on a hot drum; the starch is ground after drying to a desired particle size (Seib, 1996). Cold waters welling starch can be produced by a solvent-based method. For example, 20% starch in aqueous alcohol (20 to 30% water) is heated to 160 to 175°C for 2 to 5 min. Unlike drum dried starch or extruded starch, the end product by solvent-based method maintains granular integrity, but loses its birefringence (Thomas and Atwell, 1999).

The most important property of pregelatinized starch is that it instantly hydrates and swells in water at room temperature. However, finely ground products of pregelatinized starches are difficult to disperse in water homogeneously since they hydrate rapidly at contact with water and form lumps or fish eyes. The hydration rate can be slowed down by premixing the pregelatinized starches with other ingredients. At room temperature, the pastes of the drum cooked/dried starch reduce consistency and have a dull grainy appearance. The gel also has reduced strength. These negative attributes appear to result from the leached amylose molecules establishing a partially intractable network during drying (Seib, 1996).

Pregelatinized starch is used as a thickening agent for pie fillings, puddings, sauces, and baby foods. Starches that generate a pulpy texture are used tomodify the texture of soups, gravies, and sauces. Such starches are made by cross-linking a

normal starch followed by drum cooking/drying and grinding to a specific particle size (Trubiano and Marotta, 1971; Marotta and Trubiano, 1969). The particles swell upon rehydration, but do not disperse under heat and shear. The swollen particles resemble the cell wall material dispersed in food ingredients prepared from vegetables and fruits (Seib, 1996).

Thermal properties of pregelatinized starches of jack fruit and glutinous rice have been studied and their temperatures relevant to gelatinization of were significantly higher than those of native starches, with a much lower enthalpy of gelatinization (ΔH_{gel}) (Kittipongpatana and Kittipongpatana, 2011; Laovachirasuwan *et al.*, 2010). The increase in gelatinization temperature, compared to native starch, was adduced to the colloidal molecular structure of the starch granule, amylopectin chain length, and reordering of the crystalline structure after heat treatment. A drastic drop (60%) in the enthalpic energy required for gelatinization indicated the loss of molecular order within pregelatinized granules (Singh *et al.*, 2003). The effect of pregelatinization on functional properties of starch, such as solubility and swelling, has been found to be temperature-dependent.

Kittipongpatana and Kittipongpatana (2011) have reported that low solubility of native starch at temperatures below 70°C was improved by pregelatinization, while at higher temperatures the solubility of native starch exceeded that of pregelatinized starch of jack-fruit. Pregelatinization improves swelling properties of starch (Visavarungroj and Remon, 1990), and does significantly, at lower temperature (Kittipongpatana and Kittipongpatana, 2011).

2.2.1.2 Heat-Moisture Treatment

Heat-moisture treatment of starch is a physical treatment in which starches are treated at varying moisture levels (<35%) for a certain period of time at a

temperature above the glass transition temperature, but below the gelatinization temperature. However, the temperature is often chosen without considering the gelatinization temperature (Jacobs and Delcour, 1998).

Heat-moisture treatment of maize, wheat, yam, lentil, potato, and mucuna bean starches has no effect on the shape and size of granules. However, the wide-angle X-ray scattering patterns are altered from B-type to A- (or C-) type for potato and yam starches and C-type to A-type for arrow root and cassava starches after heat-moisture treatment. The A-type pattern of cereal starches is not changed by this treatment, but the X-ray diffraction pattern may sharpen or intensify (Hoover and Vasanthan, 1994; Hoover and Manuel, 1996). This indicates that some double helices are moving into a more perfect position in the crystalline phase. The perfection of crystallites in heat-moisture treated waxy maize or dull waxy maize starches results in the 1 to 2°C increase in melting of crystallites. Heat-moisture treatment normally increases the gelatinization temperature, broadens the gelatinization temperature range (Hoover and Vasanthan, 1994; Hoover and Manuel, 1996) and decreases swelling power. Enthalpy of gelatinization (ΔH_{gel}) for B-type starch, such as potato or yam, decreases. It indicates that some double helices are unraveled after heat moisture treatment. The enthalpy of gelatinization for A-type starch (wheat, normal, and waxy maize starches) did not change upon heat-moisture treatment, even though the onset temperature of gelatinization increased 2 to 11°C, indicating that an insignificant number of double helices unraveled (unchanged ΔH_{gel}), whereas a significant number of double helices moved into more perfect crystalline position (increased gelatinization temperature).

Heat-moisture treatment also decreases susceptibility of starch to acid hydrolysis for maize and pea starches. Impact of heat-moisture treatment on the enzyme hydrolysis of starch varies depending on botanical origin and treatment

conditions; both decreased and increased rates of enzyme hydrolysis were observed after heat-moisture treatment (Jacobs and Delcour, 1998).

From the previous works on heat-moisture treated starches, it has been established that starch granules respond to the treatment differently. Corn starch, studied by Afolabi *et al.* (2010) showed that the functional properties are temperature-dependent after heat-moisture treatment with respective lowering and elevation in swelling profile and solubility of the starch. This effect was adduced to probable changes in the packing arrangements of the starch crystallites and or interactions between starch components in the amorphous regions of the granule during hydrothermal treatment. The pasting profile of heat-moisture treated corn starch, in terms of peak viscosity, hot viscosity, cold viscosity, breakdown and setback is lower than the native starch due to weakening and breakdown of bonding forces within the granules (Rasper, 1980). The physical properties of a heat-moisture treated starch depend on the starch origin and treatment conditions used (Adebowale *et al.*, 2005). The pasting time, gelatinization temperature, final viscosity and retrogradation of heat-moisture treated yellow yam starches exhibit higher values than the corresponding native starch while an opposite trend is obtained in terms of their paste viscosity and stability. Unlike the modified white yam starches, yellow yam starches exhibit lowering of values in terms of paste viscosity and stability as the temperature of modification increases (Oladebeye *et al.*, 2011).

2.2.1.3 Annealing

Annealing of starch is a physical treatment whereby the starch is incubated in excess water (>60% w/w) or intermediate water content (40 to 55% w/w) at a temperature between the glass transition temperature and the gelatinization temperature for a certain period of time (Jacobs and Delcour, 1998; Tester and

28

Debon, 2000). Annealing increases starch gelatinization temperature and sharpens the gelatinization range. However, there are few commercial processes to be used to generate starches with higher gelatinization temperatures. Often annealing is applied unintentionally, such as the steeping step used in the maize wet-milling process.

Annealing modifies the physicochemical properties of starch without destroying the granule structure. For annealed wheat and potato starches, no changes were found in the wide-angle and small-angle X-ray scattering patterns, and no significant changes were found in crystalline type and degree of crystallinity. Annealing may induce formation of the amylose-lipid complex, but it is unlikely to affect existing amylose-lipid complexes, because their dissociation temperature is 95 to 125°C, which is far beyond the annealing temperature (Jacobs and Delcour, 1998).

Annealing elevates starch gelatinization temperature, decreases gelatinization temperature range, and reduces swelling power. Annealed starch granules contain more glassy amorphous regions and greater alignment of amylopectin double helices, resulting in the restriction of starch granule hydration during gelatinization and elevation of gelatinization temperature (Thomas and Atwell, 1999). The effects of annealing on viscosity are complex. Annealed potato and maize starches exhibit a decrease in viscosity peak with an increased onset temperature of swelling, while annealed rice and pea starches exhibit an increased viscosity (Hoover and Vasanthan, 1994).

Annealing affects the degree of susceptibility of starch to acid and enzymatic hydrolysis and the susceptibility varies with different starch sources. For example, annealing was found to increase enzymatic susceptibility of barley, oat, and wheat starches, whereas the inverse was true for potato starch (Jacobs and Delcour, 1998; Tester and Debon, 2000; Tester *et al.*, 1998).

2.2.1.4 Extrusion Modification

Extrusion combines several unit operations, including mixing, kneading, shearing, heating, cooling, shaping, and forming. Material is compressed toform a semi-solid mass under a variety of controlled conditions and forced to pass through a restricted opening at a pre-determined rate. There are two main types of cooking extruders: single-screw extruder and twin-screw extruder. The latter is further classified into co-rotating and counter-rotating, depending on the direction of screw rotation. The temperature in the extruder can be as high as 200°C, while the residence time is short (about 10 to 60 seconds) (Colonna and Mercier, 1989). Extrusion cooking is considered to be a high temperature short time (HTST) process. An extruder can be used as a bioreactor or chemical reactor for starch modifications, such as thermomechanical gelatinization, liquefaction, esterification, and etherification.

Extrusion process can be used to produce pregelatinized starch, in which granular starch with different moisture contents is compressed into a dense, compact mass, and disrupted by the high pressure, heat, and shear during the process. The extruded starch is further dried and ground to a desired particle size for food applications. Starch polymers are degraded into smaller molecules during extrusion processing, and amylopectin is more influenced than amylose. Neither short oligosaccharide nor glucose is formed, however, the formation of amyloselipid complexes occurrs during the extrusion process (Mercier *et al.*, 1980).

Starch granule and its crystalline structure are destroyed either partially or completely, depending on the ratio of amylose/amylopectin and the extrusion variables, such as moisture, temperature, and shear. Increasing severity of extrusion treatment (low moisture and high temperature) results in the decrease in initial cold viscosity, and increasing extrusion temperature causes a reduction in

the pasting consistency (Colonna and Mercier, 1989). Normally, the increase in specific energy mechanical input results in a reduction in viscosity and an increase in solubility (Colonna and Mercier, 1989).

2.2.2 CHEMICAL MODIFICATION

2.2.2.1 Oxidized Starch

Starch oxidation has been practiced since the early 1800s, and various oxidizing agents have been introduced, for instance, hypochlorite, hydrogen peroxide, periodate, permanganate, dichromate, persulphate, and chlorite (Rutenberg and Solarek, 1984).

Oxidized starch has been widely used in many industries, particularly the paper, textile, laundry finishing, and building materials industries to provide surface sizing and coating properties (Scallet and Sowell, 1967). Oxidized starch also becomes increasingly important in the food industry for its unique functional properties such as low viscosity, high stability, clarity, film forming, and binding properties.

Most oxidized starch for food applications is produced by reacting starch with a specified amount of sodium hypochlorite (NaOCl) under controlled temperature and pH (Wurzburg, 1986). Oxidation of starch mainly causes the scission of the glucosidic linkages and oxidation of hydroxyl groups to carbonyl and carboxyl groups. The scission of the glucosidic linkage results in depolymerization of amylose and amylopectin, hence decreases swelling power and paste viscosity. However, treatment with low levels of hypochlorite has been reported to increase paste viscosity (Wurzburg, 1986).

Two main reactions occur during oxidation. Firstly, starch hydroxyl groups are oxidized to carbonyl groups and then to carboxyl groups. This reaction primarily takes place on the hydroxyl groups at the C–2, C–3, and C–6 positions

(Wurzburg, 1986). Secondly, oxidation also causes degradation of starch molecules by mainly cleaving amylose and amylopectin molecules at α– (1→4)– glucosidic linkages (Wurzburg, 1986) (See Fig. 2.5). Therefore, the carboxyl and carbonyl contents and the degree of depolymerization in oxidized starch are indicators of the degree of oxidation, which can be affected by many factors, including pH, temperature, hypochlorite concentration, starch molecular structure, and starch source (Wurzburg, 1986). Formation of the carbonyl and carboxyl groups discontinuously along the chains reduces gelatinization temperature, increases solubility, and decreases gelation. The carbonyl and carboxyl groups also reduce the thermal stability of the oxidized starch that causes browning. Since the bulkiness of the carboxyls and carbonyls sterically interfere with the tendency of amylose to associate and retrograde, oxidized starches produce pastes of greater clarity and stability than those of unmodified starch.
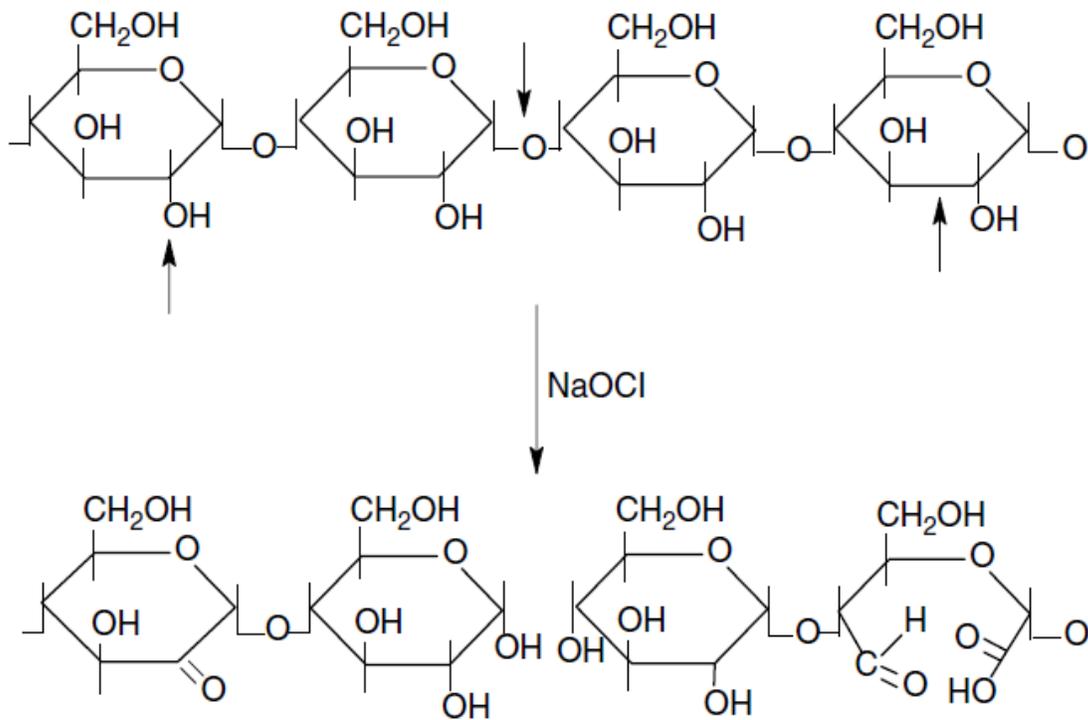
Figure 2.5: Oxidation of Starch with Formation of Carbonyl and Carboxyl Groups

Oxidized starch can be used as a coating and sealing agent in confectionary, as an emulsifier (Konoo *et al.*, 1996), as a dough conditioner for bread (Mazur *et al.*, 1989), as a gum arabic replacer (Chattopadhyay, 1997), and as a binding agent in batter applications.

Many studies have reported that starch source and structure highly influenced the extent of oxidation (Hullinger and Whistler, 1951; Kuakpetoon and Wang, 2001). Recent results by Kuakpetoon and Wang (2001) showed that potato starch was much more prone to oxidation than were corn and rice starches under the same oxidation conditions. Potato starch displays the B-type X-ray diffraction pattern, which has a looser crystalline arrangement and a lower crystallinity compared with A-type starches (Wu and Sarko, 1978a, b; Imberty and Pérez, 1988). Therefore, starches containing more loosely packed crystalline structure or more amorphous structure may provide more accessible reaction sites for the oxidizing agent. Any chemical characteristics affecting the packing of crystalline lamellae and the size of amorphous lamellae could also influence the extent of oxidation. Starches with short average chain lengths display A-type crystalline patterns, and long and intermediate average chain lengths are associated with B-type and C-type crystalline patterns, respectively (Hizukuri *et al.*, 1983; Hizukuri, 1985). Although potato and high amylase corn starches exhibit a similar B-type crystalline polymorphism, high-amylose corn starches may show different oxidation efficiency when compared to potato starch because of their high amylose contents. Jenkins and Donald (1995) investigated the influence of amylose on corn starch granule structure using small-angle X-ray scattering (SAXS) and observed that the combined size of the crystalline and amorphous lamellae was constant at 9 nm for all three corn starches varying in amylase content (0%, 28%, and 70%). However, the size of the amorphous lamellae decreased with increasing amylose content. They suggested that amylose might disrupt the packing of amylopectin

double helices by co-crystallizing with amylopectin chains and pulling some amylopectin chains from two adjacent crystalline lamellae closer to each other. Therefore, the amount of amylose may also affect the access of oxidizing agent to starch during oxidation.

2.2.2.2 Ozone-Oxidized Starch

Due to safety and environmental friendliness, chemical oxidizing agents generally are objectionable for starch modification. For example, large amounts of salts are formed in the hypochlorite oxidation process, which causes wastewater disposal problems (Kesselmans and Bleeker, 1997). In contrast, ozone does not leave a residue when it is introduced to a food product. Therefore, ozone treatment would be a good alternative to chemical treatment of food products. Ozone is a naturally occurring and industrially generated form of oxygen (Dillon *et al.*, 1992). It is a more powerful oxidant than oxygen due to its extra oxygen atom, which it can share with other substances to oxidize them. Moreover, it is a clean oxidant that has an elevated thermodynamic oxidation potential, which means that the reactions can be performed at low temperatures (Sahle-Demessie and Devulapelli, 2008).

This can be achieved by generating ozone, channeling it to the rotator reaction vessel, which holds the sample for homogenization. The unreacted ozone is trapped by potassium iodide (KI) solution. Molecules of iodine librated upon addition of approximately 10 ml of 2M H_2SO_4 are titrated with a standardized 0.2 M $Na_2S_2O_3$ solution, using starch solution as the indicator.

$$O_3 + 2KI + H_2O \rightarrow O_2 + I_2 + 2KOH \qquad …2.1$$

$$I_2 + 2Na_2S_2O_3 \rightarrow Na_2S_4O_6 + 2NaI \qquad …2.2$$
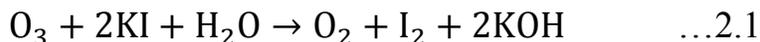
From Eqns 2.1 and 2.2, 1 mole of $Na_2S_2O_3$ consumed was equivalent to 0.5 mole of ozone.

Chan *et al.* (2009) studied the effect of ozone-oxidation on the physicochemical properties of corn, sago and tapioca starches. The Pearson correlation of their data showed a significant positive relationship between the amounts of ozone reacted with starches and carboxyl (corn, r=0.924; sago, r=0.768; and tapioca, r=0.910, P<0.01) and carbonyl contents (corn, r=0.914; sago, r=0.627; and tapioca, r=0.887, P<0.01). The extent of this interaction is influenced by the amylose-to-amylopectin ratio and phosphorus content and by the characteristics of the amylose and amylopectin in terms of molecular weight/distribution, degree of branching and branch length, and conformation (Hoover, 2001; Singh and Kaur, 2004). Ozone-oxidized starches have been found to possess decreased swelling profile than their corresponding native (unmodified) forms. Increase in solubility, resulting from depolymerization and structural weakening of the starch granule has been reported (Hodge and Osman, 1996; Parovuori *et al.*, 1995; Wang and Wang, 2003; Chan *et al.*, 2009). The physicochemical, rheological, thermal and molecular characteristics of ozone-oxidized starches are influenced by the ozone-generation time (OGT) (Chan *et al.*, 2009; Chan *et al.*, 2011).

2.2.2.3 Cross-Linked Starch

Starch contains two types of hydroxyls, primary (6–OH) and secondary (2–OH and 3–OH). These hydroxyls are able to react with multifunctional reagents resulting in cross-linked starches. Cross-linking is done to restrict swelling of the starch granule under cooking conditions or to prevent gelatinization of starch. Cross-linking of starch is effected by a low level of reagent. Starch molecules are long chain polymers, which occur in close proximity within granules. Starch molecules can be interconnected by reactions with trace amounts of a multifunctional reagent (Seib, 1996).

Cross-linking of starch with phosphorous oxychloride is a rapid reaction which produces a distarch phosphate (Fig. 2.6). The reaction is especially efficient above pH 11 and in the presence of sodium sulphate (2% based on starch) (Wu and Seib, 1990).

When phosphoryl chloride is added to a slurry of starch the first chloride ion of phosphoryl chloride reacts with water at 25°C immediately (with half life of 0.01 sec) to form a phosphorous dichloride, which is likely the crosslinking agent (Hudson and Moss, 1962).
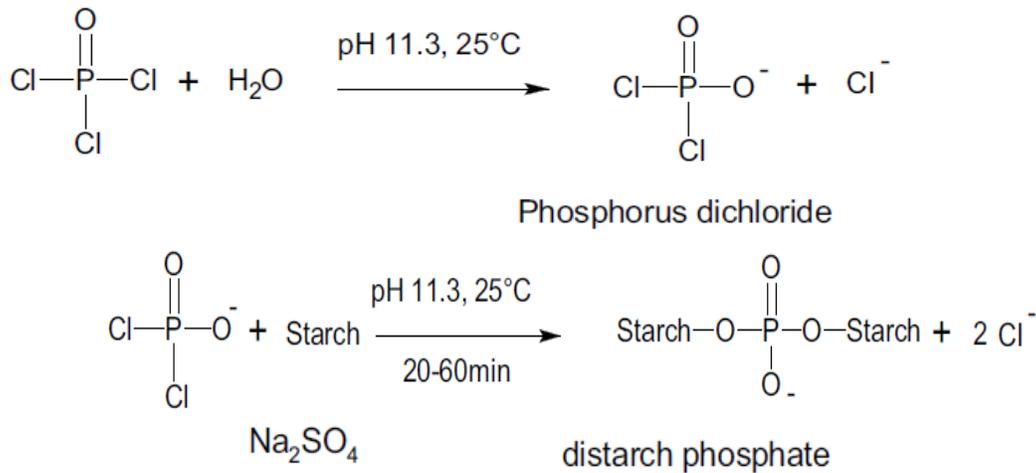
Figure 2.6: Formation of distarch phosphate

Starch with a low level of cross-linking shows a higher peak viscosity than that of native starch and reduced viscosity breakdown. The chemically bonded cross-links may maintain granule integrity to keep the swollen granules intact, hence, prevents loss of viscosity and provides resistance to mechanical shear. Increasing the level of cross-linking eventually will reduce granule swelling and decrease viscosity. At high cross-linking levels, the cross-links completely prevent

the granule from swelling and the starch cannot be gelatinized in boiling water even under autoclave conditions (Srivastava and Patel, 1973).

Cross-linked starches are used in salad dressings to provide thickening with stable viscosity at low pH and high shear during the homogenization process. Cross-linked starches with a slow gelatinization rate are used in canned foods where retort sterilization is applied; such starches provide low initial viscosity, high heat transfer, and rapid temperature increase, which are particularly suitable for quick sterilization (Rutenberg and Solarek, 1984; Evans *et al.*, 1969; Rutenberg *et al.*, 1975).

Cross-linking negatively affects the swelling of starch by immobilizing the bond flexibility between starch chains via the formation of inter-molecular bridges by phosphorous residual, causing the resistance against swelling (Koo *et al.*, 2010). Limited water solubility is associated with cross-linked starch, arising from less disintegration of starch granules during gelatinization, and resulting in increased density of cross-linkage and less molecular mobility (Koo *et al.*, 2010).

2.2.2.4 Acetylated Starch

Starch ester is a group of modified starches in which some hydroxyl groups have been replaced by ester groups. The level of substituents of the hydroxyl groups along the starch chains is often expressed as average degree of substitution (DS). The average degree of substitution is the moles of substituent per mole of D-glucose repeat residue (anhydroglucose unit). The maximum possible DS is 3.0 when all three hydroxyls are substituted on each glucose unit along a starch chain. Under alkaline conditions, starch is indirectly reacted with carboxylic anhydride. An alkali starch complex forms first, which then interacts with the carboxylic anhydride to form a starch ester with the elimination of carboxylate ion and one molecule of water (Jarowenko, 1986; Grundschober and Prey, 1963). During the

acetylation process there are two side reactions including the deacetylation of starch and the formation of sodium acetate (by product) (Fig. 2.7).
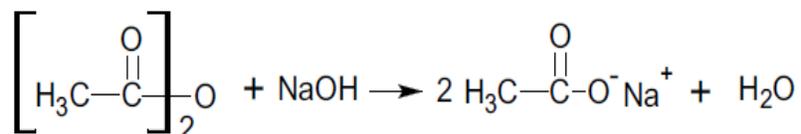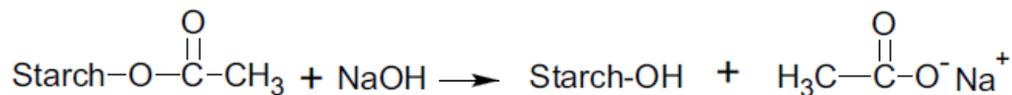
Figure 2.7: Esterification of Starch

Sodium acetate formed as a by-product must be completely removed by the washing process because it causes acetyl odours in puddings made from these starch acetates (Katcher and Ackilli, 1980).

Gelatinization temperature of starch acetate is markedly lower than that of the native starch (Liu et al., 1997). Normal corn acetate starch has a ~7°C lower gelatinization temperature and a slightly higher peak viscosity, reached at ~7°C lower than that of the unmodified starch. In the cooling cycle, the viscosity of normal corn acetate starch is lower, indicating improved cold stability (Rutenberg and Solarek, 1984).

The reduction in viscosity of normal corn acetate starch on cooling is probably due to acetate interference within the amylose portion by reducing the association of the molecules.

Acetate starches normally lack resistance to mechanical shear and acids. Cross-linked starches are resistant to viscosity breakdown and acidic conditions, but exhibit poor clarity and cold aging stability. By combining acetylation with cross-linking, both viscosity stability and clarity can be achieved, as well as low

temperature storage stability. Cross-linking also provides desired textural properties (Jarowenko, 1986).

2.2.2.5 Hydroxypropylated Starch

Unlike ester linkage such as starch acetate, which tends to deacetylate under alkaline condition, ether linkages are more stable even at high pH. Etherification gives starch excellent viscosity stability. Hydroxyalkyl starches, including hydroxyethyl and hydroxypropyl, are mainly produced for industrial applications. Hydroxyethyl starch has not yet been approved as a direct food additive, but can be used as an indirect food additive, such as a sizing agent for paper contacting food, whereas hydroxypropyl starch is primarily used for the food industry.

Propylene oxide is an unsymmetrical epoxide and a very reactive molecule, because of its highly strained three-membered epoxide ring with bond angles of ~60°. Opening of the unsymmetrical epoxide in base occurs by attacking at the sterically less hindered end of epoxide to produce 2–hydroxypropyl starch ether (Tuschhoff, 1986).

The reaction of propylene oxide with starch under alkaline conditions is a substitution, nucleophilic, bimolecular, or S_N2 type (Tuschhoff, 1986). Nucleophiles react with oxiranes in S_N2 fashion to give ring opened products (Fig. 2.8).

Starch-OH + NaOH $\longrightarrow$ StarchO$^-$ Na$^+$ + H$_2$O

StarchO$^-$ Na$^+$ + H$_3$C—HC——CH$_2$ $\xrightarrow{\text{HOH}}$ Starch—O—CH$_2$—CH—CH$_3$ + NaOH

propylene oxide   hydroxypropyl starch
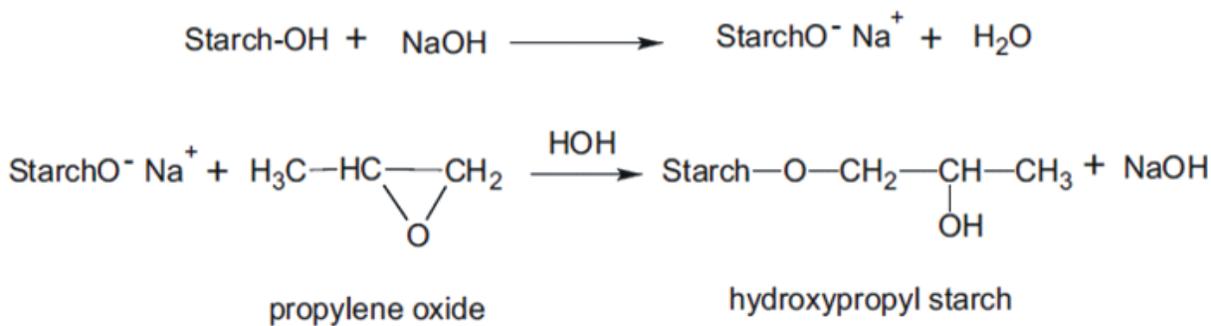
Figure 2.8: Hydroxypropylation of Starch

Depending on the degree of modification, hydroxypropylation of starch is achieved in one of two ways. At degree of substitution (DS) $\leq$ 0.25, starch is slurried in aqueous sodium hydroxide to adjust pH to approximately 11.5. Sodium sulphate, 5 to 15% (based on dry starch weight) is added to protect the starch from swelling. Propylene oxide is added up to 10% (based on starch dry weight). The mixture is warmed between 45 and 50°C and stirred for about 24 hours. After the etherification reaction, crosslinking with phosphoryl chloride is usually done to give hydroxypropyl distarch phosphate. Without cross-linking, the hydroxypropyl derivatives of starches swell excessively and give stringy pastes (Seib, 1996).

The preparation of hydroxypropyl starch with a high DS is carried out in a semi-dry state. Starch is first sprayed with aqueous sodium hydroxide until it contains approximately 20% moisture, then the alkali starch is stirred in a closed reactor with gaseous propylene oxide up to a maximum level of 25% (based on drystarch weight). Upon completion of the reaction in 24 to 36 hours, the highly hydroxypropylated starch is isolated by special washing procedures to avoid gelatinization. The end product is a cold water swelling starch (Seib, 1996; Tuschhoff, 1986).

Introduction of hydroxypropyl groups affectthe enzyme digestibility of starches. Substitution of potato, corn, waxy maize, and high-amylose maize

starches with hydroxypropyl groups decreased the extent of enzymatic hydrolysis of raw and gelatinized starches with increasing DS (Azemi and Wootton, 1984). The hydroxypropyl groups on starch chains may hinder enzymatic attack and also make neighboring bonds resistant to degradation (Björck *et al.*, 1989).

Substitution of hydroxypropyl groups on starch chains disrupts the internal bond structure resulting in the reduction of the amount of energy needed to solubilize the starch in water. As a result, the pasting temperature of starch decreases with an increase in the level of hydroxypropyl substitution. When the DS reaches a certain level, the starch becomes cold water swelling (Tuschhoff, 1986).

Hydroxypropyl groups interfere with the retrogradation of starch molecules. The substituent groups inhibit gelation and syneresis, apparently by sterically interfering with formation of junction zones and double helices in starch (Seib, 1986).

The hydroxypropyl substitution causes the repulsion between starch chains, lowering the molecular bonding force, allowing water penetration to the inside to enhance solubility (Waliszewski *et al.*, 2003). The ability of hydroxypropylation to improve swelling of starch granules has been established (Pal *et al.*, 2002; Waliszewski *et al.*, 2003).

2.3   NANOTECHNOLOGY OF STARCH

Nanotechnology has emerged as one of the most fascinating areas in the biopolymer research, which find exciting enhancement of applications in drug delivery systems, food technology and cosmetic field. This following discussion is focused on the polysaccharide nanoscience, emphasises on basic methodologies for preparing biopolymer based nanomaterials.

Nanotechnology focuses on the characterization, fabrication, and manipulation of biological and non biological structures smaller than 100 nm.

Structures on this scale have been shown to have unique and novel functional properties. The potential benefits of nanotechnology have been recognized by many industries, and commercial products are already being manufactured, such as in the microelectronics, aerospace, pharmaceutical, food and cosmetic industries (Chen *et al.*, 2006; Huaiguo *et al.*, 2006).

Worldwide commercial foods and food supplements containing added nanoparticles are becoming available. A major growth area appears to be the development of "nanoceuticals" and food supplements (Chen *et al.*, 2006).

In recent times, the application of nanocrystals of starch has gone beyond food. Interest in biomaterials and nanocomposites has now emerged (Duan *et al.*, 2011; Angellier *et al.*, 2005a, b). The quest for nanotechnology in all fields of study is the new trend of interest of both scientists and industries with the view to processing polymeric composite materials filled with rigid particles at least one dimension in nanometer range. Nanoparticles of native starch called nano starch or starch nanocrystals can be obtained by acid hydrolysis (Angellier *et al.*, 2005a). Studies on corn starch and waxy starch nanocrystals as reinforcing fillers in natural rubber have revealed possible replacement of conventional filler, carbon black with nano starch of corn (Angellier *et al.*, 2005c).

2.3.1 NANOCRYSTALS OF STARCH

Currently, the emergence of renewable biobased nanomaterials gathers the two concepts of nanotechnologies and renewable raw materials. Nanotechnology is based on the development of innovative and efficient materials while renewable raw materials focus on sustainable products for the development of future applications (LeCorre *et al.*, 2011).

As recently reviewed by LeCorre *et al.* (2012), starch nanocrystals are candidates of growing interest for the production of biobased nanomaterials. They

are crystalline platelets resulting from the disruption of the semicrystalline structure of starch granules by the hydrolysis of amorphous parts. In 2003, the morphology of starch nanocrystals extracted from waxy maize was revealed (Putaux *et al.*, 2003). Transmission electron microscopy (TEM) observations showed a longitudinal view of lamellar fragments consisting of stack of elongated elements, with a thickness of 5–7 nm, and a planar view of individualized platelets after hydrolysis. Shapes and lateral dimensions were derived from observation of individual platelets in planar view and marked 60–65° acute angles for parallel piped blocks with a length of 20–40 nm and a width of 15–30 nm were reported. However, more recent publications reported bigger starch nanocrystals (Chen *et al.*, 2008; Yu *et al.*, 2008; Chen *et al.*, 2008; Garcia *et al.*, 2009; Namazi and Dadkhah, 2010) with round edges (Wang and Zhang, 2008) and found as grape-like aggregates of 1–5 μm. The heterogeneity in particle size could be explained by the differences in starch botanic origin, as recently presented (LeCorre *et al.*, 2009), and also by the difficulty to obtain well-defined pictures of non-aggregated nanocrystals.

The dominant component of the crystalline region in native starch granules is thought to be amylopectin lamellae (Perez *et al.*, 2009; Jenkins and Donald, 1995), which pack together to form double helix crystal structure (Putaux *et al.*, 2000; O'Sullivan and Perez, 1999). In crystallites of starch, parallel stranded double helical structure is found in pairs, and all chains are packed in arrays. The pairing of double helices is identical in both polymorphs and corresponds to the interaction between double helices that has the lowest energy (Imberty *et al.*, 1991). The crystalline regions of starch granules can be isolated by mild acid hydrolysis using hydrochloric or sulfuric acid. It is believed that at temperatures below the gelatinization temperature acid molecules preferentially attack the amorphous regions of the granule (Jenkins and Donald, 1997), resulting in these

regions being more rapidly hydrolyzed than the crystalline regions (Wang *et al.*, 2003). The residue after acid hydrolysis contains the starch nanocrystals, which have high crystallinity and nanoscale platelet morphology.

Recently, starch nanocrystals have been modified to extend their end use. These include acetylated derivative of nanocrystals of corn starch for possible application in packaging industry and as nano reinforcement (Xu *et al.*, 2010) and amphiphilic starch nanocrystals, by graft copolymerization with styrene, to serve as the fillers of polymer matrix, such as natural rubber, polylacticacid, and polycaprolactone for getting nanocomposites with unique properties (Song *et al.*, 2007).

Mild acid hydrolysis has widely been used to investigate the structure and properties of starch crystallite by preferential degradation of the amorphous regions. The extent of this preferential erosion depends on the density difference between the crystalline and the amorphous phase. It has recently been demonstrated that the A–type nanocrystals obtained by hydrolysis of 'waxy', that is, amylopectin-rich maize starch granules correspond to the crystalline lamellae present in the native granule. However, additional electron diffraction data could not be collected from individual lamellae, because of their small later size and thickness.

The X-ray pattern reported for starch nanocrystals of corn by Xu *et al.* (2010) showed diffraction peaks at $2\theta = 15.2^o$, 17.1^o, 18.0^o and 23.0^o, indicating A-type X-ray pattern. X-ray pattern is, however, dependent on the degree of substitution of the nanocrystals. At low degree of substitution (DS = 0.16), the pattern of the acetylated starch nanocrystals appeared the same (A–type), although a new peak of $2\theta = 9.7^o$ was obtained. At higher degree of substitution (DS = 2.45), V-type was exhibited by destroying the A-type crystallinity, which was conspicuous with wide peaks at $2\theta = 9.2^o$ and 20.7^o (Xu *et al.*, 2010). Graft

copolymerization of nanocrystals of corn starch on styrene has been established by X-ray diffraction, suggesting that the polystyrene side chains are mainly grafted on the surface of the starch nanocrystals and arranged irregularly on the polysaccharides backbones (Song *et al.*, 2008).

2.4   NUTRITIONAL PROFILE OF STARCH
2.4.1 PROXIMATE COMPOSITION
2.4.1.1 Protein Content

Proteins are important constituents of foods for a number of different reasons. They are a major source of energy, as well as containing essential amino-acids, such as lysine, tryptophan, methionine, leucine, isoleucine and valine, which are essential to human health, but which the body cannot synthesize. Proteins have a major effect on the structure and sensory quality of numerous foods in fresh and processed conditions, for example, on the consistency and texture of meat and meat products, milk and cheese, pasta and bread.

Food quality most often depends on the structural and physicochemical quality of the protein components. Some of these functional properties are: hydration, solubility, viscosity, gel formation, texture, dough formation, emulsification, foaming, aroma binding and interaction with other food components (FAO/WHO, 1990). Crude protein is the total amount of protein in the food, but it says nothing about its digestibility. The quality of the protein is very important.

In practice, most biological methods for evaluating protein quality are, in fact, evaluating nitrogen but are expressed as crude protein (N x 6.25). Nitrogen in foods not only comes from amino acids in protein, but also exists in additional forms that may or may not be used as a part of the total nitrogen economy of

humans and animals. The nitrogen content of proteins in foods can vary between 150 and 180 g/kg (i.e. 15–18%), depending on the amino acids they comprise.

The protein content of foodstuffs is conventionally estimated from the nitrogen content determined by the Kjeldahl technique. Munro and Fleck (1969) have proposed numerous modifications of the original procedure of the Association of Official Analytical Chemists (AOAC, 1975).

2.4.1.2   Moisture Content

Moisture content is one of the most commonly measured properties of food materials. It is important to food scientists for a number of different reasons:

- *Legal and Labeling Requirements*: There are legal limits to the maximum or minimum amount of water that must be present in certain types of food.

- *Economic*: The cost of many foods depends on the amount of water they contain. Water is an inexpensive ingredient, and manufacturers often try to incorporate it as much as possible in a food, without exceeding some maximum legal requirement.

- *Microbial Stability*: The propensity of microorganisms to grow in foods depends on their water content. For this reason many foods are dried below some critical moisture content.

- *Food Quality*: The texture, taste, appearance and stability of foods depend on the amount of water they contain.

- *Food Processing Operations*: Knowledge of the moisture content is often necessary to predict the behavior of foods during processing, e.g. mixing, drying, flow through a pipe or packaging.

In principle, the moisture content of a food can therefore be determined accurately by measuring the number or mass of water molecules present in a known mass of sample. It is not possible to directly measure the number of water molecules present in a sample because of the huge number of molecules involved.

2.4.1.3   Crude Fibre

Crude fibre is indigestible carbohydrate that adds bulk to the diet. It is the organic residue after food sample has been treated under standardized conditions with light petroleum, boiling tetraoxosulphate (vi) acid, boiling sodium hydroxide and dilute hydrochloric acid (Pearson *et al.*, 1981). Sources of fiber include plant hulls, such as oat bran, or vegetable material such as beet pulp. There should be 4% or less fiber in foods intended for ferrets.

2.4.1.4   Ash Content

Ash is the inorganic residue remaining after the water and organic matter have been removed by heating in the presence of oxidizing agents, which provides a measure of the total amount of minerals within a food. Analytical techniques for providing information about the total mineral content are based on the fact that the minerals (the "analyte") can be distinguished from all the other components (the "matrix") within a food in some measurable way.

The most widely used methods are based on the fact that heating does not destroy minerals, and that they have a low volatility compared to other food components. The three main types of analytical procedure used to determine the ash content of foods is based on this principle: dry ashing, wet ashing and low temperature plasma dry ashing. The method chosen for a particular analysis depends on the reason for carrying out the analysis, the type of food analyzed and the equipment available.

Ashing may also be used as the first step in preparing samples for analysis of specific minerals, by atomic spectroscopy or the various traditional methods described below. Ash contents of fresh foods rarely exceed 5%, although some processed foods can have ash contents as high as 12%, e.g. dried beef (Anderson, 1996). Ash content is very important because it contains mostly the essential and non-essential minerals and, in fact, it is a good evaluation of the nutritive quality of food (Pearson *et al.*, 1981).

2.4.1.5   Fat Content

Fats are esters of alcohol with aliphatic fatty acids and normally occur in animal and vegetable tissue as a mixture of several pure fats plus free fatty acids. The most common of such fats are palmitin, the ester of palmitic acid; stearin, the ester of stearic acid; and olein, the ester of oleic acid. These pure chemical compounds are contained in different proportions in various natural fats and oils, and they determine the physical characteristics of each of these substances. Fats are a good source of energy and serve as the body osmoregulator (Pearson *et al.*, 1981).

2.4.2 MINERAL COMPOSITIONS

Mineral, also known as inorganic matter of food that remains after the burning off of the organic matter, is a determinant of the quality of food, health, well-being and safety of the consumer (Olaofe *et al.*, 1987). It is, therefore, imperative to have adequate knowledge of the mineral composition of food.

Minerals in food can be grouped into macromolecules and micromolecules (or trace metals). The macromolecules, which include Ca, P, Mg, K and Na are required in amount greater than 100mg/day while micromolecules are needed in lower amount than 50ppm/day e.g. Fe, Cu, Mn, Cr, Co, Pd, As, Zn, Hg, Cd and Ni.

Trace elements are classified based on their effect on health into the following categories:

- *Essential nutritive minerals:* These are minerals essential for the metabolic processes taking place in the body, although they may be harmful if taken in excess. Examples are Na, K, Ca, Cu, Mg, Fe, Co, I, Mn and Zn.

- *The non-nutritive, non-toxic minerals:* These are minerals with no harmful effect except when present in amount exceeding 100ppm. Examples are Al, B, Cr, Ni and Sn.

- *The non-nutritive, toxic minerals:* These are minerals with toxic effect even when the diet contains less than 100ppm. Examples are As, Sb, Cd, F, Pb, Hg and Se.

One of the factors influencing the uptake of macro and microelements in plants is the composition of the soil on which the plant is grown, indicating the variation of the ash and mineral contents of the agricultural products owing to the planting location.

2.5 FUNCTIONAL PROPERTIES

Oshodi and Ekperigin (1989) have defined functional properties of food as the intrinsic physicochemical characteristics, which may affect the behaviour of food system during processing and storage. Functionality is the key to marketing starches in the wide range of food and non-food applications, if pre-treated to eliminate possible toxicity (Oladebeye, 2003).

2.5.1 LEAST GELATION CONCENTRATION (LGC)

LGC is the measure of gelation capacity of starch. This measurement is based on hydrothermal process of heating and cooling. This property of starch had

been taken as the probable gel strength of starch (Oladebeye, 2003). According to Coffman and Garcia (1977), the concentration at which the starch slurry does not fall, when the test tube is inverted, is known as least gelation concentration.

2.5.2 WATER ABSORPTION CAPACITY (WAC)

Water absorption capacity (WAC) is defined as the water absorbed by the protein content of the particulate matter of a food substance after equilibration against water vapour at a known relative humidity (Mellon *et al.,* 1947). It generally depends on starch and protein contents and particle size. Fine particle size (425 *p*m) was associated with higher water absorption than coarse particle size regardless of variety of plant (Kulkarni *et al.*, 1988).

Water binding by starches has been adduced to several parameters including size, shape, conformational characteristics, steric factors, hydrophilic-hydrophobic balance in the starch molecule, lipids and carbohydrates associated with the proteins, thermodynamic properties of the system (energy of bonding, interfacial tension, etc.), physicochemical environment (pH, ionic strength, vapor pressure, temperature, presence/absence of surfactant etc.), solubility of starch molecules and others (Chou and Morr, 1979).

2.5.3 OIL ABSORPTION CAPACITY (OAC)

OAC is the measure of the affinity of the granules of food substance for oil molecules. Oil absorption capacity (OAC) is another important functional property, since it plays an important role in enhancing the mouthfeel while retaining the flavor of food products (Kinsella, 1976). It has been reported that variations in the presence of non–polar side chains, which might bind the hydrocarbon side chains of oil among the flour, explain differences in the oil binding capacity of food products (Adebowale and Lawal, 2004).

2.5.4 SWELLING POWER AND SOLUBILITY

Swelling power and solubility are measures of the magnitude of the interaction between starch chains within the amorphous and crystalline domains. The extent of this interaction is influenced by the amylose-to-amylopectin ratio and phosphorus content and by the characteristics of the amylose and amylopectin in terms of molecular weight/distribution, degree of branching and branch length, and conformation (Hoover, 2001; Singh and Kaur, 2004).

When an aqueous suspension of starch is heated above its gelatinization temperature, the granules will undergo irreversible swelling and the degree at which they swell is a function of the starch type and the presence of any physical or chemical modification. The swelling power of a starch paste is the measure of its hydration capacity and it is expressed as the ratio of the weight of the centrifuged swollen granules to the weight of the original dry starch used to make the paste (Lewandowicz *et al.*, 2002).

According to Lee and Osman (1991), the swelling power of starch depends on the water holding capacity of the starch molecules by hydrogen bonding. Hydrogen bonds stabilizing the structure of the double helices in crystallites are broken during gelatinization and are replaced by hydrogen bonds with water, and swelling is regulated by the crystallinity of the starch (Tester and Karkalas, 1996). However, the crystalline region of starches with a higher portion of long chain of amylopectin is stabilized due to longer double helices and may form more hydrogen bonds with water when they are heated in excess water than those starches with shorter chains of amylopectin (Sasaki and Matsuki, 1998).

deMan (1976) had stated that the swelling of starch granules can be inhibited in the presence of fatty acids, presumably, through the formation of insoluble complexes with the linear fraction, that is, amylose.

The hydrogen bonds are established between chains of starch granules by the hydroxyl groups, thus influencing both the physical resistance and solubility of the molecules. They allow the formation of quite compact masses, which have a certain degree of crystallinity, which is to say, a regular spatial structure. Alais *et al.* (1999) have stated that these bonds can be broken through heating; in this way the solubility is raised and the crystallinity reduced. However, solubilization occurs by assuming that a part of the amylose units is involved in the micelles network while the rest is free from entanglement and preferentially solubilized (Purshottam *et al.*, 1990).

The solubility of a starch, therefore, as described by Purshottam *et al.*, (1990), is expressed as the percentage by weight of the starch sample that is dissolved molecularly after heating in water between 65 and 95°C for about 30 minutes.

2.5.5 COLOUR PROFILE OF STARCH

Colour is an important quality of many foods. It is a quality attribute, which together with flavour and texture, plays a significant role in the acceptability of food (Ihekoronye and Ngoddy, 1985).

Basically, colour cannot be studied without considering the human sensory system. Accordingly, colour can be defined as a psychological interpretation of a physiological response by the eye and brain to the physical stimulus of light radiation at different wavelength. The human eye, however, is limited when it comes to high resolution of colours.

In spectrophotometric measurement of colour, three attributes are considered namely: hue, L value and chroma. Hue is the quality by which one colour is distinguished from another, as red from yellow, green, blue or purple; L value is the measure of lightness from completely opaque to completely transparent and

chroma is the measure of strength and weakness of a colour (Bakker and Arnold, 1993). Aboubakar *et al.* (2008) have characterized the colour of starch on the basis of L*, a* and b* values, where L* represents whiteness, a* redness and b* yellowness.

The color of starch due to the presence of polyphenolic compounds, ascorbic acid and carotene has impact on its quality. Any pigmentation in the starch is carried over to the final product. This reduces the quality, hence acceptability of starch product (Galvez and Resurreccion, 1992). A low value for chroma and a high value for lightness are desired for the starch to meet the consumer preference. It has been hypothesized that the variation in b* value among samples may be attributed to the amount of carbohydrate and proteins content due to their role in development of non enzymatic browning (Jamin and Flores, 1998).

2.6   RHEOLOGICAL STUDIES

The recrystallization process of starch results in 'solid' or 'solid-like' material called starch gel, which is a full three-dimensional polymer network. Hence, it is natural that the course of this structure development be monitored by rheological or mechanical testing. Rheology involves the application of large forces of shearing stresses to a starch gel or dispersion that can cause permanent structural damage or shear thinning, thus making it difficult to study the visco-elastic properties of the system. However, small deformation dynamic mechanical devices, which enable visco–elastic properties to be studied non-destructively have become increasingly popular (Karim *et al.*, 2000).

According to Launay *et al.* (1986), rheological behaviour of starch systems would depend upon:

1. the volume fraction occupied by the dispersed phase (swollen granules);
2. the viscoelastic properties of the dispersed (soluble) phase;

3. the rheological properties of the continuous phase; and

4. the interactions between dispersed and continuous phases.

2.6.1 PASTING PROPERTIES OF STARCH

The pasting behavior of starch is a function of its tendency to retrograde, which is usually studied by observing changes in viscosity during programmed heating and cooling of a starch suspension, using a variety of instruments. The Brabender Amyloviscograph has been used widely for studying starch pasting behavior (Karim *et al.*, 2000). However, the Rapid Visco Analyser (RVA) has several advantages over the viscoamylograph (Deffenbaugh and Walker, 1989; Ross *et al.*, 1987; Walker *et al.*, 1988). These include small sample sizes and ability to set temperature profiles. Results are commonly reported in Rapid Viscoanalyser Units (RVU), which are approximately equal to cP×10, but may also be reported in cP. However, use of the latter method for data reporting may give the incorrect impression that the measurement is an absolute viscosity (Zhou *et al.*, 1998). The RVA differs from the Brabender Amyloviscograph in two important features: a more rapid rate of heating and a stronger mixing action. Nevertheless, when heating rate is controlled at $1.5^{\mathrm{o}}\mathrm{Cmin}^{-1}$, the results obtained on an RVA have been observed to be similar to those on the amyloviscograph (Deffenbaugh and Walker, 1989).

Five characteristic parameters are usually measured from the pasting curve (Dengate, 1984): (i) the peak viscosity (P), which is the highest apparent viscosity obtained during pasting, i.e. programmed heating to $95^{\mathrm{o}}\mathrm{C}$ at $1.5^{\mathrm{o}}\mathrm{C}$ min^{-1}, and peak viscosity temperature (PT); (ii) the ease of cooking, indicated by the apparent viscosity at $95^{\mathrm{o}}\mathrm{C}$ in relation to the peak viscosity; (iii) the paste stability (H) or resistance to breakdown, indicated by the apparent viscosity after cooking for a period of time (20–60 min) at $95^{\mathrm{o}}\mathrm{C}$; it illustrates the stability of paste during

cooking; (iv) setback or cold paste viscosity (C), indicated by the apparent viscosity of the paste after programmed cooling to $50^{\circ}C$, and (v) stability of the cooked paste, indicated by the apparent viscosity after stirring at $50^{\circ}C$ for periods of up to 1 h (Fig. 2.9).

The setback values are indicative of the retrogradation tendency of starch. Since the initial gel network development is dominated by amylose gelation (Miles *et al.*, 1985), setback is more likely related to the retrogradation tendency of amylose (Karim *et al.*, 2000).

2.6.2 TEXTURE PROFILE ANALYSIS

Texture is an essential factor in consumers' perception of food quality and has been studies for several decades (Walter *et al.*, 2000). In a Texture Profile Analysis (TPA) test, a sample of specific dimensions is compressed uniaxially; the compressive force is then removed and the sample is re-compressed. Such a compressive sequence represents two ``bites''. During the test, compressive force is recorded as a function of the amount of compression (distance). Thus, two force against distance plots or TPA curves would be derived (Fig. 2.10).

Several parameters may be derived from the TPA curves: the maximum force (H), which occurs at the end of the first compression, equates to "hardness"; the force of the first maximum (F) is called "fracturability" (not all foods show this peak); the work done to compress the sample on the "first and second bites" is given as the area under the respective curves (A1and A2), and the ratio A2/A1is related to cohesiveness (C); the distance S is called "springiness"; and the negative area 3 is the "adhesiveness" or "stickiness". Textural characteristics such as gumminess (hardness $\times$ cohesiveness) and chewiness (hardness $\times$ cohesiveness $\times$ springiness) are derived functions.
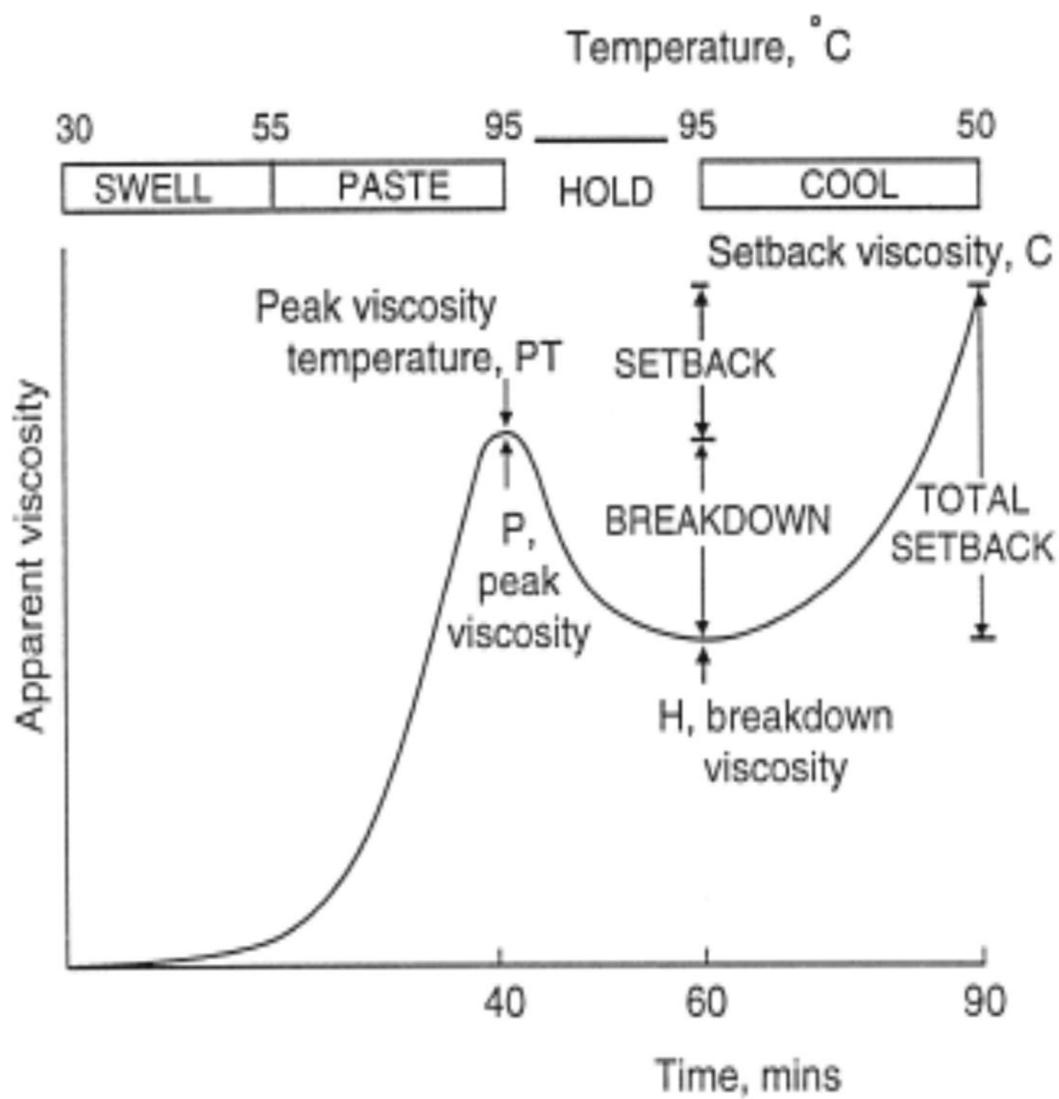
Figure 2.9: A pasting cycle curve, typical of wheat starch, showing definition of pasting parameters (Dengate, 1984)
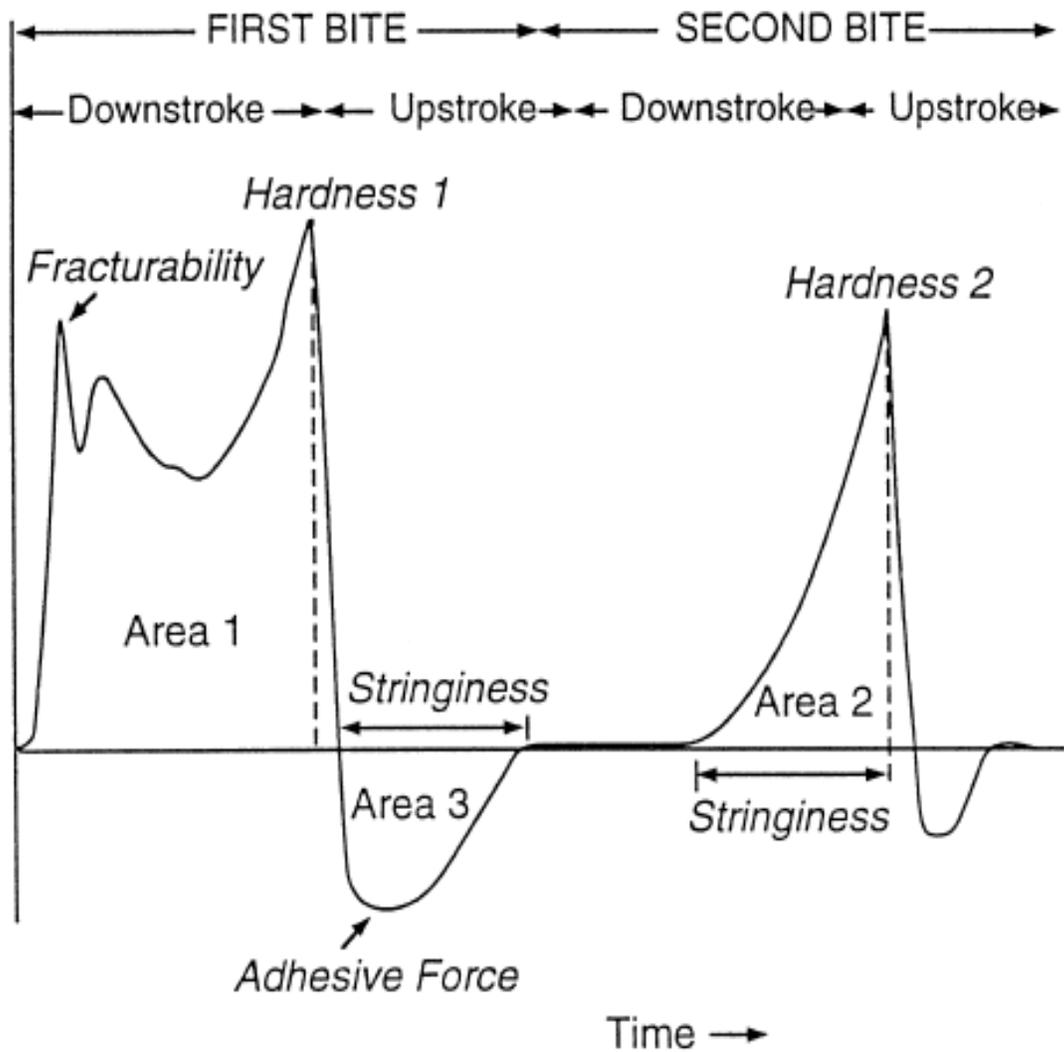
***Figure 2.10: Generalized texture profile curve obtained using the Instron
Testing Machine*** *(Bourne, 1978)*

The use of Texture Analyzer for studying the gel properties of starch has been published (Ji *et al.*, 2003; Seetharaman *et al.*, 2001). Gunaratne and Corke (2007) have studied the gel properties of root and tuber starches of true yam, gourd yam, taro, lotus and sweet potato, using a Texture Analyzer, where the maximum force peak in the TPA profile represents the gel hardness (or gel strength).

2.6.3 FLOW BEHAVIOUR OF STARCH

Flow behaviour is part of starch paste rheological study besides the viscoelastic properties. Flow behavior measurement may reveal flow behaviour of materials, which leads to improved efficiency in processing and helps formulator or end users to decide the type of starch, which is optimal for their individual needs. A study of the rheological properties of the starch pastes also enables the engineering scale up in production (Jackman, 1991), quality control as well as improvement of final products (Race, 1991). Characterizing flow behaviour of a polysaccharide such as starch enables researchers to establish a relationship between the microstructural processes and the macroscopic behaviour.

Applications of starch (such as thickeners, sizing and coating papers, sizing textile, adhesive formulations and other applications) always involve gelatinization of starch, that breaks the inter-chains hydrogen bonding so as the rheological properties of starch paste can be utilized effectively (Solorza-Feria *et al.*, 2002).

Gelatinization of starch induces a complex structural modification, leading to dramatic apparent viscosity changes. Depending upon the degree to which starch granules are swollen and the extent of solubility, a wide range of properties can be exhibited (Lee *et al.*, 2004).

The Herschel–Bulkley model is usually used to fit a flow curve of the flow behavior test to obtain parameters such as the consistency coefficients (K), flow behaviour indices (n), and yield stresses (σ_o). Starches normally exhibit non-

Newtonian behavior, that is, the viscosity decreases when shear rate increases. This behaviour is defined as shear-thinning and occurs when stress is applied to shear the paste, which causes the paste's structure to be broken down, as evidenced by n < 1.

Sanchez-Rivera *et al.* (2009) have observed that oxidized banana starch shows a decrease in n values compared to its native form. In addition, the Pearson correlation analysis for all starch data reported by Chan *et al.* (2011) revealed a significant positive correlation between yield stress and n values (corn, r = 0.844; sago, r = 0.931, and tapioca, r = 0.484, p < 0.01) at different ozone generation time (OGT). The initial stress applied to the starch paste is believed to cause the arrangement of macromolecules inside the matrix to disorganize, thereby the paste flows more freely and behaves like a Newtonian fluid (n=1). The different flow behaviours of starches might be attributed to their differences in amylose content, rate and susceptibility of amylose/amylopectin to oxidation, and the rate of oxidation of carbonyl and carboxyl groups (Chan *et al.*, 2011).

2.7 THERMAL ANALYSIS

Thermal analysis of starch has attracted attention since 1913, when Bautlin, historically, first reported on the product yields from the decomposition of rice starch that had been heated from 373 to 773 K over a period of 7 h (Tomasik *et al.*, 1989). Among the thermoanalytical methods, Differential Thermal Analysis (DTA) and Differential Scanning Calorimetry (DSC) have proven most useful in providing basic information on starch retrogradation. However, Differential Scanning Calorimetry (DSC) is widely accepted as the most suitable instrument for the evaluation of starch gelatinization (Zaidul *et al.*, 2008), and starch retrogradation, which results from the storage of the gelatinized starch. Differential scanning calorimetry (DSC) was first used for measuring gelatinization of starch

by Stevens and Elton (1971). DSC has since become an important tool for study of starch gelatinization, and numerous studies have been published (Krueger *et al.*, 1987).

In DSC, when a thermal transition occurs, the energy absorbed by the sample is replenished by increased energy input to the sample to maintain the temperature balance. Because this energy input is precisely equivalent in magnitude to the energy absorbed in the transition, a recording of this balancing energy yields a direct calorimetric measurement of the energy transition, which is then recorded as a peak. The area under the peak is directly proportional to the enthalpic change (ΔH) and its direction indicates whether the thermal event is endothermic or exothermic. In the case of retrograded starch, the value of ΔH provides a quantitative measure of the energy transformation that occurs during the melting of recrystallized amylopectin as well as precise measurements of the transition temperatures (i.e. onset, T_o; peak, T_p; and conclusion, T_c) of this endothermic event (Karim *et al.*, 2000).

Countless research works have been done on gelatinization and retrogradation profile of different starches, both their native forms and their modified derivatives. In all cases, results have shown that the transition temperatures of retrogradation were found to be lower than the gelatinization temperatures. This might be due to the fact that recrystallization of amylopectin branched chains occurred in a less ordered manner in stored gels, as it is present in native form (Sandhu and Singh, 2007; Karim *et al.*, 2000; Chen *et al.*, 2010).

At times, a single method of analysis may not supply elucidative information on the intrinsic behaviours of starches. This, therefore, necessitates further support for the role of amylopectin in starch gelatinization and retrogradation by comparing DSC results with results obtained by X-ray diffraction (Miles *et al.*, 1985). Both the X-ray and DSC data are congruous with the view that starch

gelatinization and general granule disruption in water is dependent upon starch crystallites with varied degrees of perfection (or internal order) that become disordered at temperatures that are contingent upon the amount of water available for melting (Zobel *et al.*, 1988).

2.7.1 GELATINIZATION

Gelatinization, a thermal transition (55–80°C) of hydrated starch, remains an important phenomenon for cereal and legume starches. The process causes disruption of the starch granule structure and swelling up to several times their original size. When starch granules are heated in excess water, they undergo a process called gelatinization (Ratnayake and Jackson, 2009; Sablani, 2009), which has been described as follows: when a mixture of starch granules in an excess of water is heated to temperatures above what is known as the initial gelatinization temperature, the granules swell as hydrogen bonds in amorphous regions are disrupted and water, which acts as a plasticizer, is absorbed. As the temperature increases, more hydration and more swelling occurs in amorphous regions, pulling apart crystallites, which regions also eventually undergo hydration and melt. This disruption of amorphous and crystalline structures results in an irreversible loss of crystalline, double-helical (Cooke and Gidley, 1992), lamellar, and orientational orders (Parker and Ring, 2001) and granule properties related to that order. Leaching of starch polymer molecules, especially amylose also occurs.

The loss of crystalline order involves melting of the crystallites of amylopectin and is dependent on the crystalline polymorph present, its degree of perfection, and the amount of water present (Parker and Ring, 2001). Water is the plasticizer for starch granules. In fact, amorphous regions are plasticized by water into a rubbery state even at ambient temperature (Waigh *et al.*, 2000). Loss of

order in amorphous regions is a non-equilibrium, glass transition process (Slade and Levine, 1993).

Thus, reaction kinetics pertaining to gelatinization provides definite set of process parameters (temperature, time, viscosity and mechanical strength) for a specific starch. These data could be useful for process and equipment design for a specific starch or a blend. Differential Scanning Calorimetry (DSC) has been mostly used for starch gelatinization and its quantification by measuring process enthalpy (Baik, *et al.*, 1997; Riva *et al.*, 1994; Spigno and De Faveri, 2004).

Noda *et al.* (2004) have reported that T_o and T_p of all potato starch samples ranged between 60.4 and $64.7^{o}C$ and between 63.5 and $67.7^{o}C$, respectively. In most cases, the T_o and T_p were $6–7^{o}C$ and $3–4^{o}C$ lower than the pasting temperature measured by RVA, respectively. In another study, gelatinization transition temperatures (T_o, T_p and T_c) and enthalpies of gelatinization (ΔH) of canna starch were reported to decrease with increase in the level of molar substitution (MS), especially for starch with MS at 0.11. The values of T_p of the hydroxypropyl derivative decreased by $1–9^{o}C$, compared to the native starch, showing significant comparison with those ($1–8^{o}C$) of pasting temperature determined by RVA of same starches (Chuenkamol *et al.*, 2007). Same trend have also been reported for hydroxypropylation of starches of potato (Singh *et al.*, 2004; Kim and Eliasson, 1993), rice (Seow and Thevamalar, 1993) and pea (Hoover *et al.*, 1988).

2.7.2 RETROGRADATION

Starch retrogradation, a non-equilibrium, polymer crystallization process (Slade and Levine, 1986 and 1989), has been defined as the process, which occurs when the molecular chains in gelatinized starches begin to reassociate in an ordered structure (Atwell *et al.*, 1988). In other words, storage of starch gels results

in structure transformation called recrystallization or retrogradation. During retrogradation, amylose forms double-helical associations of 40–70 glucose units (Jane and Robyt, 1984) whereas amylopectin crystallization occurs by reassociation of the outermost short branches (Ring *et al.*, 1987). Although both amylose and amylopectin are capable of retrograding, the amylopectin component appears to be more responsible for long-term quality changes in foods (Miles *et al.*, 1985; Ring *et al.*, 1987; Silverio *et al.*, 1996), depending on the storage temperature.

The first (short-term) phase of retrogradation occurs as the paste cools and involves network formation, that is, entanglements and/or junction zone formation between amylose molecules (Doublier and Choplin, 1989; Eidam *et al.*,1995; Ellis and Ring, 1985; Gidley, 1989; Silverio *et al.*, 1996), forming an elastic gel. This short-term phase may last up to 48 h. Embedded within the network are granule ghosts and remnants (Keetels *et al.*, 1996a, b; Miles *et al.*, 1985; Ellis and Ring, 1985), making the gel a filled gel, that is, a network forming the continuous phase filledwith dispersed particles (Zasypkin *et al.*, 1997). In starches that do not contain amylose, amylopectin molecules can associate to formweak gels (Cameron *et al.*, 1994; Durrani and Donald, 1995). The chain lengths affect the rate of retrogradation of amylopectin molecules, with longer chain lengths resulting in faster retrogradation rates (Kalichevsky *et al.*, 1990). Because of the reduced energy in chain segments and whole molecules, phase separation probably increases as pastes cool, resulting in increased network formation and even particles of amylose in an amylopectin matrix (Jacobson *et al.*, 1997). However, there is evidence that at least partial co-crystallization of amylose and amylopectin molecules of at least some starches can occur (Gomand *et al.*, 2010a, b; Miles *et al.*, 1985).

That the endothermic transition temperatures (T_o, T_p, andT_c) and melting enthalpies of retrograded gels are usually below the gelatinization temperatures and melting enthalpies of gelatinization (ΔH_g) suggest that retrogradation results in reassociation of the gelatinized starch molecules, but in a less ordered and hence less stable way than those existing in the native starch granules (Karim *et al.*, 2000).

2.8   FTIR SPECTROSCOPY

Infra-red spectroscopy (IR) has been suggested in the past as a suitable method for estimating the degree of substitution of various modified starches (e.g. acetyl value). Modern instruments which utilize interferometers offer the advantage of rapid acquisition of many scans, yielding a high signal to noise ratio in a short time (the Multiplex advantage). Furthermore, the spectra are obtained in digital form, and are therefore amenable to manipulation. In this regard, facile spectral subtraction, and the availability of resolution enhancement procedures such as second derivative spectra, and Fourier self-deconvolution are of major importance (Forrest and Cove, 1992).

The combined technique of Fourier Transform Infra-red (FTIR) spectroscopy with attenuated total reflectance (ATR) has been used to follow starch retrogradation (Goodfellow and Wilson, 1990; Smits *et al.*, 1998; Van Soest *et al.*, 1994a, b; Wilson *et al.*, 1987; Wilson *et al.*, 1991). Of particular interest are the peaks at 1047 cm^{-1} (characteristic of the crystalline regions of a starch system) and 1022 cm^{-1} (characteristic of amorphous starch). Retrogradation has been observed to cause an increase in the ratio of the peak intensities at 1047 and 1022 cm^{-1}, which suggests a reduction in amorphousness or an increase in organisation of the structure (Smits *et al.*, 1998).

It has also been shown that the FTIR/ATR method could provide high-quality spectra of the starch fraction of bread (Wilson and Belton, 1988) from which processes similar to those seen in starch gels could be observed. The potential of near infra-red reflectance (NIR) spectroscopy to study the disorder-order transition in the starch fraction of bread crumbs has been explored by Wilson *et al.* (1991). This is based on the assumption that since starch polymers are extensively hydrogen-bonded, both intra-molecularly and to solvent water, changes in the hydrogen bonding network of the system may be reflected in the NIR reflectance spectra.

However, previous works on hydroxypropylation of starch have not shown detailed FTIR spectra of the starches investigated. This may be due to the low molar substitution (MS) of less than 1 reported for various starches (Xu and Shei, 1997; Karim *et al.*, 2008; Lawal, 2011), which is too low for formation of new peaks, in spite of introduction of new hydroxyl groups.

2.9   MORPHOLOGY OF STARCH

In nature, starch exists in the form of granules, which can differ in size and shape. The origin of starch granules can be inferred from their size, shape, and, the hilum position (the original growing point of granule). Tuber starch granules are generally voluminous and oval shaped with an eccentric hilum. Cereal starch granules such as maize, oat, and rice have polygonal or round shapes. High amylose maize starch exhibits filamentous granules (bud-like protrusions). Legume seed starch granules are bean-like with a central elongated or starred hilum. The hilum is not always distinguishable, especially in very small granules (Pomeranz, 1985; Blanshard, 1987; Hoover, 2001).

The size of starch granules vary from 2 to 100 μm in diameter. The size of starch granules is usually expressed as a range or as an average of the length of the

longest axis. Potato starch has the largest granules among all the starches. The size of most cereal starch granules is smaller than that of tuber and legume starches.

Under polarized light in a microscope, a typical birefringence cross is observed as two intersecting band, which indicates that the starch granule has a radial orientation of crystallites or there exists a high degree of molecular order within the granule (Cui, 2005).

Various methods are used to study granule morphology. Microscopy shows the distribution of various structures in the granule and some of their details. The complementary methods of transmission electron microscopy (TEM), scanning electron microscopy (SEM), and atomic force microscopy (AFM) have been widely used. The external surface area of starch granule can be determined by the shape and size of the particle which is usually determined using optical microscopy or light scattering.

Starches isolated from corn, sorghum, millet, large granules of wheat, rye, and barley were found to have pores on their surfaces by SEM (Fanon *et al.*, 1992). However, some granules contain many pores, others a few. For some starch granules, there are no surface pores observed. The presence of pores in starch granules would result in a macroporous structure whose available surface area would be much greater than the boundary surface area (Cui, 2005).

The use of SEM in studying the morphology of native and modified starches from different sources has been numerously reported (Baker *et al.*, 2001; Baldwin *et al.*, 1997; Juszczak *et al.*, 2003a, b; Krok *et al.*, 2000; Ohtani *et al.*, 2000; Ridout *et al.*, 2002; Karim *et al.*, 2008; Lawal, 2011).

With recent trend in nanotechnology of starch, the morphology of the nanocrystals has recently been studied with Transmission Electron Microscopy (TEM) and Atomic Force Microscopy (AFM) (Angellier *et al.*, 2009; Angellier *et al.*, 2006b; Xu *et al.*, 2010). Although the use of SEM has been reported to study

the morphology of nanocrystals of starch (Song *et al.*, 2008), detailed and high quality images can be obtained with TEM or AFM. Gallant *et al.* (1997) have reported that, according to Abbe's formula, the resolution of a light microscope is at least 10 times better with SEM and 1000 times better with TEM.

CHAPTER THREE

3.0   MATERIALS AND METHODS

3.1   MATERIALS

3.1.1 SOURCES OF MATERIALS

Corms of white and red cocoyam (*Colocasia esculenta*) cultivars and tubers of white yam (*Dioscorea rotundata*) and yellow yam (*Dioscorea cayenensis*) were purchased at Uchi Market, Auchi, Nigeria. The seeds of lima bean (*Phaseolus lunatus*) and pigeon pea (*Cajanus cajan*) were purchased at Jattu Market, Edo State, Nigeria while seeds of jack beans (*Canavalia ensiformis*) were harvested from the residential orchards, both in Owo, Ondo State and Auchi, Edo State, Nigeria. All the chemicals used were analytical grades and were used directly without further purification.

3.1.2 ISOLATION OF NATIVE STARCHES FROM TUBERS

The extraction of native starches from the tubers was carried out by adopting the method described by Asiedu (1989). The general scheme used for the extraction was schematized as shown in Fig. 3.1.
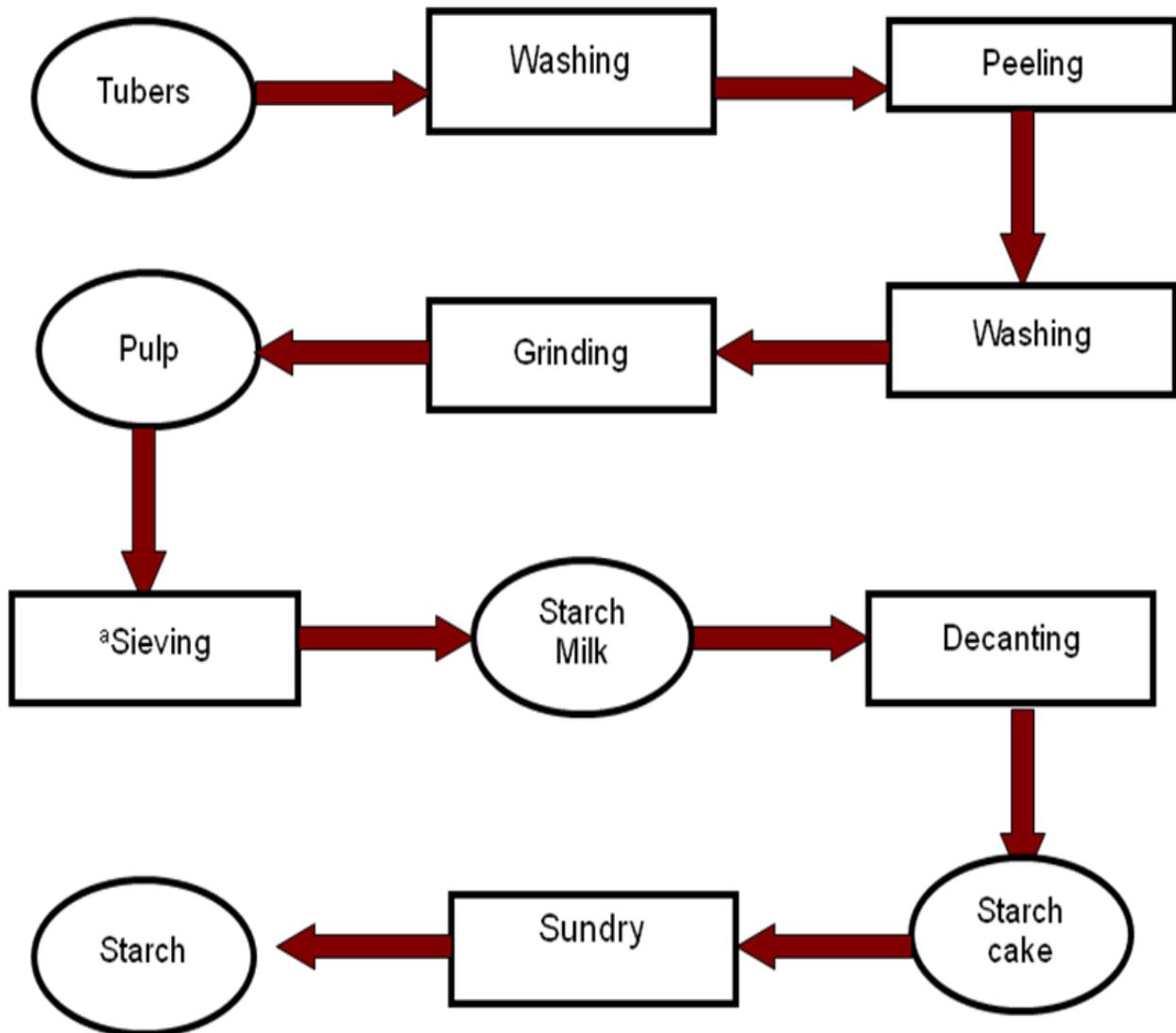
Figure 3.1: Isolation of Native Starch from Tubers

3.1.2 ISOLATION AND PURIFICATION OF LEGUME STARCHES

The extraction of starches from the legumes was carried out by adopting the method described by Galvez and Resurreccion (1992). The general scheme used for the extraction was schematized as shown in Fig. 3.2, which included cleaning the seeds, washing prior to stepping process, steeping, wet-milling and settling procedure to isolate starch from the suspension and sieving, disinfection and drying.
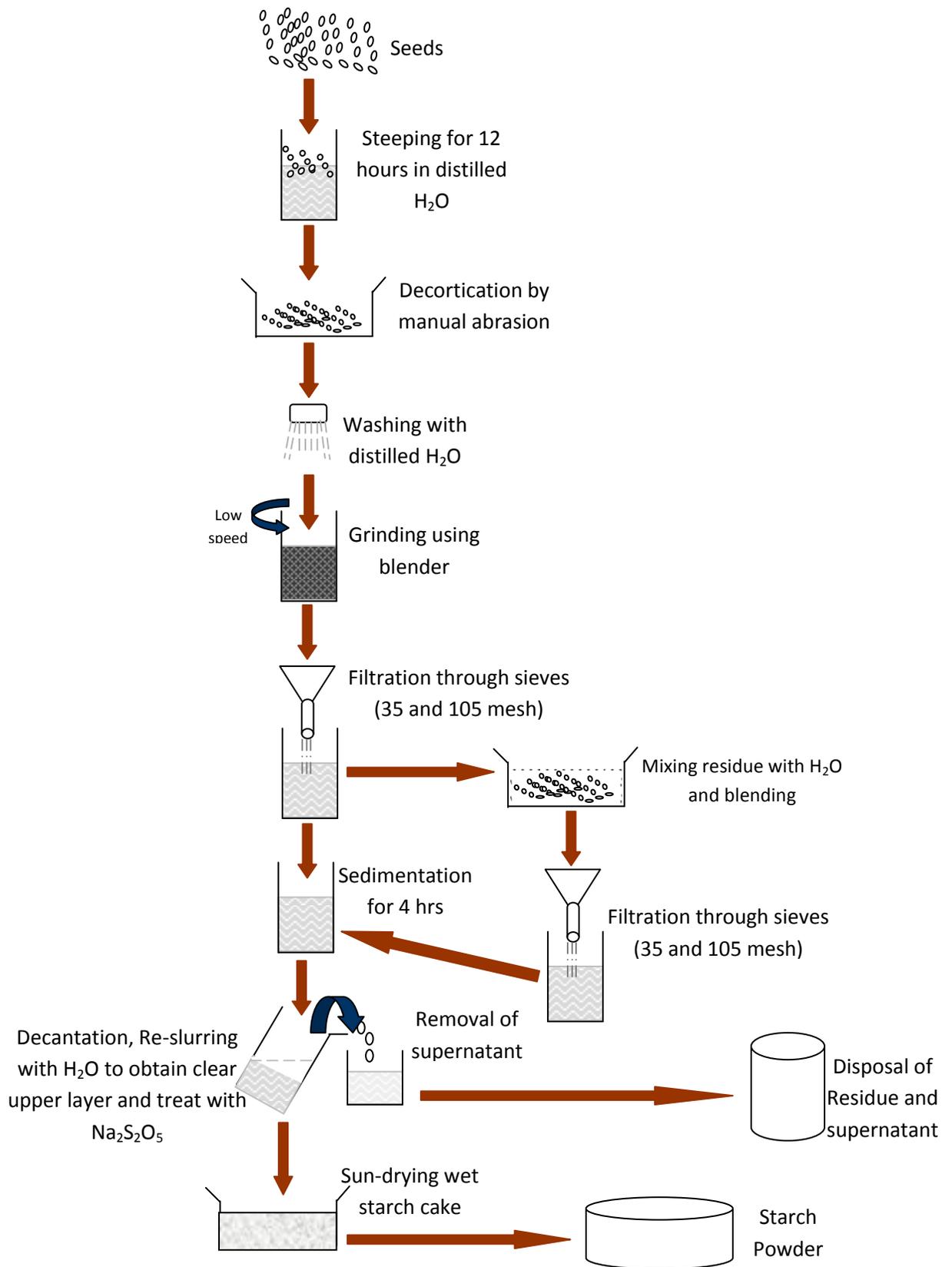
Figure 3.2: Isolation of Native Starch from Legumes

3.1.3 PREPARATION OF OZONE-OXIDIZED STARCHES

Ozone (O_3) oxidation was carried out in a rotating vessel designed for an evaporator that was connected to an ozone generator (SA-100P Ozonizer, Ishimori Seisakusho Co. Ltd., Japan) and an oxygen (O_2) cylinder (Fig. 3.3) as described by Chan *et al.* (2009). Ozone was generated by corona discharge reactor cells in which diatomic oxygen was flowed though a high-voltage electric field produced between conductive and dielectric surfaces. The reaction vessel, generator, and O_2 cylinder were connected by Teflon tubing, and all connections were firmly sealed. The flow rate of O_2 gas from the cylinder was 8 ± 0.2 mL/s, which was determined by a bubble type flow meter. This flow rate was assumed to be the rate of O_3 flow to the reaction vessel. Two potassium iodide (KI) traps were placed at the end of the reaction vessel to trap unreacted ozone.

The concentration of the KI solution was 4%, and an appropriate amount (total 1 L) was placed in each trap to react with O_3 by the following equation:

$$O_3 + 2KI + H_2O \rightarrow O_2 + I_2 + 2KOH \ \text{…………………………..3.1}$$

To perform the reaction, a starch sample (in the powder form) was placed in the reaction vessel. O_3 was generated for 5, 10 and 15 min ozone generation times (OGTs), and the reaction vessel was rotated at 150 rpm to ensure homogeneous contact between starch and O_3 during the reaction. Next, 10 min of contact time elapsed to allow the reaction (oxidation) to take place between O_3 and starch with both the gas inlet and the outlet closed. Finally, O_2 was flushed through the vessel for 20 min to flush out O_3 that did not react with the starch. When this procedure was completed, the oxidized starch was removed from the vessel.
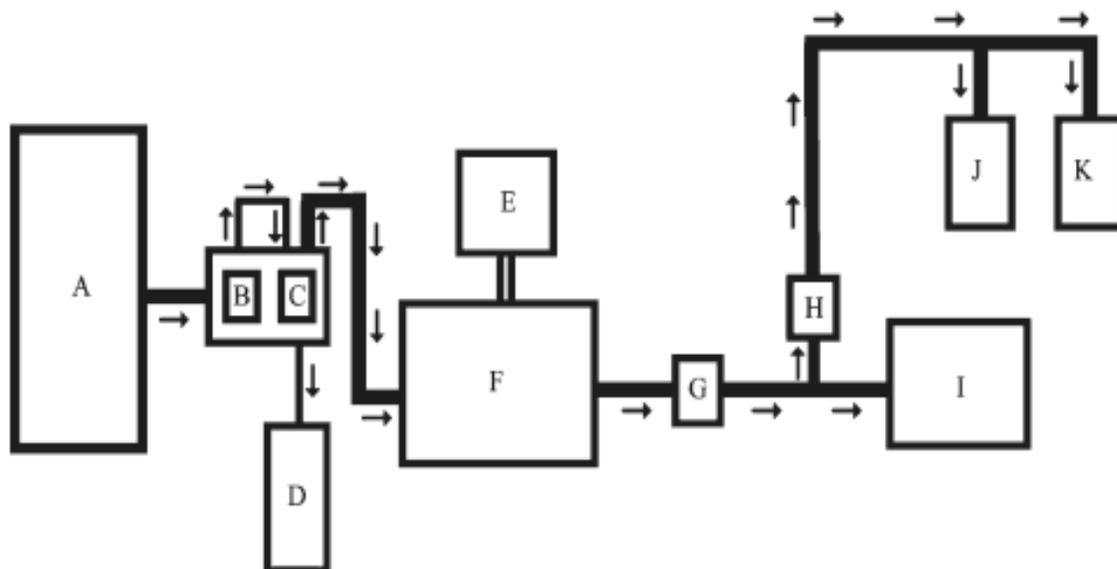
A: Oxygen cylinder
B: Flow rate controller for oxygen
C: Controller for oxygen gas
　(to bubble-type flow meter or to ozonizer)
D: Bubble-type flow meter
E: Transformer
F: Ozonizer
G: Gas inlet
H: Gas outlet
I: Rotating vessel
J & K: Potassium iodide (KI) traps

▬▬▬ Teflon tubing

▬▬ Tubing

▬▬ Wire

──▶ Gas flow

Figure 3.3: Schematic Diagram of the Setup of Ozone-Oxidation System
(Chan et al., 2009)

The amount of O_3 that did not react with the starch was determined by titration of the KI solutions in the traps. Approximately 10 mL of 2M H_2SO_4 was added to the KI solution, and the amount of I_2 released was determined by titration with a standardized 0.2 M $Na_2S_2O_3$ solution (by using starch solution as the indicator) as follows:

$$I_2 + 2Na_2S_2O_3 \rightarrow Na_2S_4O_6 + 2NaI$$……………………..3.2

Therefore, 1 mol of $Na_2S_2O_3$ consumed was equivalent to 0.5 mol of ozone. Prior to the reaction of starch with O_3, a blank test was conducted following exactly the same procedure but without starch. A calibration curve was obtained by plotting the amount of O_3 generated (A) against OGT (min). The amount of O_3 reacted with starch was calculated by subtracting the unreacted amount from the amount generated. Duplicate samples for each OGT were prepared from each starch type.

3.1.4 PREPARATION OF HYDROXYPROPYLATED STARCH

The method described by Choi and Kerr (2003) was used to prepare the hydroxypropylated starches with some slight modifications. Starch (50 g, db) was suspended in 110 ml distilled water containing 10 g Na_2SO_4 in a 250 ml screw-cap jar. The jar was screwed with cap and the slurry stirred at 150 rpm at 35°C in an orbital incubator shaker SI-600R (JEIO Tech, Seoul, Korea) for 40 mins. Then, the slurry was adjusted to pH 11 with 1.0 M NaOH. Propylene oxide (10% and 20%, db) was added and the jar was immediately capped and shaken vigorously at 150 rpm at 35°C in an orbital incubator shaker SI-600R (JEIO Tech, Seoul, Korea) for 24 hours to prevent sedimentation. After 24 hours, the starch suspension was adjusted to pH 5.5 with 1.0 M HCl. The resulting starch slurry was washed with distilled water, centrifuged about five to seven times for 15 mins at 2300 g. The

starch cake was isolated, oven-dried at 40°C for 2–3 days, mill-ground and sieved with 250 μm mesh.

3.1.5 PREPARATION OF STARCH NANOCRYSTALS

The acid hydrolysis method described by Angellier *et al.* (2005a) was adopted. 37 g of native starch granules was mixed with 250 ml of 3.16M H$_2$SO$_4$. The suspension was placed over a water-bath at a regulated temperature of 40°C for 5 days. Continuous stirring was ensured by means of homogenizer set at 100 rpm. After 5 days, the suspension was washed by centrifugation in distilled water until neutral. The aggregate was freeze-dried at 4°C with several drops of chloroform.

3.2 METHODS
3.2.1 PROXIMATE COMPOSITIONS OF STARCH SAMPLES
3.2.1.1 Determination of Moisture Content

The air-oven method was used to determine the moisture content of the starch samples. The crucibles were first washed, dried in the oven, allowed to cool in the desiccator and weighed (W$_1$). Each of the starch samples was put in the crucibles; both the crucible and the sample were weighed as W$_2$. The crucibles containing the samples were then dried in the oven at 105°C for 3 hours. The crucibles were taken out, allowed to cool in the desiccator and weighed. The process of drying, cooling and weighing was continued until constant weights (W$_3$) were obtained (AOAC, 1975),

The percentage moisture was calculated as follows:

$$\% \text{ Moisture content} = \frac{\text{Weight Lost}}{\text{Weight of Sample}} \times 100$$

$$\% \text{ Moisture content} = \frac{W_2 - W_3}{W_2 - W_1} \times 100$$

3.2.1.2 Determination of Ash Content

Each of the samples was put in a clean preweighed and dried crucibles (W_1) and they were weighed (W_2). The crucibles with the samples were then transferred into a muffle furnace at 550°C for 6 hours to burn off the organic matter until grey/white ash was obtained. The crucibles were then removed, allowed to cool in a desiccator and then weighed. The process of heating in the furnace, cooling in a desiccator and weighing was continued until a constant weight (W_3) was obtained (AOAC, 1990). The ash content was calculated thus:

$$\% \text{ Ash} = \frac{\text{Weight of Ash}}{\text{Weight of Sample}} \times 100$$

$$\% \text{ Ash} = \frac{W_3 - W_1}{W_2 - W_1} \times 100$$

3.2.1.3 Determination of Crude Protein

Microkjeldahl method was used to determine the crude protein content of the starch samples (AOAC, 1990). Two (2) grams (W_1) of the sample was measured into a Kjeldahl flask and a tablet of Kjeldahl catalyst (selenium catalyst) was added to the sample along with 25cm^3 of conc. H_2SO_4. The flask was gently placed in the digestor housed by a fume cupboard and heated until a clear solution was obtained. The clear solution was cooled, poured into a 100cm^3 volumetric flask, made up to the mark with distilled water and 10cm^3 of the resulting mixture was measured into the distillation unit. About 5cm^3 of 2% boric acid was pipetted into a 100ml conical flask with 2 drops of mixed indicator and was placed at the receiving end of the distillator. The conical flask was placed in such a way that the delivery tube was dipped completely into the boric acid inside the conical flask. 40% NaOH was added to the sample until alkaline condition was attained. As soon as the alkaline

condition was reached, the sample was distilled into the boric acid. The liberated ammonia was trapped in the boric acid solution and about $50cm^3$ of the solution was collected into the conical flask. The solution in the flask was titrated with 0.01M HCl until the first permanent colour change was observed. The same procedure was followed for the blank.

$$\% \text{ Crude Protein} = \frac{\text{Molarity of HCl} \times 0.0014 \times \text{Titre Value} \times D_f \times C_f}{\text{Weight of Sample}} \times 100$$

where, D_f = Dilution factor and C_f = Conversion factor = 6.25

3.2.1.4   Determination of Crude Fat

The fat contents of the samples were determined in a soxhlet extractor (Pearson *et al.*, 1981). Two grams of each of the samples was weighed (W_1) into a preweighed filter paper (W_2), folded neatly and the total weight noted (W_3). The filter papers, holding the samples were then inserted into the thimble and extraction was carried out with petroleum ether (b.pt. 40–60°C) for 5 hours. After the extraction, the filter papers with the samples were removed, dried in the oven at 100°C for about 30 minutes, allowed to cool in a dessicator and weighed (W_4).

$$\% \text{ Crude fat} = \frac{\text{Loss in Weight}}{\text{Weight of Sample}} \times 100$$

$$\% \text{ Crude fat} = \frac{W_3 - W_4}{W_1} \times 100$$

3.2.1.5   Determination of Crude Fibre

200ml freshly prepared 1.25% H_2SO_4 was added to 2g of the residue after fat extraction and quickly brought to boiling. Boiling and refluxing was done for 30 minutes in a fume cupboard housing the digestion apparatus. The mixture was filtered through Whatman filter paper by gravity. The beaker holding the mixture was rinsed with distilled water and the residue on the paper equally washed with

distilled water until the filtrate was free of acid. To the residue, which was transferred quantitatively into a digestion flask, 200ml freshly prepared 1.25% NaOH was added and the mixture was quickly brought to boiling. Boiling and refluxing continued for 30 minutes. The mixture was filtered using Whatman filter paper. The beaker was rinsed with distilled water and the residue equally washed with distilled water until the filtrate was free of alkali. The resulting residue was washed with methylated spirit and subsequently with petroleum ether three times each in small quantity. The solvents were allowed to drain properly and the residue was transferred into a crucible, which had been previously ignited at 600°C and cooled in a dessicator. The crucible and the residue were dried to a constant weight at 105°C (weight A). The organic matter was burnt off by igniting in muffle furnace for 6 hours at 600°C. The residue obtained was cooled in a dessicator and weighed (weight B). The loss in weight during incineration represented the weight of crude fibre in the sample (AOAC, 1990).

$$\% \text{ Crude Fibre} = \frac{\text{Weight A-Weight B}}{\text{Weight of Sample}} \times 100$$

3.2.1.6 Carbohydrate by Difference

The carbohydrate contents of the samples were determined by difference. % Carbohydrate = 100% − (Sum of the percentages of moisture content, ash, fat, crude fibre and crude protein).

3.2.2 MINERAL COMPOSITION

2 g of the sample was ignited in a muffle furnace for 6 hours at 550°C and the resulting ash was cooled in a desiccator after which 0.1M HCI solution was added to break up the ash. It was then filtered through acid washed Whatman

number 43 filter paper into 100ml volumetric flask and diluted to 100ml with the distilled water. The solution was analysed for metals using atomic absorption spectrometer with different hollow cathode lamps for calcium, sodium, potassium, iron, zinc, magnesium, mercury, lead, cadmium, copper, manganese and nickel (Pearson *et al.*, 1981). The phosphorus content for each sample was determined by pipetting $5cm^3$ of the ash solution into a $100cm^3$ volumetric flask and made up to the mark with distilled water. About $4cm^3$ of ammonium molybdate was added and shaken followed by the addition of $0.7cm^3$ of 2% tin (ii) chloride solution and shaken. The solution was analyzed for phosphorus using a colorimeter using a red filter (Ceirwyn, 1995).

3.2.3 FUNCTIONAL PROPERTIES

3.2.3.1   Colour Analysis

The method of Bakker and Arnold (1993) was adopted. A recording spectrophotometer model PU8740 was used with glass cells of 2 mm path length to obtain the absorption spectra from which L*a*b* values were calculated, using illuminant D65 and a 10° observer. The L* value was measured as the lightness from completely opaque (0) to completely transparent (100), a* was measured as the redness and b* the yellowness. Hue angle (H) was calculated from $H = \tan^{-1}$ (b*/a*) and chroma (C) from $C = [(a*)^2+(b*)^2]^{0.5}$.

3.2.3.2   Least Gelation Concentration

The modified method of Coffman and Garcia (1977) was adopted to determine the least gelation concentrations of the starch samples. 2–20% suspensions of each of the samples were prepared with distilled water. 10ml of each suspension was put in a test tube and heated for 1 hour on boiling water bath, followed by a rapid cooling in a bath of cold water. The test tubes were further

cooled at 4°C for 2 hours. The concentrations at which the gels did not fall down from the inverted test tubes were taken as the least gelation concentration of the starch samples

3.2.3.3 Water and Oil Absorption Capacities

The centrifugal method of Beuchat (1977) was used to determine the oil and water absorption capacities of the isolated bean starches and the bean flour. About one gram of sample was mixed with 10 ml distilled water/oil (Thermolyne, type 37600 mixer, Maxi mix II, Iowa, U.S.A) for 30 s. The samples were then allowed to stand at 21°C for 30 min, centrifuged at 5000 rpm for 30 min, and the volume of the supernatant noted in a 10 ml graduated cylinder. Density of distilled water was assumed to be 1 g/ml and that of oil (Gino, vegetable cooking oil, Thailand) was found to be 0.89 g/ml.

3.2.3.4 Determination of Molar Substitution and Degree of Substitution

0.1 gram of hydroxypropylated starch was weighed into a 100-ml volumetric flask and 25 ml of 0.5M tetraoxosulphate (vi) acid was added. A sample of unmodified starch of the same source was prepared in the same manner. The flasks were placed in a boiling water bath and heated until clear solutions were obtained. The resulting clear solutions were cooled and made up to 100ml with distilled water. One (1) ml of each of the solutions was pipette into 25ml graduated test tube with glass stopper. The tubes were immersed in cold water while 8 ml of concentrated tetraoxosulphate (vi) acid were added dropwisely to each tube. After thorough shaking, the tubes were placed in boiling water-bath, one after the other, for exactly three (3) minutes. Immediately, the tubes were transferred to an ice-bath until the solutions were chilled. About 0.6 ml of ninnydrin reagent (3 g/100ml ninhydrin in 5 g/100ml of $Na_2S_2O_5$) was carefully added by allowing the reagent to

run down the walls of the test tubes. Immediately, the test tubes were shaken well and placed in a water-bath for 100 minutes at 25°C. The volume of the solution in each tube was adjusted to 25 ml with concentrated tetraoxosulphate (vi) acid, followed by mixing and inverting the tubes several times. The tubes were not shaken. Immediately, portions of the solutions were transferred to 1-cm cells designed for a Beckman Model B Spectrophotometer, and after 10 minutes, the absorbance was taken at 590 nm, using the starch blank as the reference. A calibration curve was prepared with 1-ml aliquots of standard aqueous solutions containing 10, 20, 30, 40, and 50 μg of propylene glycol per ml (Joint FAO/WHO Expert committee on Food Additives (2001)).

Calculations:

$$\% \text{ Hydroxypropyl Group (\% HP)} = \frac{C \times 0.7763 \times 10 \times F}{w}$$

where, c = amount of propylene glycol in the sample read from the calibration curve, F = dilution factor (if a further dilution has been necessary) and w = weight of the sample

$$\text{Molar Substitution (MS)} = \frac{162W}{100M - (M-1)W}$$

where, W = equivalent hydroxypropyl group in 100 mg of starch and M = molecular weight of propylene glycol (C_3H_6O)

The degree of substitution, DS was estimated from the hydroxypropyl content of the starch samples, using the following equation (Wurzburg, 1986):

$$\text{Degree of Substitution, DS} = \frac{162 \times \left(\frac{\%HP}{58}\right)}{100 - \left[\frac{57}{58} \times \%HP\right]}$$

3.2.3.5   Carbonyl Content

The carbonyl content was determined by following the titrimetric method of Smith (1967) with some modifications. Four grams of starch was gelatinized in boiling water-bath for 20 min, cooled to 40°C, adjusted to pH 3.2 with 0.1 M HCl, and added to 15 ml of hydroxylamine reagent. The flask was stoppered and placed in a 40°C waterbath for 4 h with slow stirring. The excess hydroxylamine was determined by rapidly titrating the reaction mixture to pH 3.2 with standardized 0.1M HCl. A blank determination with only hydroxylamine reagent was prepared by first dissolving 25 g hydroxylamine hydrochloride in 100 ml of 0.5 M NaOH before adjusting the final volume to 500mL with distilled water. Carbonyl content was calculated as follows:

$$\text{Carbonyl Content (g/100g)} = \frac{[\text{Blank-Sample}]\text{ml}\times\text{acid Molarity}\times0.028}{\text{Weight of Sample}} \times 100$$

3.2.3.6   Carboxyl Content

The carboxyl content of oxidized starch was determined according to the modified procedure of Chattopadhyay *et al.* (1997). A starch sample (2 g) was mixed with 25 ml of 0.1M HCl, and the slurry was stirred occasionally for 30 min with a magnetic stirrer. The slurry was then vacuum filtered through a 150 ml medium porosity fritted glass funnel and washed with 400 ml of distilled water. The starch cake was then carefully transferred into a 500 ml beaker, and the volume was adjusted to 300 ml with distilled water. The starch slurry was heated in a boiling water bath with continuous stirring for 15 min to ensure complete gelatinization. The hot starch dispersion was then adjusted to 450 ml with distilled water and titrated to pH 8.3 with standardized 0.01M NaOH. A blank test was performed with unmodified starch. Carboxyl content was calculated as follows:

$$\text{Carboxyl Content (g/100g)} = \frac{[\text{Sample-Blank}] \text{ml} \times \text{ Molarity of NaOH } \times 0.045}{\text{Weight of Sample}} \times 100$$

3.2.3.7 Determination of Solubility and Swelling Power

Swelling power and solubility of the starches were determined by adopting the standard chemical method described by Leach *et al.* (1959) with some modifications. 100 mg of the starch sample was quantitatively and accurately weighed into a clean dried test tube and re-weighed as W_1. The starch sample was dispersed in 50 ml distilled water and mixed using vortex mixer. The resulting slurry was heated at 90°C for 30 mins in a water-bath. The mixture was cooled to $28 \pm 2^\circ$C and centrifuged at 2200 rpm for 15 mins to separate the gel and supernatant. The supernatant was removed and poured in a dish for solubility determination. The weight of the swollen sediment was determined (W_2). The supernatant was dried to a constant weight in an air-oven at 100°C for 4 hours.

$$\text{Swelling Power (g/g)} = \frac{W_2 - W_1}{\text{Weight of Sample}}$$

$$\text{Solubility (\%)} = \frac{\text{Dry Weight of Solubles}}{\text{Weight of Sample}} \times 100$$

3.2.4 RHEOLOGICAL PROPERTIES

3.2.4.1 Pasting Properties

The pasting profile of the starches (8% w/w, dry weight basis) was determined using the Rapid Visco Analyzer (model RVA-4, Newport Scientific Pvt. Ltd., Warriewood, Australia). The samples were equilibrated at 50°C for 1 min and then raised to 95°C in 3.75 min, held for 2.5 min, cooled to 50°C in 3.75min, and held for 5 min. The paddle speed was set at 960 rpm for the first 10 s to evenly disperse the starch slurry and reduced to 160 rpm throughout the remaining period of the experiment. The units of viscosity were expressed as rapid visco units (RVUs).

3.2.4.2 Textural Analysis

The textural behaviours of the gels were investigated, using the method described by Gunaratne and Corke (2007) with some modifications. These were determined on the starch gel made in the RVA testing using a TA-XT2 texture analyzer (Stable Micro Systems, Godalming, England). After RVA testing, the paddle was removed and the starch paste in the canister was covered by parafilm wrap and stored at 4^oC for 7 days for proper gel formation. The gel was allowed to equilibrate to room temperature and was compressed at a pre-set speed of 5 mm/s, test speed of 0.5 mm/s and post speed of 5 mm/s to a distance of 10 mm with a 6-mm cylindrical probe and trigger force of 5g. The maximum force peak (hardness) in the TPA profile represented the gel strength while other parameters such as gumminess, springiness, chewiness and cohesiveness were deduced by extrapolations from the TPA curve.

3.2.4.3 Flow Behaviour Measurement

The flow behaviours of the starches were measured using CSL^2100 Carri-Med Rheometer (AR 1000, TA Instruments Ltd) with plate-plate geometry (40 mm diameter) at a gap of 55 μm by adopting the method of Lee *et al.* (2004) with some modifications. Starch sample (5%, w/w) was weighed into a 100 ml screw-cap conical flask and topped with deionized water to a total of 30g. The mixture was heated on a hot plate while stirring with a magnetic bar at 160 rpm until the suspension turned from opaque to translucent solution. The flask was immediately transferred to a water-bath preset at 95^oC and held for 15 min. The flask was subsequently transferred to another water-bath preset at 80^oC for another 10 min for full viscosity development. The sample was held at 80^oC throughout the experiment to prevent gelatinization. Continuous shear test was carried out by monitoring the shear rate from 0 to 900 s^{-1} in 180 s and subsequently returned to

the initial rate. With this, a plot of shear stress (or viscosity) and shear rate was obtained. Torque was fixed at logarithmic ramp to minimize the inertia effect of the rheometer. Herschel–Bulkley rheological model, $\sigma = \sigma_o + K\gamma^n$, was used to express the flow behaviour parameters. Each sample was freshly prepared and all measurements were carried out at 25^oC and in triplicates.

3.2.5 DETERMINATION OF MOLAR MASS DISTRIBUTION

The standard method described by Politz *et al.* (1994) was adopted for the GPC analysis of the starch samples with some modifications. 45 mg of the starch sample were added to 5ml of dimethylacetamide (DMAC) in 10ml Reacta-Vials (Pierce, Rockford, IL) in a heating block. Thetemperature was raised to 150^oC for 1hr 15 mins. After cooling to 100^oC, dried LiCl (to 8% w/v) was added. The vials were capped, agitated by hand and heated at 100^oC for 1 hr. The temperature was then lowered to 50^oC, and the vials were stirred overnight. The next day, vials were removed and placed on a reciprocating shaker for 30 mins. The samples were then returned to the heating block and incubation (at 50^oC) continued until the samples were visually clear. The resulting solutions were quantitatively diluted to 50 ml with DMAC. Prior to injection, solutions were filtered *in vacuo* through Teflon solvent-resistant disposable filters (Millex SR, 0.5pm, Millipore) using 4 ml glass vials (WISP, Waters) in a Baker 10 extraction apparatus fitted with glass syringes ($10 \, cm^3$). The mobile-phase solvent for gel permeation chromatography (GPC) was DMAC containing 5% LiCl. The GPC system consisted of an automatic sampler (Waters WISP) with an HPLC pump (Waters Model 590), detected by multi-angle laser light scattering (MALLS) (DAWN EOS, Wyatt Technology Corp, Santa Barbara, CA) and differential refractive index (RI) (Waters Corp., Milford, MA) detectors. The RI calibration constant was measured with a series of NaCl standards. The 90°-photodiode detector of MALLS was calibrated using toluene

(HPLC grade). This system was equipped with four columns (Ultra-styragel 10^3, 10^4 and 10^5 (Baxter, Muskegon, MI) and 10^6 (Phenomenex, Torrance, CA)) connected in series and preceded by a guard column (Phenogel, linear, Phenomenex). The system was maintained at 50^oC. Standard injection volume was 40 μL and the mobile phase was pumped at a rate of 1.0 ml min^{-1}. Run times were 60 min. The software package Unical based upon ASYST (Unical, Version 3.02, Viscotek) was used for data acquisition and analysis. The system was calibrated with the polystyrene standards. Data were obtained from two dissolutions per sample with two GPC runs per dissolution.

3.2.6 AMYLOSE AND AMYLOPECTIN CONTENTS

The amylose contents of the starch samples were determined following the method described by Williams *et al.* (1970) with some modifications. 100 mg of starch sample was dispersed in 1ml of 95% ethanol and 9 ml 1M NaOH with the test tube covered with paraffin foil and vortex to ensure homogeneity. The dispersed starch solution was heated for 10 min on a boiling water–bath to gelatinize the starch followed by cooling. 1 ml of the extract was pipette and made up to 10 ml in a volumetric flask with distilled water. An aliquot of test starch solution (0.5 ml) was pipetted into the 10 ml volumetric flask and 0.1ml of 1 M acetic acid was then added, followed by the addition of 0.2 ml of iodine reagent (2g of potassium iodide and 0.2g of resublimed iodine in 100ml of distilled water). The solution was made up to 10 ml with distilled water and was left for 20 min for colour development. The solution was vortexed and test portions were transferred to 1-cm cells (cuvette) and absorbance was taken at 620 nm, using Beckman Model B Spectrophotometer. The measurement of the amylose was determined from a standard curve developed using a standard sample of known amylose

content. The value of amylopectin was deducted by estimate (% Amylopectin Content = 100% – % Amylose Content).

3.2.7 X-RAY DIFFRACTION PATTERNS

The x-ray diffraction studies were carried out using a Siemens D5000 X-ray Powder Diffractometer (20° Geometry, Madison, USA). The starch samples were equilibrated with distilled water in a dessicator for 48 h before determination to improve resolution of the X-ray diffractogram pattern. The fine samples were filled into a sample holder and packed as densely as possible. The finished surface was smoother and flushed. The samples were mounted in a X-ray diffractometer and copper Kα, 2λ (λ = 1.540 μm and 1.544 Å; 40 KV; 35 mA) was generated to determine X-ray pattern. The scan was made from a diffraction angle (2θ) of 1.5 to 60° at 0.05 step size with a count time of 3 s. From the resulting X-ray patterns, peak positions were identified using the instrument's software and these peak positions were used to determine the crystalline natures of the starch samples (Jayakody *et al.*, 2007).

Calculation:

$$\text{Crystallinity, } X_{cr}(\%) = \frac{A_{cr}}{A_{cr} + A_{am}} \times 100\%$$

where, A_{cr} and A_{am} are the integrated areas of crystalline and amorphous phases respectively.

$$\text{Cyrstallite size, } D_{(hkl)} = \frac{k\lambda}{B_{(hkl)}cos\theta}$$

where, k = Scherrer constant (0.84), λ = 0.154 nm, $B_{(hkl)}$ (FWHM – Full Width Half Maximum), and θ = corresponding Bragg's angle to FWHM.

3.2.8 THERMAL PROPERTIES

The thermal characteristics of starches were studied using a Differential Scanning Calorimeter (DSC-Q100, TA Instruments, New Castle, DE, USA). 3.0 ±0.01 mg of the starch sample was placed in a pre-weighed aluminium sample pan with the required amount of water to make slurry. A Starch slurry was prepared at 1:3 dry starch/water ratio and was immediately hermetically sealed using a DuPont encapsulation press (DuPont Co., Delaware, USA), and reweighed. The samples were allowed to stand at room temperature for minimum of 1 hour to equilibrate. The instrument was conditioned at $75^{\circ}C$ for 120 min, followed by indium check, using a standard reference pan (empty pan) and indium pan (16.6 mg) at the rate of $10^{\circ}C$/min between $30–180^{\circ}C$ for 20 min. The samples were run for thermal properties by replacing the indium pan with the sample pans at heating rate of $5^{\circ}C$/min from $20–100^{\circ}C$, using the standard reference pan (empty pan) as reference. The DSC cell was purged with nitrogen gas at a flow rate of 100 ml/min. Onset temperature (T_o), peak temperature (T_p), conclusion temperature (T_c) and enthalpy of gelatinization (ΔH_{gel}) were computed from the thermograms, using TA Instruments Universal Analysis software. The gelatinization temperature range (R) and peak height index (PHI) were calculated as ($T_c–T_o$) and $\frac{\Delta H}{(Tp–To)}$ respectively. After the DSC run, gelatinized starch samples (in the original sealed pan) were stored at $4^{\circ}C$ for 7 days for retrogradation studies. After 7 days, samples were removed and allowed to equilibrate at room temperature for 1 h before being rescanned using the DSC with the same heating programme. Likewise, Onset temperature (T_o), peak temperature (T_p), conclusion temperature (T_c) and enthalpy of retrogradation (ΔH_{ret}) were evaluated automatically and percentage of retrogradation (%R) was calculated as:

$$\%R = \frac{\text{Enthalpy of Retrogradation}}{\text{Enthalpy of Gelatinization}} \times 100$$

3.2.9 ATR-FTIR SPECTROSCOPY

A Nicolet AVATAR 360 Fourier Transform Infrared Spectrophotometer configured for attenuated total reflectance (ATR) at ambient temperature was used to obtain the infrared spectra of the starch samples. The spectra were obtained at a resolution of 4 cm^{-1} in the range 4000–500 cm^{-1}. The spectra were acquired using OMIC software.

3.2.10 MORPHOLOGICAL PROPERTIES

3.2.10.1 Scanning Electron Microscopy (SEM)

The starch samples were sprinkled onto the aluminum specimen stubs with double-sided adhesive tape while the non-sticking portion was blown off. The samples were coated with a 30 nm layer of gold using a sputter coater [Polaron (Fisons) SC 515 VG Microtech, Sussex, UK]. The coated starch samples were observed using a Scanning Electron Microscope (FESEM Leo Supra 50VP, Carl-Zeiss SMT, Oberkochen, Germany). Images were captured at different magnifications of 1000 K×, 2000 K× and 5000 K× for morphological studies.

3.2.10.2 Transmission Electron Microscopy (TEM)

The suspension of nanocrystals of starch was dispersed in ethanol (100%, v/v) and sonicated for homogeneity of the nanocrystals for 3 mins, using Sonicor (Copiague, NT). A drop of dilute nanocrystal suspension was spread on a glow-discharged copper-coated TEM grid and was allowed to dry for 3 mins. The preparation was negatively stained with 2% (w/v) uranyl acetate, and was allowed to spread for 1 min. The grid holding the stained nanocrystals was placed in a petri-dish for 15 mins to dry. The dry grid was observed using a Philips CM 12 microscope (FEI Company, Eindhoven, Netherlands) operating at 80 kV. Images were recorded on Kodak S0163 film.

3.2.11 SOLUBILITY TEST OF STARCH NANOCRYSTALS

The method described by Xu *et al.* (2010) was adopted for the determination of solubility of starch nanocrystals in organic solvents with some modifications. Five (5) organic solvents and one (1) inorganic solvent were used. The solvents used were toluene, xylene, acetic acid, trichloromethane (chloroform), ethanol and deionized water. Five (5) mg/ml concentration of the nanocrystals was prepared each with the solvents at room temperature. The resulting contents were slightly agitated and left undisturbed for about 30 mins after which the contents were observed and photographs taken. The contents were left for 24 h to investigate any change in the solubility.

3.2.12 STATISTICAL ANALYSIS

Duncan's New Multiple Range Testing was used to compare means at the 5% significance level. Simple Pearson correlation and regression analysis were conducted using SPSS 17.0 software (SPSS Inc., Chicago, IL).

4.0   RESULTS

Table 4.1: Percentage Yield of Native and Nano Starches

Starch	% Yield	
	Native	**Nanocrystals**
WCS	31.70	6.67
RCS	31.68	5.68
WYS	42.66	6.22
YYS	41.72	6.78
PPS	20.57	10.54
LBS	20.36	10.81
JBS	20.26	13.51

WCS – white cocoyam starch; RCS – red cocoyam starch; WYS – white yam starch; YYS – yellow yam starch; PPS – pigeon peas starch; LBS – lima beans starch; JBS – jack beans starch

Table 4.2: Molar Substitution and Degree of Substitution of Hydroxypropylated Starches

Starch	Level of Substitution	Amount of Propylene Glycol (μg/ml)	Hydroxypropyl Group (% HP)	Molar Substitution (MS)	Degree of Substitution (DS)
WCS	Low	10.97	0.85	0.26	0.02
	High	13.40	1.04	0.32	0.03
RCS	Low	9.67	0.75	0.23	0.02
	High	13.40	1.04	0.32	0.03
WYS	Low	9.81	0.76	0.23	0.02
	High	10.95	0.85	0.26	0.02
YYS	Low	15.05	1.17	0.37	0.03
	High	16.39	1.27	0.67	0.04
PPS	Low	11.19	0.87	0.27	0.02
	High	13.57	1.05	0.33	0.03
LBS	Low	10.99	0.85	0.26	0.02
	High	15.13	1.17	0.37	0.03
JBS	Low	10.13	0.79	0.24	0.02
	High	12.48	0.97	0.30	0.03

WCS – white cocoyam starch; RCS – red cocoyam starch; WYS – white yam starch; YYS – yellow yam starch; PPS – pigeon peas starch; LBS – lima beans starch; JBS – jack beans starch

Table 4.3: Amount of Reacted Ozone with Starch Samples (mmol)

Starch	OGT (min)		
	5	**10**	**15**
WCS	0.60 ± 0.06^{a}	1.40 ± 0.75^{ab}	1.83 ± 0.00^{b}
RCS	0.03 ± 0.00^{a}	0.13 ± 0.00^{b}	1.00 ± 0.06^{c}
WYS	0.50 ± 0.06^{a}	1.30 ± 0.06^{b}	1.53 ± 0.00^{c}
YYS	0.33 ± 0.00^{a}	0.50 ± 0.06^{a}	1.13 ± 0.20^{b}
PPS	1.13 ± 0.00^{a}	1.90 ± 0.06^{c}	1.46 ± 0.23^{b}
LBS	1.46 ± 0.06^{a}	2.10 ± 0.12^{b}	2.46 ± 0.06^{c}
JBS	0.83 ± 0.00^{a}	1.43 ± 0.00^{c}	1.25 ± 0.27^{b}

OGT – Ozone Generation Time. Results are expressed as means±standard deviations (n = 3). Values in the same row with the same superscript letters are not significantly different ($p < 0.05$)

Table 4.4: Carbonyl and Carboxyl Contents of Ozone-Oxidized Starches

Starch	OGT (min)	Carbonyl Content (%)	Carboxyl Content (%)
WCS	5	0.322 ± 0.001^a	0.201 ± 0.001^a
	10	0.538 ± 0.001^b	0.254 ± 0.001^b
	15	0.711 ± 0.002^c	0.311 ± 0.001^c
RCS	5	0.320 ± 0.001^a	0.190 ± 0.001^a
	10	0.542 ± 0.001^b	0.225 ± 0.001^b
	15	0.623 ± 0.002^c	0.430 ± 0.001^c
WYS	5	0.322 ± 0.001^a	0.182 ± 0.001^a
	10	0.546 ± 0.001^b	0.223 ± 0.001^b
	15	0.587 ± 0.001^c	0.280 ± 0.001^c
YYS	5	0.433 ± 0.002^a	0.224 ± 0.001^a
	10	0.535 ± 0.001^b	0.264 ± 0.001^b
	15	0.541 ± 0.001^c	0.270 ± 0.001^c
PPS	5	0.232 ± 0.002^a	0.151 ± 0.002^a
	10	0.422 ± 0.001^b	0.181 ± 0.001^b
	15	0.542 ± 0.001^c	0.227 ± 0.001^c
LBS	5	0.531 ± 0.002^a	0.175 ± 0.002^a
	10	0.622 ± 0.002^b	0.243 ± 0.002^b
	15	0.680 ± 0.001^c	0.252 ± 0.001^c
JBS	5	0.533 ± 0.002^a	0.167 ± 0.001^a
	10	0.663 ± 0.002^b	0.222 ± 0.001^b
	15	0.670 ± 0.002^c	0.240 ± 0.001^c

Results are expressed as means±standard deviations (n = 3). Values in the same column with the same superscript letters are not significantly different ($p < 0.05$)

Table 4.5: Proximate Composition of Unmodified Starches

Starch	Moisture Content (%)	Protein Content (%)	Crude Fat (%)	Crude Fibre (%)	Ash Content (%)	Carbohydrate By Difference (%)
WCS	10.28 ± 0.01^b	2.10 ± 0.01^c	1.02 ± 0.01^a	1.22 ± 0.01^a	1.20 ± 0.01^d	84.18 ± 0.03^f
RCS	10.76 ± 0.01^g	1.45 ± 0.01^a	1.07 ± 0.01^c	1.47 ± 0.01^c	1.13 ± 0.01^a	84.12 ± 0.02^e
WYS	10.23 ± 0.01^a	2.24 ± 0.01^d	1.06 ± 0.01^c	1.26 ± 0.01^b	1.17 ± 0.01^c	84.04 ± 0.01^d
YYS	10.45 ± 0.01^d	1.80 ± 0.01^b	1.09 ± 0.01^d	1.23 ± 0.01^a	1.15 ± 0.01^b	84.28 ± 0.02^g
PPS	10.55 ± 0.01^e	5.64 ± 0.01^e	1.04 ± 0.01^b	1.77 ± 0.01^f	1.20 ± 0.01^d	79.81 ± 0.01^c
LBS	10.35 ± 0.01^c	6.58 ± 0.01^f	1.16 ± 0.01^e	1.63 ± 0.01^e	1.26 ± 0.01^e	79.01 ± 0.03^b
JBS	10.67 ± 0.01^f	7.01 ± 0.02^g	1.04 ± 0.01^b	1.52 ± 0.01^d	1.15 ± 0.01^b	78.61 ± 0.02^a

Results are on dry weight basis. Results are expressed as means±standard deviations (n = 3). Values in the same column with the same superscript letters are not significantly different ($p < 0.05$)

Table 4.6: Mineral Compositions of Unmodified Starch Samples

Sample	Mineral (ppm)						
	Na	**Ca**	**Mg**	**K**	**P**	**Fe**	**Zn**
WCS	182.30 ± 0.14^c	36.40 ± 0.14^b	59.45 ± 0.21^c	3482.35 ± 0.21^d	2362.35 ± 0.21^c	2.15 ± 0.07^a	2.35 ± 0.07^b
RCS	163.50 ± 0.28^a	36.35 ± 0.07^b	77.70 ± 0.14^e	3262.65 ± 0.21^b	1925.40 ± 8.94^b	2.25 ± 0.07^{ab}	2.35 ± 0.07^b
WYS	201.25 ± 0.07^d	36.50 ± 0.14^b	65.65 ± 0.21^e	3582.25 ± 0.07^e	2660.35 ± 6.86^e	2.55 ± 0.07^c	2.55 ± 0.07^c
YYS	214.40 ± 0.28^e	37.45 ± 0.07^c	54.35 ± 0.07^a	3366.45 ± 0.21^c	2481.15 ± 0.07^d	2.35 ± 0.07^b	2.35 ± 0.07^b
PPS	246.00 ± 0.42^g	62.25 ± 0.07^e	60.50 ± 0.14^d	4332.70 ± 0.14^g	3331.25 ± 0.07^g	2.35 ± 0.07^b	2.25 ± 0.07^{ab}
LBS	224.65 ± 0.21^f	56.45 ± 0.21^d	55.25 ± 0.07^b	4201.05 ± 0.21^f	3221.45 ± 0.35^f	2.25 ± 0.07^{ab}	2.55 ± 0.07^c
JBS	171.25 ± 0.07^b	32.30 ± 0.14^a	85.55 ± 0.07^f	3195.35 ± 0.21^a	1793.45 ± 0.21^a	2.25 ± 0.07^{ab}	2.15 ± 0.07^a

Results are expressed as means±standard deviations (n = 3). Values in the same column with the same superscript letters are not significantly different (p < 0.05)

Continuation of Table 4.6: Mineral Compositions of Unmodified Starch Samples

Starch	Mineral (ppm)					
	Cu	**Mn**	**Pb**	**Ni**	**Cd**	**Hg**
WCS	0.35 ± 0.01^e	0.75 ± 0.01^b	ND	ND	ND	ND
RCS	0.15 ± 0.01^a	0.95 ± 0.01^d	ND	ND	ND	ND
WYS	0.30 ± 0.00^d	0.85 ± 0.01^c	ND	ND	ND	ND
YYS	0.35 ± 0.01^e	0.95 ± 0.01^d	ND	ND	ND	ND
PPS	0.20 ± 0.00^b	0.65 ± 0.01^a	ND	ND	ND	ND
LBS	0.25 ± 0.01^c	0.85 ± 0.01^c	ND	ND	ND	ND
JBS	0.25 ± 0.01^c	1.15 ± 0.01^e	ND	ND	ND	ND

ND − Not detected. Results are expressed as means±standard deviations (n = 3). Values in the same column with the same superscript letters are not significantly different ($p < 0.05$)

Table 4.7: Colour Characteristics, Least Gelation Concentration (LGC),Water Absorption Capacity (WAC) and Oil Absorption Capacity (OAC) of Unmodified Starches

Starch	Colour Characteristics			LGC (%)	WAC (%)	OAC (%)
	L^*	a^*	b^*			
WCS	70.35 ± 0.02^e	5.78 ± 0.01^b	12.43 ± 0.01^d	6.00 ± 0.00^a	92.58 ± 0.01^a	4.32 ± 0.03^c
RCS	70.45 ± 0.01^f	6.34 ± 0.01^e	12.15 ± 0.01^c	6.00 ± 0.00^a	93.36 ± 0.01^b	4.62 ± 0.01^e
WYS	70.35 ± 0.01^e	6.34 ± 0.01^e	12.06 ± 0.01^b	6.00 ± 0.00^a	95.47 ± 0.01^e	4.56 ± 0.01^d
YYS	69.17 ± 0.02^b	5.90 ± 0.12^c	12.22 ± 0.01^d	6.00 ± 0.00^a	93.65 ± 0.01^c	4.17 ± 0.01^a
PPS	69.97 ± 0.01^c	6.06 ± 0.01^d	12.05 ± 0.01^{ab}	8.00 ± 0.00^b	94.47 ± 0.01^d	4.60 ± 0.02^e
LBS	68.55 ± 0.01^a	5.64 ± 0.02^a	12.58 ± 0.02^e	8.00 ± 0.00^b	96.23 ± 0.01^e	4.20 ± 0.01^b
JBS	70.22 ± 0.01^d	6.36 ± 0.01^e	12.03 ± 0.01^a	6.00 ± 0.00^a	94.47 ± 0.01^d	4.77 ± 0.01^f

Results are expressed as means±standard deviations (n = 3). Values in the same column with the same superscript letters are not significantly different (p < 0.05)

Table 4.8: Swelling Power and Solubility of Native and Ozone-Oxidized Starches

Starch	OGT (min)	Swelling Power (g/g)	Solubility (%)
WCS	Native	12.70 ± 0.06^c	11.58 ± 0.04^a
	5	10.38 ± 0.04^a	12.76 ± 0.04^b
	10	10.77 ± 0.04^b	13.38 ± 0.08^c
	15	13.65 ± 0.04^d	13.74 ± 0.03^d
RCS	Native	12.14 ± 0.05^d	12.20 ± 0.02^a
	5	10.71 ± 0.04^b	12.73 ± 0.03^b
	10	10.83 ± 0.03^c	13.84 ± 0.08^d
	15	10.44 ± 0.04^a	13.67 ± 0.08^c
WYS	Native	13.13 ± 0.14^a	2.77 ± 0.04^a
	5	14.78 ± 0.08^d	4.27 ± 0.07^c
	10	13.78 ± 0.06^b	3.80 ± 0.11^b
	15	14.10 ± 0.07^c	4.42 ± 0.05^c
YYS	Native	13.89 ± 0.13^{bc}	2.29 ± 0.04^a
	5	12.90 ± 0.09^a	7.75 ± 0.11^d
	10	13.65 ± 0.09^{ab}	2.81 ± 0.02^b
	15	13.92 ± 0.04^c	6.33 ± 0.02^c
PPS	Native	9.58 ± 0.04^b	3.73 ± 0.05^a
	5	9.83 ± 0.04^c	5.38 ± 0.04^c
	10	9.31 ± 0.02^a	4.14 ± 0.06^b
	15	10.30 ± 0.11^d	4.25 ± 0.06^b
LSB	Native	11.59 ± 0.03^a	4.78 ± 0.02^a
	5	13.15 ± 0.05^c	5.13 ± 0.04^c
	10	12.75 ± 0.04^b	4.70 ± 0.03^a
	15	12.88 ± 0.08^b	4.93 ± 0.04^b
JBS	Native	10.69 ± 0.07^a	6.17 ± 0.07^c
	5	12.27 ± 0.07^d	5.86 ± 0.05^c
	10	12.06 ± 0.06^c	6.05 ± 0.04^b
	15	11.59 ± 0.08^b	4.44 ± 0.06^a

Results are expressed as means±standard deviations (n = 2). Values in the same column with the same superscript letters are not significantly different ($p < 0.05$)

Table 4.9: Swelling Power and Solubility of Native and Hydroxypropylated Starches

Starch	Level of Substitution	Swelling Power (g/g)	Solubility (%)
WCS	Native	12.70 ± 0.06^a	11.58 ± 0.04^a
	Low	15.05 ± 0.07^b	16.54 ± 0.12^b
	High	21.29 ± 0.10^c	21.15 ± 0.08^c
RCS	Native	12.14 ± 0.05^a	12.20 ± 0.02^a
	Low	15.54 ± 0.11^b	24.13 ± 0.07^b
	High	18.11 ± 0.06^c	25.32 ± 0.06^c
WYS	Native	13.13 ± 0.14^a	2.77 ± 0.04^a
	Low	13.61 ± 0.08^b	5.45 ± 0.04^b
	High	16.13 ± 0.06^c	9.13 ± 0.04^c
YYS	Native	13.89 ± 0.13^b	2.29 ± 0.04^b
	Low	13.85 ± 0.11^b	7.05 ± 0.06^c
	High	8.94 ± 0.08^a	1.83 ± 0.02^a
PPS	Native	9.58 ± 0.04^a	3.73 ± 0.05^a
	Low	10.59 ± 0.10^b	7.91 ± 0.04^b
	High	10.80 ± 0.06^b	11.42 ± 0.08^c
LBS	Native	11.59 ± 0.03^a	4.78 ± 0.02^a
	Low	11.69 ± 0.08^a	6.20 ± 0.07^b
	High	11.69 ± 0.15^a	11.65 ± 0.08^c
JBS	Native	10.69 ± 0.07^c	6.17 ± 0.07^b
	Low	9.80 ± 0.11^a	5.53 ± 0.04^a
	High	10.29 ± 0.04^b	12.57 ± 0.07^c

Results are expressed as means±standard deviations (n = 2). Values in the same column with the same superscript letters are not significantly different (p < 0.05)

Table 4.10: Pasting Properties of Native and Ozone-Oxidized Starch Samples

Starch	OGT (min)	Peak Viscosity (RVU)	Hot Paste Viscosity (RVU)	Breakdown (RVU)	Cold Paste Viscosity (RVU)	Setback (RVU)	Peak Time (mins)	Pasting Temperature (^{o}C)
WCS	Native	75.31 ± 3.83^b	60.56 ± 4.51^c	14.75 ± 0.74^a	95.94 ± 6.14^c	35.39 ± 1.71^d	4.49 ± 0.08^b	83.98 ± 0.03^d
	5	64.08 ± 2.13^a	49.67 ± 2.44^{ab}	14.42 ± 0.31^a	74.58 ± 2.14^b	24.92 ± 0.30^b	4.45 ± 0.01^b	83.15 ± 0.04^b
	10	66.92 ± 1.86^a	50.58 ± 1.58^b	16.33 ± 0.28^a	77.50 ± 1.70^b	26.92 ± 0.12^c	4.25 ± 0.03^a	83.25 ± 0.05^c
	15	74.17 ± 3.83^b	45.00 ± 1.34^a	29.17 ± 2.49^b	67.83 ± 1.32^a	22.83 ± 0.02^a	4.18 ± 0.02^a	82.40 ± 0.02^a
RCS	Native	58.47 ± 2.84^a	48.89 ± 3.00^c	9.59 ± 0.29^a	81.47 ± 5.51^c	32.52 ± 2.53^b	4.76 ± 0.10^b	83.51 ± 0.94^b
	5	56.67 ± 1.22^a	37.58 ± 1.13^b	19.08 ± 0.09^b	59.25 ± 1.04^b	21.67 ± 2.15^a	4.45 ± 0.03^{ab}	83.29 ± 0.04^{ab}
	10	54.58 ± 1.14^a	33.83 ± 1.22^a	20.75 ± 0.08^c	53.75 ± 1.50^a	19.92 ± 0.28^a	4.38 ± 0.08^a	82.53 ± 0.03^a
	15	56.83 ± 2.40^a	32.83 ± 1.73^a	24.00 ± 0.67^d	51.67 ± 1.77^a	18.83 ± 0.04^a	4.45 ± 0.35^{ab}	82.48 ± 0.02^a
WYS	Native	126.55 ± 2.23^c	109.00 ± 1.84^b	17.56 ± 1.18^a	161.78 ± 3.61^c	52.78 ± 2.35^d	5.87 ± 0.04^d	80.78 ± 0.03^b
	5	128.00 ± 3.15^c	108.17 ± 2.35^b	19.83 ± 0.80^b	140.08 ± 5.03^b	31.92 ± 2.68^c	5.52 ± 0.01^a	81.62 ± 0.01^c
	10	121.00 ± 3.05^b	104.50 ± 1.60^a	16.50 ± 1.45^a	132.83 ± 2.62^a	28.33 ± 1.02^b	5.72 ± 0.01^b	80.46 ± 0.03^a
	15	116.92 ± 2.13^a	101.25 ± 1.87^a	15.67 ± 0.26^a	126.58 ± 1.37^a	25.33 ± 0.50^a	5.78 ± 0.01^c	81.67 ± 0.02^d
YYS	Native	115.91 ± 0.88^d	111.08 ± 2.18^d	4.83 ± 1.51^b	159.55 ± 3.56^a	48.47 ± 1.63^c	6.16 ± 0.03^a	84.92 ± 0.03^b
	5	99.25 ± 0.80^c	97.25 ± 0.86^c	2.00 ± 0.06^a	124.50 ± 0.60^c	27.25 ± 0.26^b	6.72 ± 0.01^c	85.72 ± 0.02^c
	10	90.17 ± 0.83^a	87.75 ± 0.35^a	2.42 ± 0.48^a	113.17 ± 1.19^a	25.42 ± 0.84^a	6.52 ± 0.01^b	85.77 ± 0.03^c
	15	92.25 ± 0.50^b	90.33 ± 0.67^b	1.92 ± 0.17^a	117.17 ± 0.83^b	26.83 ± 1.50^{ab}	6.92 ± 0.01^d	84.86 ± 0.02^a
PPS	Native	45.42 ± 2.02^a	43.75 ± 1.95^a	1.67 ± 0.14^c	58.86 ± 2.87^{ab}	15.11 ± 0.93^b	6.94 ± 0.03^b	86.54 ± 0.83^a
	5	47.75 ± 0.44^c	46.92 ± 0.36^b	0.83 ± 0.08^a	58.75 ± 0.48^{ab}	11.83 ± 0.12^a	6.92 ± 0.01^b	88.14 ± 0.01^b
	10	47.33 ± 0.32^{ab}	46.08 ± 0.47^b	1.25 ± 0.15^b	57.33 ± 0.28^a	11.25 ± 0.19^a	6.85 ± 0.01^a	86.47 ± 0.30^a
	15	48.08 ± 0.36^c	47.17 ± 0.34^{bc}	0.92 ± 0.02^a	58.67 ± 0.43^b	11.50 ± 0.09^a	6.92 ± 0.02^b	86.53 ± 0.01^a
LBS	Native	84.67 ± 2.47^{ab}	63.63 ± 2.05^{ab}	21.03 ± 2.44^{ab}	74.28 ± 2.96^b	10.64 ± 0.97^b	5.01 ± 0.10^a	86.54 ± 0.75^a
	5	88.75 ± 0.44^c	64.83 ± 0.35^{bc}	23.92 ± 0.09^c	74.25 ± 0.50^b	9.42 ± 0.15^a	5.12 ± 0.01^{bc}	86.53 ± 0.02^a
	10	86.50 ± 0.62^b	64.00 ± 0.32^b	22.50 ± 0.30^{bc}	73.33 ± 0.29^{ab}	9.33 ± 0.03^a	5.05 ± 0.01^{ab}	87.38 ± 0.01^b
	15	81.50 ± 0.49^a	61.67 ± 0.26^a	19.83 ± 0.23^a	70.75 ± 0.36^a	9.08 ± 0.10^a	5.18 ± 0.01^c	87.33 ± 0.04^b
JBS	Native	32.52 ± 1.99^a	29.50 ± 1.80^a	3.03 ± 0.65^{ab}	38.92 ± 2.30^a	9.42 ± 0.82^b	5.65 ± 0.88^a	86.31 ± 1.96^b
	5	55.75 ± 0.50^c	51.67 ± 0.43^d	4.08 ± 0.06^b	62.58 ± 0.47^c	10.92 ± 0.04^c	5.45 ± 0.01^a	84.96 ± 0.02^{ab}
	10	50.17 ± 0.72^{bc}	46.67 ± 0.42^c	3.50 ± 0.30^b	56.00 ± 0.65^{bc}	9.33 ± 0.23^b	5.18 ± 0.03^a	84.15 ± 0.01^a
	15	44.58 ± 0.41^{ab}	42.00 ± 0.70^b	2.58 ± 0.30^a	50.17 ± 0.73^b	8.17 ± 0.03^a	5.92 ± 0.01^a	84.91 ± 0.01^{ab}

Results are expressed as means±standard deviations (n = 3). Values in the same column with the same superscript letters are not significantly different ($p < 0.05$)

Table 4.11: Pasting Properties of Native and Hydroxypropylated Starch Samples

Starch	Level of Substitution	Peak Viscosity (RVU)	Hot Paste Viscosity (RVU)	Breakdown (RVU)	Cold Paste Viscosity (RVU)	Setback (RVU)	Peak Time (mins)	Pasting Temperature (^oC)
WCS	Native	75.31 ± 3.83^{bc}	60.56 ± 3.00^{c}	14.75 ± 0.74^{a}	95.94 ± 6.14^{c}	35.39 ± 2.71^{c}	4.49 ± 0.08^{c}	83.98 ± 0.03^{c}
	Low	67.17 ± 2.05^{a}	41.50 ± 1.22^{b}	25.67 ± 0.91^{b}	66.92 ± 2.11^{b}	25.42 ± 1.13^{b}	3.92 ± 0.02^{b}	79.85 ± 0.01^{b}
	High	71.25 ± 2.11^{b}	36.58 ± 1.33^{a}	34.67 ± 0.77^{c}	57.42 ± 1.54^{a}	20.83 ± 0.32^{a}	3.38 ± 0.02^{a}	75.20 ± 0.01^{a}
RCS	Native	58.47 ± 2.84^{c}	48.89 ± 3.00^{c}	9.59 ± 0.29^{a}	81.47 ± 5.51^{c}	32.52 ± 2.53^{c}	4.76 ± 0.10^{c}	83.51 ± 0.94^{c}
	Low	49.75 ± 1.12^{a}	29.33 ± 0.52^{b}	20.42 ± 0.70^{b}	48.67 ± 2.13^{b}	19.33 ± 1.65^{b}	3.98 ± 0.03^{b}	78.33 ± 0.02^{b}
	High	57.33 ± 1.88^{b}	26.83 ± 1.23^{a}	30.50 ± 0.64^{c}	42.58 ± 1.90^{a}	15.75 ± 0.67^{a}	3.45 ± 0.02^{a}	73.53 ± 0.03^{a}
WYS	Native	126.55 ± 2.23^{a}	109.00 ± 1.84^{c}	17.56 ± 1.18^{a}	161.78 ± 3.61^{c}	52.78 ± 2.35^{c}	5.87 ± 0.04^{c}	80.78 ± 0.03^{c}
	Low	163.25 ± 4.24^{b}	104.44 ± 2.36^{b}	58.81 ± 1.93^{b}	149.50 ± 3.24^{b}	45.06 ± 0.87^{b}	4.05 ± 0.00^{b}	78.40 ± 0.05^{b}
	High	194.11 ± 4.65^{c}	90.59 ± 1.42^{a}	103.53 ± 3.23^{c}	118.11 ± 1.49^{a}	27.53 ± 0.09^{a}	3.40 ± 0.04^{a}	72.98 ± 0.50^{a}
YYS	Native	115.91 ± 0.88^{a}	111.08 ± 2.18^{c}	4.83 ± 1.51^{a}	159.55 ± 3.56^{b}	48.47 ± 1.63^{b}	6.16 ± 0.03^{c}	84.92 ± 0.03^{c}
	Low	151.67 ± 0.89^{b}	102.92 ± 0.67^{b}	48.75 ± 0.15^{b}	159.00 ± 1.15^{b}	56.08 ± 0.45^{c}	4.45 ± 0.02^{b}	81.50 ± 0.01^{b}
	High	178.33 ± 1.12^{c}	89.58 ± 1.04^{a}	88.75 ± 0.10^{c}	122.83 ± 1.56^{a}	33.25 ± 0.52^{a}	3.78 ± 0.02^{a}	76.00 ± 0.01^{a}
PPS	Native	45.42 ± 2.02^{a}	43.75 ± 1.95^{a}	1.67 ± 0.14^{b}	58.86 ± 2.87^{a}	15.11 ± 0.93^{a}	6.94 ± 0.03^{c}	86.54 ± 0.83^{c}
	Low	52.50 ± 1.32^{b}	51.31 ± 0.99^{c}	1.19 ± 0.49^{a}	76.33 ± 1.76^{bc}	25.03 ± 1.06^{b}	5.03 ± 0.17^{b}	82.75 ± 0.55^{b}
	High	58.22 ± 1.06^{c}	50.67 ± 0.88^{b}	7.56 ± 0.20^{c}	75.36 ± 0.84^{b}	24.70 ± 0.05^{b}	4.52 ± 0.07^{a}	79.00 ± 0.50^{a}
LBS	Native	84.67 ± 4.47^{b}	63.63 ± 2.05^{c}	21.03 ± 2.44^{a}	74.28 ± 2.96^{ab}	10.64 ± 0.97^{a}	5.01 ± 0.10^{c}	86.54 ± 0.75^{c}
	Low	105.88 ± 2.30^{c}	57.71 ± 1.47^{b}	48.17 ± 0.83^{c}	95.54 ± 2.89^{c}	37.83 ± 1.41^{c}	4.15 ± 0.04^{b}	82.35 ± 0.07^{b}
	High	78.36 ± 2.25^{a}	45.67 ± 1.34^{a}	32.69 ± 0.92^{b}	72.45 ± 2.71^{a}	26.78 ± 1.38^{b}	3.87 ± 0.04^{a}	76.24 ± 0.41^{a}
JBS	Native	32.52 ± 1.99^{a}	29.50 ± 1.80^{b}	3.03 ± 0.65^{a}	38.92 ± 2.30^{a}	9.42 ± 1.82^{a}	5.65 ± 0.88^{c}	86.31 ± 1.96^{c}
	Low	35.00 ± 0.50^{b}	30.22 ± 0.51^{c}	4.78 ± 0.13^{b}	54.36 ± 1.29^{bc}	24.14 ± 0.79^{b}	4.63 ± 0.08^{b}	82.46 ± 0.10^{b}
	High	37.80 ± 0.25^{c}	28.83 ± 0.17^{a}	8.97 ± 0.19^{c}	54.72 ± 0.67^{b}	25.89 ± 0.59^{c}	3.94 ± 0.10^{a}	74.59 ± 0.48^{a}

Results are expressed as means±standard deviations (n = 3). Values in the same column with the same superscript letters are not significantly different (p < 0.05)

Table 4.12: Textural Properties of Native and Ozone-Oxidized Starch Gels

Starch	OGT (min)	Gel Strength (N)	Springiness	Cohesiveness	Gumminess (N)	Chewiness (Nm)	Resilience
WCS	Native	8.29	0.99	0.31	1.69	1.68	0.04
	5	7.22	0.80	0.59	1.61	1.29	0.35
	10	7.36	0.98	0.37	1.12	1.10	0.05
	15	2.83	0.91	0.71	1.13	1.02	0.44
RCS	Native	5.39	1.00	0.34	2.79	2.78	0.05
	5	2.71	0.98	0.41	2.95	2.90	0.04
	10	3.00	0.99	0.32	2.32	2.30	0.03
	15	1.60	0.88	0.62	1.76	1.54	0.37
WYS	Native	6.25	0.58	0.33	2.04	1.17	0.07
	5	4.95	0.81	0.38	1.88	1.52	0.11
	10	4.20	0.52	0.35	1.48	0.76	0.09
	15	3.35	0.55	0.33	1.11	0.61	0.11
YYS	Native	2.35	0.65	0.39	0.91	0.59	0.06
	5	2.08	0.44	0.39	0.82	0.36	0.09
	10	2.29	0.43	0.39	0.90	0.39	0.09
	15	1.93	0.40	0.36	0.69	0.28	0.08
PPS	Native	5.23	0.92	0.30	1.59	1.46	0.06
	5	4.95	0.92	0.35	1.75	1.60	0.06
	10	2.83	0.82	0.62	1.75	1.44	0.36
	15	5.42	0.86	0.31	1.66	1.42	0.07
LSB	Native	5.28	0.88	0.31	1.64	1.43	0.06
	5	4.84	0.67	0.30	1.46	0.98	0.07
	10	4.84	0.64	0.33	1.58	1.01	0.07
	15	4.38	0.65	0.28	1.23	0.80	0.07
JBS	Native	3.79	0.60	0.38	1.44	0.86	0.07
	5	3.74	0.61	0.36	1.36	0.83	0.07
	10	2.98	0.78	0.56	1.66	1.30	0.34
	15	4.20	0.49	0.37	1.55	0.75	0.11

Table 4.13: Textural Properties of Native and Hydroxypropylated Starch Gels

Starch	Level of Substitution	Gel Strength (N)	Springiness	Cohesiveness	Gumminess (N)	Chewiness(Nm)	Resilience
WCS	Native	8.29	0.99	0.31	1.69	1.68	0.04
	Low	0.87	0.56	0.51	0.45	0.12	0.87
	High	0.80	0.37	1.64	1.31	0.05	0.80
RCS	Native	5.39	1.00	0.34	2.79	2.78	0.05
	Low	0.85	0.49	0.89	0.75	0.14	0.85
	High	0.82	0.57	1.15	0.94	0.29	0.82
WYS	Native	6.25	0.58	0.33	2.04	1.17	0.07
	Low	0.97	0.90	0.04	0.04	0.27	0.97
	High	0.95	0.72	0.60	0.57	0.13	0.95
YYS	Native	2.35	0.65	0.39	0.91	0.59	0.06
	Low	0.93	0.47	0.24	0.22	0.03	0.93
	High	0.89	0.61	0.44	0.39	0.16	0.89
PPS	Native	5.23	0.92	0.30	1.59	1.46	0.06
	Low	0.55	0.34	0.72	0.40	0.03	0.55
	High	0.93	0.65	0.35	0.33	0.05	0.93
LSB	Native	5.28	0.88	0.31	1.64	1.43	0.06
	Low	0.87	0.32	1.33	1.16	0.04	0.87
	High	0.88	0.75	1.28	1.13	0.36	0.88
JBS	Native	3.79	0.60	0.38	1.44	0.86	0.07
	Low	0.59	0.36	0.95	0.56	0.04	0.59
	High	0.92	0.73	0.93	0.86	0.38	0.92

Table 4.14: Herschel-Bulkley Parameters for Native and Ozone-Oxidized Starches

Starch	OGT (mins)	σ_0 (Pa)	K (Pa.s^n)	N
WCS	Native	0.71 ± 0.41^a	0.34 ± 0.09^a	0.63 ± 0.05^a
	5	15.17 ± 4.93^b	1.81 ± 0.17^c	0.60 ± 0.03^a
	10	8.98 ± 0.46^b	1.09 ± 0.01^b	0.62 ± 0.00^a
	15	11.58 ± 4.05^b	1.29 ± 0.36^b	0.60 ± 0.03^a
RCS	Native	7.27 ± 1.79^{ab}	6.46 ± 0.45^c	0.52 ± 0.02^a
	5	1.34 ± 0.15^a	1.43 ± 0.04^b	0.58 ± 0.01^b
	10	12.61 ± 5.81^b	0.86 ± 0.08^a	0.66 ± 0.01^c
	15	6.47 ± 1.13^a	0.87 ± 0.07^a	0.64 ± 0.01^c
WYS	Native	0.46 ± 0.05^a	0.10 ± 0.04^a	0.69 ± 0.03^b
	5	11.32 ± 2.35^c	1.04 ± 0.24^b	0.64 ± 0.03^b
	10	13.52 ± 1.02^c	0.97 ± 0.31^b	0.67 ± 0.03^b
	15	3.07 ± 0.68^b	0.82 ± 0.08^b	0.58 ± 0.01^a
YYS	Native	0.24 ± 0.04^a	0.06 ± 0.03^a	0.73 ± 0.00^c
	5	2.92 ± 1.12^b	0.73 ± 0.05^d	0.60 ± 0.02^a
	10	3.18 ± 0.73^b	0.52 ± 0.09^c	0.64 ± 0.01^b
	15	0.76 ± 0.27^a	0.26 ± 0.01^b	0.65 ± 0.01^b
PPS	Native	0.18 ± 0.05^a	0.02 ± 0.01^a	0.86 ± 0.02^c
	5	0.32 ± 0.08^a	0.18 ± 0.04^b	0.70 ± 0.03^b
	10	1.31 ± 0.28^b	0.54 ± 0.02^d	0.62 ± 0.02^a
	15	0.40 ± 0.06^a	0.40 ± 0.08^c	0.62 ± 0.01^a
LSB	Native	2.86 ± 0.08^{ab}	0.83 ± 0.03^b	0.62 ± 0.00^b
	5	3.79 ± 0.26^b	1.05 ± 0.02^c	0.60 ± 0.00^{ab}
	10	2.45 ± 0.37^a	0.89 ± 0.06^b	0.58 ± 0.02^a
	15	2.45 ± 0.94^a	0.61 ± 0.06^a	0.62 ± 0.01^b
JBS	Native	0.65 ± 0.13^a	0.08 ± 0.02^a	0.76 ± 0.02^c
	5	2.95 ± 0.42^b	0.16 ± 0.02^a	0.71 ± 0.01^b
	10	2.65 ± 0.20^b	0.32 ± 0.07^b	0.65 ± 0.01^a
	15	2.10 ± 0.81^b	0.33 ± 0.13^b	0.64 ± 0.01^a

Results are expressed as means±standard deviations (n = 3). Values in the same column with the same superscript letters are not significantly different ($p < 0.05$)

Table 4.15: Herschel-Bulkley Parameters for Native and Hydroxypropylated Starches

Starch	Level of Substitution	σ_0 (Pa)	K (Pa.s^n)	N
WCS	Native	0.72 ± 0.41^a	0.34 ± 0.09^a	0.63 ± 0.05^b
	Low	1.89 ± 0.30^a	1.30 ± 0.70^b	0.63 ± 0.03^b
	High	4.21 ± 1.90^b	2.15 ± 0.26^b	0.54 ± 0.01^a
RCS	Native	7.27 ± 1.79^b	2.60 ± 0.45^a	0.52 ± 0.02^a
	Low	1.51 ± 0.03^a	0.96 ± 0.25^a	0.66 ± 0.01^b
	High	0.87 ± 0.05^a	0.71 ± 0.09^a	0.67 ± 0.01^b
WYS	Native	0.46 ± 0.05^a	0.10 ± 0.04^a	0.69 ± 0.03^b
	Low	4.07 ± 0.73^c	1.69 ± 0.36^b	0.63 ± 0.01^a
	High	2.59 ± 0.11^b	1.98 ± 0.05^b	0.61 ± 0.00^a
YYS	Native	0.24 ± 0.04^a	0.06 ± 0.03^a	0.73 ± 0.00^c
	Low	6.87 ± 0.08^b	3.84 ± 0.42^b	0.55 ± 0.02^b
	High	8.93 ± 0.09^c	4.38 ± 0.28^b	0.52 ± 0.00^a
PPS	Native	0.18 ± 0.05^a	0.02 ± 0.01^a	0.86 ± 0.02^c
	Low	5.49 ± 0.77^c	1.22 ± 0.12^c	0.61 ± 0.02^a
	High	0.56 ± 0.01^b	0.13 ± 0.01^b	0.73 ± 0.00^b
LSB	Native	2.86 ± 0.08^{ab}	0.83 ± 0.03^a	0.62 ± 0.00^a
	Low	6.46 ± 6.00^a	1.97 ± 0.72^b	0.60 ± 0.02^a
	High	1.20 ± 0.05^a	1.13 ± 0.11^a	0.65 ± 0.01^b
JBS	Native	0.64 ± 0.13^a	0.08 ± 0.02^a	0.76 ± 0.02^c
	Low	9.25 ± 0.84^b	0.86 ± 0.16^b	0.65 ± 0.00^b
	High	1.89 ± 0.23^b	1.42 ± 0.12^c	0.62 ± 0.01^a

Results are expressed as means±standard deviations (n = 3). Values in the same column with the same superscript letters are not significantly different (p < 0.05)

Table 4.16: Gelatinization Profile of Native and Ozone-Oxidized Starches

Starch	OGT(mins)	T_o (°C)	T_P (°C)	T_C (°C)	ΔH_{gel} (J/g)	[a]R (°C)	PHI (J/g.°C)
WCS	Native	77.24 ± 0.11^b	79.52 ± 0.01^b	86.14 ± 0.58^a	15.19 ± 3.12^a	8.91 ± 0.69^a	6.64 ± 0.04^a
	5	76.57 ± 0.01^a	78.73 ± 0.11^a	86.16 ± 3.54^a	15.32 ± 1.90^a	9.59 ± 3.52^{ab}	7.08 ± 0.55^{ab}
	10	76.44 ± 0.00^a	78.70 ± 0.04^a	91.30 ± 1.90^a	20.34 ± 2.29^a	14.86 ± 1.90^b	9.01 ± 0.88^b
	15	78.52 ± 0.04^c	80.90 ± 0.12^c	89.02 ± 0.88^a	15.00 ± 0.95^a	10.50 ± 0.84^{ab}	6.32 ± 0.19^a
RCS	Native	75.96 ± 0.07^b	78.66 ± 0.04^b	89.20 ± 0.13^c	13.61 ± 0.66^a	13.24 ± 0.21^c	5.04 ± 0.20^a
	5	75.40 ± 0.19^a	78.24 ± 0.26^a	84.91 ± 1.81^b	14.24 ± 1.39^a	9.44 ± 1.61^b	5.59 ± 1.97^a
	10	75.38 ± 0.21^a	78.17 ± 0.08^a	84.29 ± 0.16^{ab}	13.17 ± 2.68^a	8.91 ± 0.37^{ab}	4.70 ± 0.75^a
	15	75.14 ± 0.12^a	78.13 ± 0.12^a	82.11 ± 0.23^a	14.68 ± 4.50^a	6.97 ± 0.35^a	4.87 ± 1.11^a
WYS	Native	71.23 ± 0.01^b	74.52 ± 0.06^c	84.32 ± 3.03^a	13.94 ± 1.51^{ab}	13.09 ± 3.04^a	4.23 ± 0.38^a
	5	71.04 ± 0.01^a	73.90 ± 0.03^a	80.51 ± 1.61^a	11.99 ± 0.79^{ab}	9.47 ± 1.63^a	4.19 ± 0.21^a
	10	71.07 ± 0.04^a	74.28 ± 0.00^b	83.85 ± 0.32^a	14.43 ± 0.31^b	12.78 ± 0.28^a	4.50 ± 0.04^a
	15	71.14 ± 0.06^{ab}	74.21 ± 0.01^b	79.49 ± 0.05^a	11.94 ± 0.06^a	8.35 ± 0.01^a	3.89 ± 0.07^a
YYS	Native	71.55 ± 0.54^b	74.80 ± 0.17^{bc}	81.80 ± 1.15^{ab}	10.80 ± 0.57^a	10.25 ± 1.69^a	3.34 ± 0.21^a
	5	70.63 ± 0.28^a	74.59 ± 0.01^{ab}	81.27 ± 2.03^{ab}	15.43 ± 2.11^b	10.64 ± 1.75^a	3.89 ± 0.24^b
	10	71.13 ± 0.03^{ab}	74.93 ± 0.06^c	83.29 ± 0.36^b	10.84 ± 0.11^a	12.16 ± 0.33^a	2.86 ± 0.01^a
	15	70.76 ± 0.14^{ab}	74.35 ± 0.14^a	79.70 ± 0.19^a	13.14 ± 0.04^{ab}	8.94 ± 0.50^a	3.67 ± 0.13^{ab}
PPS	Native	76.82 ± 0.32^a	81.22 ± 0.12^a	89.39 ± 0.06^a	6.29 ± 1.02^a	12.57 ± 0.38^a	1.43 ± 0.16^a
	5	76.07 ± 0.65^a	81.27 ± 0.12^a	91.28 ± 2.36^a	7.22 ± 0.62^a	15.21 ± 1.70^a	1.40 ± 0.02^a
	10	76.15 ± 0.87^a	80.99 ± 0.14^a	90.16 ± 1.32^a	7.63 ± 1.66^{ab}	14.01 ± 1.19^a	1.57 ± 0.11^{ab}
	15	75.46 ± 0.25^a	81.20 ± 0.05^a	91.07 ± 1.52^a	11.73 ± 2.31^b	15.62 ± 1.07^a	1.87 ± 0.21^b
LSB	Native	75.45 ± 0.77^{ab}	79.89 ± 0.11^b	86.41 ± 0.68^b	8.34 ± 0.47^c	10.97 ± 1.45^a	1.89 ± 0.17^b
	5	76.61 ± 0.06^b	80.05 ± 0.00^b	88.03 ± 0.04^c	3.24 ± 0.05^a	11.42 ± 0.10^a	0.94 ± 0.00^a
	10	72.59 ± 0.11^a	79.36 ± 0.06^a	84.62 ± 0.93^a	7.85 ± 0.83^c	12.03 ± 0.82^a	1.16 ± 0.13^a
	15	74.71 ± 0.69^a	79.41 ± 0.12^a	84.18 ± 0.01^a	5.29 ± 1.11^b	9.47 ± 0.68^a	1.12 ± 0.10^a
JBS	Native	77.54 ± 0.01^c	80.93 ± 0.15^b	88.99 ± 0.39^a	10.51 ± 0.71^c	11.45 ± 0.38^a	3.10 ± 0.07^c
	5	76.83 ± 0.23^b	80.66 ± 0.00^a	89.07 ± 0.09^a	9.25 ± 0.15^{ab}	12.24 ± 0.32^b	2.46 ± 0.04^b
	10	74.10 ± 0.08^a	80.73 ± 0.03^{ab}	88.93 ± 0.06^a	9.99 ± 0.06^{bc}	14.83 ± 0.14^c	1.50 ± 0.02^a
	15	77.22 ± 0.02^c	80.50 ± 0.09^a	88.88 ± 0.13^a	8.50 ± 0.06^a	11.67 ± 0.11^{ab}	2.50 ± 0.00^b

[a]R = range of temperature; Results are expressed as means±standard deviations (n = 3). Values in the same column with the same superscript lowercase letters are not significantly different ($p < 0.05$)

Table 4.17: Gelatinization Profile of Native and Hydroxypropylated Starches

Starch	Level of Substitution	T_o (^{o}C)	T_P (^{o}C)	T_C (^{o}C)	ΔH_{gel} (J/g)	R (^{o}C)	PHI (J/g.^{o}C)
WCS	Native	77.24±0.11[c]	79.52±0.01[c]	86.14±0.58[a]	15.19±3.11[a]	8.91±0.69[a]	6.64±1.04[b]
	Low	73.08±0.42[b]	77.03±0.16[b]	86.43±1.61[a]	13.30±0.87[a]	13.35±1.18[b]	3.39±0.45[a]
	High	64.98±1.56[a]	72.19±0.23[a]	83.09±2.36[a]	15.68±2.76[a]	18.11±0.81[c]	2.20±0.16[a]
RCS	Native	75.96±0.07[c]	78.60±0.04[c]	89.20±0.13[c]	13.61±0.66[a]	13.24±0.21[a]	5.04±0.20[c]
	Low	71.10±0.03[b]	75.74±0.00[b]	87.63±0.10[b]	13.49±0.16[a]	16.53±0.13[b]	2.91±0.02[b]
	High	62.64±0.09[a]	71.64±0.04[a]	84.07±0.00[a]	21.47±0.01[b]	21.44±0.09[c]	2.39±0.01[a]
WYS	Native	71.23±0.01[b]	74.52±0.06[a]	84.32±3.03[a]	13.94±1.51[a]	13.09±3.04[a]	4.23±0.37[b]
	Low	67.68±0.01[ab]	70.92±0.06[a]	85.52±1.51[a]	21.77±1.12[b]	17.84±1.50[a]	6.72±0.23[c]
	High	63.50±2.45[a]	69.71±4.24[a]	78.81±2.62[a]	12.39±2.31[a]	15.31±0.18[a]	2.03±0.21[a]
YYS	Native	71.55±0.54[c]	74.80±0.17[c]	81.80±1.15[a]	10.80±0.57[ab]	10.25±1.69[a]	3.34±0.21[b]
	Low	67.50±0.13[b]	72.20±0.23[b]	79.38±0.43[a]	9.02±0.11[a]	11.88±0.56[a]	1.92±0.07[a]
	High	60.66±0.58[a]	68.48±0.04[a]	80.02±1.46[a]	13.52±1.88[b]	19.36±2.04[b]	1.73±0.12[a]
PPS	Native	76.82±0.32[c]	81.22±0.12[c]	89.39±0.06[a]	6.29±1.02[a]	12.57±0.38[a]	1.43±0.16[b]
	Low	68.21±0.47[b]	76.64±0.42[b]	88.85±0.21[a]	10.61±0.33[b]	20.64±0.67[b]	1.26±0.04[ab]
	High	63.12±2.02[a]	72.23±0.00[a]	88.43±0.48[a]	11.12±0.33[b]	25.31±1.54[c]	1.05±0.02[a]
LSB	Native	75.45±0.77[c]	79.89±0.11[c]	86.41±0.68[b]	8.34±0.47[b]	10.97±1.45[a]	1.89±0.17[b]
	Low	66.06±0.13[b]	75.43±0.00[b]	89.23±0.21[c]	16.44±0.21[c]	23.17±0.08[b]	1.76±0.01[b]
	High	59.36±0.79[a]	69.10±0.71[a]	83.17±0.22[a]	7.17±0.23[a]	23.81±1.01[b]	0.74±0.03[a]
JBS	Native	77.54±0.01[b]	80.93±0.15[b]	88.99±0.39[a]	10.51±0.71[a]	11.45±0.38[a]	3.10±0.07[c]
	Low	72.00±3.70[b]	76.28±4.45[ab]	87.00±1.99[a]	11.16±1.77[a]	15.00±1.75[a]	2.61±0.02[b]
	High	62.22±0.20[a]	72.52±0.42[a]	86.32±2.95[a]	13.16±2.20[a]	24.10±2.75[b]	1.28±0.18[a]

[a]R = range of temperature; Results are expressed as means±standard deviations (n = 3). Values in the same column with the same superscript lowercase letters are not significantly different (p < 0.05)

Table 4.18: Retrogradation Profile of Native and Ozone-Oxidized Starches (After 7 Days)

Starch	OGT	T_o (°C)	T_P (°C)	T_C (°C)	ΔH_{ret} (J/g)	[a]R (°C)	[b]% R
WCS	Native	43.32±0.98[a]	54.67±0.11[a]	69.86±1.98[a]	8.97±1.92[a]	26.55±2.96[a]	58.99±0.50[c]
	5	43.57±1.77[a]	54.87±0.00[a]	70.29±1.08[a]	8.59±0.73[a]	26.72±0.69[a]	56.18±2.20[b]
	10	42.92±0.56[a]	54.84±0.41[a]	71.70±0.81[a]	9.83±0.27[a]	28.78±0.87[a]	48.57±4.15[a]
	15	44.68±0.88[a]	56.24±0.87[b]	71.24±1.44[a]	8.41±0.30[a]	26.56±2.32[a]	56.12±1.56[b]
RCS	Native	43.27±0.49[a]	55.86±0.54[b]	70.31±0.17[a]	8.99±0.01[a]	27.04±0.66[a]	66.13±3.13[a]
	5	42.84±1.27[a]	54.75±0.00[ab]	70.16±1.17[a]	8.12±0.69[a]	27.33±2.44[a]	57.02±0.74[a]
	10	42.11±0.93[a]	54.18±0.59[a]	68.89±2.85[a]	8.02±2.26[a]	26.78±3.78[a]	60.39±4.84[a]
	15	42.63±0.74[a]	54.77±0.00[ab]	71.24±0.12[a]	8.94±0.63[a]	28.60±0.86[a]	63.17±15.06[a]
WYS	Native	43.49±0.27[b]	56.33±0.91[a]	72.69±1.09[a]	6.98±0.54[b]	29.20±0.82[a]	50.12±1.53[b]
	5	42.79±0.12[a]	55.15±2.46[a]	74.69±0.13[ab]	5.22±0.81[a]	31.90±0.25[ab]	43.41±3.86[a]
	10	43.19±0.05[ab]	57.86±0.64[a]	76.49±0.86[ab]	9.17±0.12[c]	33.30±0.91[ab]	63.52±0.54[c]
	15	42.83±0.35[a]	57.83±1.00[a]	76.80±2.39[b]	8.87±0.28[c]	33.97±2.74[b]	74.25±1.96[d]
YYS	Native	43.09±0.04[a]	64.09±0.11[b]	86.91±0.49[b]	11.70±0.28[b]	43.82±0.54[b]	108.42±3.20[c]
	5	44.58±0.11[c]	59.26±2.61[a]	78.77±4.29[a]	7.91±1.50[a]	34.19±4.40[a]	51.04±2.79[a]
	10	43.50±0.11[ab]	56.74±0.00[a]	77.91±1.27[a]	7.87±0.54[a]	34.41±1.38[a]	72.54±4.26[b]
	15	44.17±0.55[bc]	58.54±0.00[a]	74.65±0.21[a]	8.83±0.11[a]	30.48±0.76[a]	67.16±0.59[b]
PPS	Native	43.21±0.57[ab]	56.05±1.69[a]	74.83±5.48[a]	7.54±2.02[a]	31.62±6.05[a]	118.83±12.92[b]
	5	44.06±0.30[b]	57.06±0.07[ab]	76.19±0.96[a]	7.60±0.14[a]	32.14±0.66[a]	105.57±7.14[ab]
	10	42.34±0.13[a]	59.24±0.00[b]	74.11±0.06[a]	7.65±0.32[a]	31.78±0.19[a]	102.24±18.11[ab]
	15	43.78±1.00[ab]	56.97±0.08[ab]	74.45±1.18[a]	8.69±0.06[a]	30.67±2.18[a]	75.64±15.39[a]
LSB	Native	43.01±0.64[a]	56.55±0.00[d]	71.67±0.47[a]	5.45±0.13[a]	28.66±1.10[ab]	65.35±2.04[a]
	5	43.25±0.19[ab]	56.00±0.00[c]	72.65±0.08[b]	5.75±0.06[a]	29.40±0.11[b]	177.60±0.76[c]
	10	42.35±0.28[a]	55.49±0.08[b]	76.32±0.18[c]	8.20±0.21[b]	33.98±0.46[c]	104.91±8.45[b]
	15	44.17±0.20[b]	55.01±0.00[a]	71.31±0.35[a]	6.75±0.91[a]	27.14±0.55[a]	128.74±9.65[d]
JBS	Native	44.62±0.54[b]	59.28±0.13[b]	71.53±0.37[a]	4.73±0.37[a]	26.91±0.92[a]	44.99±0.47[a]
	5	42.91±0.18[a]	57.12±0.14[ab]	72.17±0.22[a]	6.66±0.14[b]	29.26±0.04[a]	72.04±0.37[c]
	10	43.38±0.56[a]	56.07±0.52[a]	71.98±1.13[a]	6.77±0.02[b]	28.61±1.69[a]	67.76±0.22[b]
	15	43.30±0.24[a]	55.92±1.52[a]	72.03±1.20[a]	7.18±0.04[b]	28.73±0.96[a]	84.47±0.22[d]

[a]R = temperature range; [b]%R = percentage retrogradation; Results are expressed as means±standard deviations (n = 3). Values in the same column with the same superscript lowercase letters are not significantly different (p < 0.05)

Table 4.19: Retrogradation Profile of Native and Hydroxypropylated Starches (After 7 Days)

Starch	Level of Substitution	T_o (°C)	T_P (°C)	T_C (°C)	ΔH_{ret} (J/g)	[a]R (°C)	[b]% R
WCS	Native	43.32 ± 0.98^a	54.67 ± 0.11^a	69.86 ± 1.98^a	8.97 ± 1.92^b	8.97 ± 1.92^b	58.99 ± 0.50^c
	Low	42.74 ± 1.92^a	56.60 ± 2.76^a	70.95 ± 1.68^a	7.32 ± 1.01^b	7.32 ± 1.01^b	54.89 ± 4.02^b
	High	44.89 ± 1.15^a	57.66 ± 0.07^a	69.12 ± 2.91^a	2.74 ± 0.78^a	2.74 ± 0.78^a	17.27 ± 1.97^a
RCS	Native	43.27 ± 0.49^a	55.86 ± 0.54^a	70.31 ± 0.17^a	8.99 ± 0.01^c	8.99 ± 0.01^c	65.79 ± 2.64^c
	Low	42.54 ± 0.71^a	56.20 ± 1.17^a	69.44 ± 1.71^a	6.62 ± 0.57^b	6.62 ± 0.57^b	49.04 ± 3.66^b
	High	46.69 ± 0.50^b	56.99 ± 2.76^a	69.13 ± 1.06^a	2.16 ± 0.07^a	2.16 ± 0.07^a	10.06 ± 0.34^a
WYS	Native	43.49 ± 0.27^a	56.33 ± 0.91^a	72.69 ± 1.09^a	6.98 ± 0.54^b	6.98 ± 0.54^{ab}	50.12 ± 1.53^b
	Low	43.92 ± 0.56^a	62.34 ± 1.00^b	73.46 ± 0.53^{ab}	8.21 ± 1.01^c	8.21 ± 1.01^b	37.63 ± 2.70^a
	High	50.09 ± 0.62^b	64.14 ± 1.39^c	76.04 ± 0.17^b	4.68 ± 0.81^a	4.68 ± 0.81^a	37.80 ± 0.49^a
YYS	Native	43.09 ± 0.04^a	64.09 ± 0.11^a	86.91 ± 0.49^b	11.70 ± 0.28^b	11.70 ± 0.28^b	108.37 ± 3.13^b
	Low	46.92 ± 0.92^a	66.37 ± 0.01^a	84.08 ± 0.42^b	11.65 ± 0.86^b	11.65 ± 0.86^b	129.18 ± 8.05^c
	High	47.55 ± 2.57^a	64.26 ± 1.03^b	75.02 ± 1.54^a	5.43 ± 1.67^a	5.43 ± 1.67^a	39.69 ± 6.82^a
PPS	Native	43.21 ± 0.57^a	56.05 ± 1.69^a	74.83 ± 5.48^a	7.54 ± 2.02^a	7.54 ± 2.02^a	118.83 ± 12.92^c
	Low	43.14 ± 0.05^a	57.13 ± 0.00^a	75.66 ± 0.54^a	8.75 ± 0.22^a	8.75 ± 0.22^a	82.47 ± 0.52^b
	High	46.70 ± 1.20^b	63.72 ± 0.63^b	75.51 ± 1.93^a	6.53 ± 0.08^a	6.53 ± 0.08^a	58.74 ± 0.95^a
LSB	Native	43.01 ± 0.64^a	56.55 ± 0.00^a	71.67 ± 0.47^a	5.45 ± 0.13^a	5.44 ± 0.13^a	65.10 ± 2.40^b
	Low	43.53 ± 0.12^{ab}	59.48 ± 0.71^a	73.88 ± 1.56^a	6.23 ± 0.21^a	6.23 ± 0.21^a	37.89 ± 1.72^a
	High	45.09 ± 0.91^b	58.96 ± 5.23^a	72.77 ± 0.17^a	5.23 ± 1.08^a	5.22 ± 1.08^a	72.72 ± 12.75^b
JBS	Native	44.62 ± 0.54^a	59.28 ± 0.13^a	71.53 ± 0.37^a	4.73 ± 0.37^a	4.73 ± 0.37^a	44.98 ± 0.47^a
	Low	45.17 ± 0.65^a	61.00 ± 0.00^c	72.18 ± 1.41^a	4.77 ± 0.56^a	4.77 ± 0.56^a	42.84 ± 1.78^a
	High	43.76 ± 0.33^a	60.62 ± 0.13^b	72.51 ± 1.32^a	6.88 ± 1.00^a	6.88 ± 1.01^a	52.40 ± 1.12^b

[a]R = temperature range; [b]%R = percentage retrogradation; Results are expressed as means±standard deviations (n = 3). Values in the same column with the same superscript lowercase letters are not significantly different (p < 0.05)

Table 4.20: Major Peak Characteristics of Native and Selected Ozone-Oxidized Starches Analyzed with XRD[a]

Starch	OGT (min)	Peak 1				Peak 2				Peak 3			
		I	2θ	d	RI (%)	I	2θ	d	RI (%)	I	2θ	d	RI (%)
WCS	Native	307	14.95	5.95	54.00	365	16.95	5.23	64.00	327	22.10	3.95	49.00
	10	286	15.20	5.81	86.40	320	17.30	5.18	100.00	313	23.35	3.80	85.20
RCS	Native	253	15.25	5.73	54.30	304	17.30	4.90	68.50	285	22.11	3.85	64.20
	10	266	15.35	5.32	46.80	312	17.50	5.12	68.00	292	23.00	3.32	33.10
						(319)	(18.30)	(4.83)	(64.50)				
WYS	Native	184	5.80	15.15	5.90	222	15.05	5.82	72.80	327	17.40	5.04	100.00
	10	154	5.85	15.03	36.30	322	17.35	5.17	67.90	231	23.40	3.59	44.10
YYS	Native	209	5.75	15.40	52.40	246	14.25	5.91	62.40	399	17.10	5.20	100.00
	10	192	5.70	15.23	51.40	358	17.25	5.14	100.00	262	24.10	3.60	65.40
PPS	Native	258	15.25	5.87	75.50	308	17.10	5.16	94.20	237	22.80	3.85	75.80
	15	231	15.25	5.92	55.80	300	17.40	4.88	70.50	244	23.05	3.77	64.30
LBS	Native	244	15.20	5.76	82.20	303	17.20	5.15	100.00	266	22.90	3.87	87.80
	5	238	15.15	5.84	78.50	303	17.35	5.12	100.00	243	23.20	3.84	80.20
JBS	Native	271	15.25	5.80	89.50	305	17.00	5.12	100.00	260	22.75	3.91	85.20
	5	224	15.20	5.99	66.6	290	17.85	5.07	97.00	268	23.20	3.82	90.30

[a]OGT (Ozone Generation Time); I – Intensity (counts); 2θ – Bragg's angle; d – d-spacing; RI – Relative intensity; values in parentheses show additional values (intensity, Bragg's angle, d-spacing and relative intensity).

Table 4.21: Major Peak Characteristics of Native and Selected Hydroxypropylated Starches Analyzed with XRD[a]

Starch	LS	Peak 1				Peak 2				Peak 3			
		I	2θ	d	RI (%)	I	2θ	d	RI (%)	I	2θ	d	RI (%)
WCS	Native	307	14.95	5.95	54.00	365	16.95	5.23	64.00	327	22.10	3.95	49.00
	Low	235	15.30	5.79	80.40	279	18.20	4.88	94.30	273	23.20	3.83	92.20
RCS	Native	253	15.25	5.73	54.30	304	17.30	4.90	68.50	285	22.11	3.85	64.20
	Low	207	15.30	5.79	76.7	252	17.90	4.85	92.20	243	23.45	3.84	90.00
WYS	Native	184	5.80	15.15	5.90	222	15.05	5.82	72.80	327	17.40	5.04	100.00
	High	162	9.80	7.59	50.70	190	15.10	5.32	60.10	273	17.25	5.11	76.30
YYS	Native	209	5.75	15.40	52.40	246	14.25	5.91	62.40	399	17.10	5.20	100.00
	High	181	5.45	15.60	92.80	326	17.10	5.19	90.60	234	23.70	3.70	59.20
PPS	Native	258	15.25	5.87	75.50	308	17.10	5.16	94.20	237	22.80	3.85	75.80
	High	192	15.10	5.60	57.10	268	17.40	5.14	85.70	230	22.85	3.85	78.70
LBS	Native	244	15.20	5.76	82.20	303	17.20	5.15	100.00	266	22.90	3.87	87.80
	Low	232	15.20	5.80	81.00	289	17.25	5.15	100.00	240	23.05	3.97	71.60
JBS	Native	271	15.25	5.80	89.50	305	17.00	5.12	100.00	260	22.75	3.91	85.20
	High	212	14.90	5.94	68.40	250 (250)	16.85 (17.95)	5.13 (4.93)	72.80 (81.30)	232	22.65	3.86	71.50

[a]LS – Level of substitution (10% and 20% db);I – Intensity (counts); 2θ – Bragg's angle; d – d-spacing; RI – Relative intensity.

Table 4.22: Crystallinity and Crystallite Size of Native and Ozone–Oxidized Starches Analyzed with XRD[a]

Starch	OGT (min)	A_{cr} (cps.$2\theta^o$)	A_{am} (cps.$2\theta^o$)	Crystallinity, X_{cr} (%)	B(hkl) ($2\theta^o$)	θ ($2\theta^o$)	Crystallite Size, D(hkl)
WCS	Native	88.35	190.15	31.70	1.76	17.53	0.08
	10	10.57	79.66	11.71	0.38	17.13	0.36
RCS	Native	74.64	174.06	30.01	0.93	17.72	0.15
	10	9.11	72.76	11.13	0.53	18.38	0.26
WYS	Native	57.74	164.86	25.94	0.97	17.41	0.14
	10	3.60	45.90	7.27	0.18	17.42	0.75
YYS	Native	62.25	159.85	28.03	0.85	17.10	0.16
	10	7.47	65.11	10.29	0.24	17.22	0.56
PPS	Native	63.41	176.19	26.46	1.70	17.66	0.08
	15	11.18	94.82	10.55	0.31	17.32	0.44
LBS	Native	58.02	178.98	24.48	1.24	17.59	0.11
	5	2.57	62.88	3.93	0.11	17.33	1.23
JBS	Native	49.04	179.46	21.46	1.18	17.56	0.11
	5	3.33	46.05	6.74	0.25	17.95	0.54

[a]A_{cr} (integrated area of the crystalline phases); A_{am} (integrated area of the amorphous phases); $B_{(hkl)}$(FWHM – Full Width Half Maximum), θ(corresponding Bragg's angle to FWHM); $D_{(hkl)} = \dfrac{k\lambda}{B_{(hkl)}cos\theta}$

Table 4.23: Crystallinity and Crystallite Size of Native and Hydroxypropylated Starches Analyzed with XRD[a]

Starch	LS	A_{cr} (cps.$2\theta^o$)	A_{am} (cps.$2\theta^o$)	Crystallinity, X_{cr} (%)	B(hkl) ($2\theta^o$)	θ ($2\theta^o$)	Crystallite Size, D(hkl)
WCS	Native	88.35	190.15	31.70	1.76	17.49	0.08
	Low	2.09	30.74	6.37	0.15	18.16	0.91
RCS	Native	74.64	174.06	30.01	0.93	18.02	0.15
	Low	5.07	45.70	9.99	0.29	18.17	0.47
WYS	Native	57.74	164.86	25.94	0.97	17.41	0.14
	High	4.34	48.58	8.20	0.30	17.35	0.45
YYS	Native	62.25	159.85	28.03	0.85	17.10	0.16
	High	9.64	51.74	15.71	0.39	17.03	0.35
PPS	Native	63.41	176.19	26.46	1.70	17.63	0.08
	High	5.62	63.27	8.16	0.29	17.28	0.47
LBS	Native	58.02	178.98	24.48	1.24	17.49	0.11
	Low	0.19	43.02	0.44	0.09	17.22	1.50
JBS	Native	49.04	179.46	21.46	1.18	17.38	0.11
	High	5.33	57.90	8.43	0.48	17.93	0.28

[a]A_{cr} (integrated area of the crystalline phases); A_{am} (integrated area of the amorphous phases); $B_{(hkl)}$(FWHM – Full Width Half Maximum), θ(corresponding Bragg's angle to FWHM); $D_{(hkl)} = \dfrac{k\lambda}{B_{(hkl)}cos\theta}$

Table 4.24: Molecular Mass Distribution of Native and Selected Ozone-Oxidized Starches[a, b]

Starch	OGT (min)	Amylose Content (%)	Amylopectin Content (%)	M_w $\times 10^6$	M_n $\times 10^6$	DP_w $\times 10^4$	DP_n $\times 10^3$	Polydispersity Ratio ($\frac{M_w}{M_n}$)
WCS	Native	19.62±0.05	80.39±0.05	3.29±0.01	1.07±0.01	2.03±0.01	6.60±0.01	3.08±0.01
	10	25.63±0.05	74.38±0.05	5.88±0.01	0.56±0.01	3.63±0.01	3.46±0.01	10.59±0.15
RCS	Native	20.75±0.05	79.26±0.05	3.59±0.01	1.10±0.01	2.22±0.01	6.79±0.01	3.27±0.01
	10	24.71±0.05	75.30±0.05	6.09±0.01	0.59±0.01	3.76±0.01	3.64±0.01	10.42±0.15
WYS	Native	19.73±0.10	80.28±0.10	3.63±0.01	1.06±0.01	2.24±0.01	6.54±0.01	3.44±0.03
	10	25.62±0.05	74.38±0.05	5.95±0.01	0.52±0.01	3.67±0.01	3.21±0.01	11.56±0.13
YYS	Native	20.05±0.05	79.96±0.05	3.18±0.01	1.10±0.01	1.96±0.01	6.79±0.01	2.91±0.04
	10	25.52±0.10	74.48±0.10	5.70±0.01	0.54±0.01	3.52±0.01	3.33±0.01	10.66±0.16
PPS	Native	20.33±0.05	79.68±0.05	3.14±0.01	1.06±0.01	1.94±0.01	6.54±0.01	2.97±0.03
	15	25.87±0.10	74.13±0.10	6.16±0.01	0.58±0.01	3.80±0.01	3.58±0.01	10.72±0.11
LBS	Native	19.44±0.10	80.56±0.10	3.06±0.01	1.03±0.01	1.89±0.01	6.36±0.01	2.97±0.05
	5	24.96±0.11	75.05±0.11	3.44±0.01	1.05±0.01	2.12±0.01	6.48±0.01	3.28±0.06
JBS	Native	20.29±0.20	79.71±0.20	3.43±0.01	1.08±0.01	2.11±0.01	6.67±0.01	3.19±0.03
	5	23.93±0.06	76.07±0.06	3.57±0.01	1.06±0.01	2.20±0.01	6.54±0.01	3.39±0.01

[a]M_w= weight average; M_n= number average; DP_w = weight average degree of polymerization (calculated by dividing M_w by 162 i.e. the molecular weight of anhydrous glucose); DP_n = number average degree of polymerization (calculated by dividing M_w by 162 i.e. the molecular weight of anhydrous glucose); [b]Results are expressed as means±standard deviations (n = 2).

Table 4.25: Chain Length Distribution of Amylopectin (%) of Native and Selected Ozone-Oxidized Starches

Starch	OGT (min)	Chain Length Distribution (%)			
		A (DP 6–12)	B1 (DP 13–24)	B2 (DP 25–36)	B3[†] (DP ≥37)
WCS	Native	25.50±0.71	31.50±0.71	24.50±0.71	18.50±0.71
	10	22.50±2.12	32.50±0.71	25.50±0.71	19.50±0.71
RCS	Native	26.00±0.00	31.50±0.71	24.50±0.71	18.00±0.00
	10	23.50±0.71	34.00±0.00	25.50±0.71	17.00±0.00
WYS	Native	25.50±0.71	33.50±0.71	25.50±0.71	15.50±0.71
	10	21.50±0.71	31.50±0.71	26.00±1.41	21.00±0.71
YYS	Native	27.50±0.71	32.50±0.71	25.50±0.71	14.50±0.00
	10	24.00±1.41	33.00±1.41	23.50±0.71	19.50±0.71
PPS	Native	27.50±0.71	31.50±0.71	25.50±0.71	15.50±0.71
	15	21.50±0.71	34.50±0.71	24.00±1.41	20.00±1.41
LBS	Native	25.50±0.71	34.50±0.71	24.50±0.71	15.50±0.71
	5	23.00±1.41	35.50±0.71	25.00±1.41	16.50±0.71
JBS	Native	25.50±0.71	33.50±0.71	25.50±0.71	15.50±0.71
	5	23.00±1.41	35.50±0.71	25.00±1.41	16.50±0.71

Results are expressed as means±standard deviations (n = 2).

Table 4.26: Molecular Weights of Native and Selected Hydroxypropylated Starches[a, b]

Starch	Level of substitution	Amylose Content (%)	Amylopectin Content (%)	M_w $\times 10^6$	M_n $\times 10^6$	DP_w $\times 10^4$	DP_n $\times 10^3$	Polydispersity Ratio ($\frac{M_w}{M_n}$)
WCS	Native	19.62±0.05	80.38±0.05	3.29±0.01	1.07±0.01	2.03±0.01	6.60±0.01	3.08±0.01
	Low	23.54±0.10	76.46±0.10	3.63±0.01	1.03±0.01	2.24±0.01	6.36±0.01	3.54±0.02
RCS	Native	20.75±0.05	79.25±0.05	3.59±0.01	1.10±0.01	2.22±0.01	6.79±0.01	3.27±0.01
	Low	23.68±0.20	76.32±0.20	6.54±0.01	2.22±0.02	4.37±0.01	13.70±0.02	2.96±0.04
WYS	Native	19.72±0.10	80.28±0.10	3.63±0.01	1.06±0.01	2.24±0.01	6.54±0.01	3.44±0.03
	High	24.50±0.15	75.50±0.15	6.44±0.01	0.57±0.01	3.98±0.01	3.52±0.01	11.40±0.17
YYS	Native	20.04±0.05	79.96±0.05	3.18±0.01	1.10±0.01	1.96±0.01	6.79±0.01	2.91±0.04
	High	25.13±0.05	74.87±0.05	5.86±0.01	0.64±0.01	3.62±0.01	3.95±0.01	9.23±0.09
PPS	Native	20.32±0.05	79.68±0.05	3.14±0.01	1.06±0.01	1.94±0.01	6.54±0.01	2.97±0.03
	High	25.42±0.05	74.58±0.05	6.24±0.01	0.58±0.01	3.85±0.01	3.58±0.01	10.86±0.11
LBS	Native	19.44±0.10	80.56±0.10	3.06±0.01	1.03±0.01	1.89±0.01	6.36±0.01	2.97±0.05
	Low	23.22±0.05	76.78±0.05	3.57±0.03	1.12±0.01	2.20±0.01	6.91±0.01	3.21±0.01
JBS	Native	20.29±0.20	79.71±0.20	3.43±0.01	1.08±0.01	2.11±0.01	6.67±0.01	3.19±0.03
	High	24.74±0.10	75.26±0.10	6.36±0.01	0.61±0.01	3.93±0.01	3.77±0.01	10.43±0.37

[a]M_w= weight average; M_n= number average; DP_w = weight average degree of polymerization (calculated by dividing M_w by 162 i.e. the molecular weight of anhydrous glucose); DP_n = number average degree of polymerization (calculated by dividing M_w by 162 i.e. the molecular weight of anhydrous glucose); [b]Results are expressed as means±standard deviations (n = 2).

Table 4.27: Chain Length Distribution of Amylopectin (%) of Native and Selected Hydroxypropylated Starches

Sample	Level of Substitution	Molecular Weight			
		A (DP 6–12)	B1 (DP 13–24)	B2 (DP 25–36)	B3[†] (DP ≥37)
WCS	Native	25.50±0.71	31.50±0.71	24.50±0.71	18.50±0.71
	Low	21.50±0.71	36.00±1.41	23.50±0.71	19.00±0.00
RCS	Native	26.00±1.41	31.50±0.71	24.50±0.71	18.00±1.41
	Low	17.50±0.71	34.00±1.41	24.50±0.71	24.00±1.41
WYS	Native	25.50±0.71	33.50±0.71	25.50±0.71	15.50±0.71
	High	22.50±0.71	35.00±1.41	25.50±0.71	17.00±1.41
YYS	Native	27.50±0.71	32.50±0.71	25.50±0.71	14.50±1.41
	High	22.50±0.71	34.50±0.71	25.50±0.71	17.50±1.41
PPS	Native	27.50±0.71	31.50±0.71	25.50±0.71	15.50±0.71
	High	21.00±1.41	33.50±0.71	26.50±0.71	19.00±1.41
LBS	Native	25.50±0.71	34.50±0.71	24.50±0.71	15.50±0.00
	Low	22.50±2.12	35.50±0.71	24.50±0.71	17.50±0.00
JBS	Native	25.50±0.71	33.50±0.71	25.50±0.71	15.50±0.00
	High	21.50±0.71	35.50±0.71	25.50±0.71	17.50±0.00

Results are expressed as means±standard deviations (n = 2). Values in the same column with the same superscript letters are not significantly different (p < 0.05).

Table 4.28: Solubility Test of Nanocrystals of Starches

Starch	Solvent					
	Toluene	**Xylene**	**Chloroform**	**Acetic Acid**	**Ethanol**	**De-ionized Water**
WCS	Insoluble	Insoluble	Precipitate formed	Insoluble	Insoluble	Insoluble
RCS	Insoluble	Insoluble	Precipitate formed	Insoluble	Insoluble	Insoluble
WYS	Insoluble	Insoluble	Precipitate formed	Insoluble	Insoluble	Insoluble
YYS	Insoluble	Insoluble	Precipitate formed	Insoluble	Insoluble	Insoluble
PPS	Insoluble	Insoluble	Precipitate formed	Insoluble	Insoluble	Suspension Formed
LBS	Insoluble	Insoluble	Precipitate formed	Sparingly soluble	Sparingly soluble	Sparingly Soluble
JBS	Insoluble	Insoluble	Precipitate formed	Insoluble	Insoluble	Suspension Formed
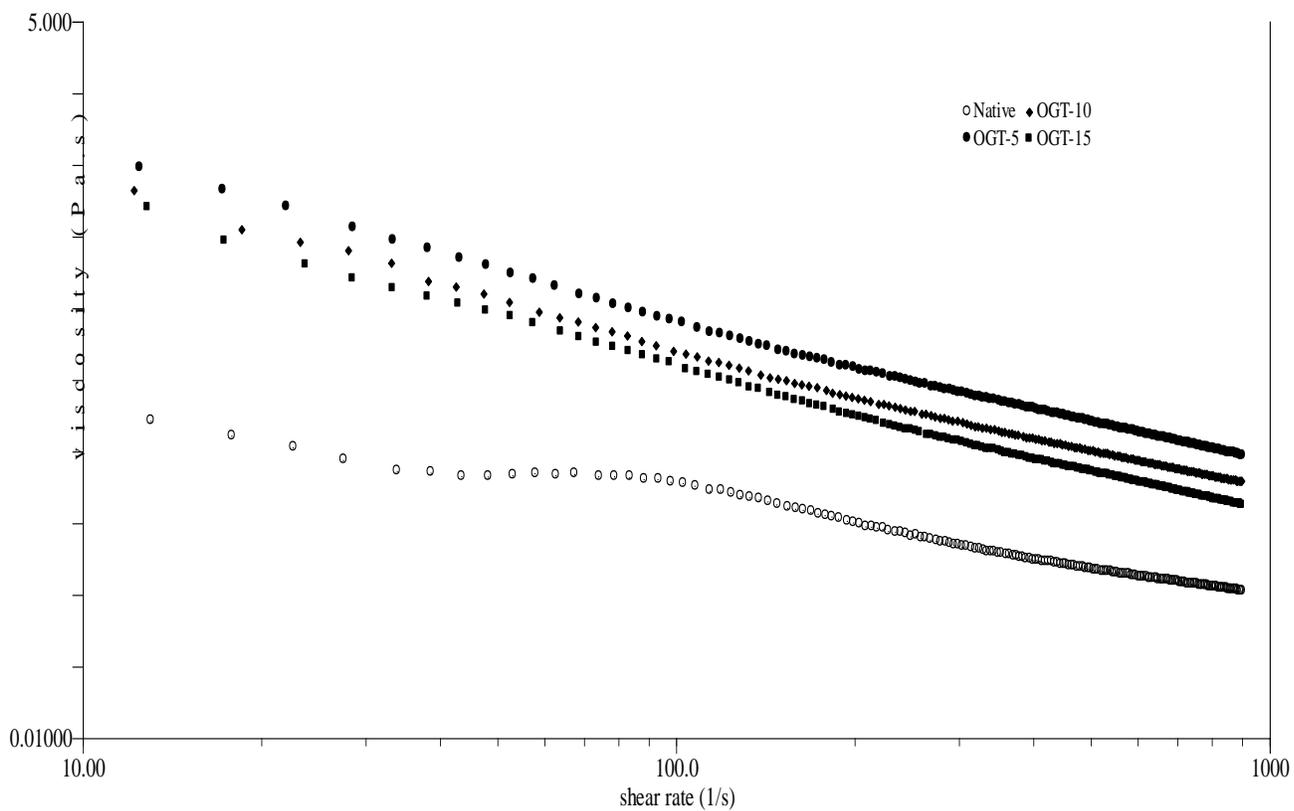
Figure 4.1: Effect of shear rate on shear viscosity of native and ozone–oxidized white cocoyam starches (WCS)
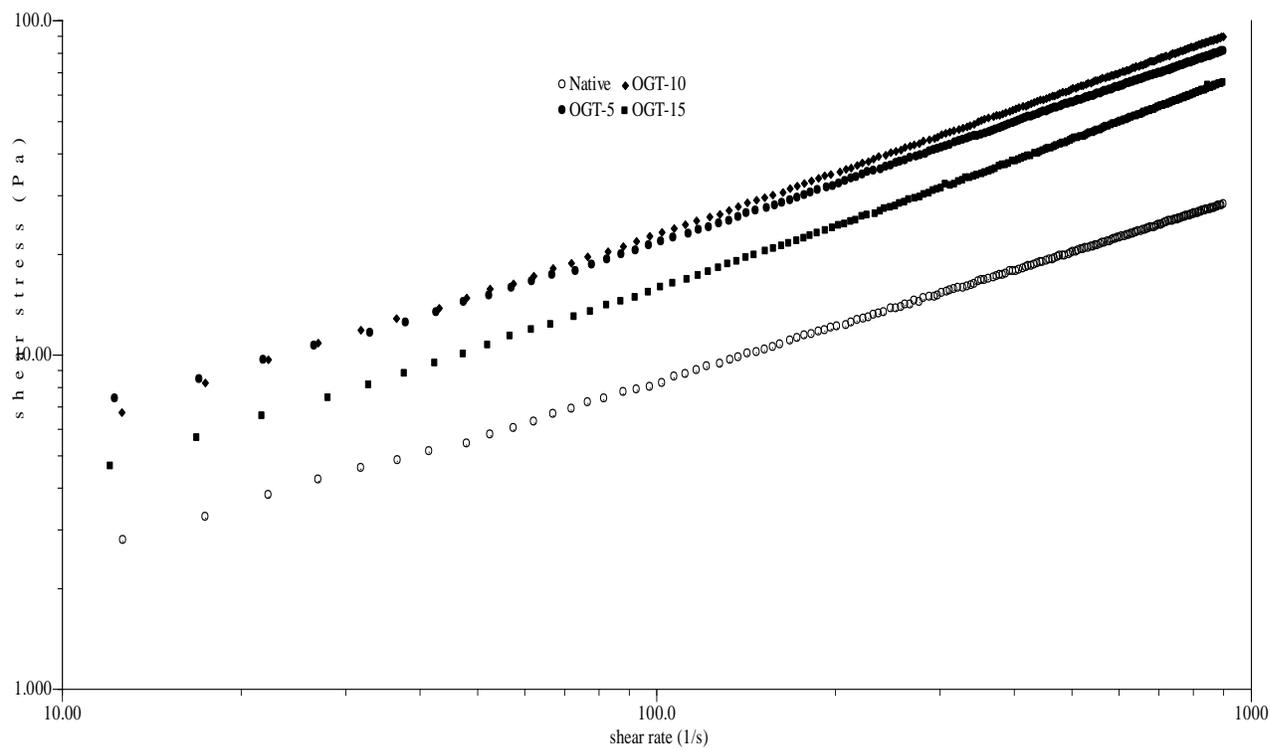
Figure 4.2: Effect of shear rate on shear viscosity of native and ozone–oxidized red cocoyam starches (RCS)
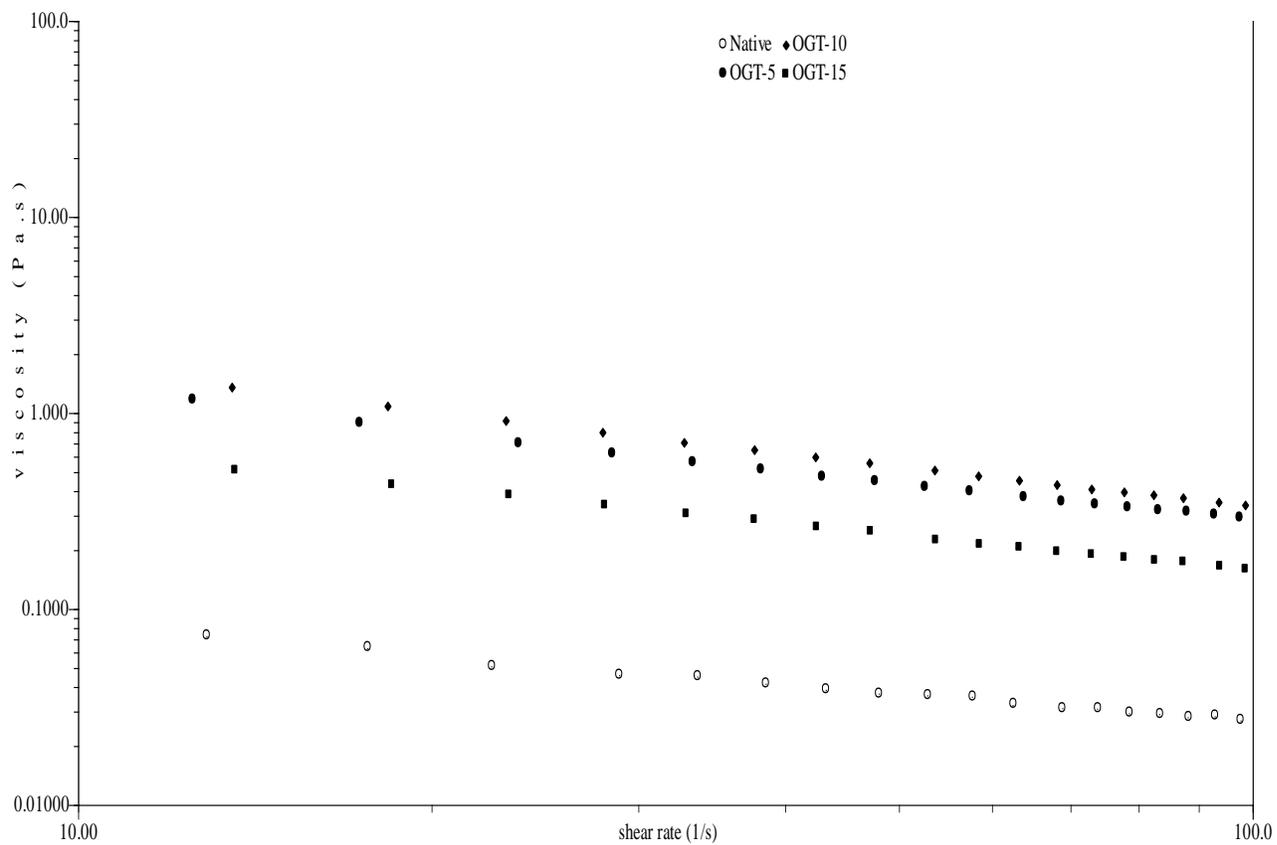
***Figure 4.3: Effect of shear rate on shear viscosity of native and ozone–oxidized
white yam starches (WYS)***
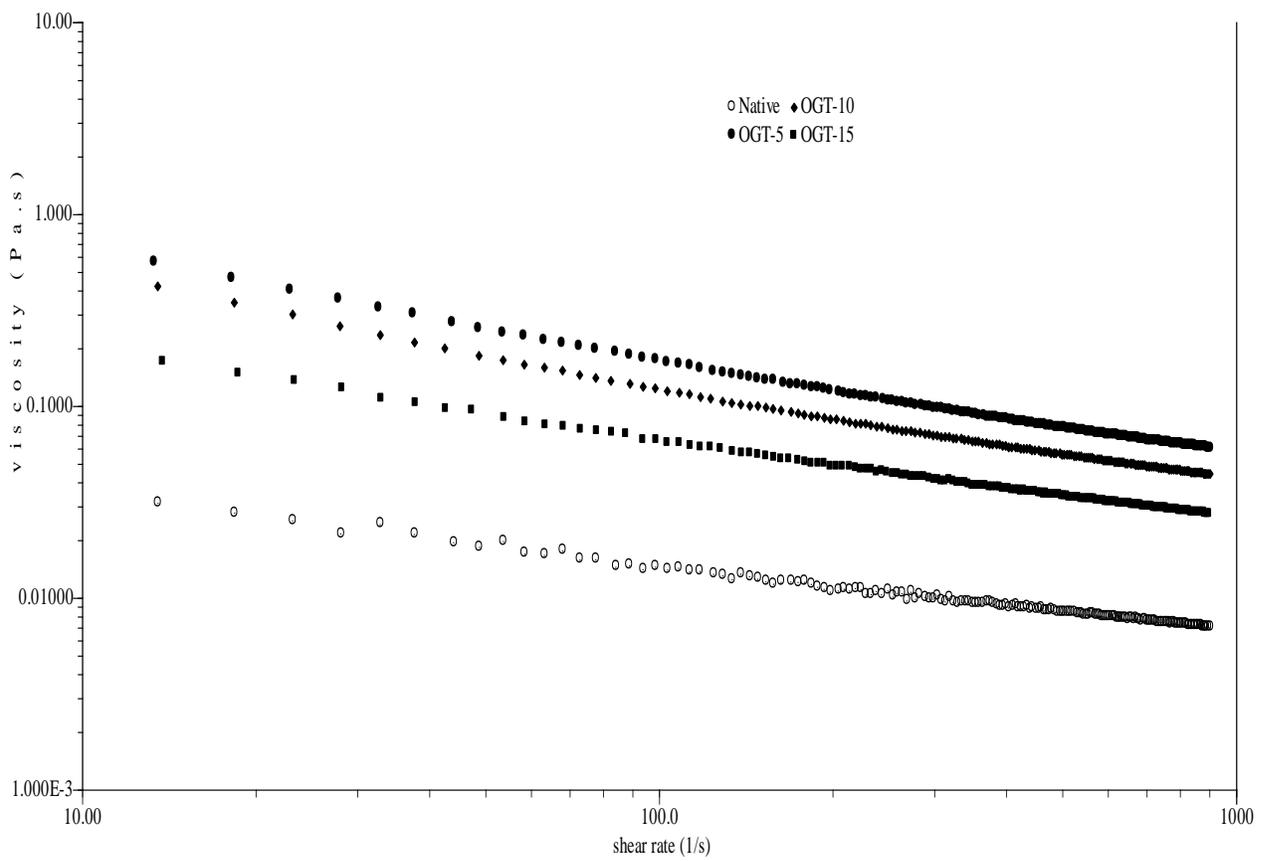
Figure 4.4: Effect of shear rate on shear viscosity of native and ozone–oxidized yellow yam starches (YYS)
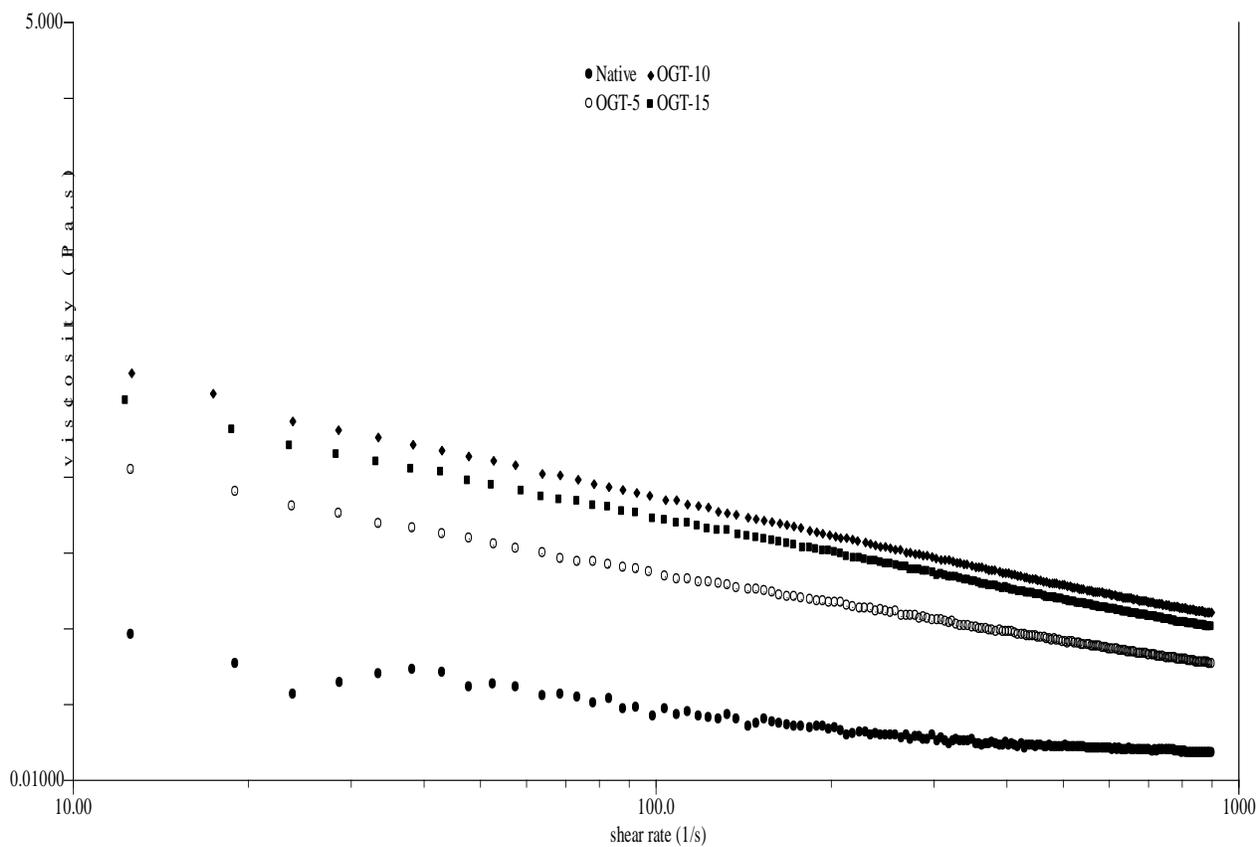
Figure 4.5: Effect of shear rate on shear viscosity of native and ozone–oxidized

pigeon pea starches (PPS)
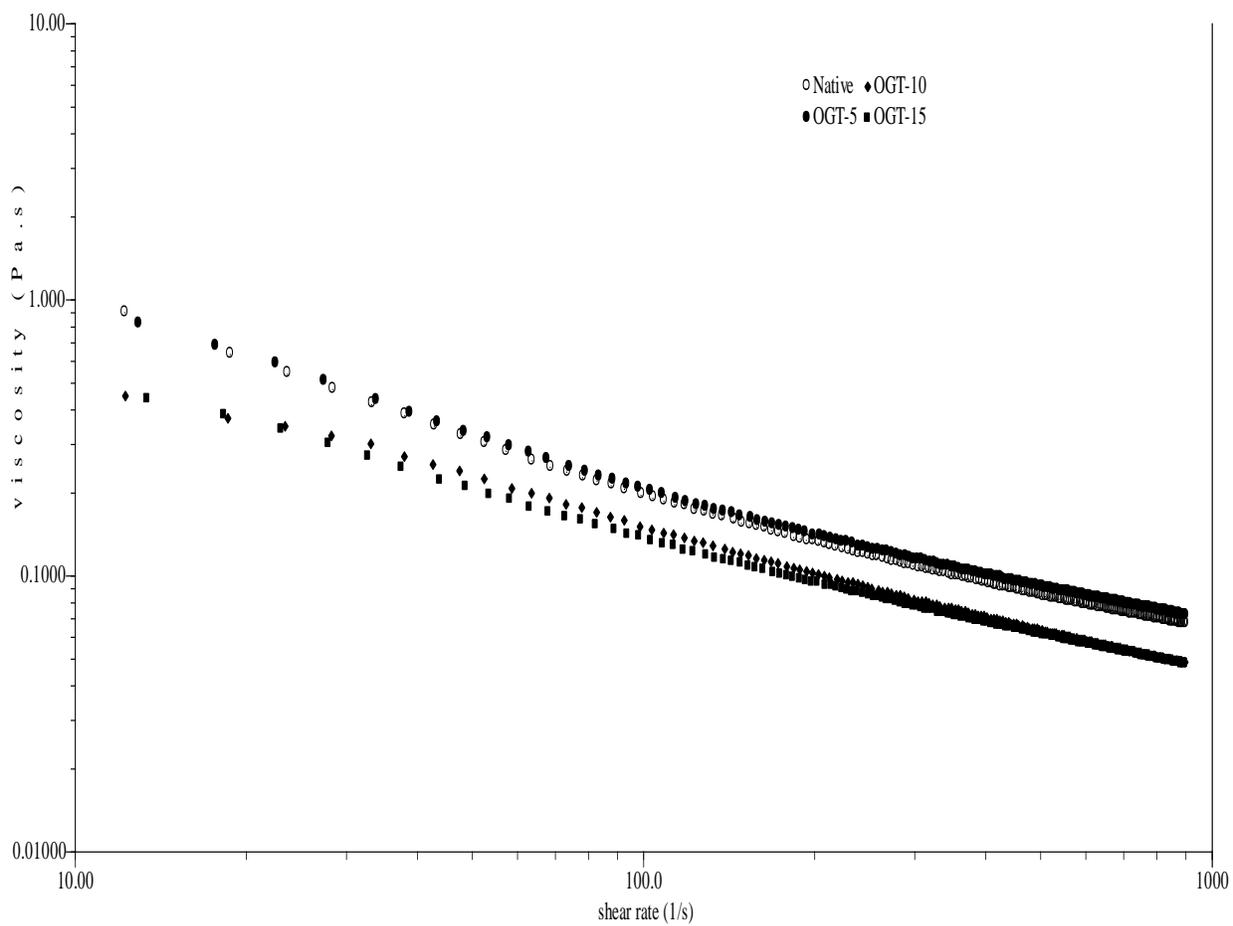
Figure 4.6: Effect of shear rate on shear viscosity of native and ozone–oxidized lima bean starches (LBS)
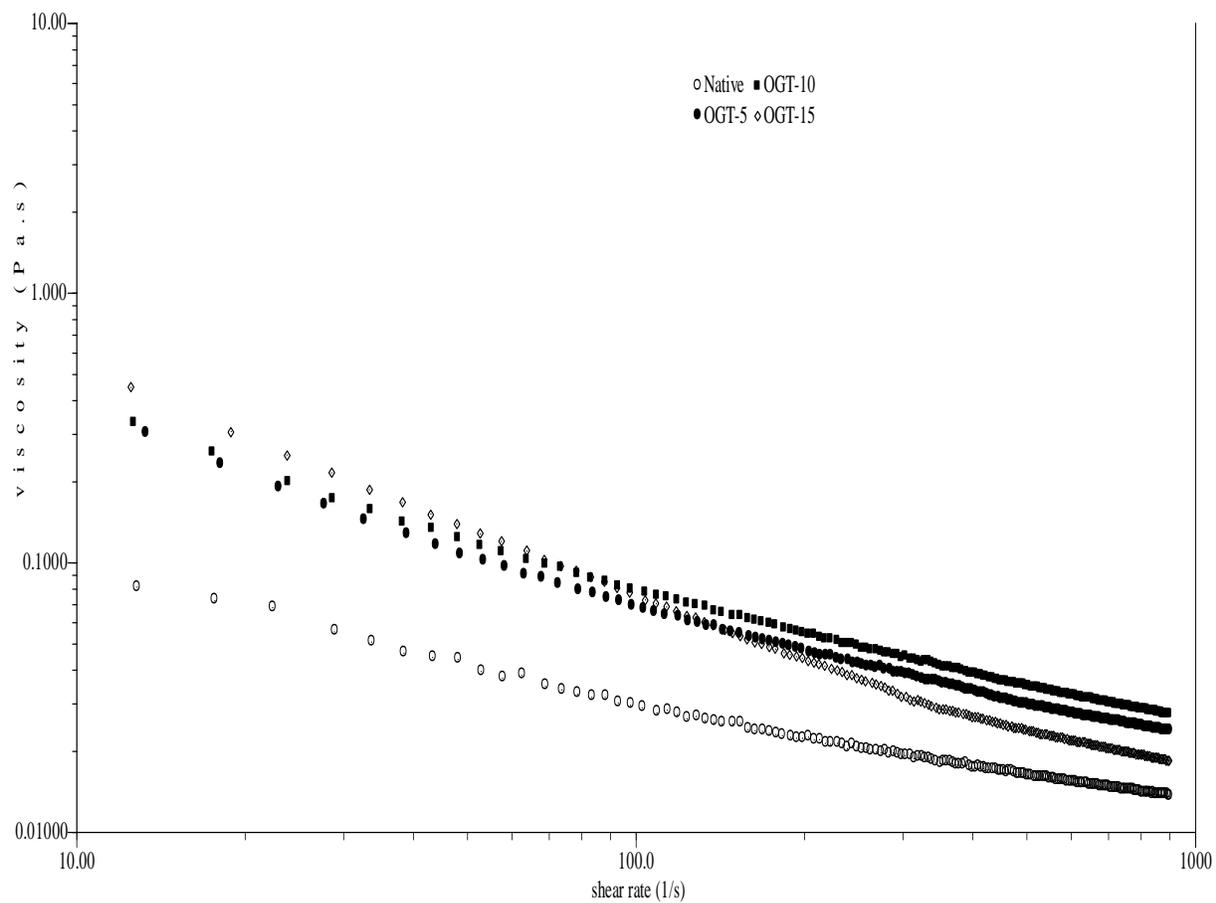
Figure 4.7: Effect of shear rate on shear viscosity of native and ozone–oxidized jack bean starches (JBS)
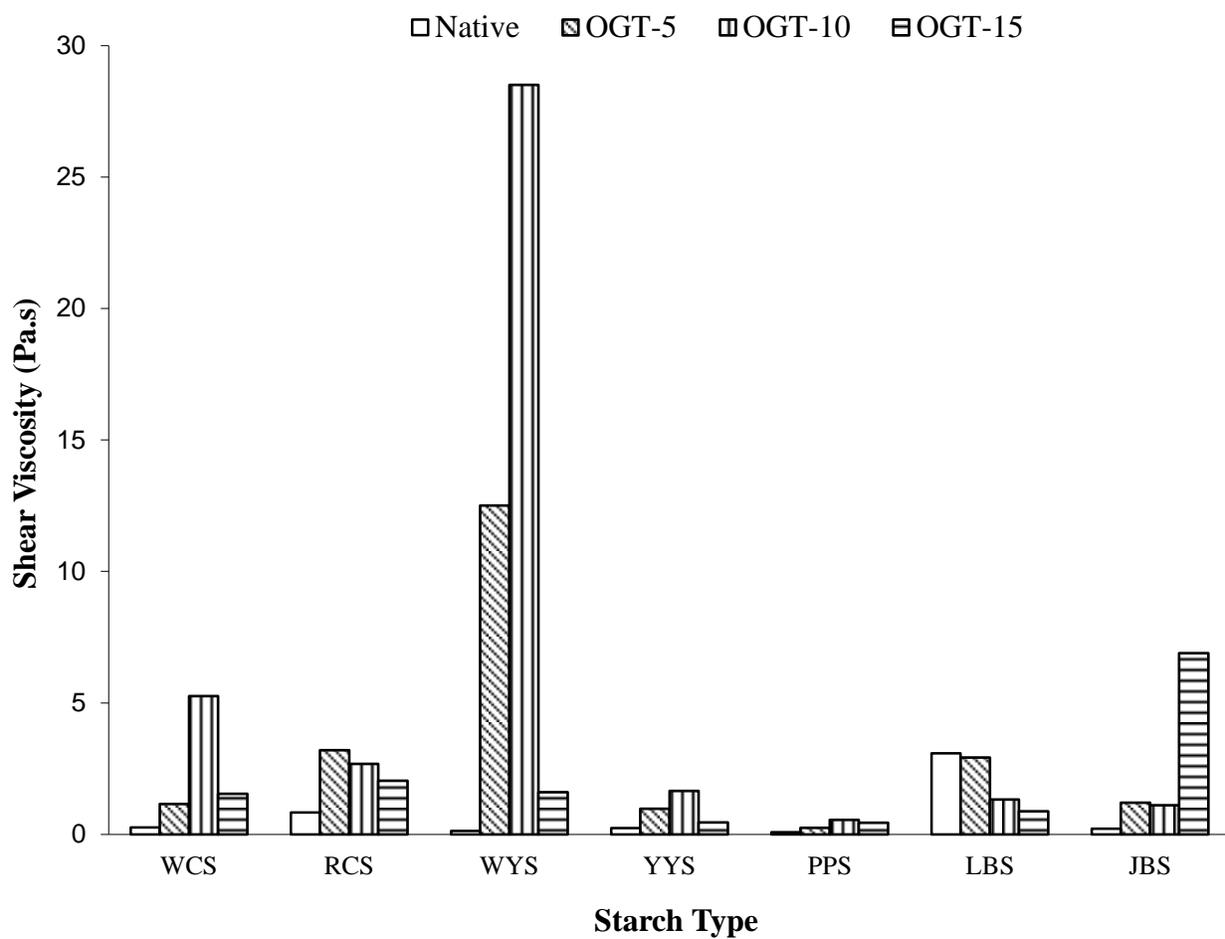
Figure 4.8: Shear viscosities of native and ozone-oxidized starches at 25^oC
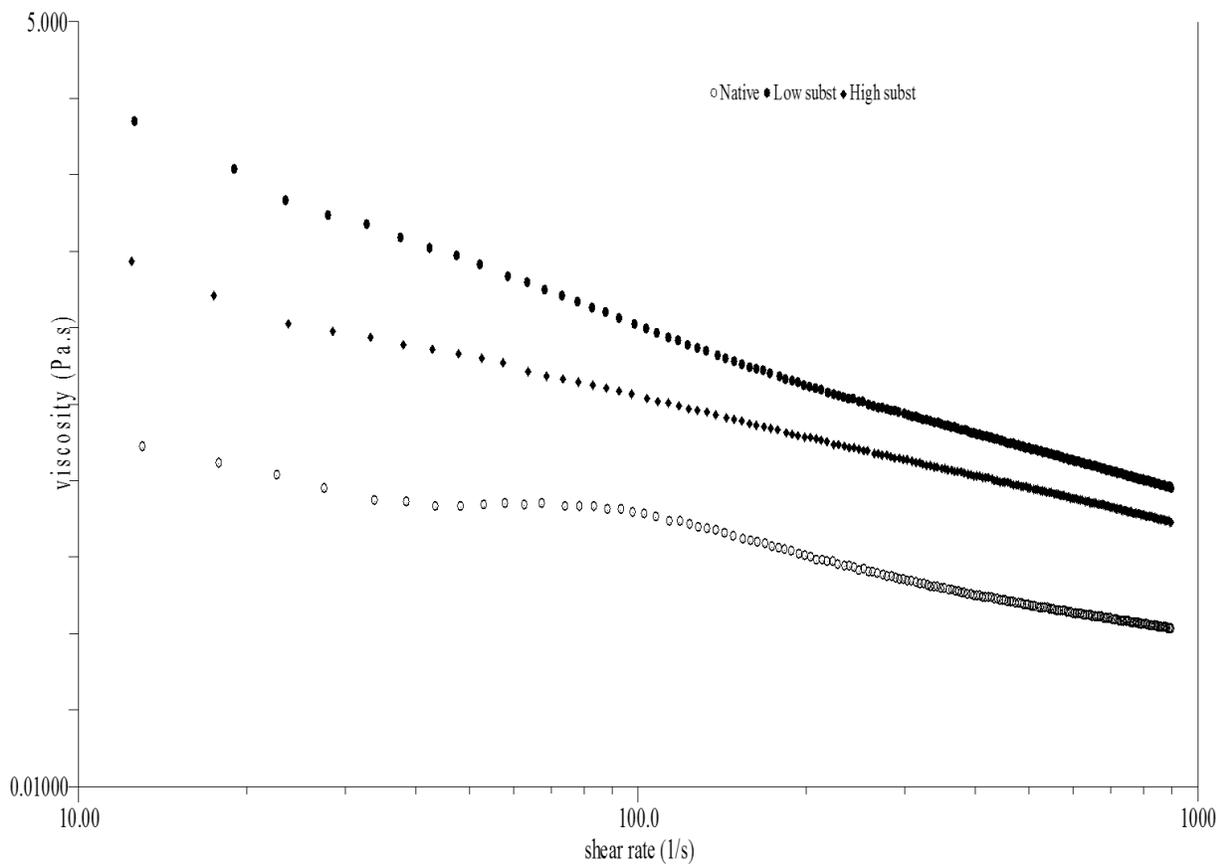
Figure 4.9: Effect of shear rate on shear viscosity of native and hydroxypropylated white cocoyam starches (WCS)
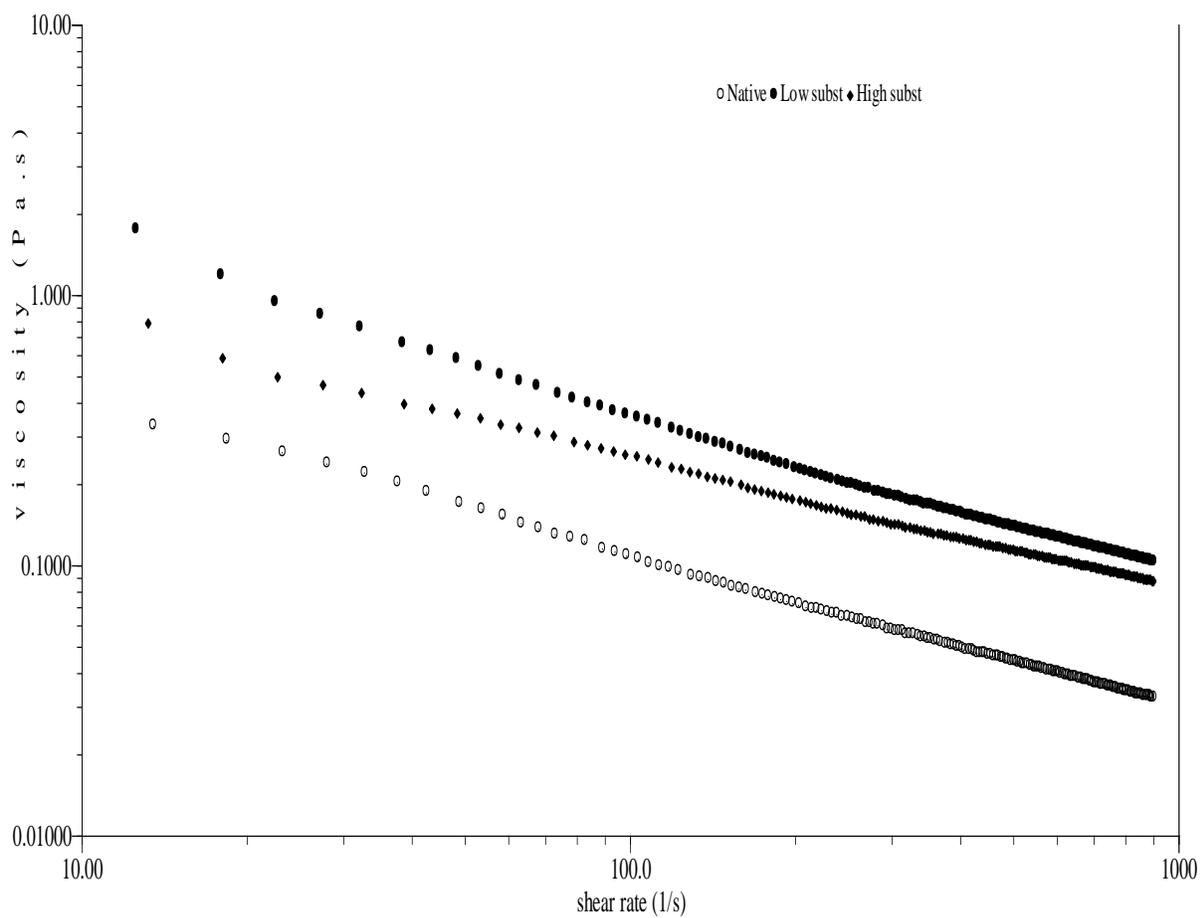
Figure 4.10: Effect of shear rate on shear viscosity of native and hydroxypropylated
red cocoyam starches (RCS)
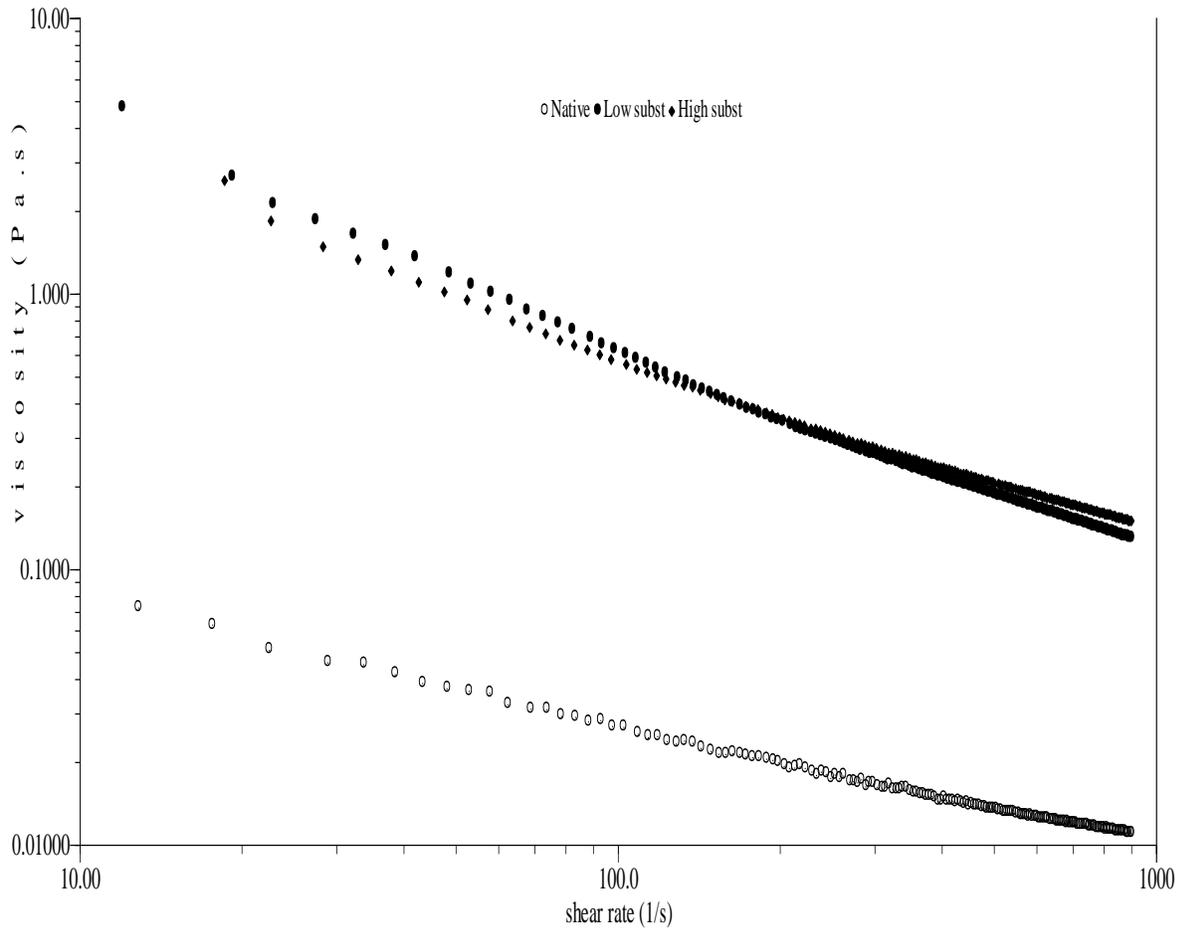
Figure 4.11: Effect of shear rate on shear viscosity of native and hydroxypropylated
white yam starches (WYS)
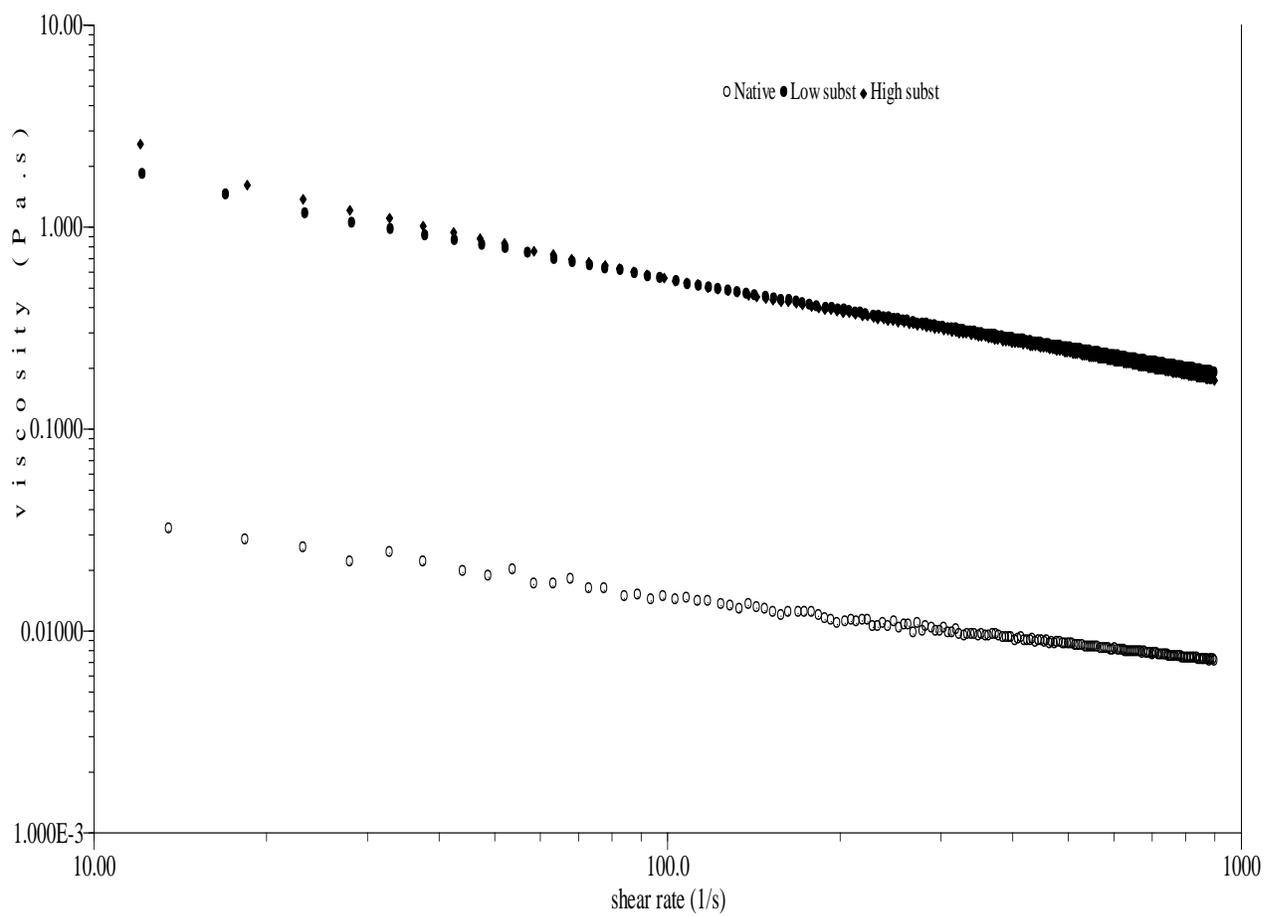
Figure 4.12: Effect of shear rate on shear viscosity of native and hydroxypropylated yellow yam starches (YYS)
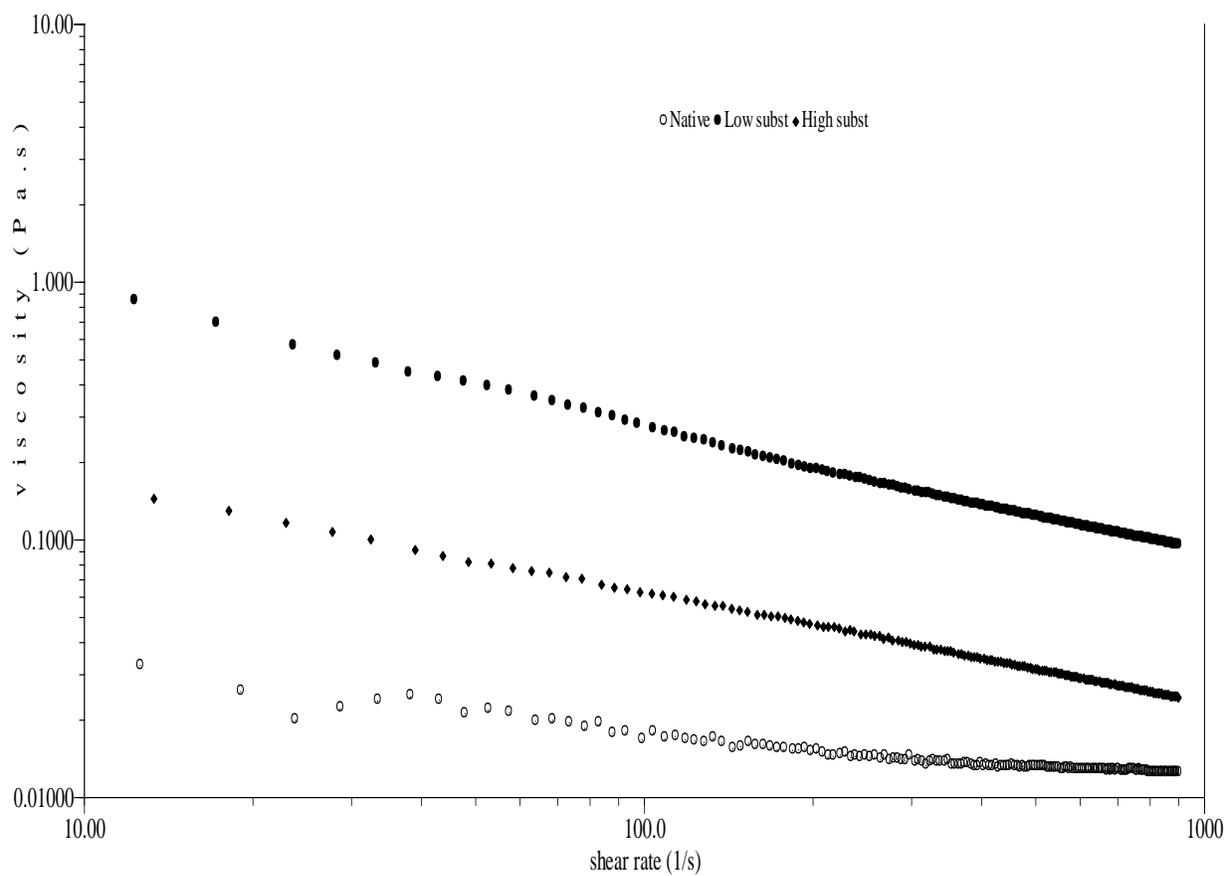
Figure 4.13: Effect of shear rate on shear viscosity of native and hydroxypropylated pigeon pea starches (PPS)
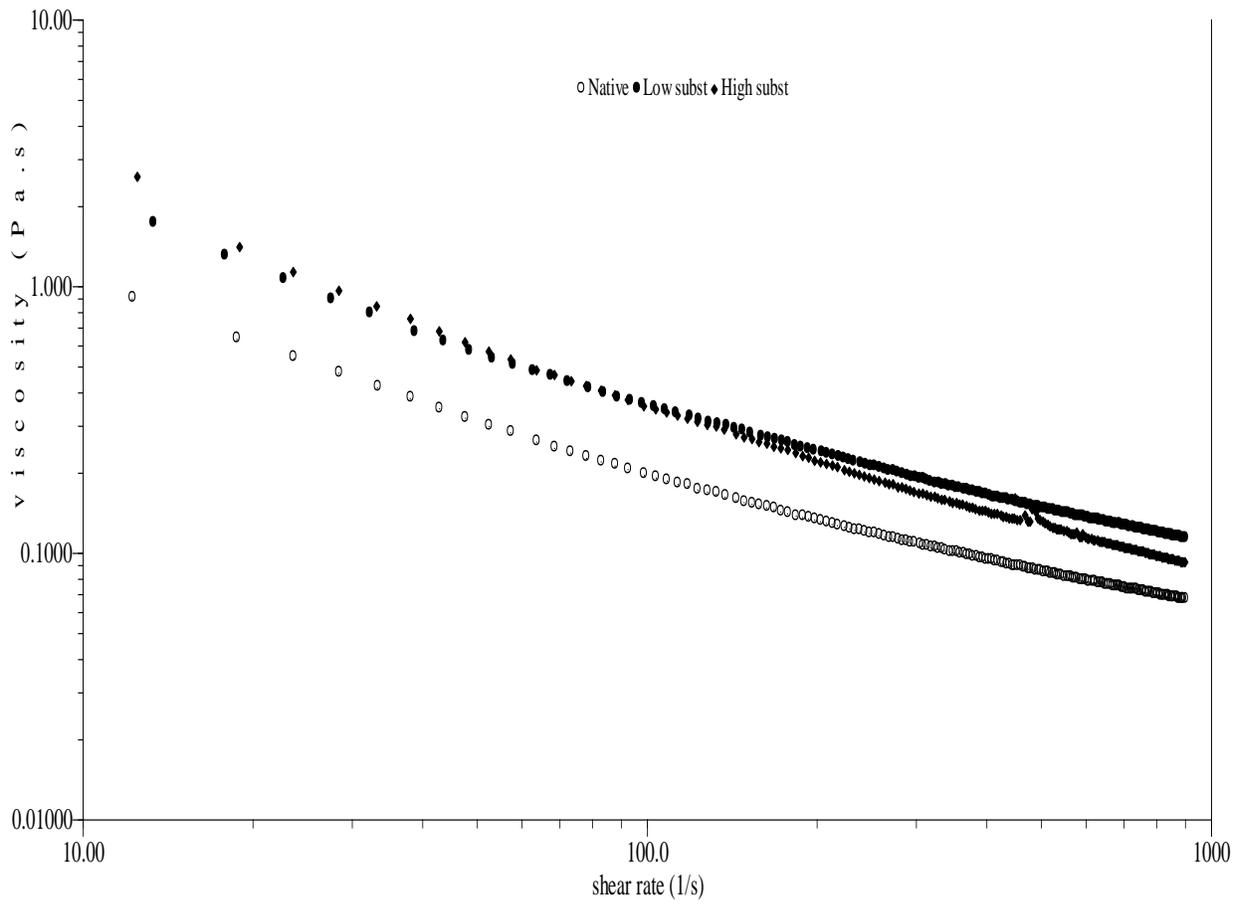
Figure 4.14: Effect of shear rate on shear viscosity of native and hydroxypropylated lima bean starches (LBS)
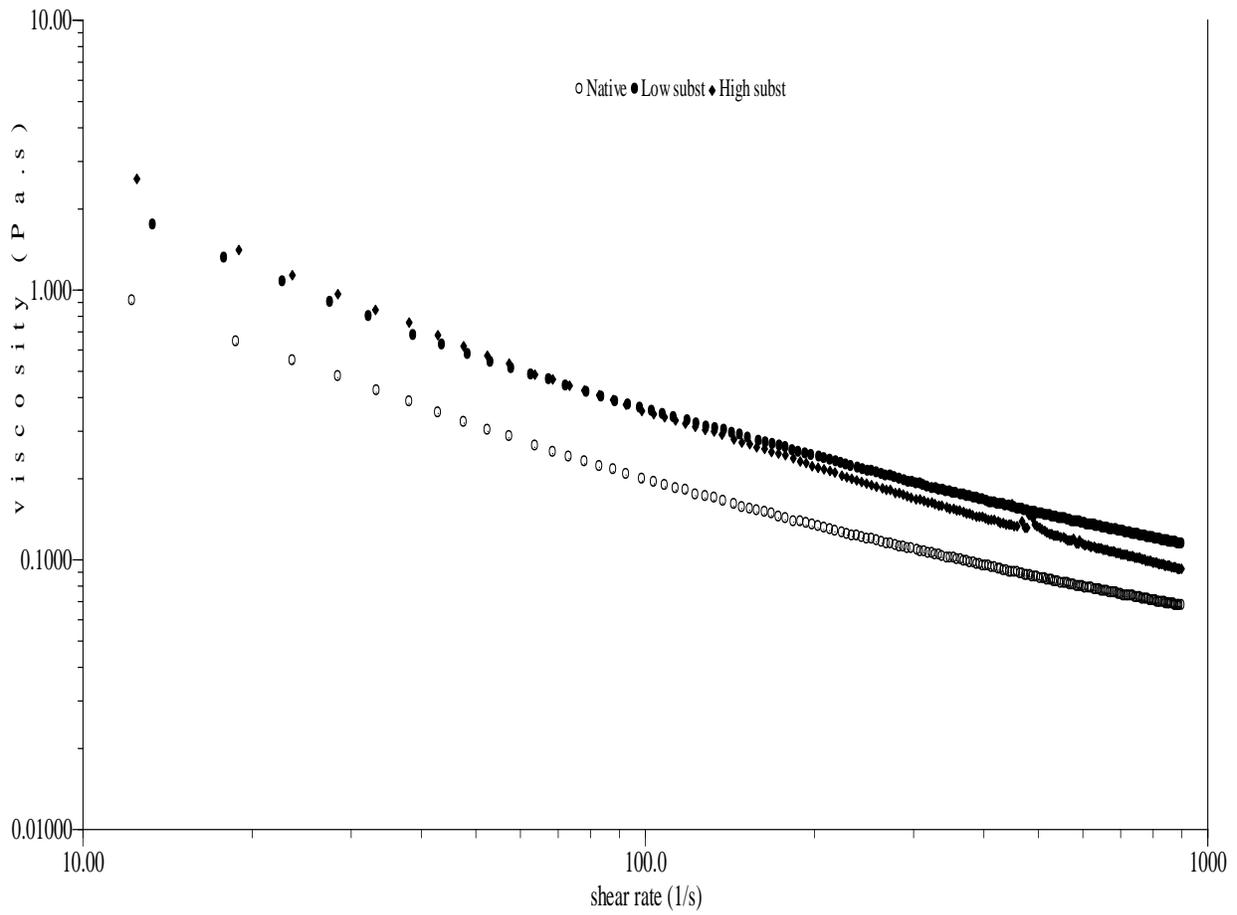
Figure 4.15: Effect of shear rate on shear viscosity of native and hydroxypropylated jack bean starches (JBS)
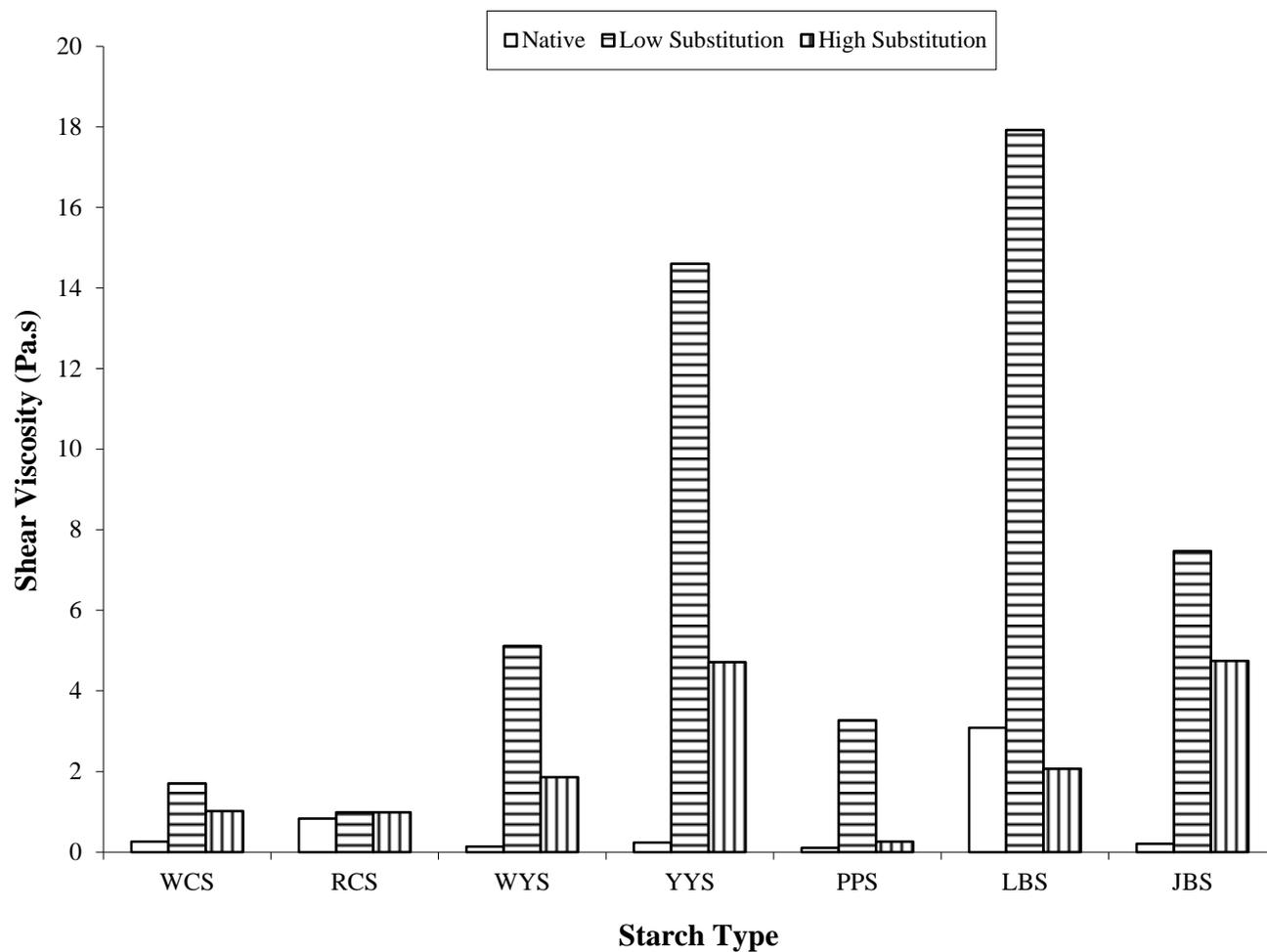
Figure 4.16: Shear viscosities of native and hydroxypropylated starches at 25°C
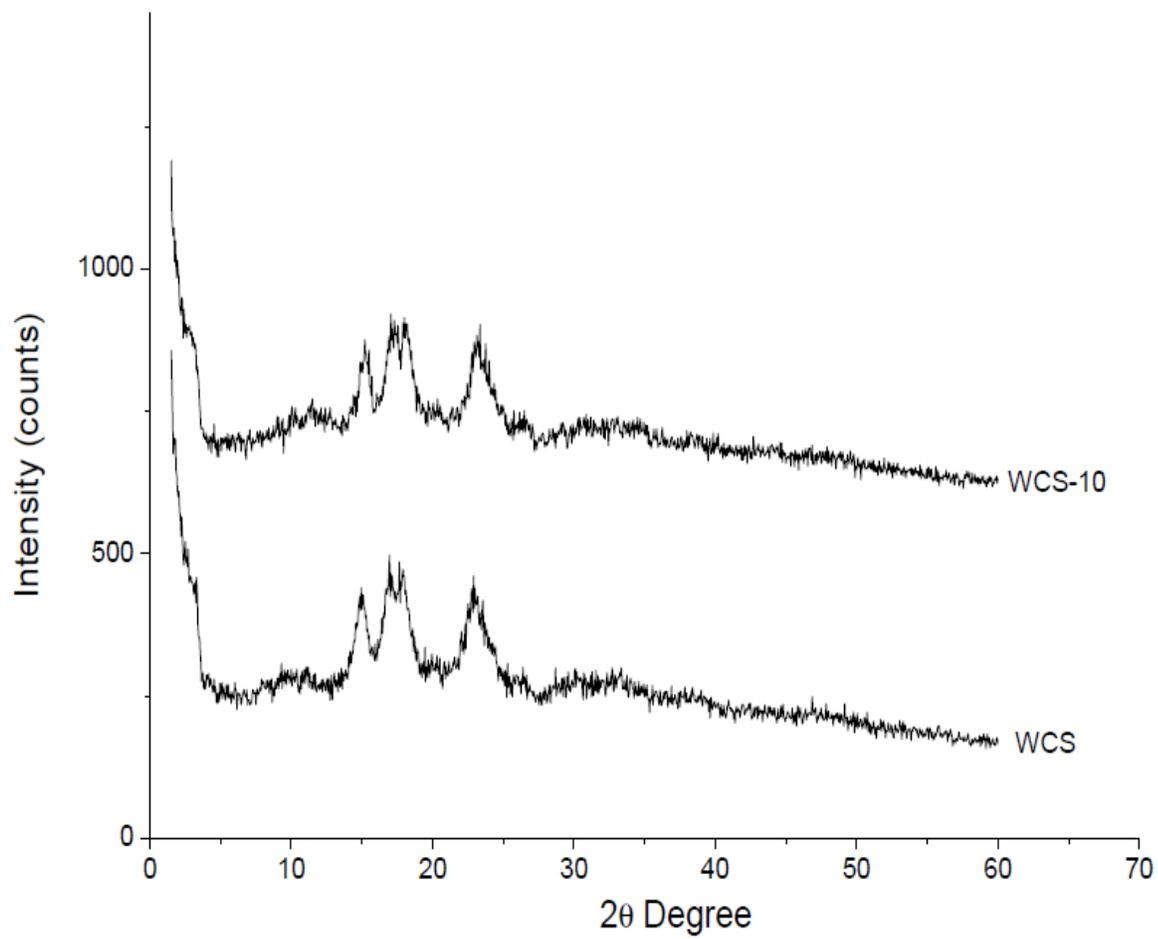
Figure 4.17: X-ray patterns of native and ozone-oxidized white cocoyam starches (WCS)
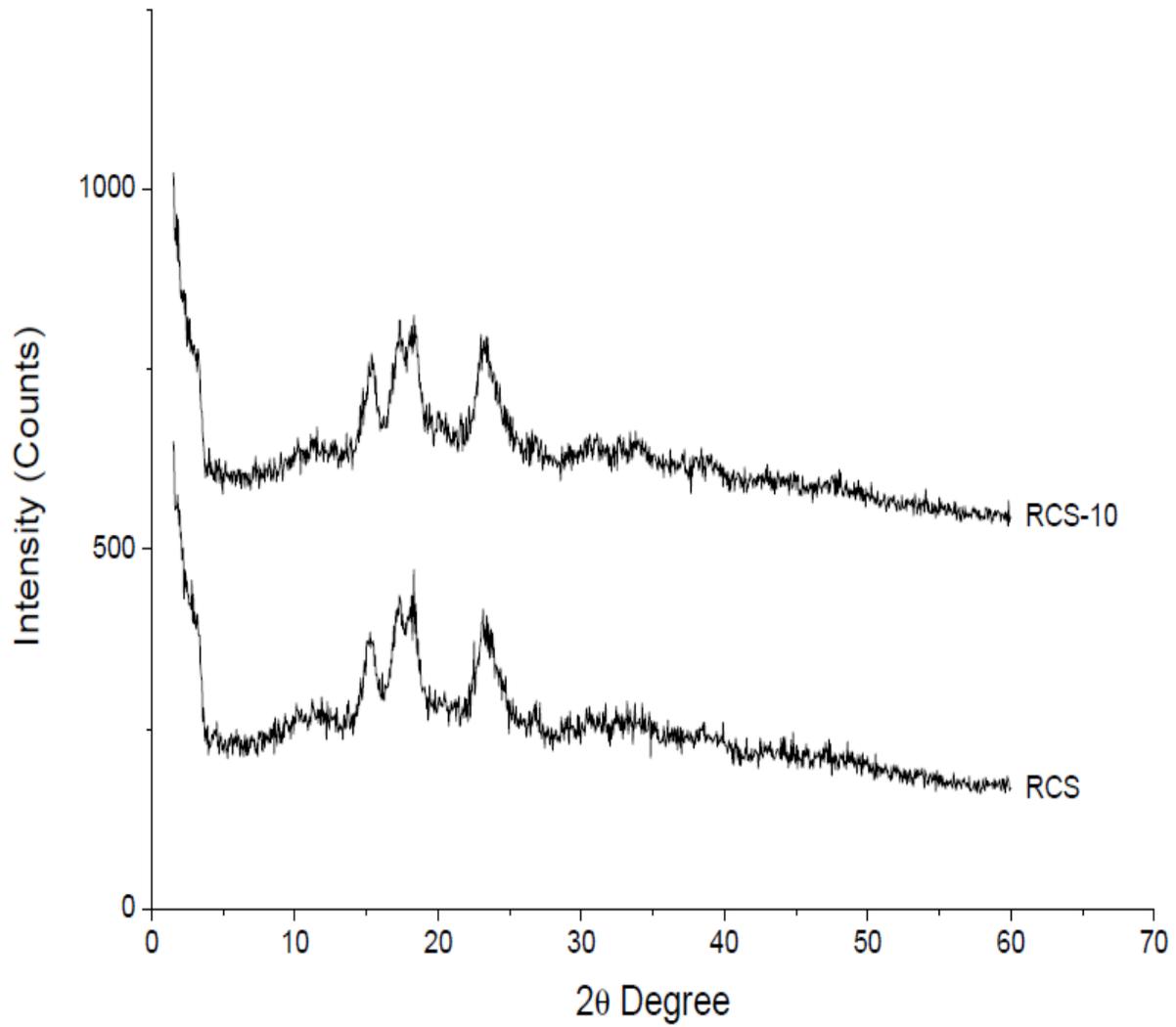
Figure 4.18: X-ray patterns of native and ozone-oxidized red cocoyam starches (RCS)
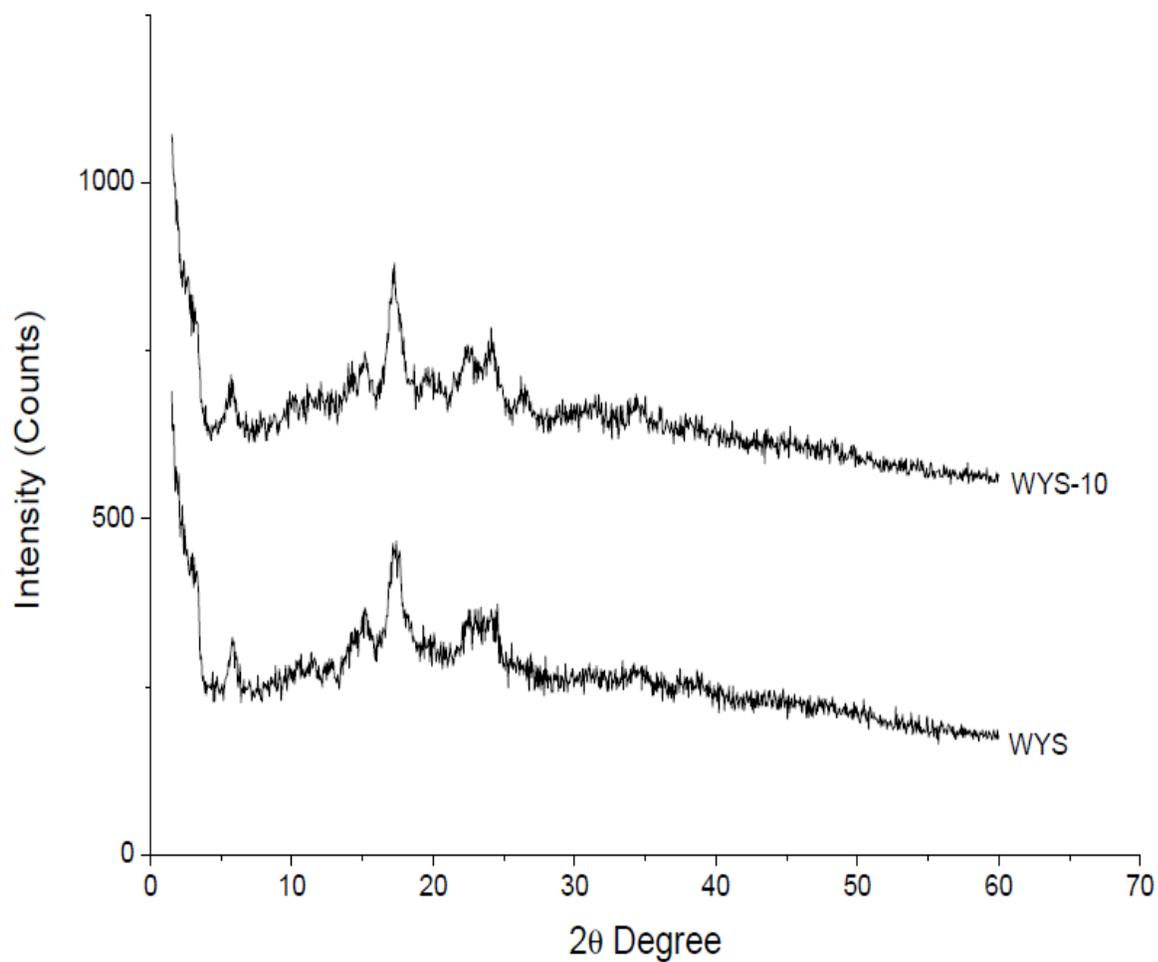
Figure 4.19: X-ray patterns of native and ozone-oxidized white yam starches (WYS)
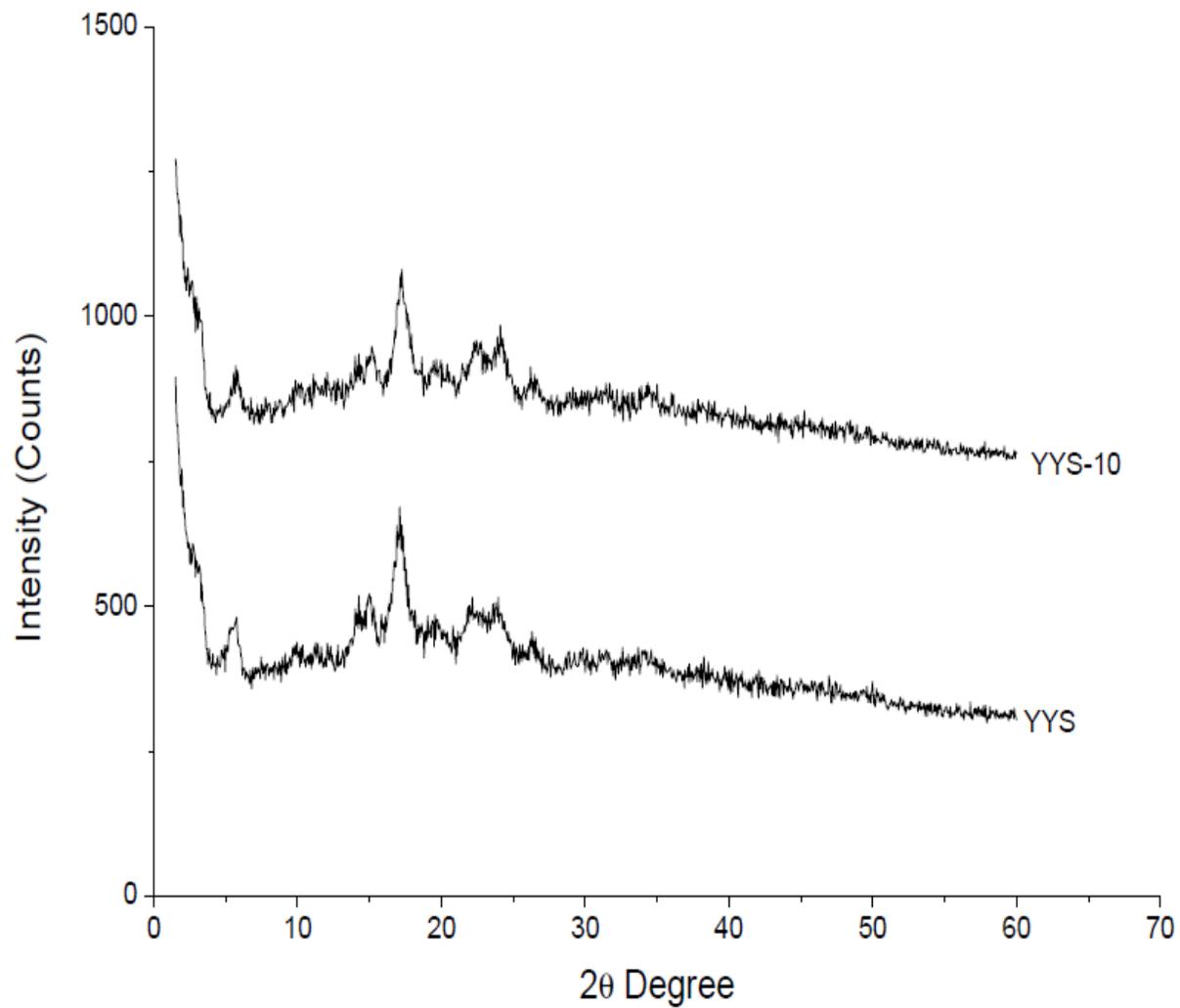
Figure 4.20: X-ray patterns of native and ozone-oxidized yellow yam starches (YYS)
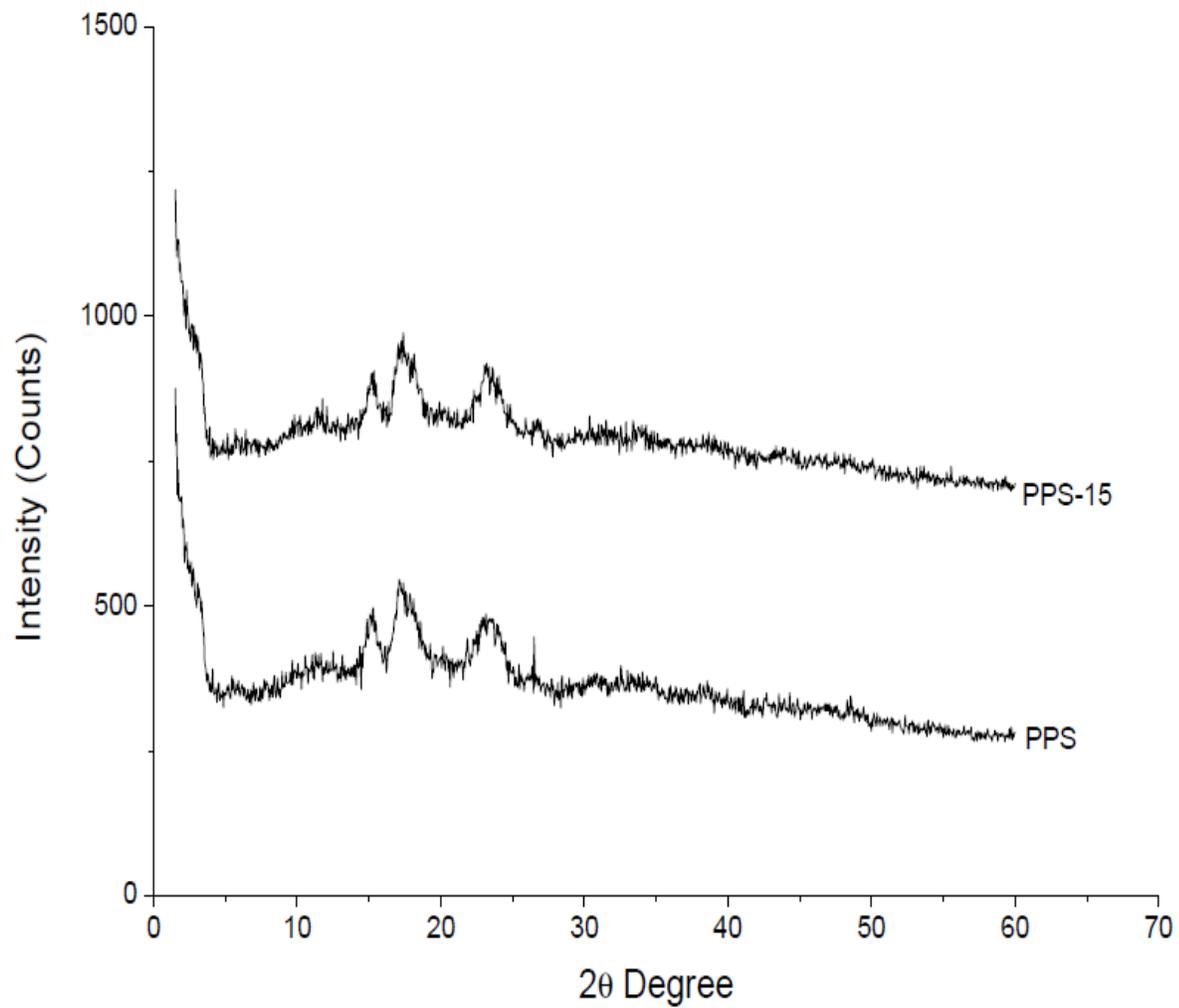
Figure 4.21: X-ray patterns of native and ozone-oxidized pigeon pea starches (PPS)
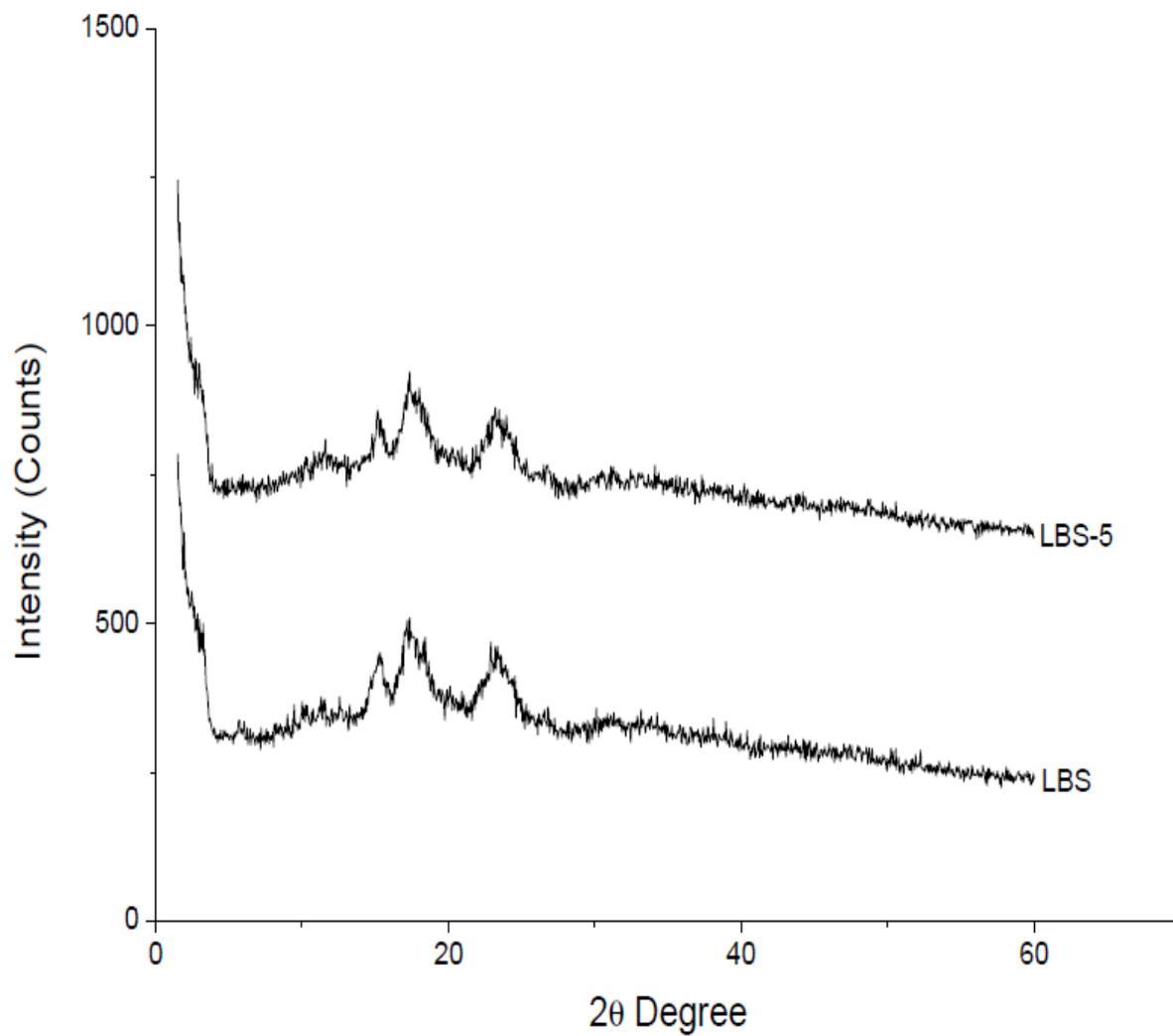
Figure 4.22: X-ray patterns of native and ozone-oxidized lima bean starches (LBS)
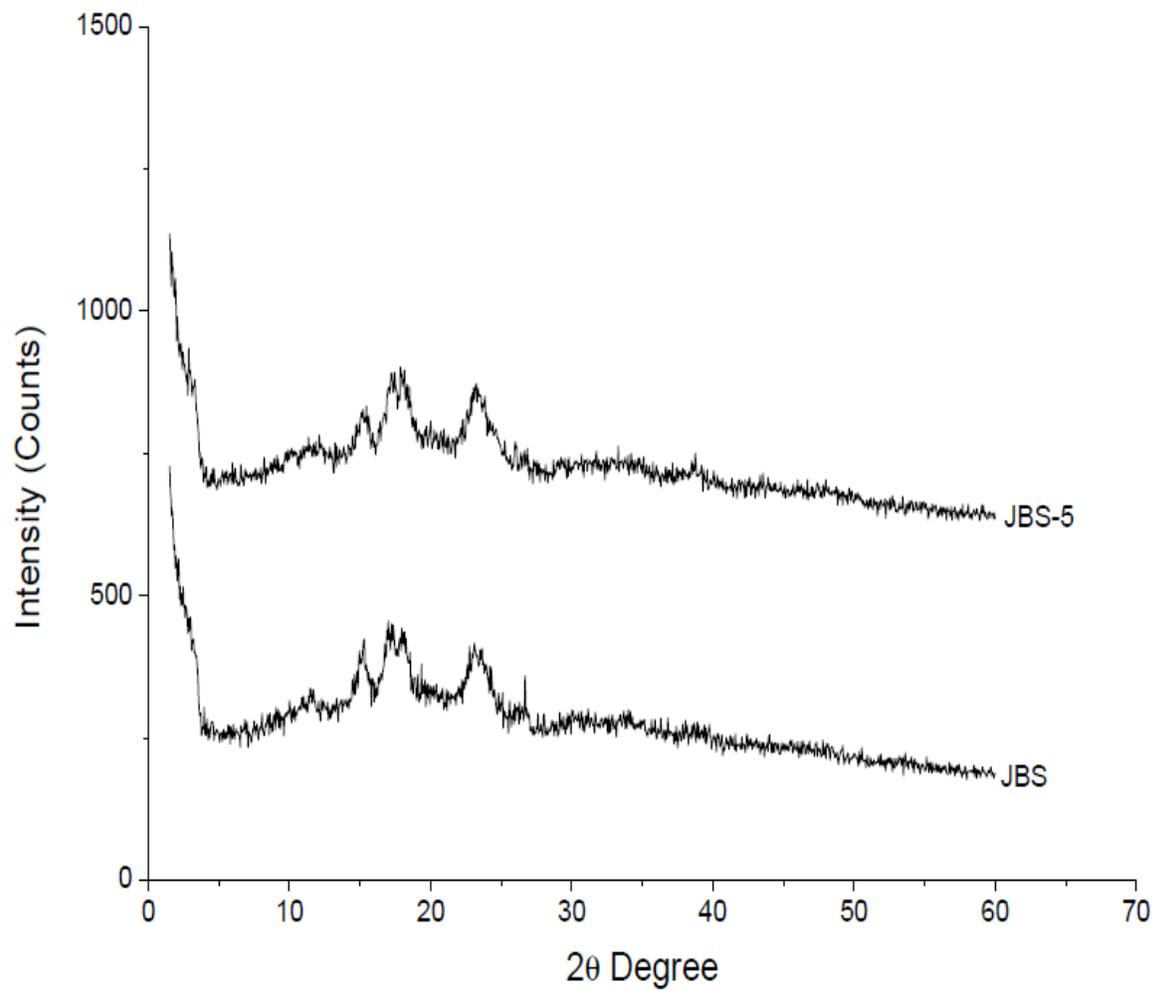
Figure 4.23: X-ray patterns of native and ozone-oxidized jack bean starches (JBS)
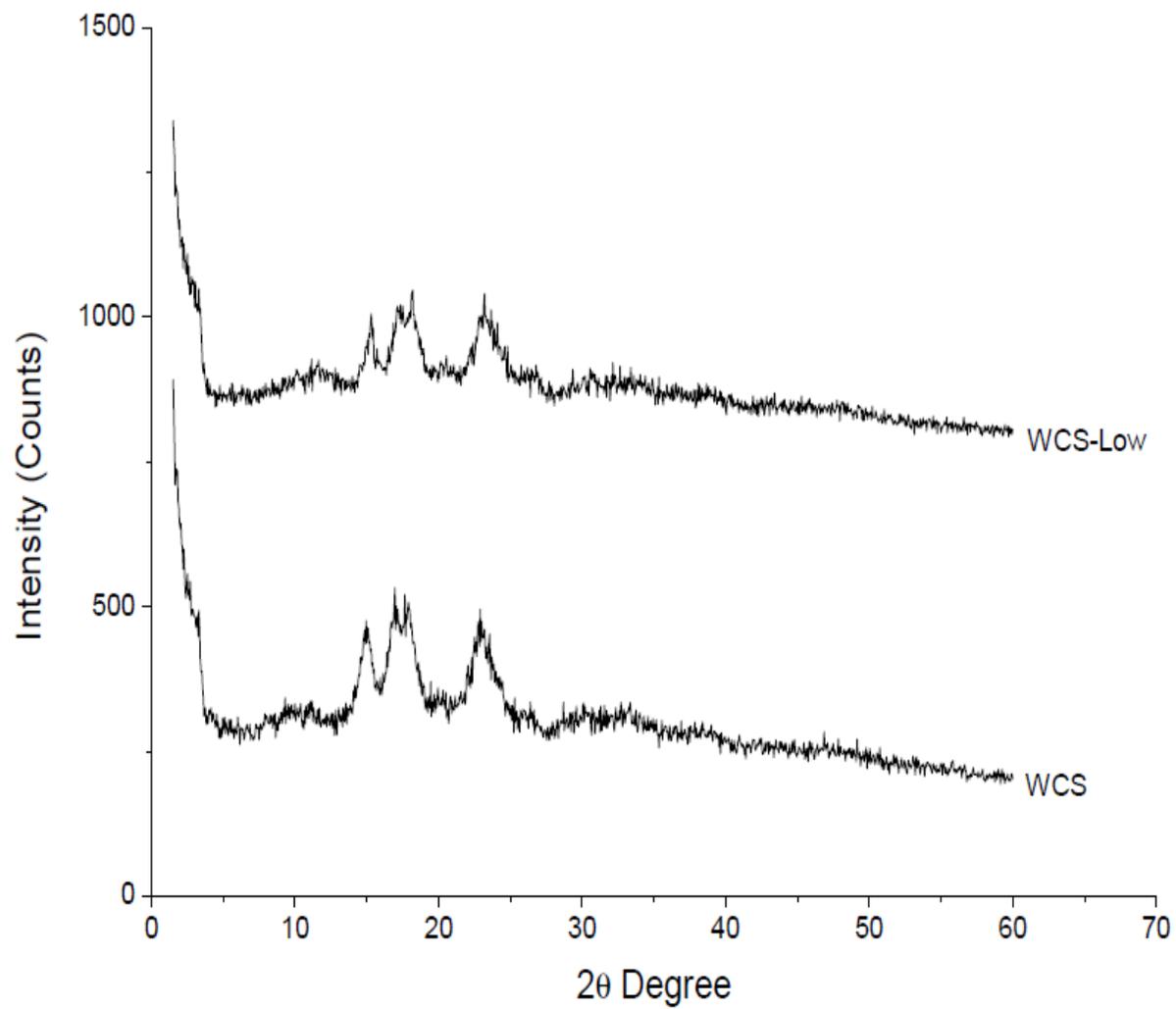
Figure 4.24: X-ray patterns of native and hydroxypropylated white cocoyam starches (WCS)
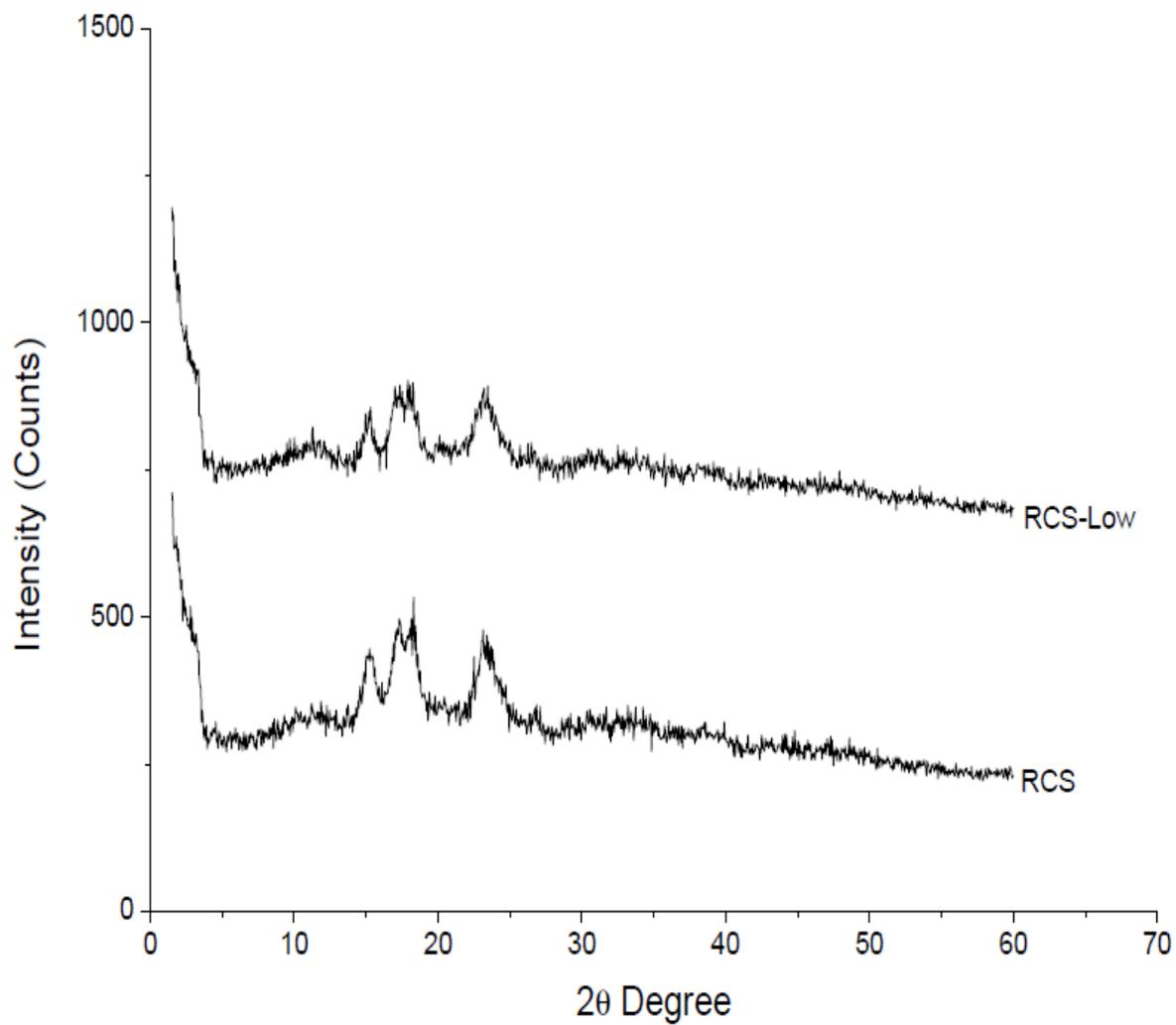
Figure 4.25: X-ray patterns of native and hydroxypropylated red cocoyam starches (RCS)
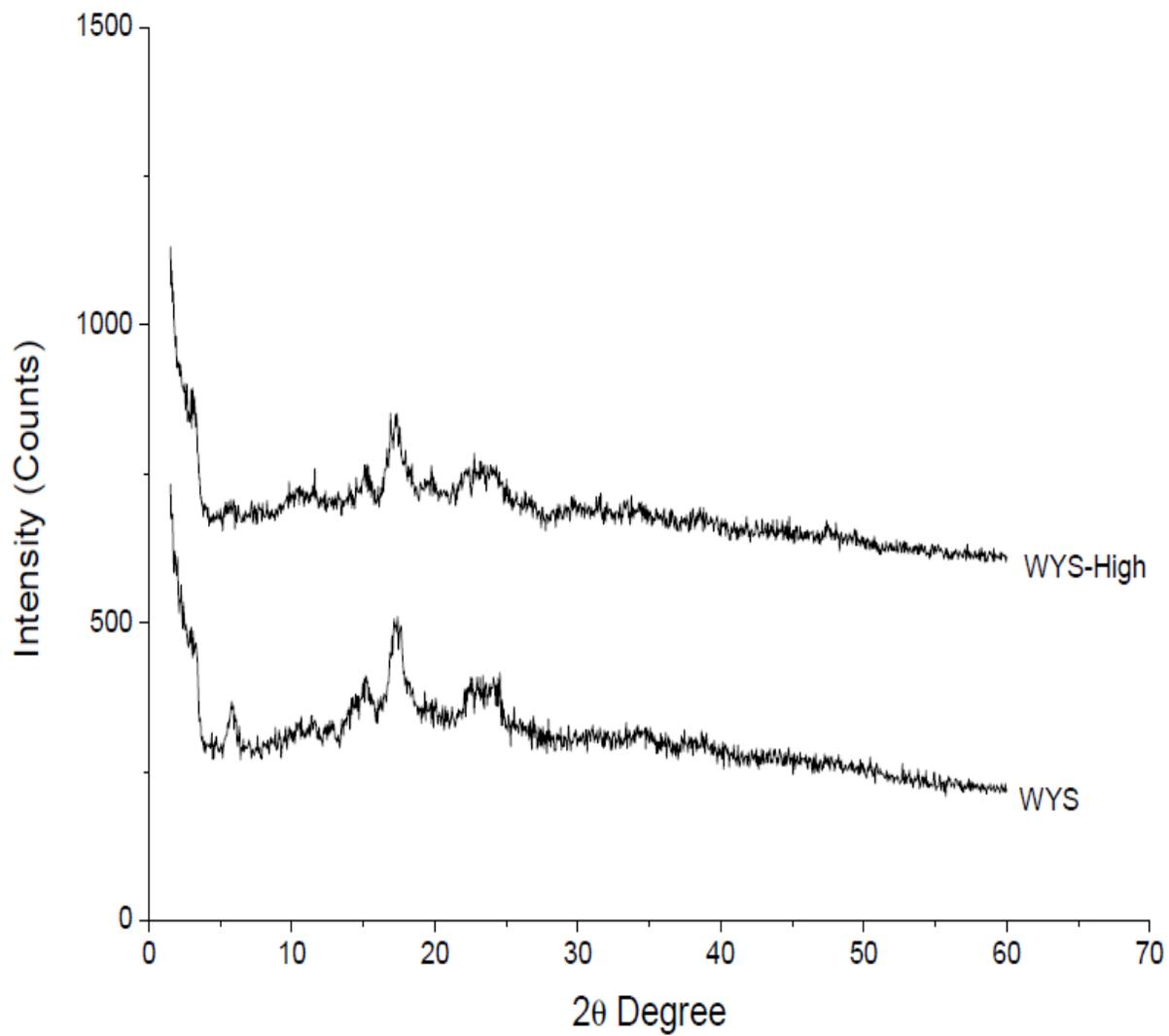
Figure 4.26: X-ray patterns of native and hydroxypropylated white yam starches (WYS)
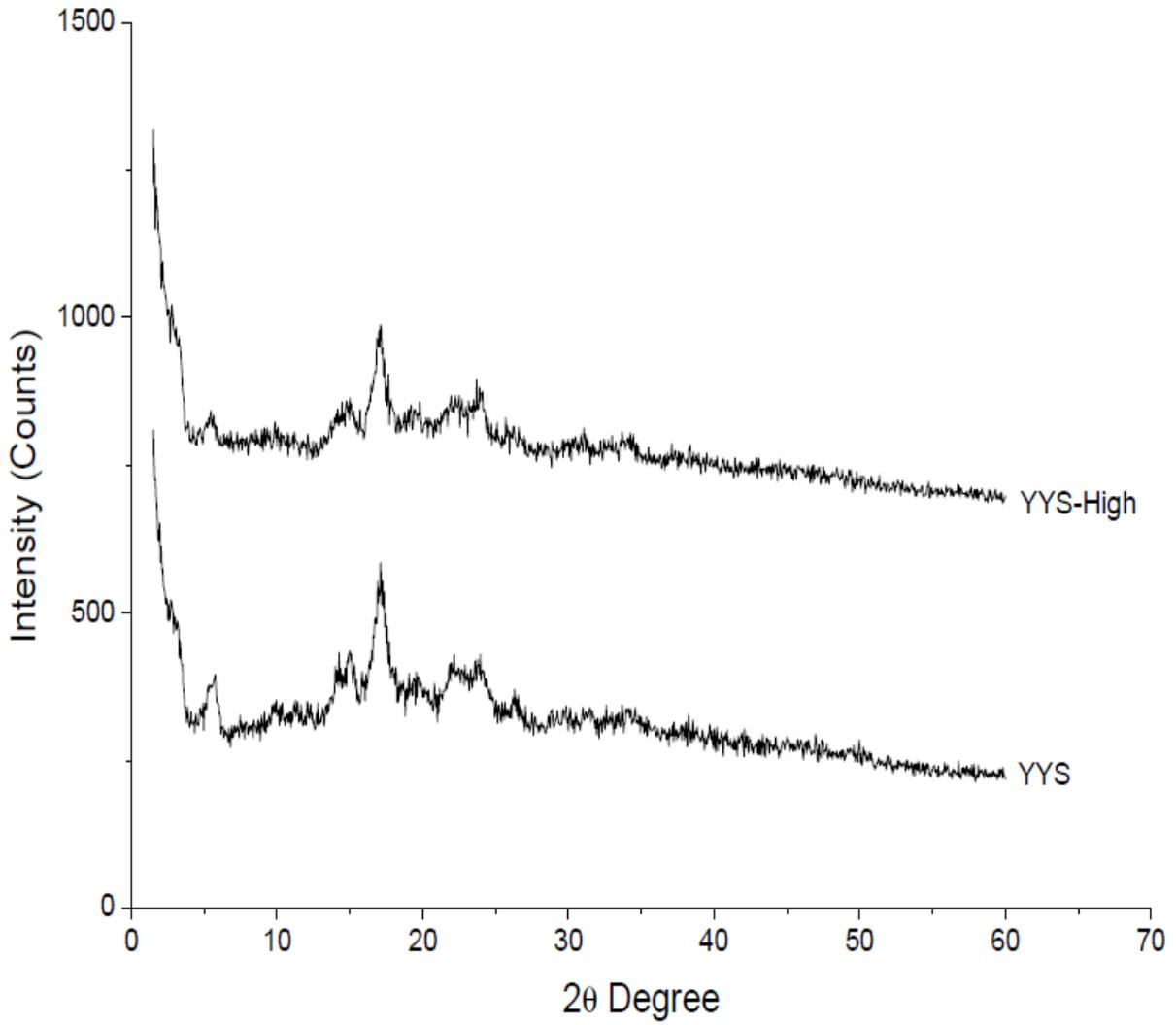
Figure 4.27: X-ray patterns of native and hydroxypropylated yellow yam starches (YYS)
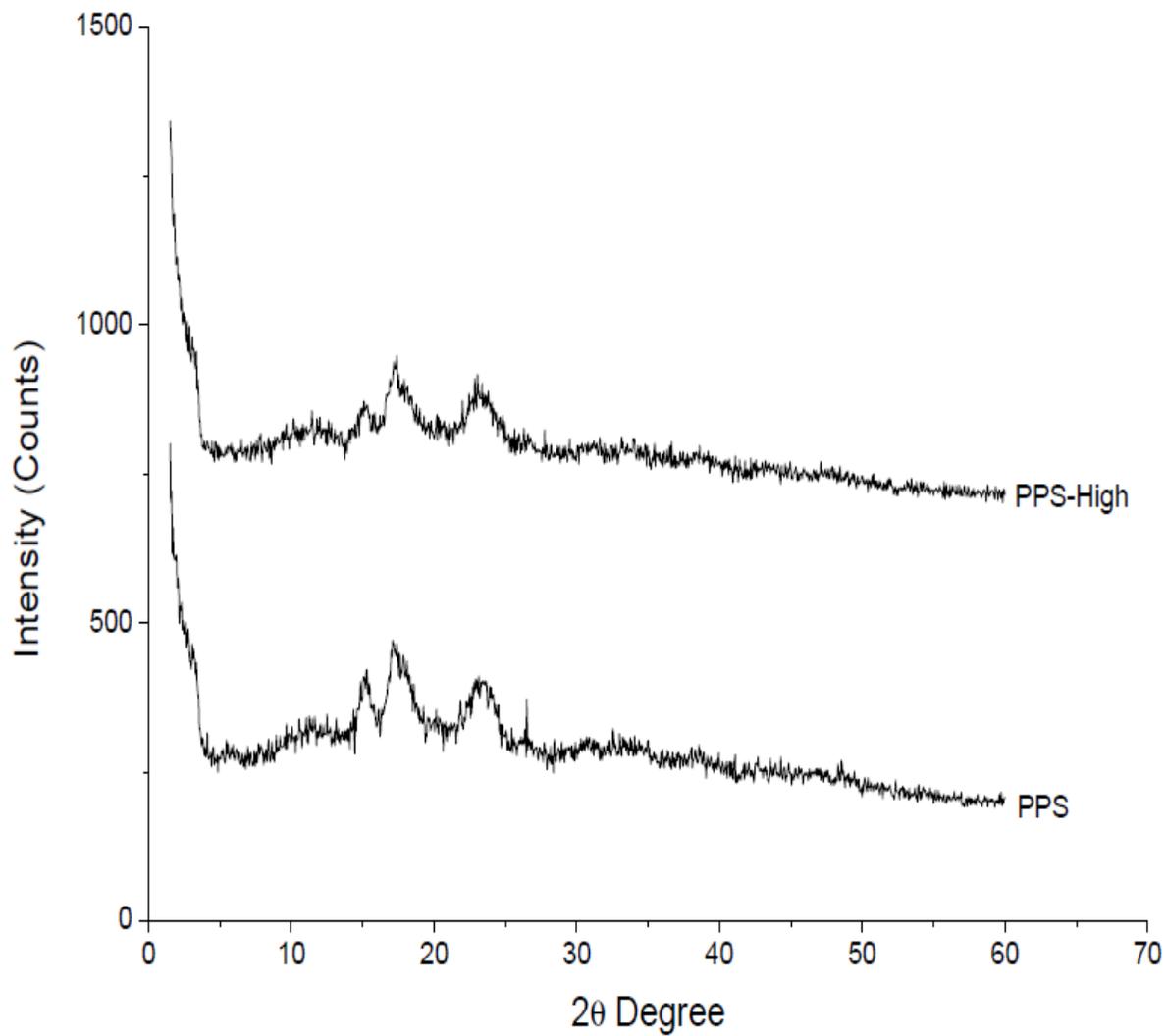
Figure 4.28: X-ray patterns of native and hydroxypropylated pigeon pea starches (PPS)
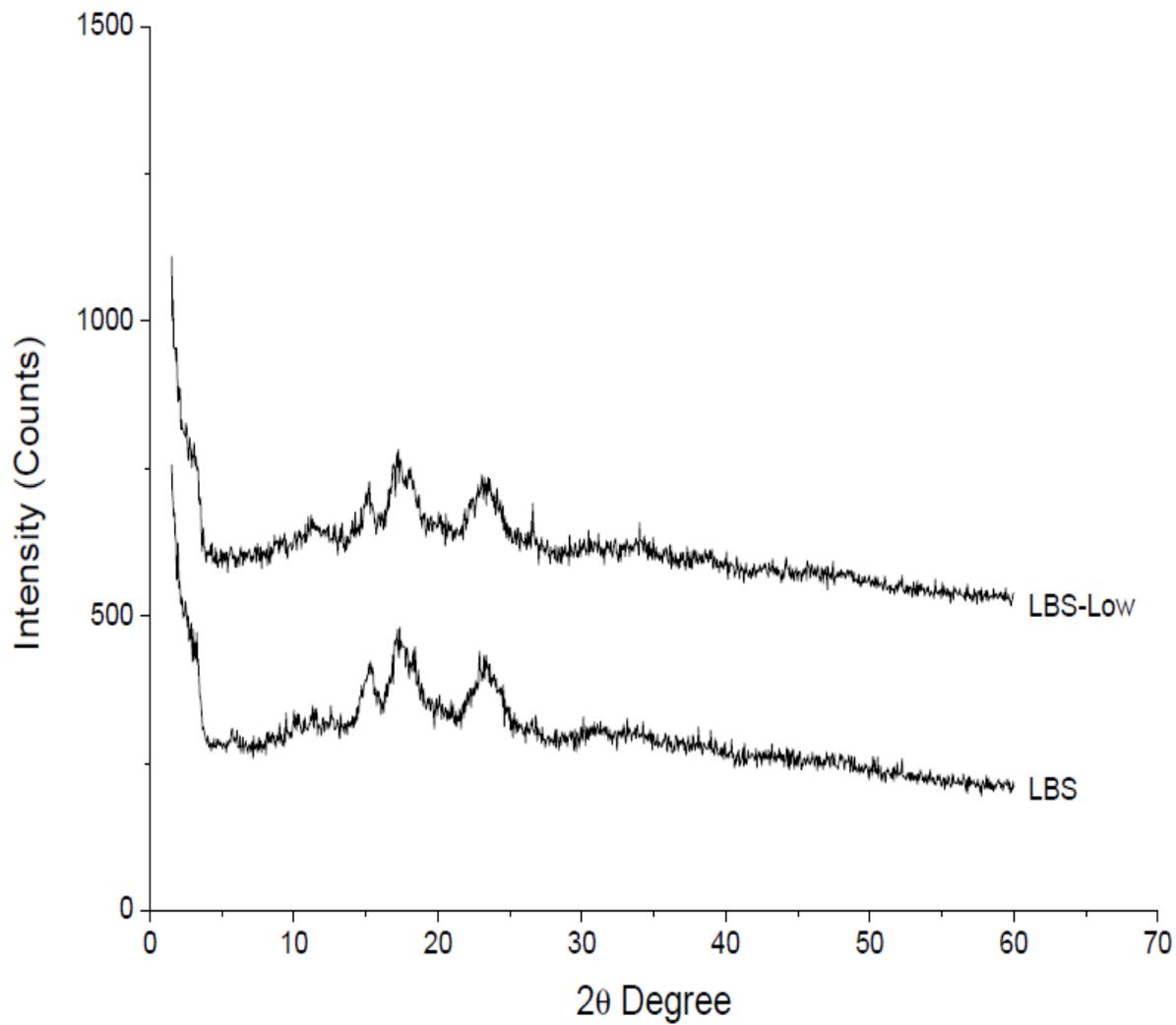
Figure 4.29: X-ray patterns of native and hydroxypropylated lima bean starches (LBS)
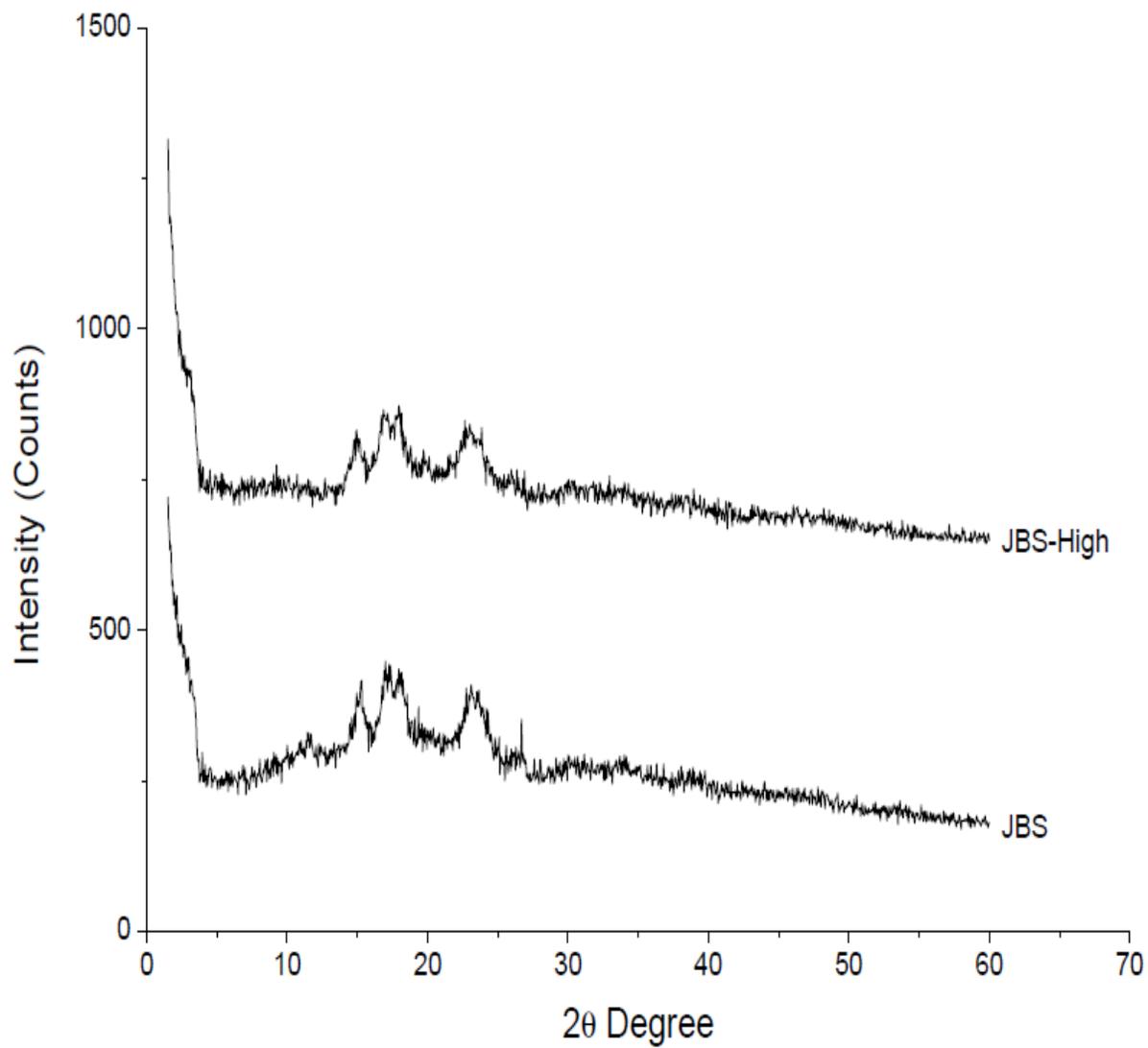
Figure 4.30: X-ray patterns of native and hydroxypropylated jack bean starches (JBS)
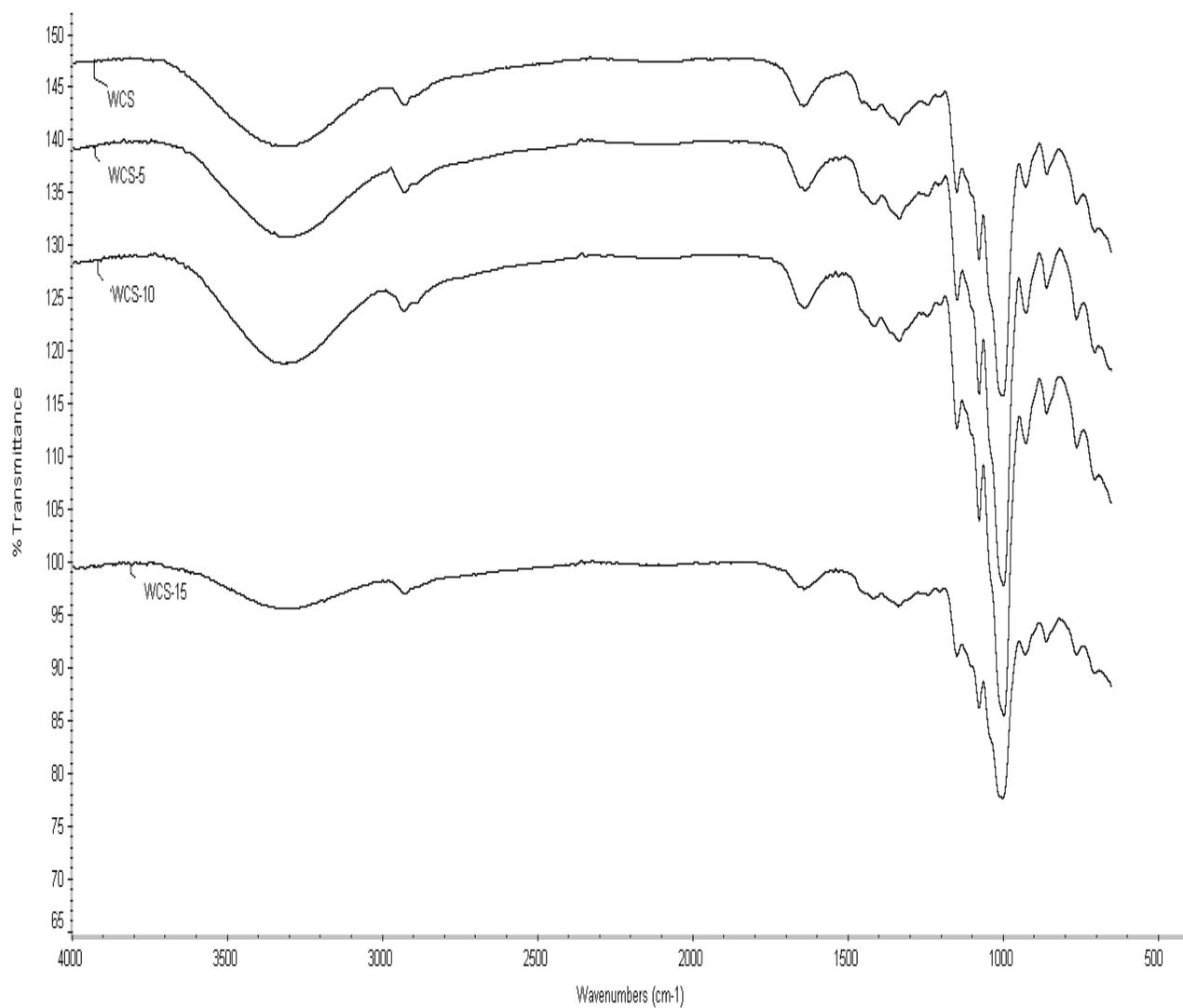
Figure 4.31: ATR-FTIR spectroscopy spectra of native and ozone-oxidized WCS
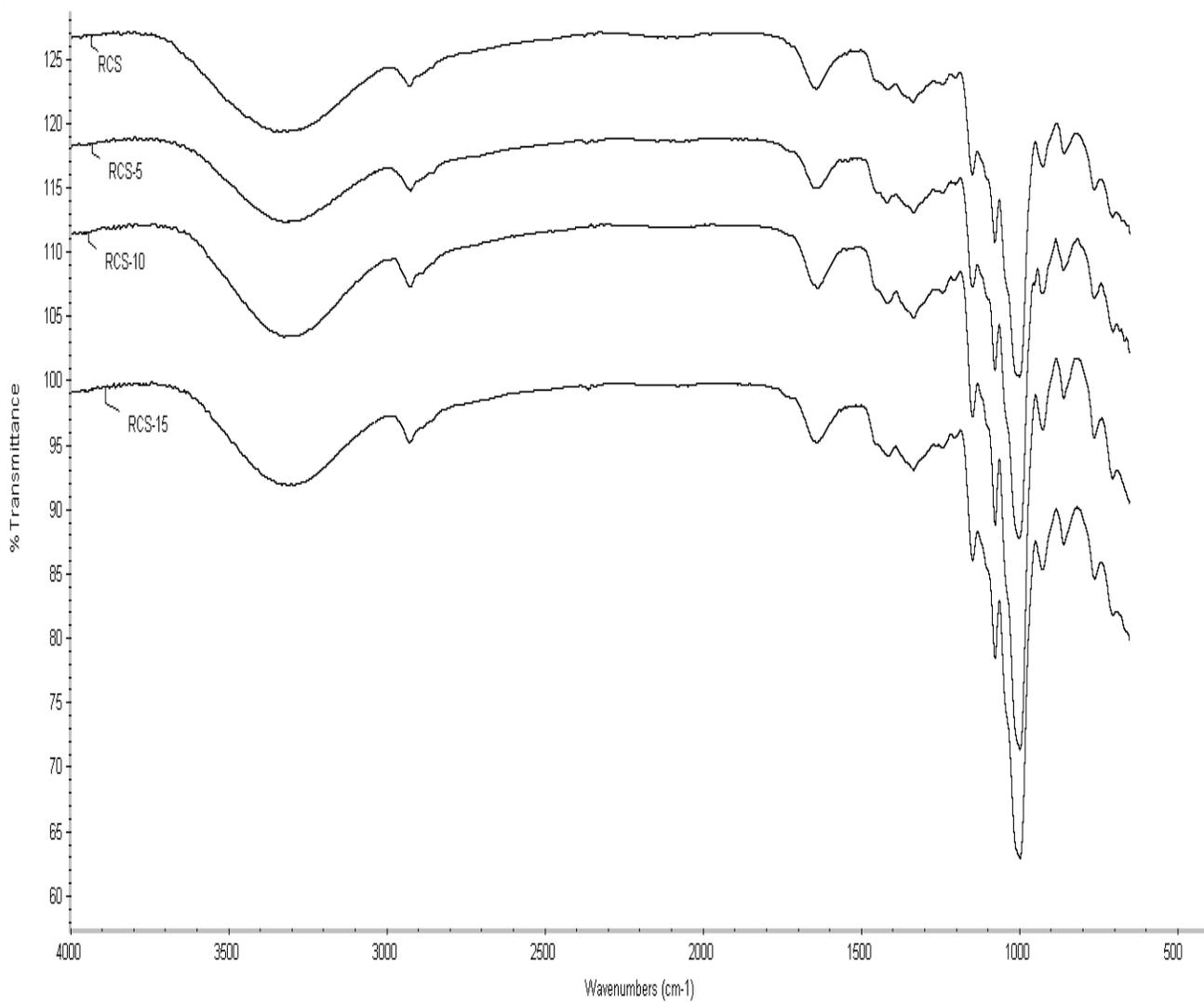
Figure 4.32: ATR-FTIR spectroscopy spectra of native and ozone-oxidized RCS
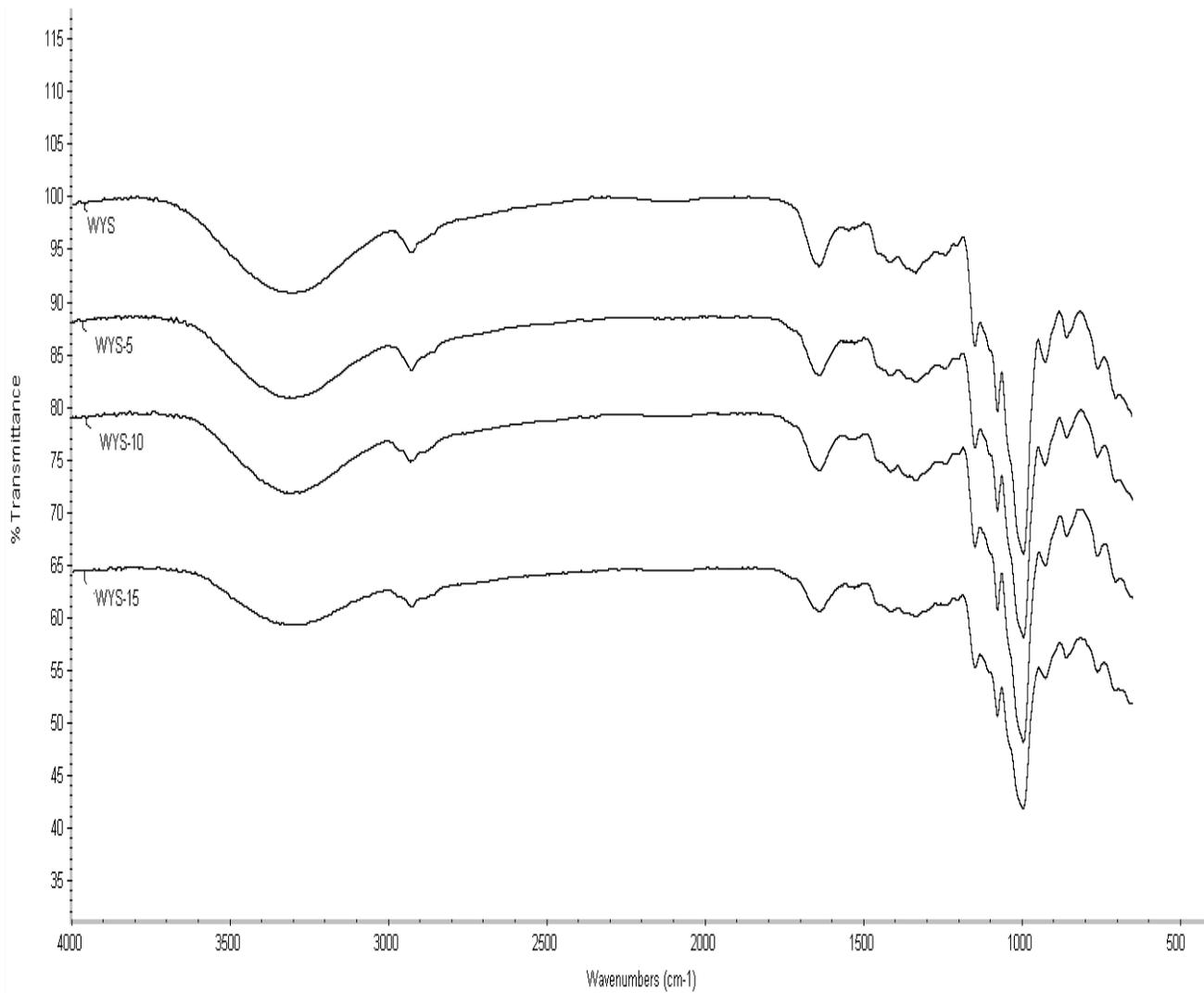
Figure 4.33: ATR-FTIR spectroscopy spectra of native and ozone-oxidized WYS
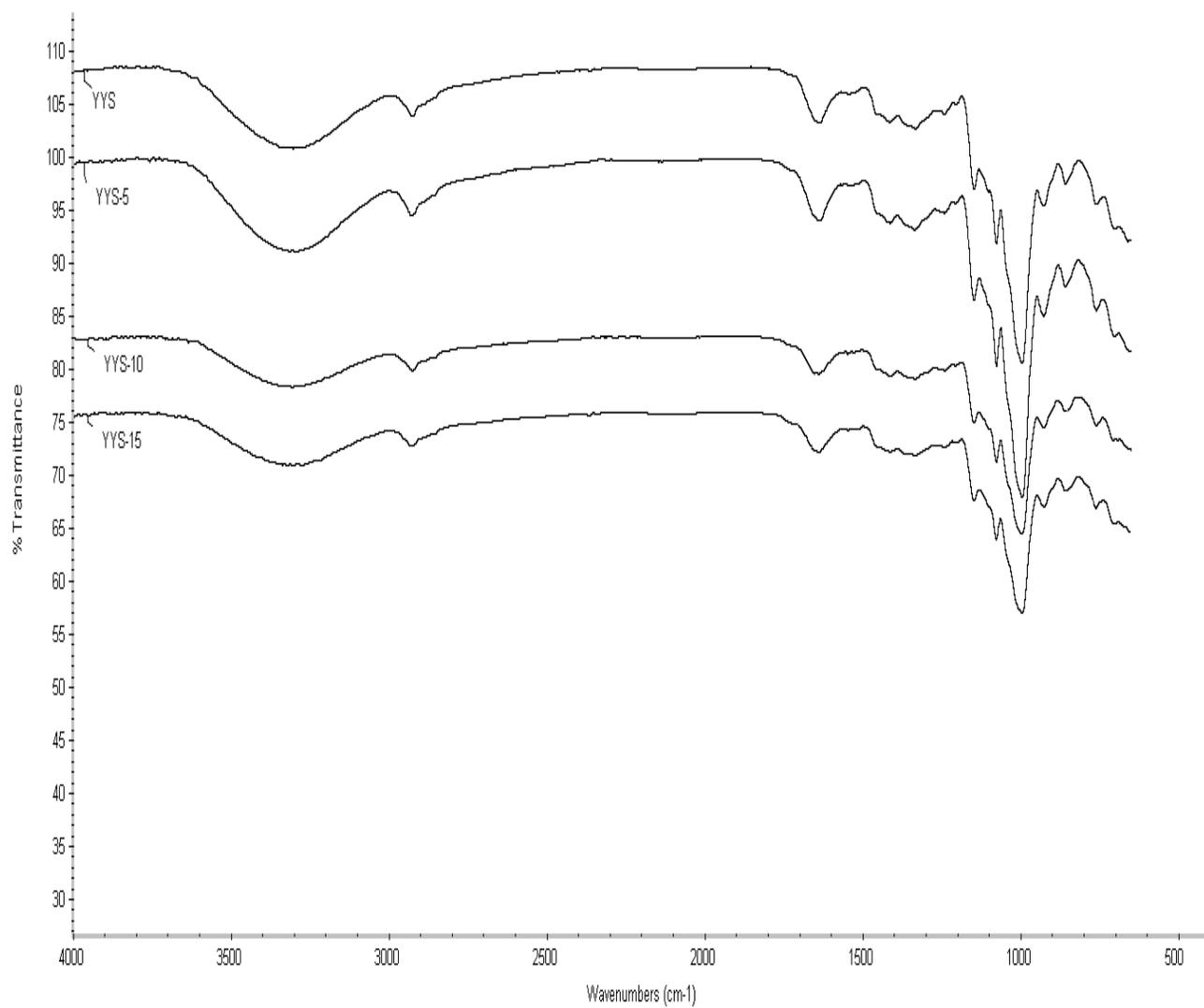
Figure 4.34: ATR-FTIR spectroscopy spectra of native and ozone-oxidized YYS
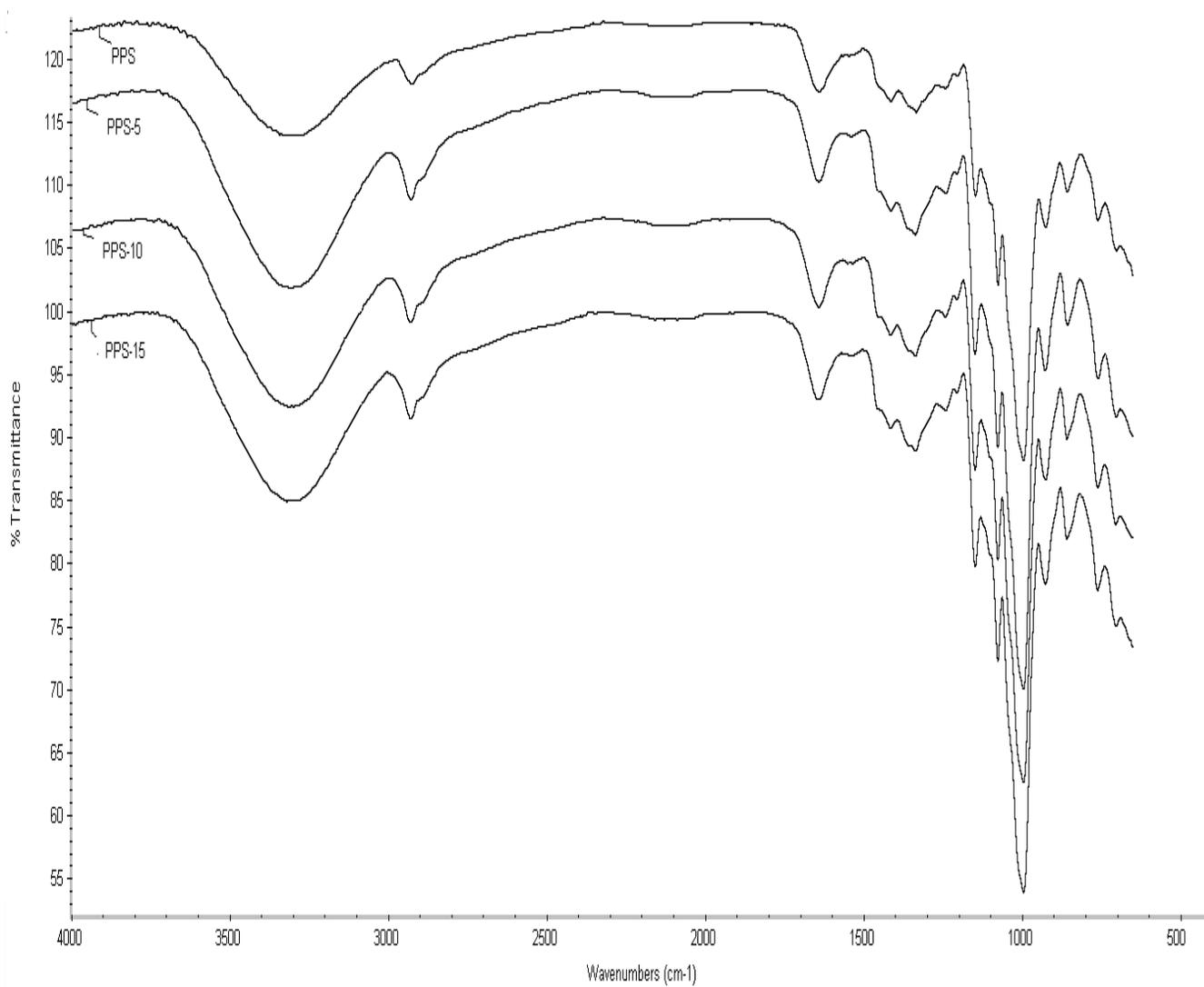
Figure 4.35: ATR-FTIR spectroscopy spectra of native and ozone-oxidized PPS
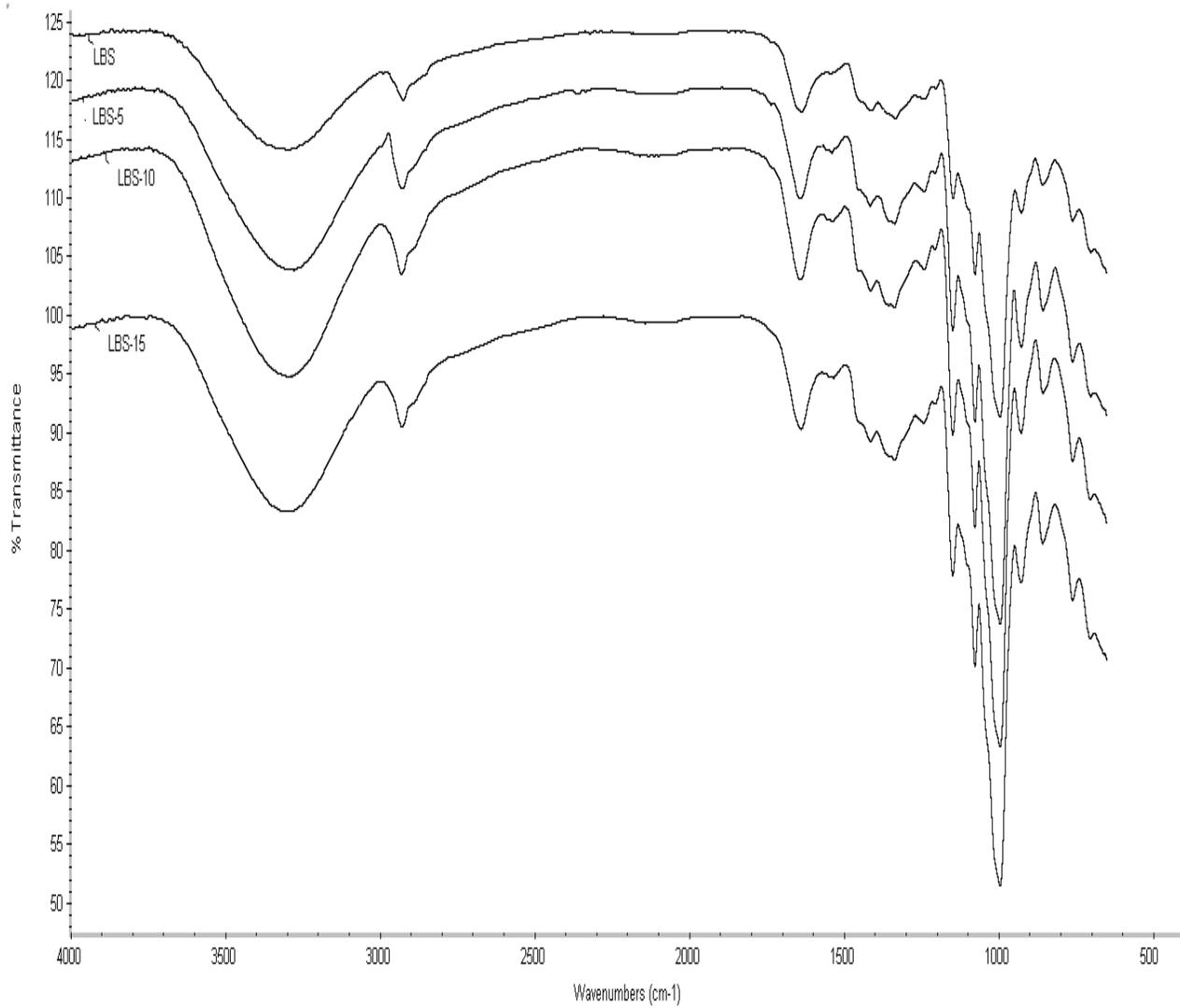
Figure 4.36: ATR-FTIR spectroscopy spectra of native and ozone-oxidized LBS
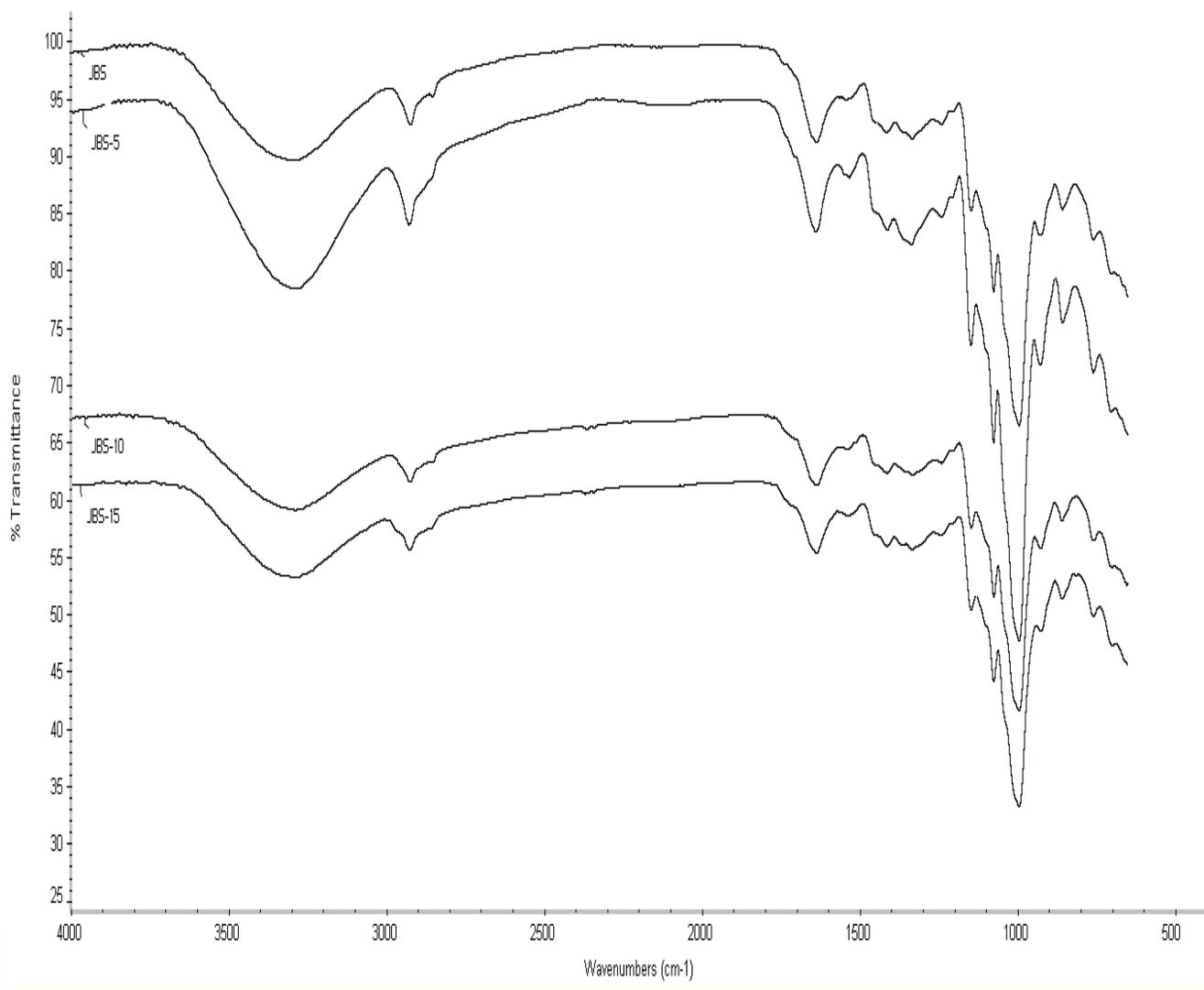
Figure 4.37: ATR-FTIR spectroscopy spectra of native and ozone-oxidized JBS
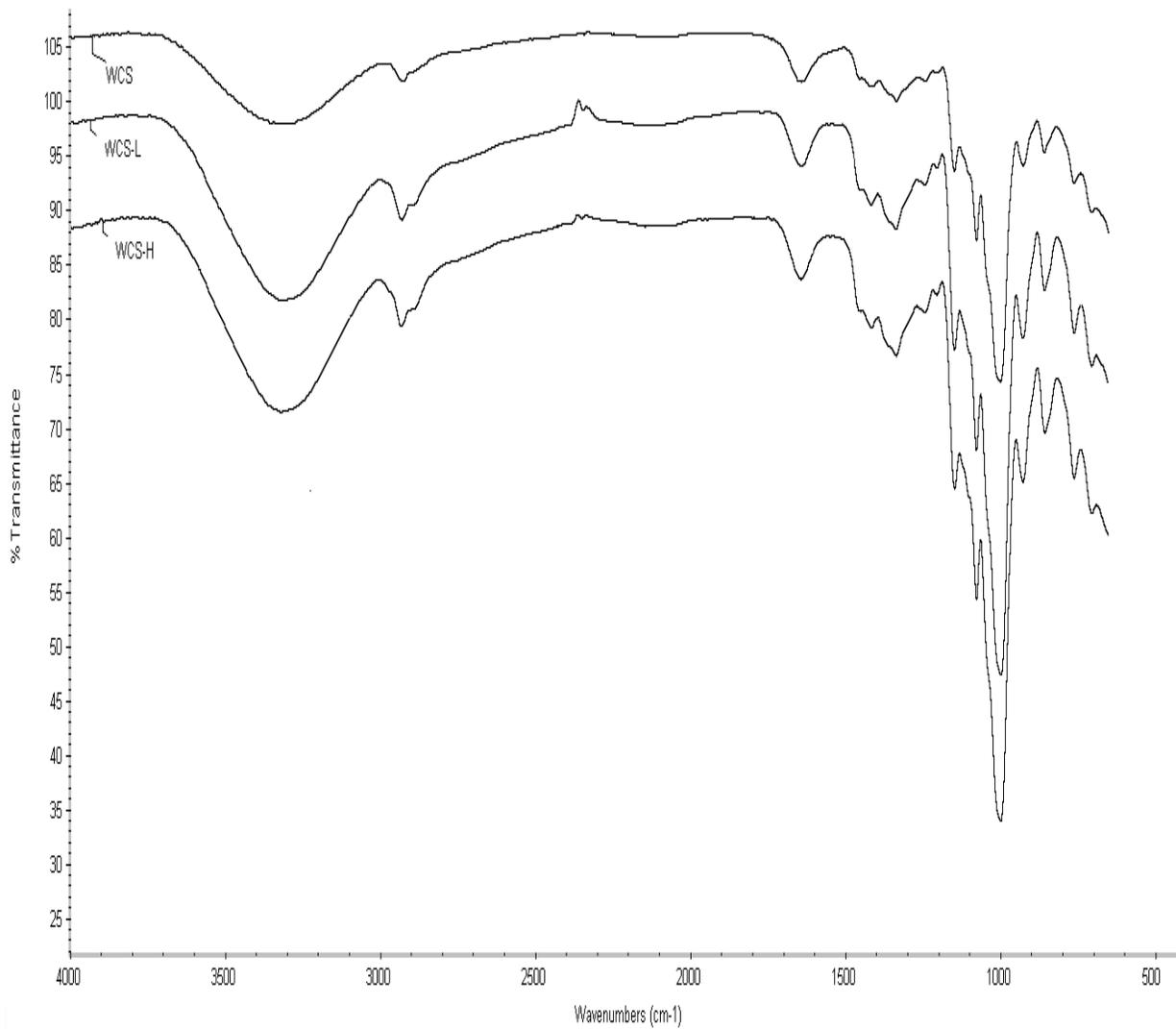
Figure 4.38: ATR-FTIR spectroscopy spectra of native and hydroxypropylated WCS
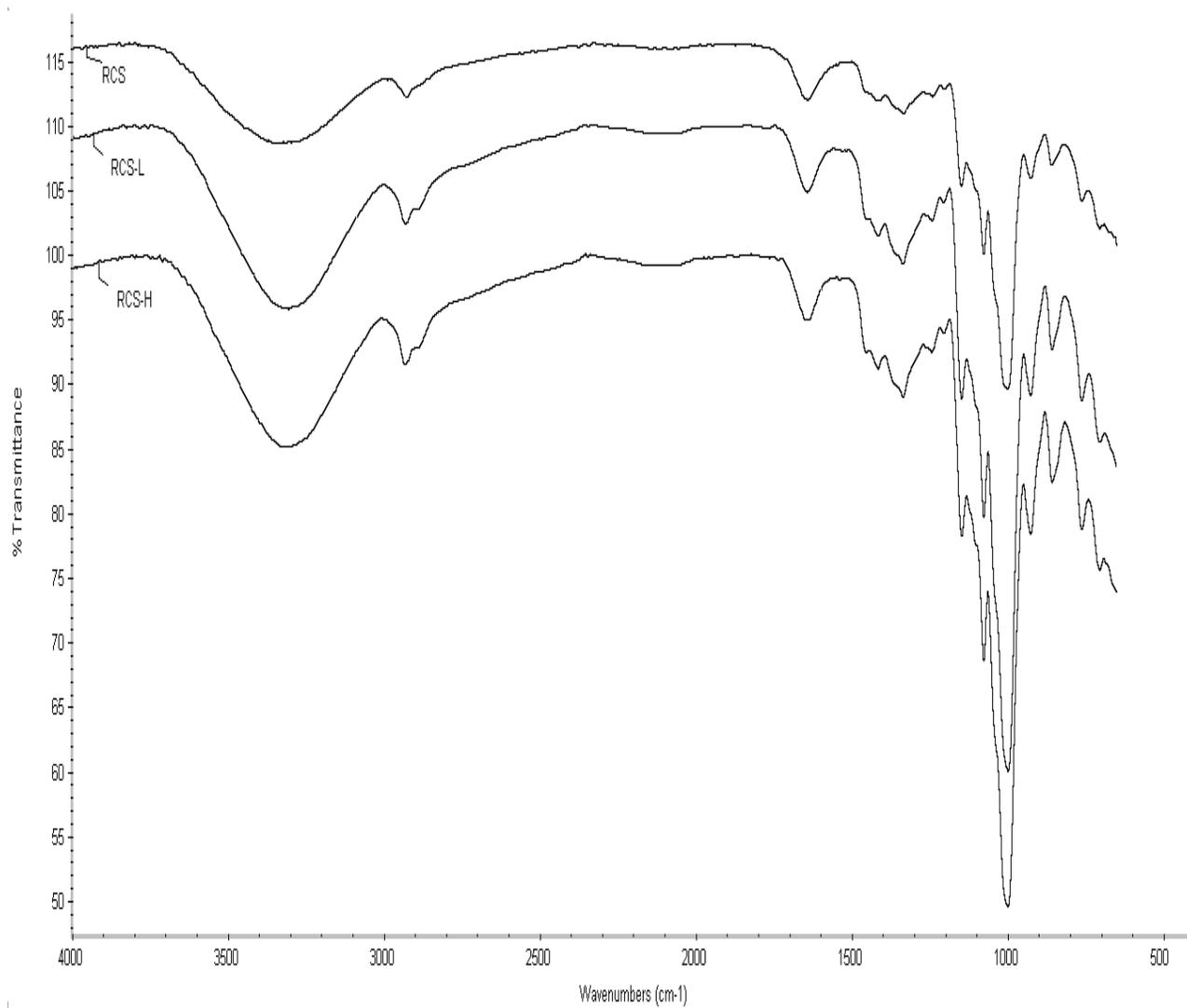
Figure 4.39: ATR-FTIR spectroscopy spectra of native and hydroxypropylated RCS
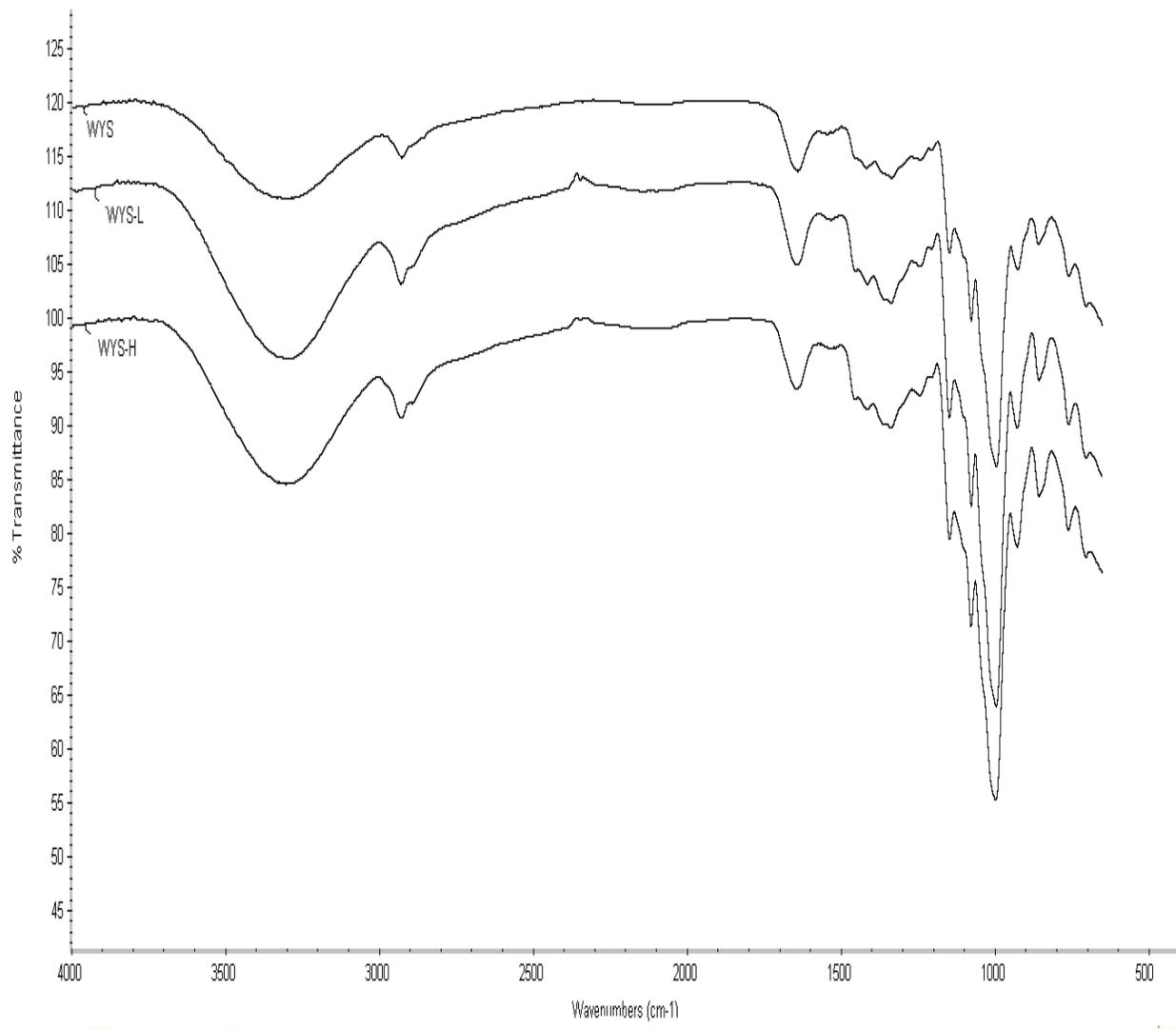
Figure 4.40: ATR-FTIR spectroscopy spectra of native and hydroxypropylated WYS
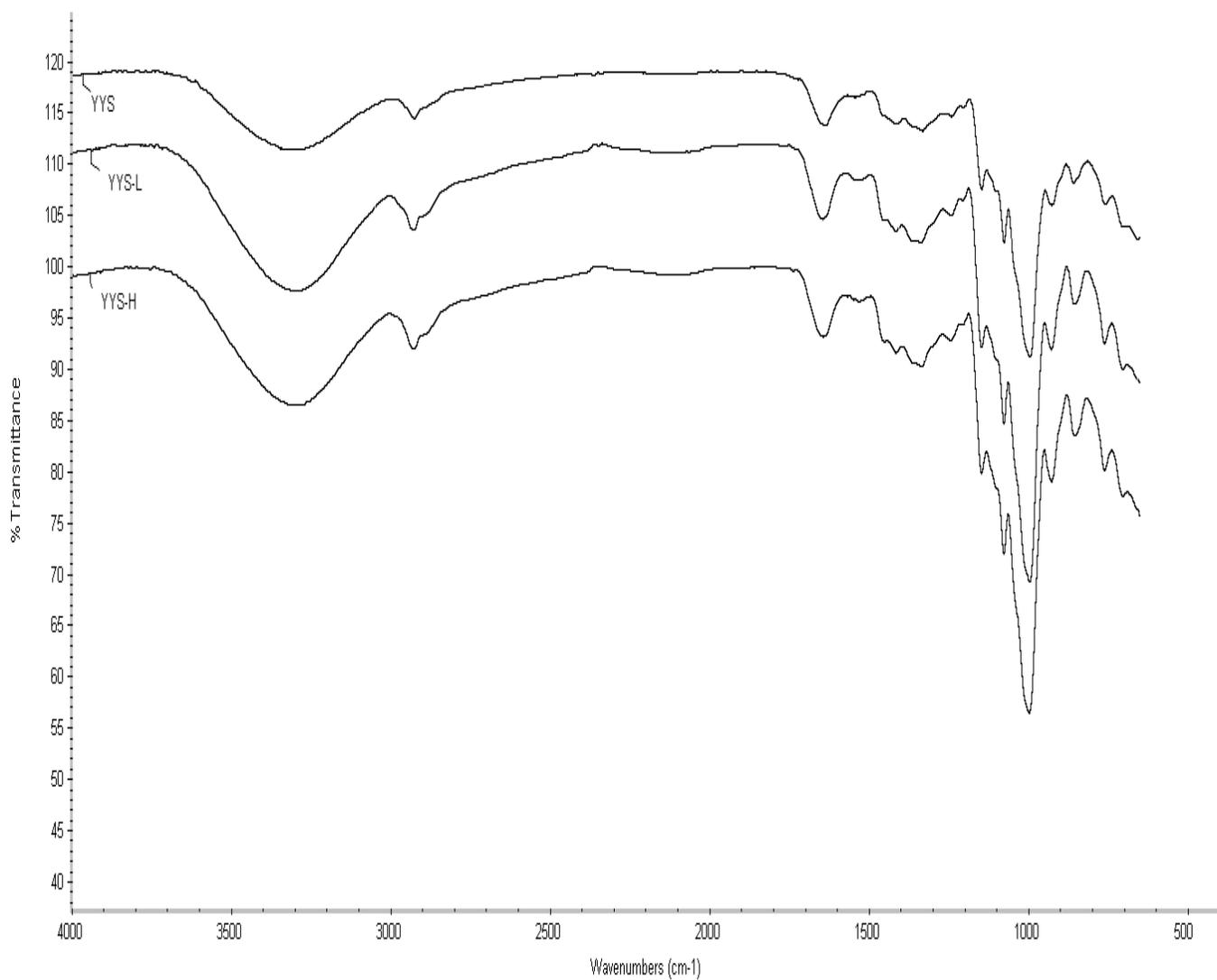
Figure 4.41: ATR-FTIR spectroscopy spectra of native and hydroxypropylated YYS
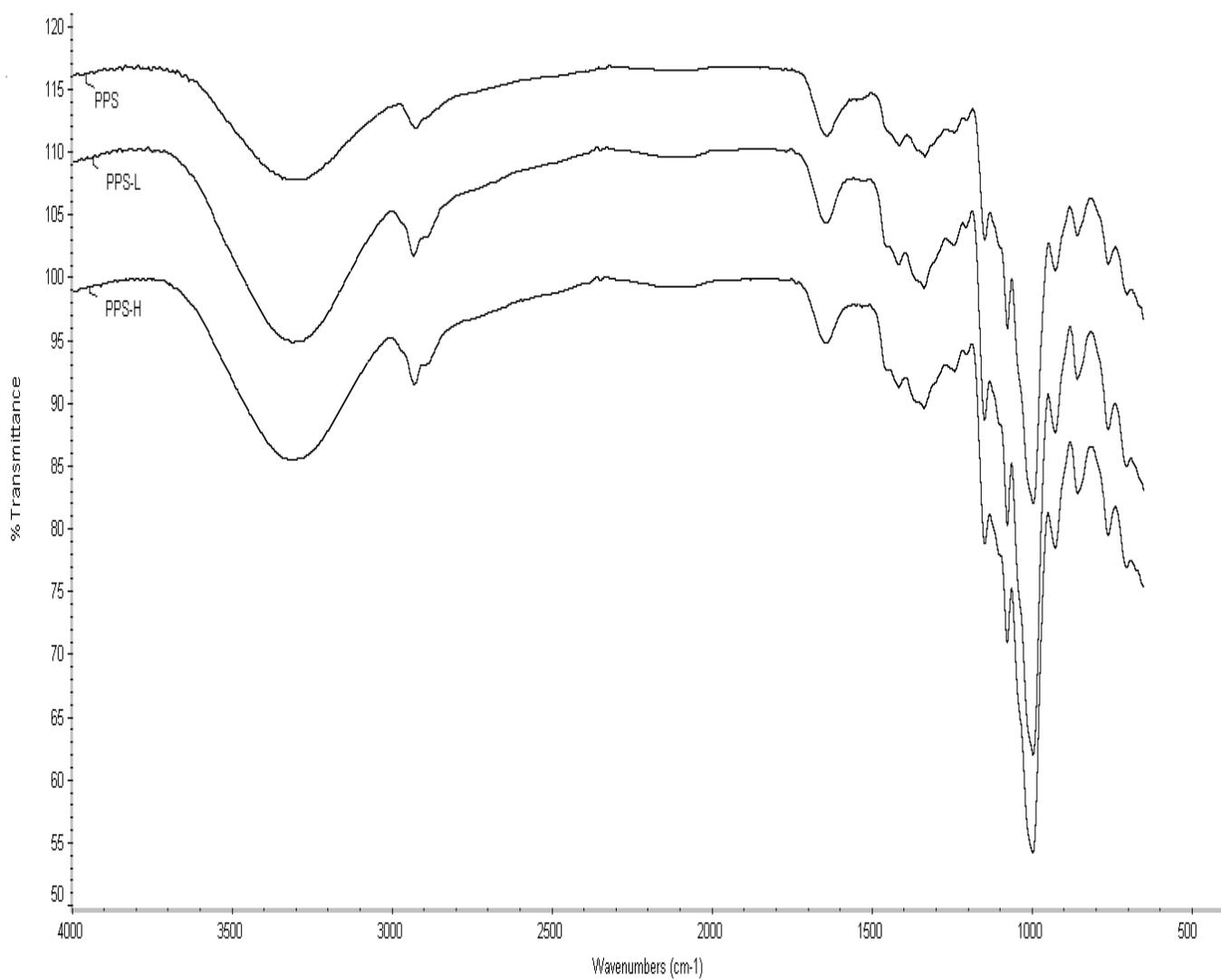
Figure 4.42: ATR-FTIR spectroscopy spectra of native and hydroxypropylated PPS
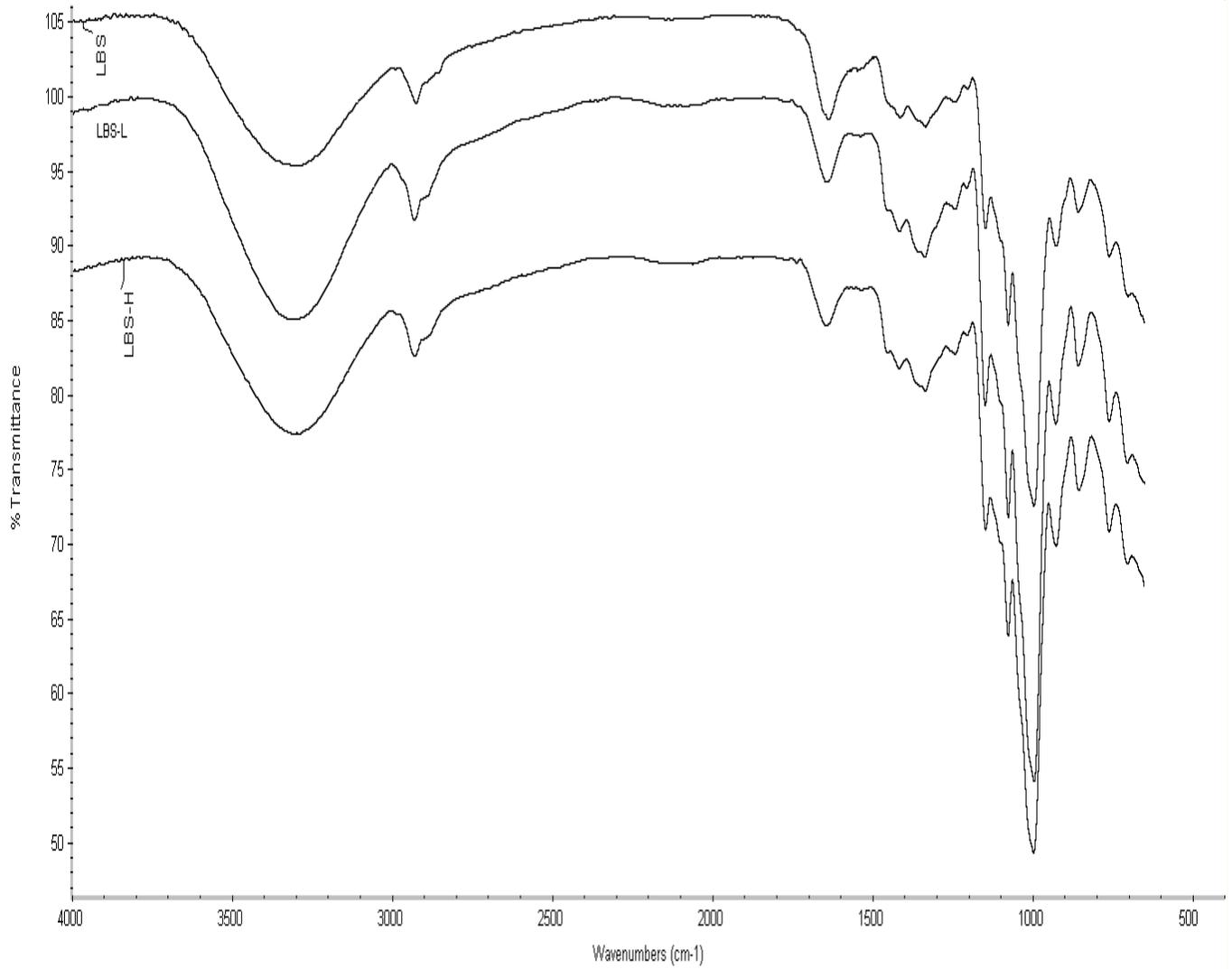
Figure 4.43: ATR-FTIR spectroscopy spectra of native and hydroxypropylated LBS
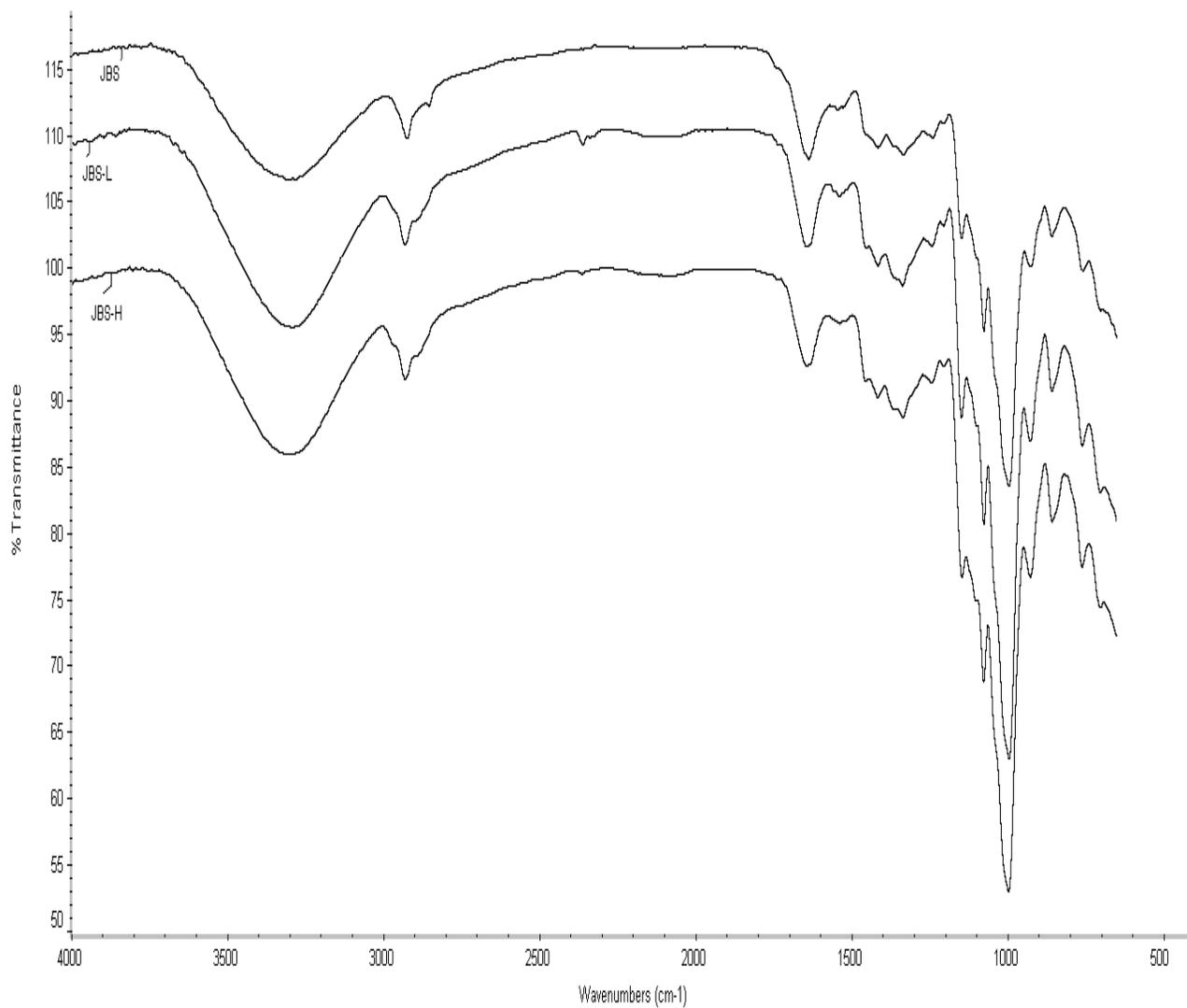
Figure 4.44: ATR-FTIR spectroscopy spectra of native and hydroxypropylated JBS
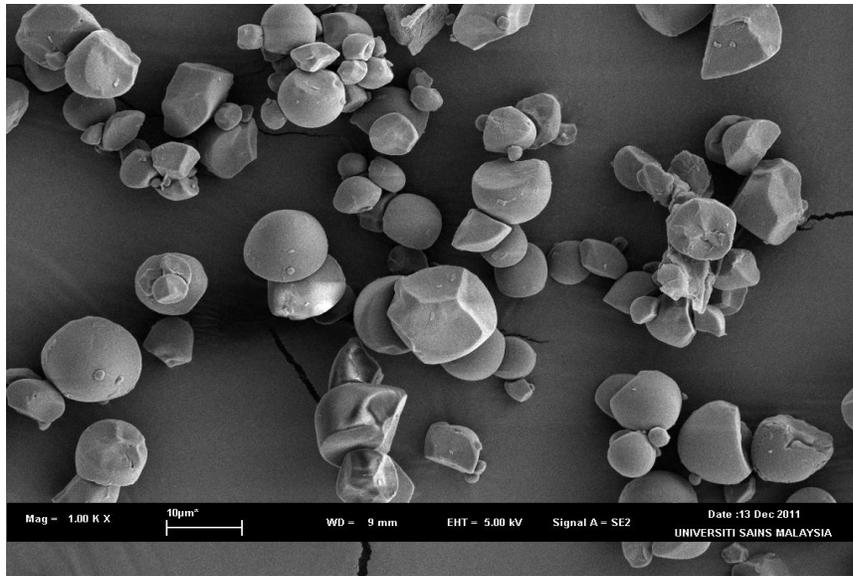
(a)
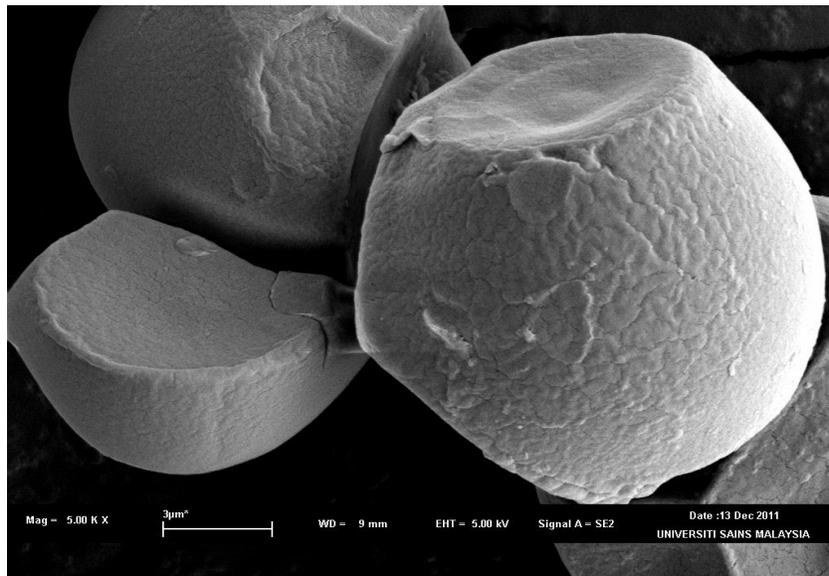
(b)

Figure 4.45: Scanning electron micrographs of WCS at: (a) 1.00K ✕, 10 μm; (b) 5.00K ✕, 3 μm
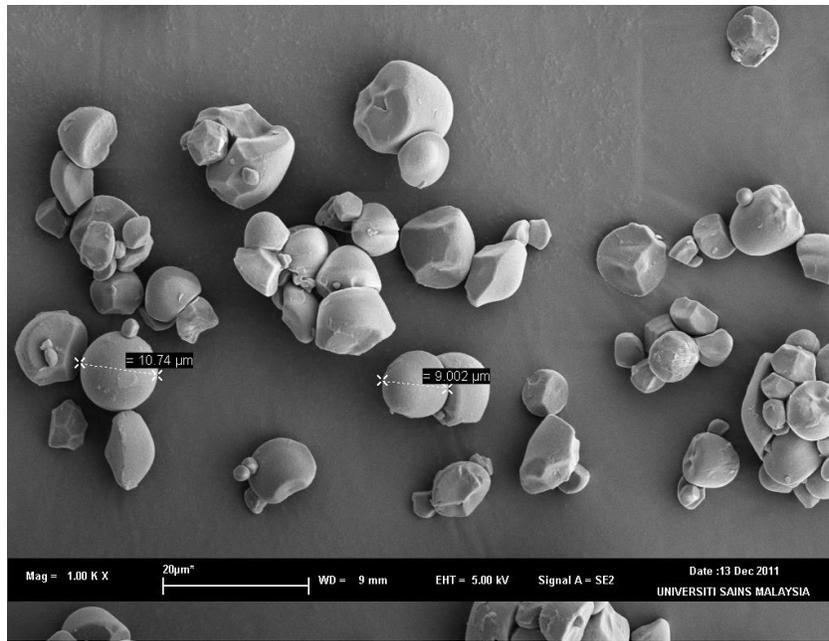
(a)
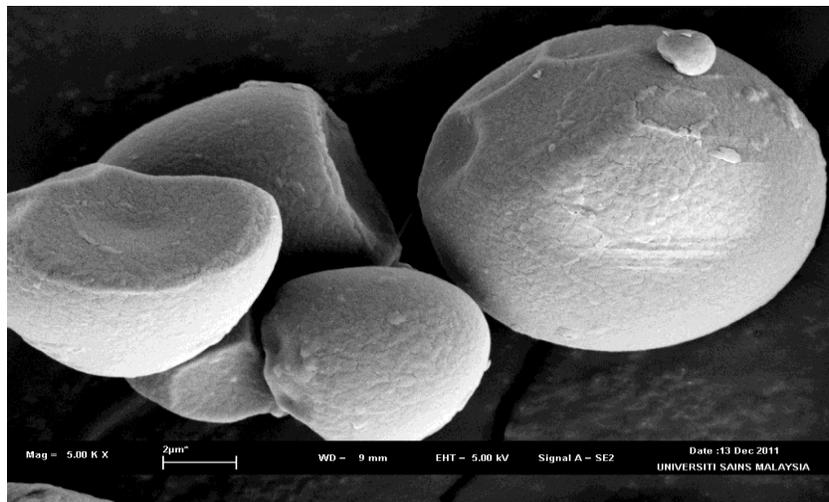
(b)

Figure 4.46: Scanning electron micrographs of RCS at: (a) 1.00K ✕, 10 μm; (b) 5.00K ✕, 3 μm
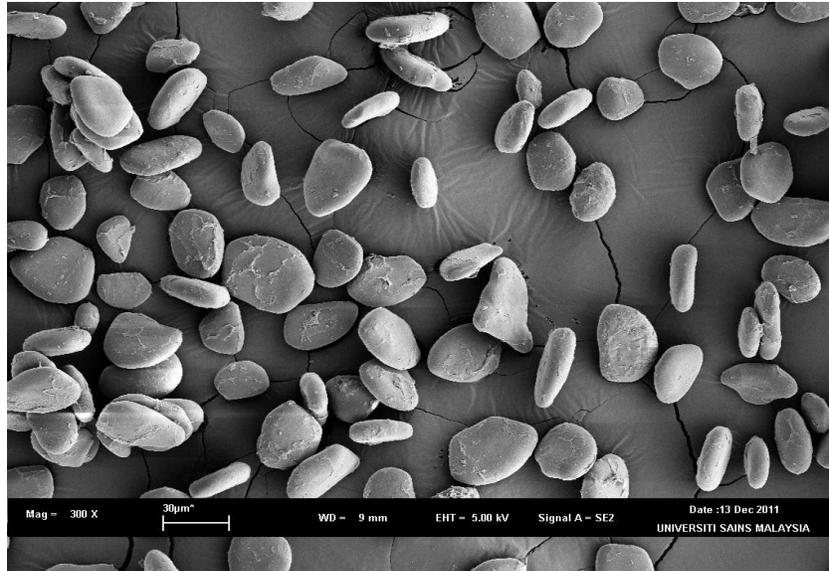
(a)
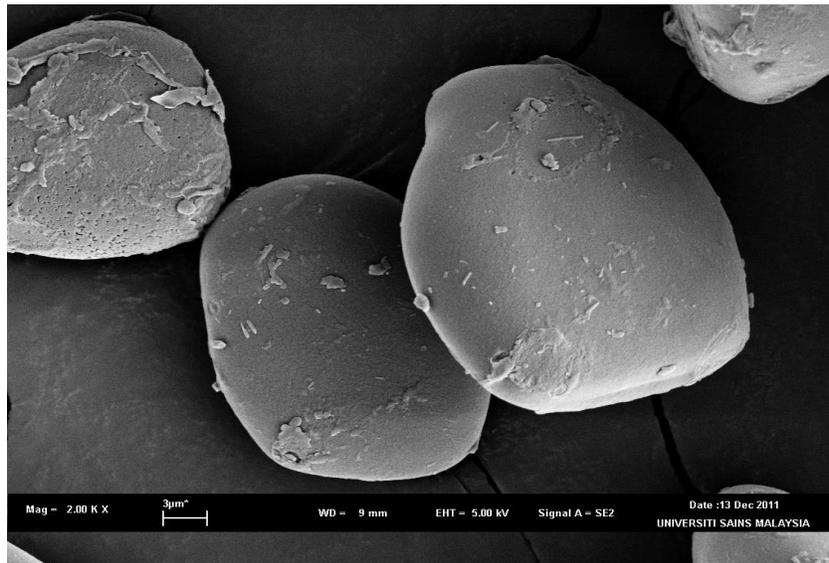
(b)

Figure 4.47: Scanning electron micrographs of WYS at: (a) 0.300K ✕, 30 µm; (b) 2.00K ✕, 3 µm
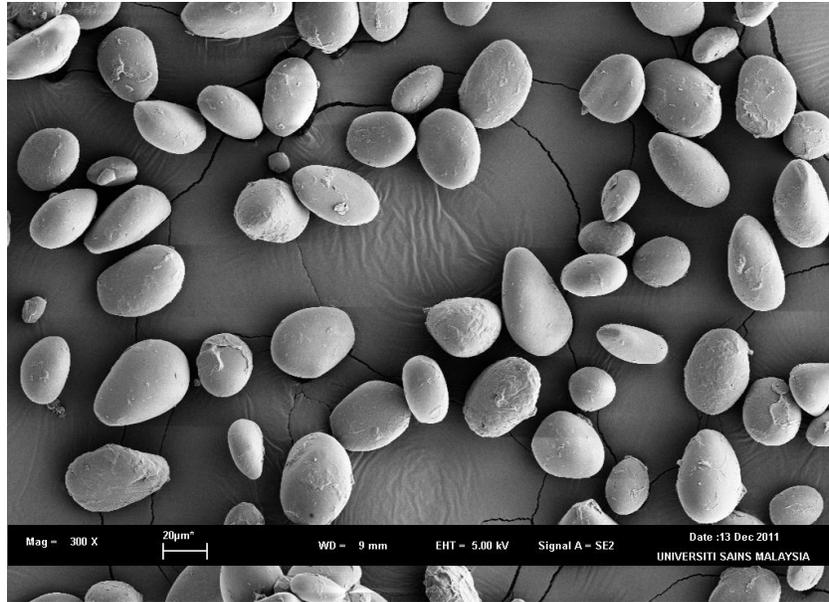
(a)
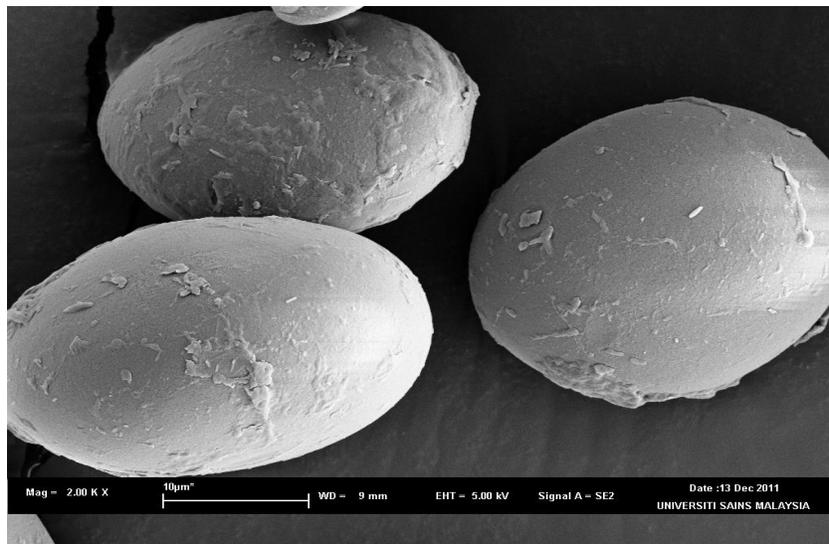
(b)

Figure 4.48: Scanning electron micrographs of YYS at: (a) 0.300K ✕, 20 µm; (b) 2.00K ✕, 10 µm
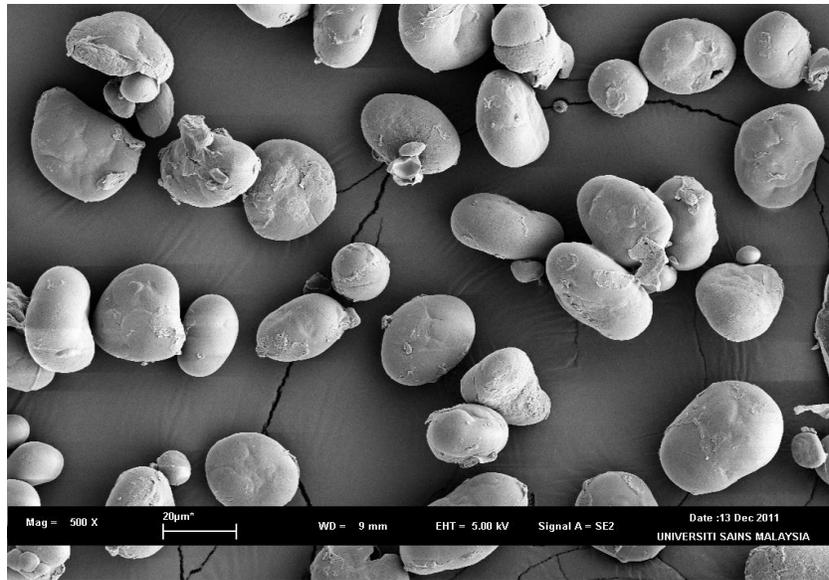
(a)
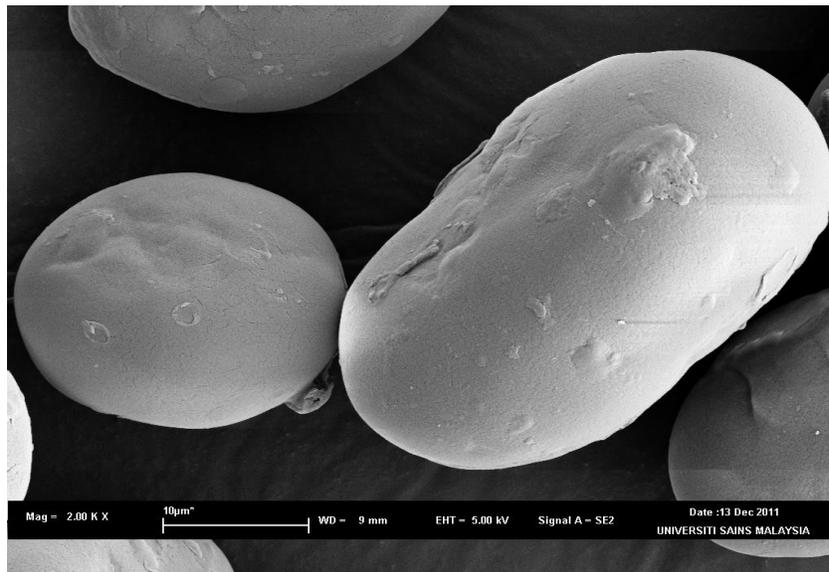
(b)

Figure 4.49: Scanning electron micrographs of PPS at: (a) 0.500K ✕, 20 μm; (b) 2.00K ✕, 10 μm
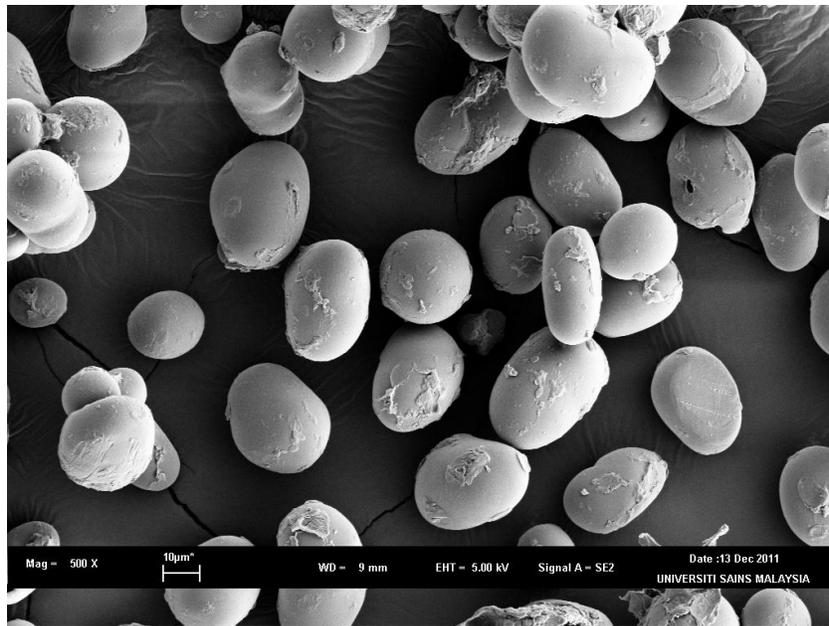
(a)
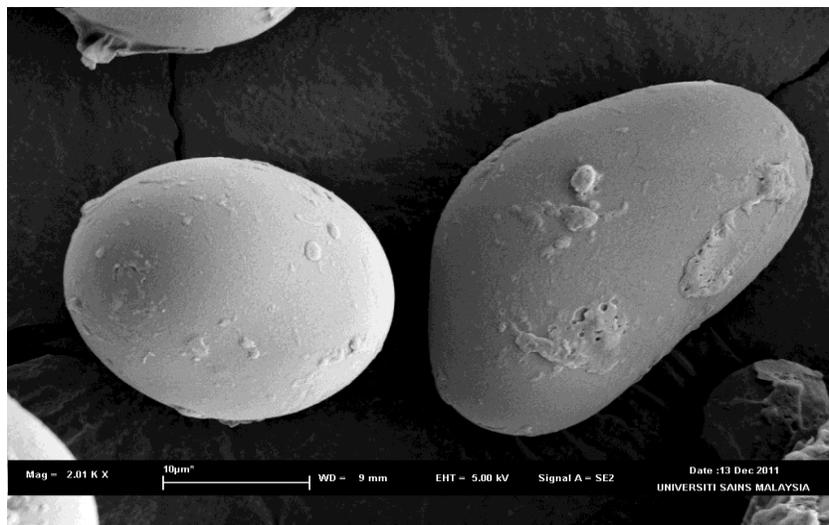
(b)

Figure 4.50: Scanning electron micrographs of LBS at: (a) 0.500K ✕, 10 μm; (b) 2.00K ✕, 10 μm
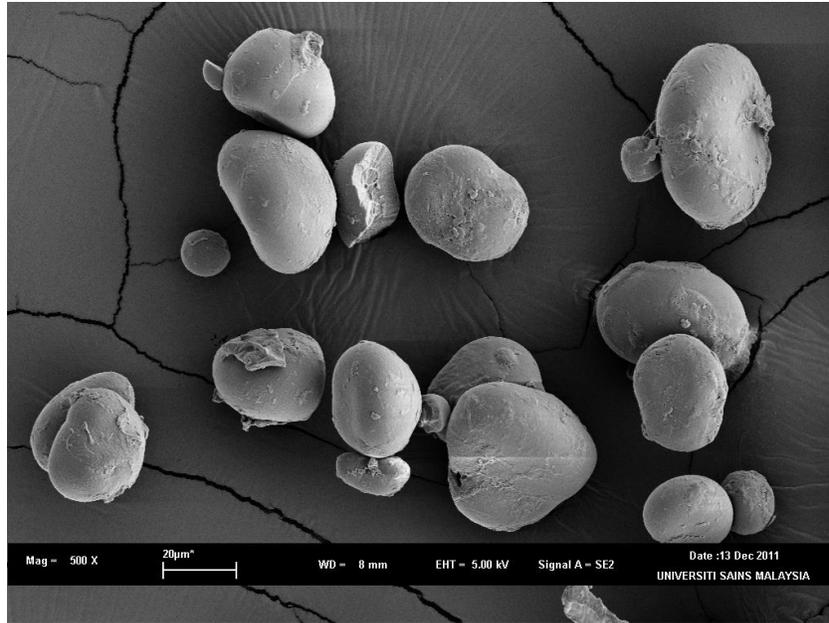
(a)
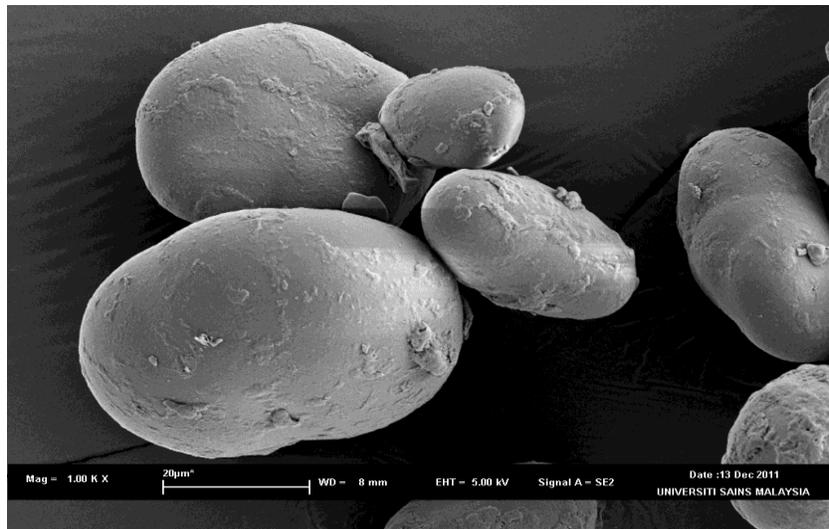
(b)

Figure 4.51: Scanning electron micrographs of JBS at: (a) 0.500K ⨯, 10 µm; (b) 2.00K ⨯, 3 µm
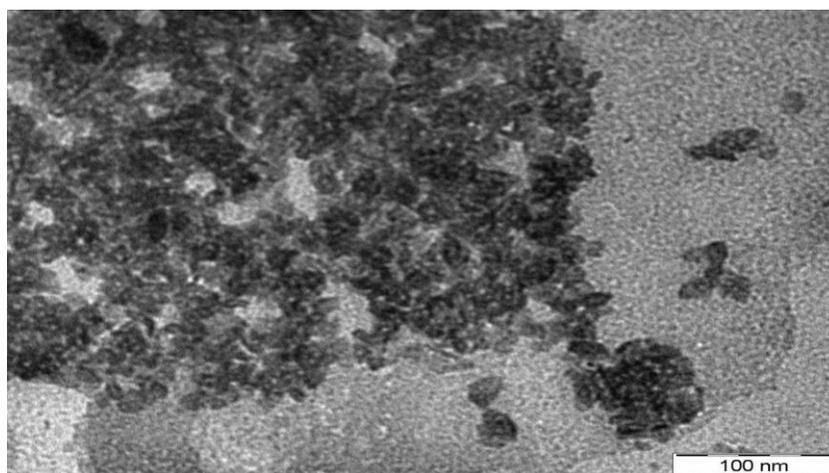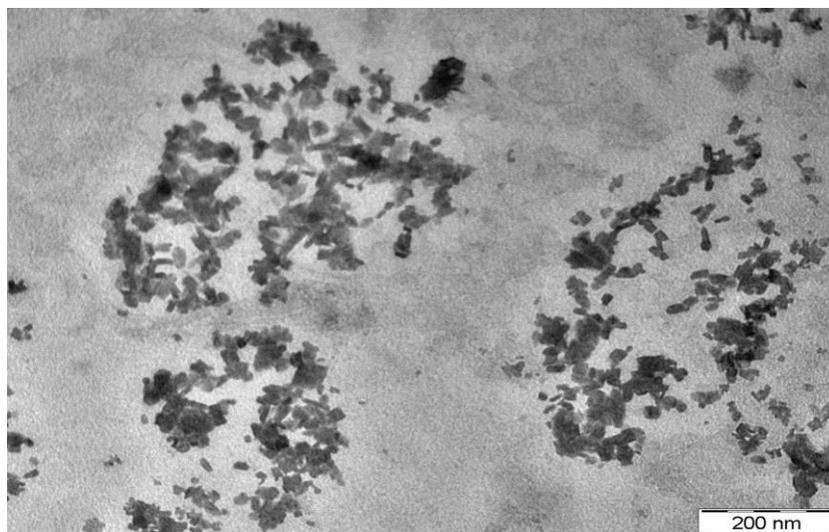
Figure 4.52: Transmission electron micrographs of negatively stained preparations from WCS granules treated with H_2SO_4 at 40°C under continuous stirring (200 nm, 100 nm)
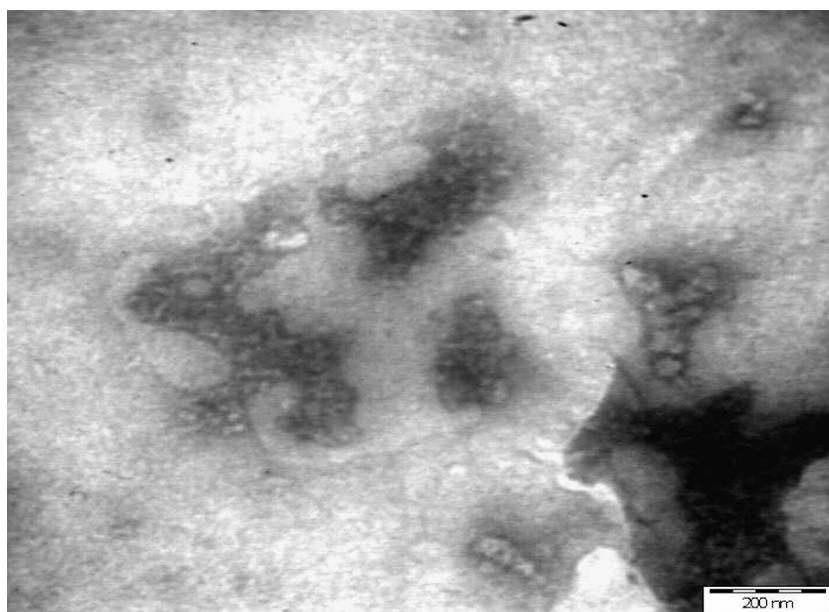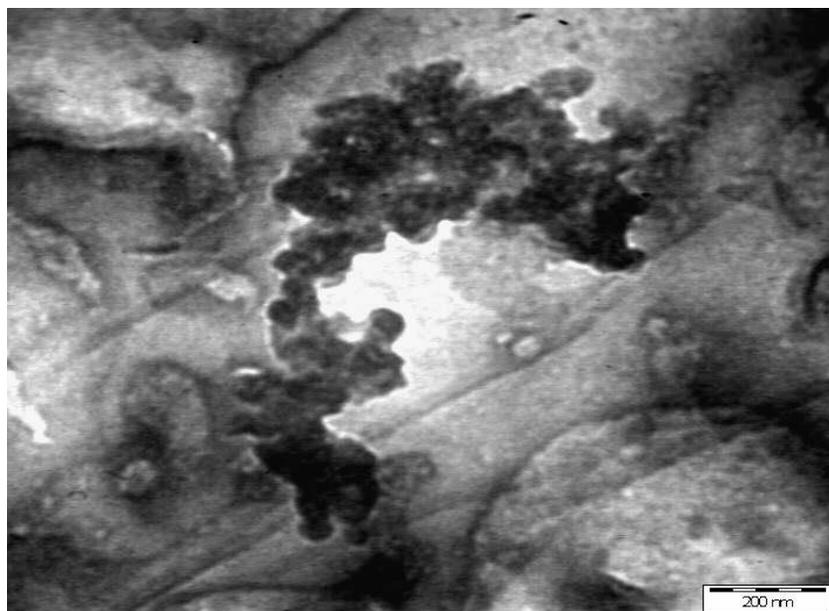
Figure 4.53: Transmission electron micrographs of negatively stained preparations from RCS granules treated with H_2SO_4 at 40°C under continuous stirring (200 nm)
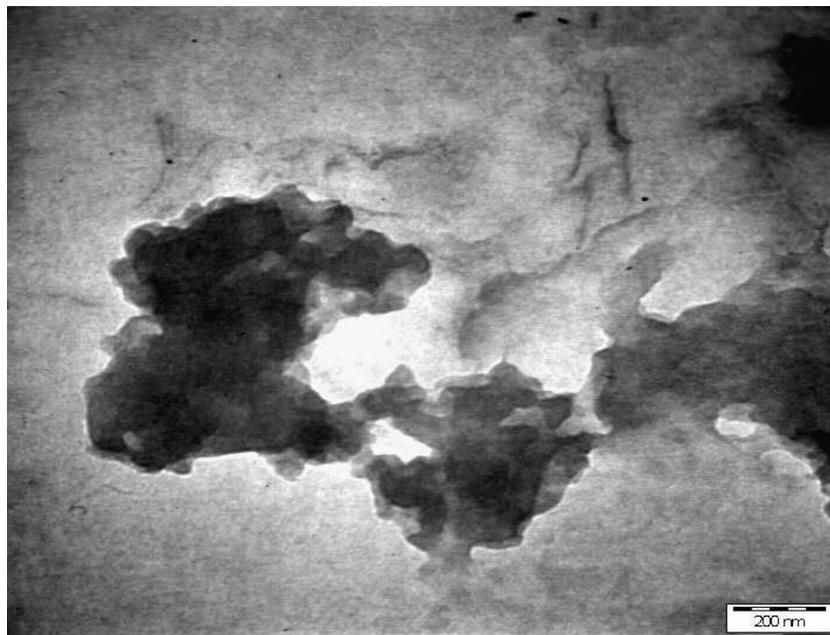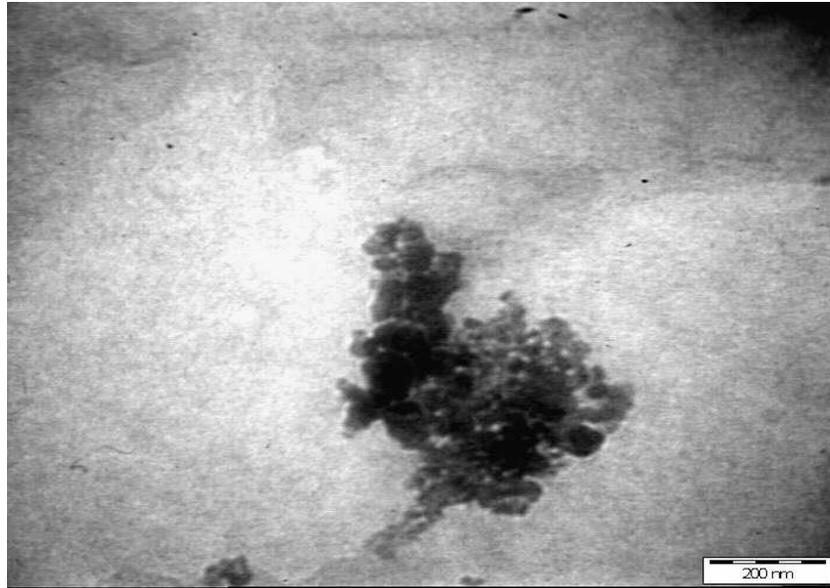
Figure 4.54: Transmission electron micrographs of negatively stained preparations from WYS granules treated with H_2SO_4 at 40°C under continuous stirring (200 nm)
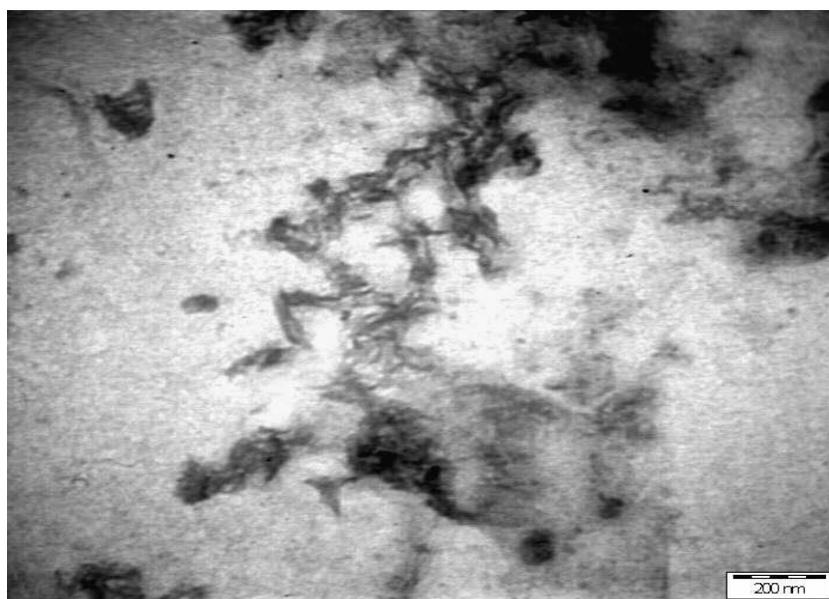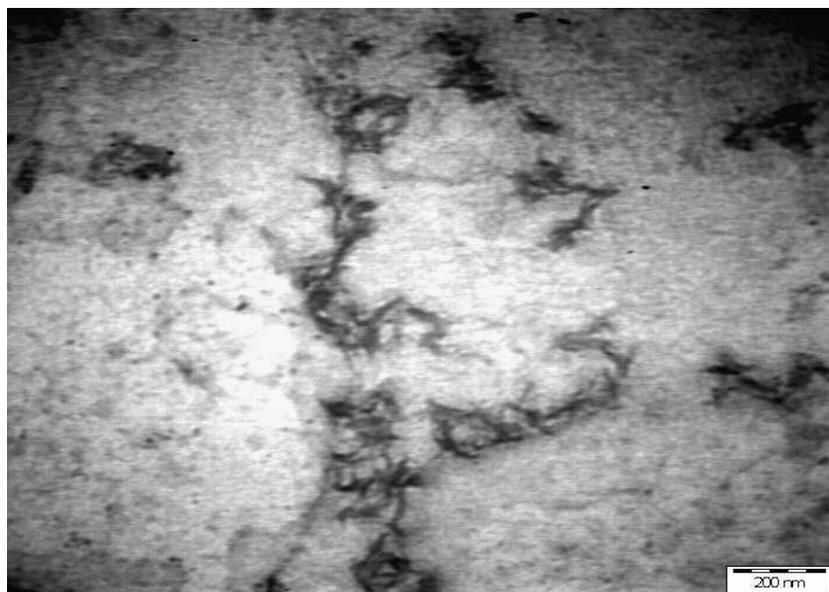
Figure 4.55: Transmission electron micrographs of negatively stained preparations from YYS granules treated with H_2SO_4 at 40^oC under continuous stirring (200 nm)
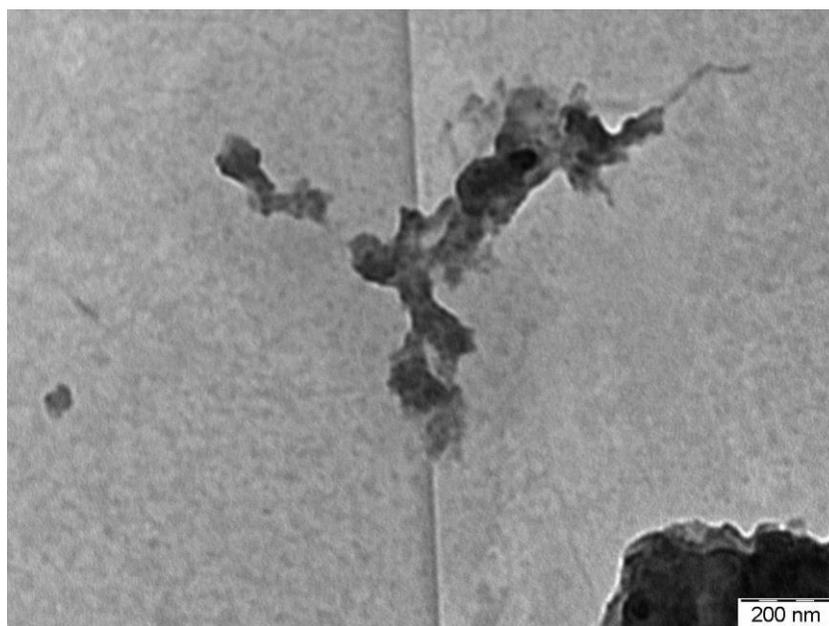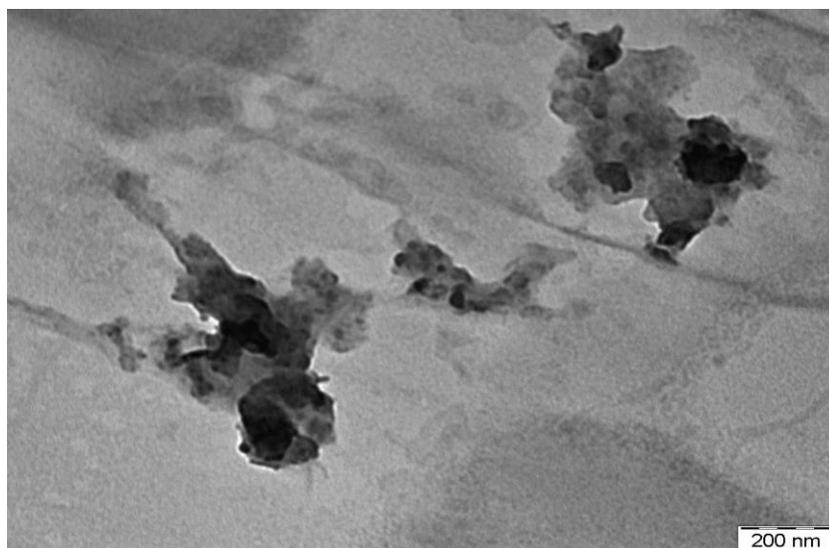
Figure 4.56: Transmission electron micrographs of negatively stained preparations from PPS granules treated with H_2SO_4 at 40°C under continuous stirring (200 nm)
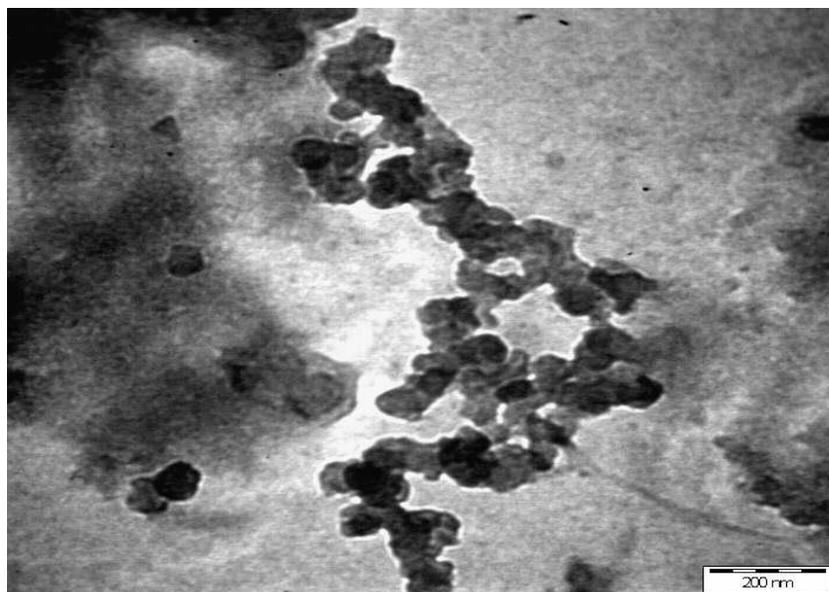
Figure 4.57: Transmission electron micrographs of negatively stained preparations from LBS granules treated with H_2SO_4 at 40°C under continuous stirring (200 nm)
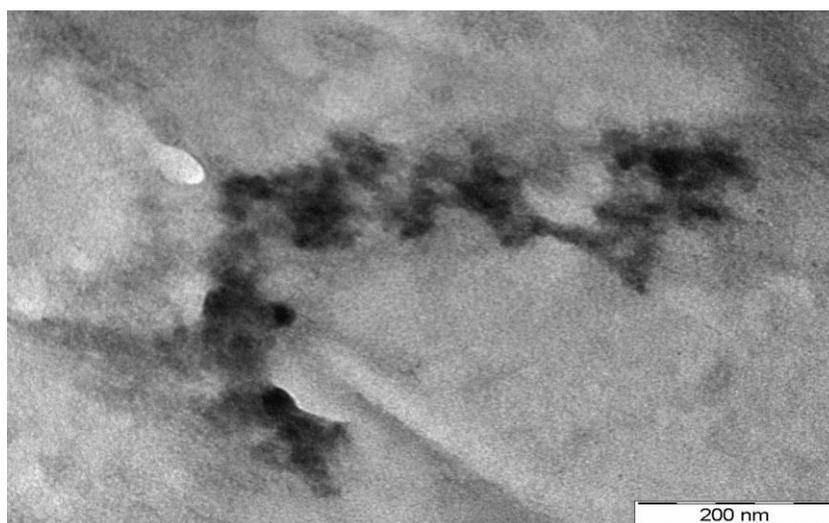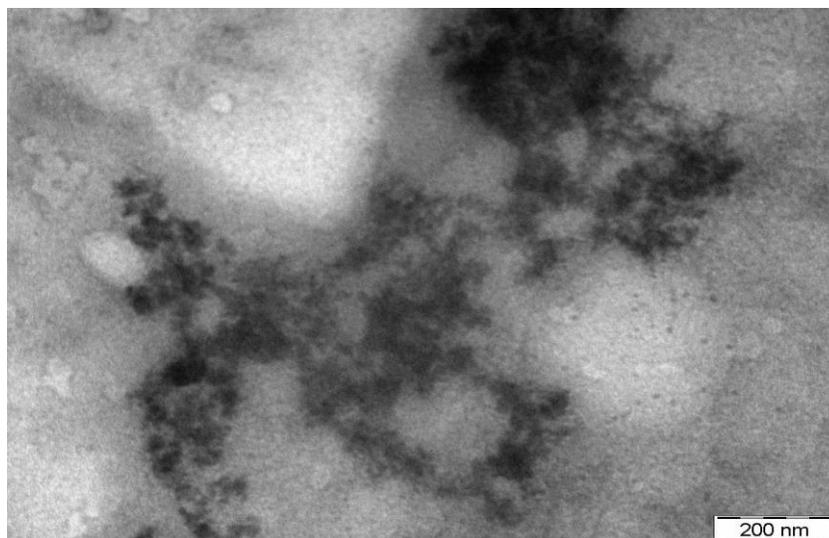
Figure 4.58: Transmission electron micrographs of negatively stained preparations from JBS granules treated with H_2SO_4 at 40°C under continuous stirring (200 nm)
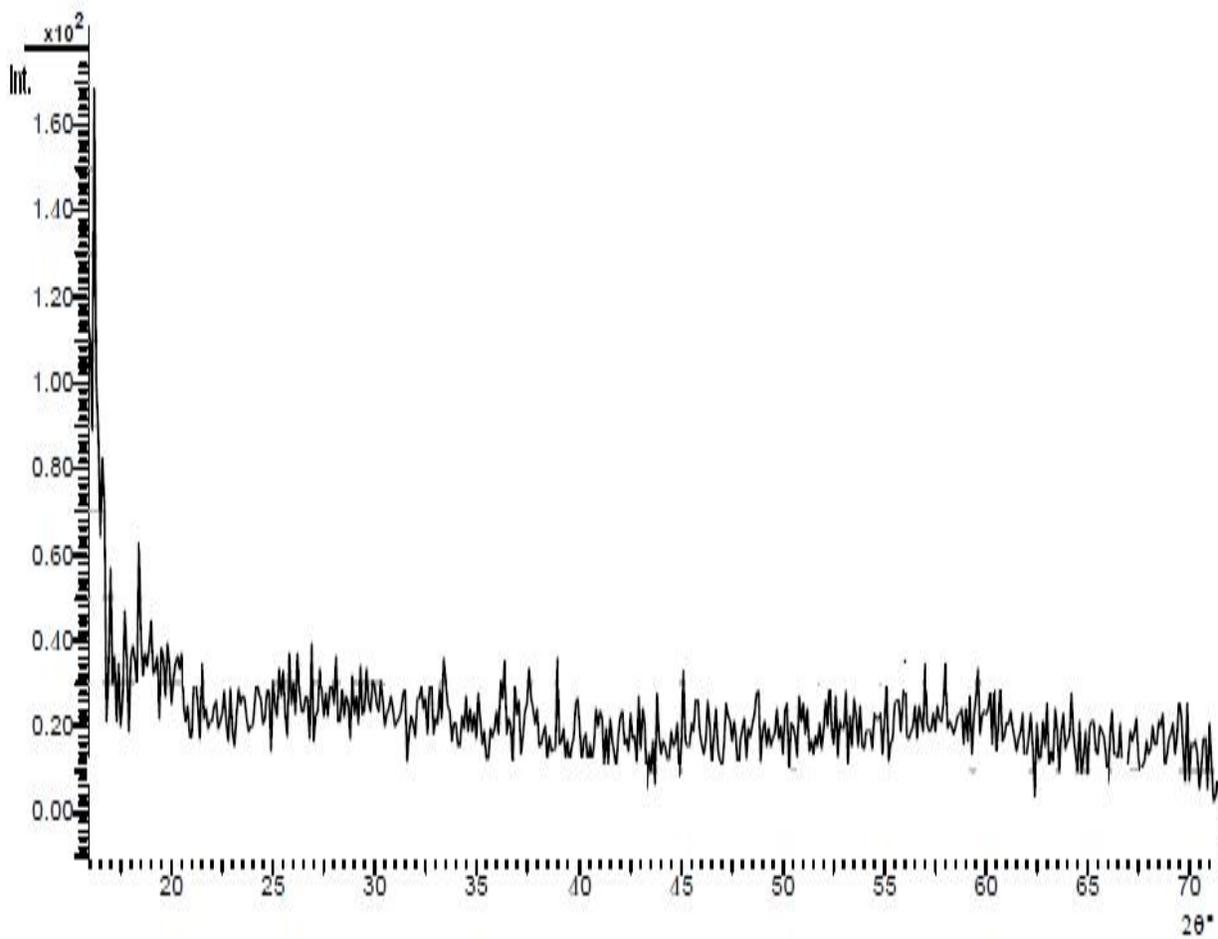
Figure 4.59: X-ray pattern of nanocrystals of WCS
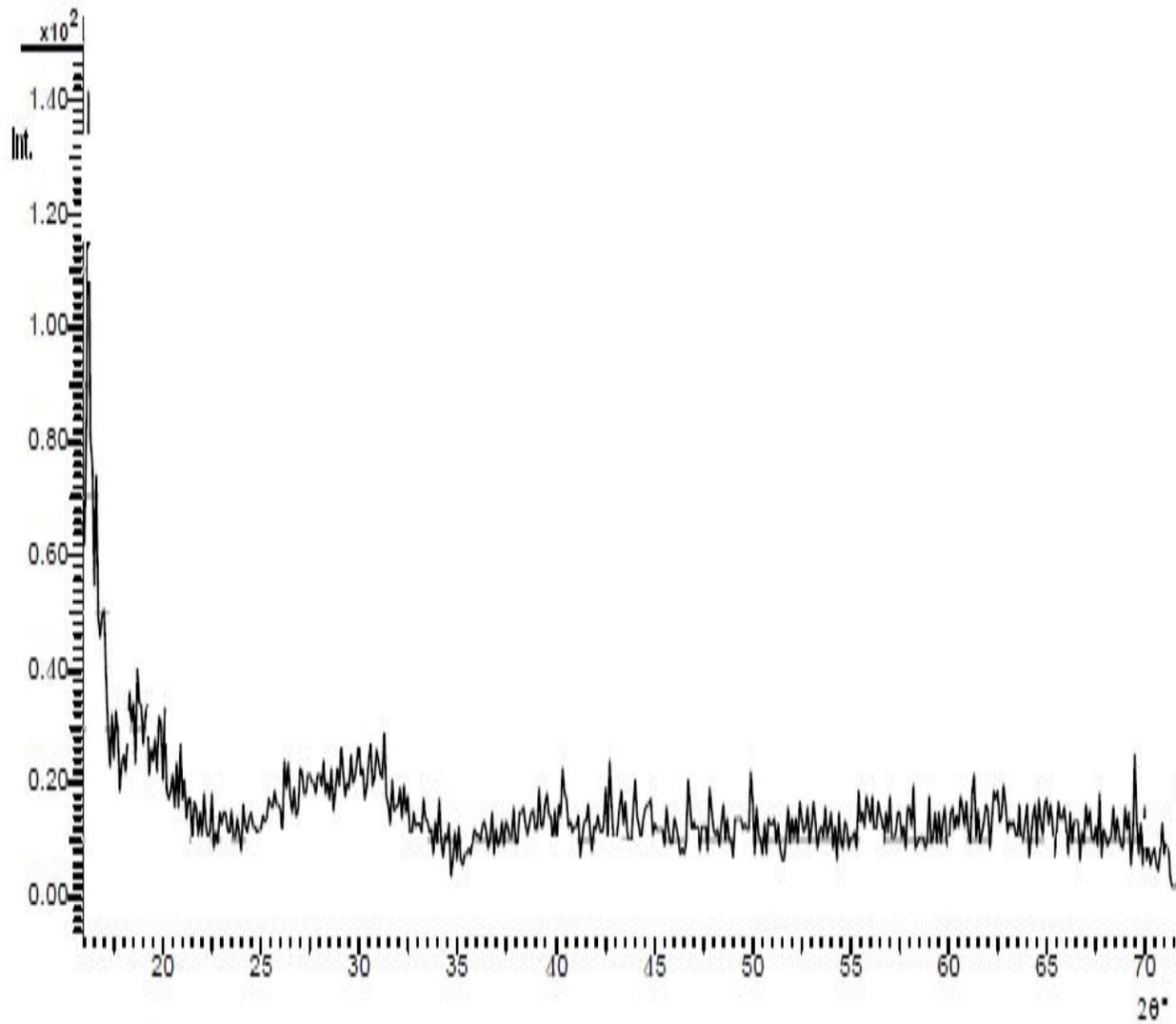
Figure 4.60: X-ray pattern of nanocrystals of RCS
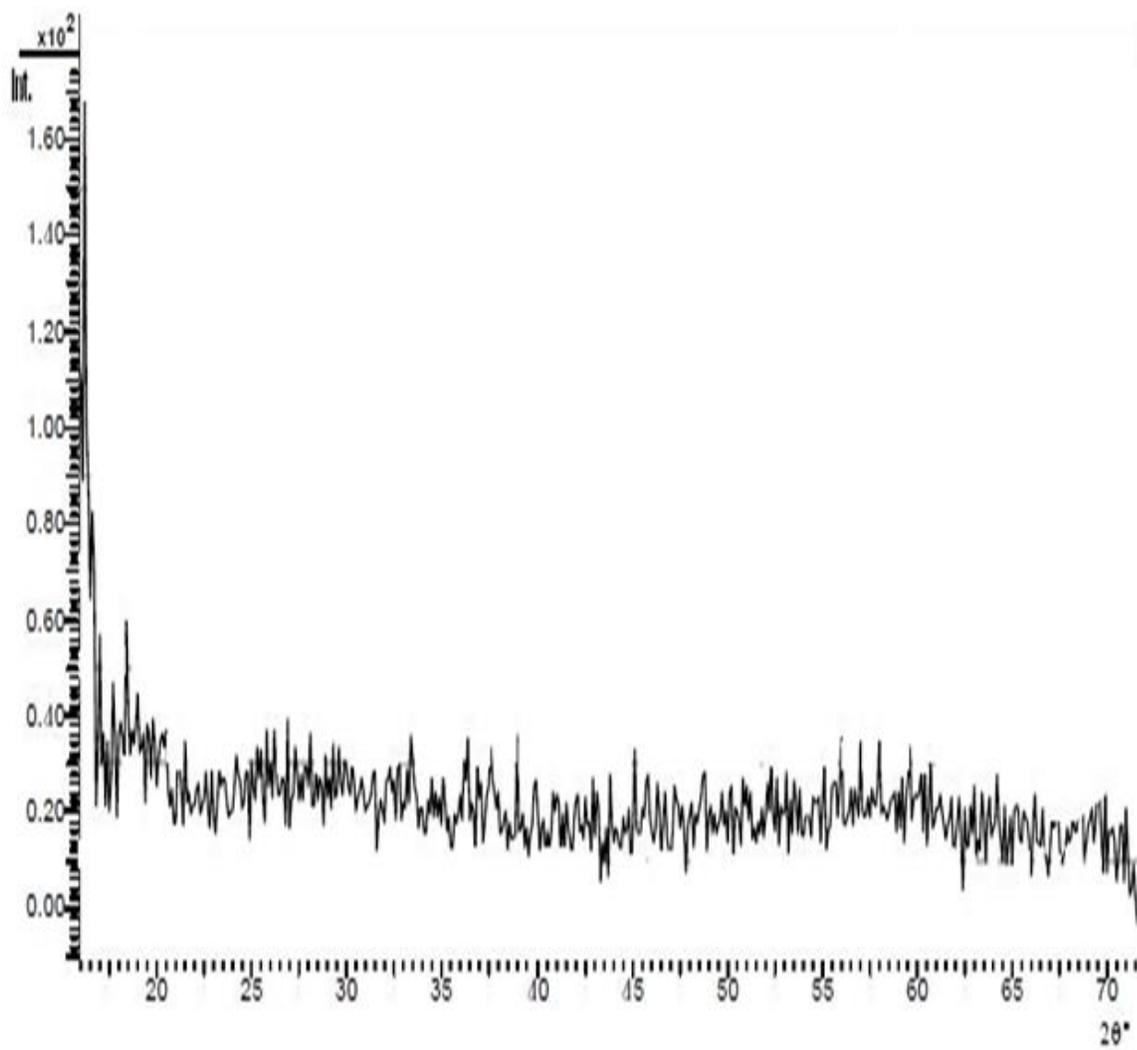
Figure 4.61: X-ray pattern of nanocrystals of WYS
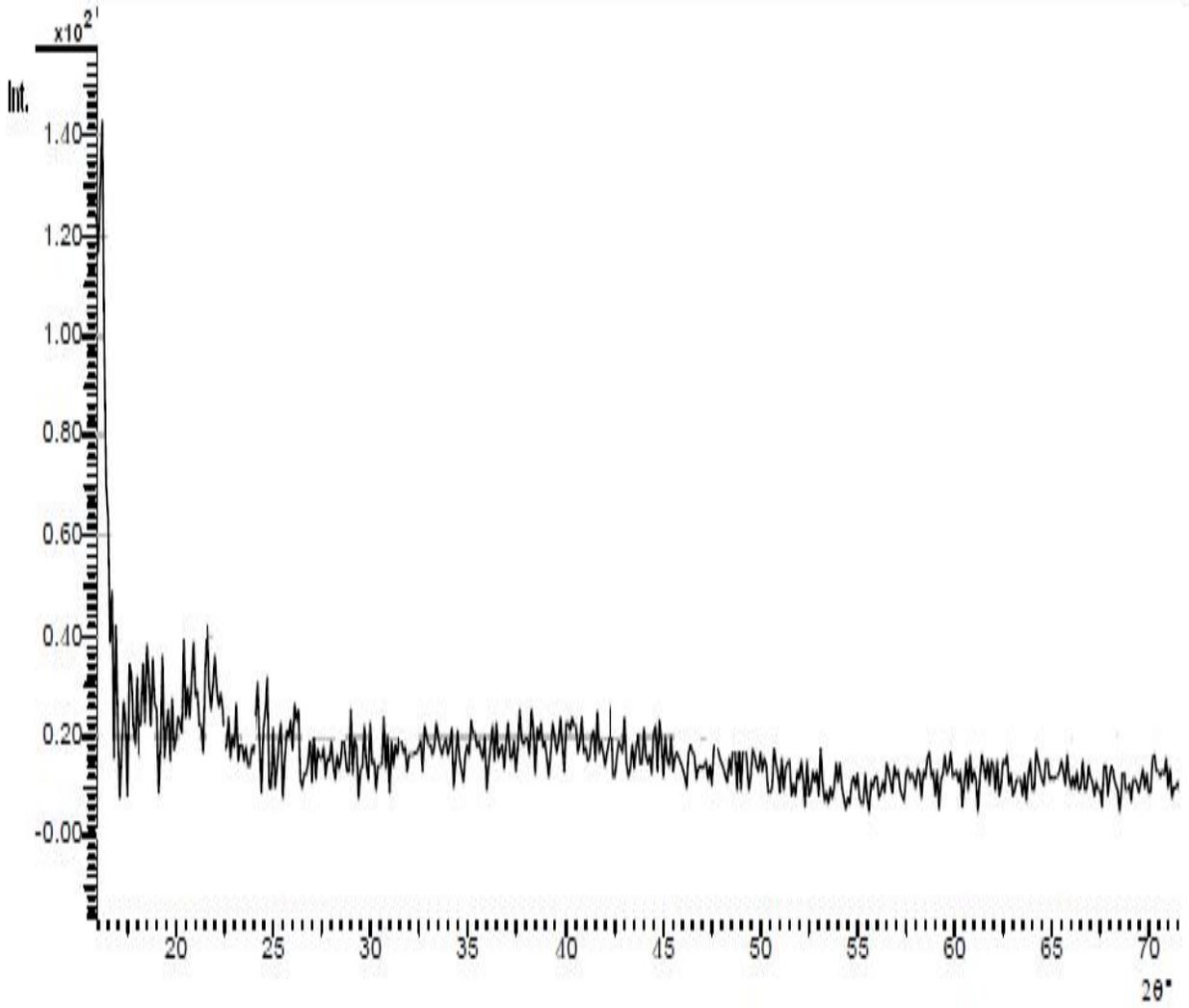
Figure 4.62: X-ray pattern of nanocrystals of YYS
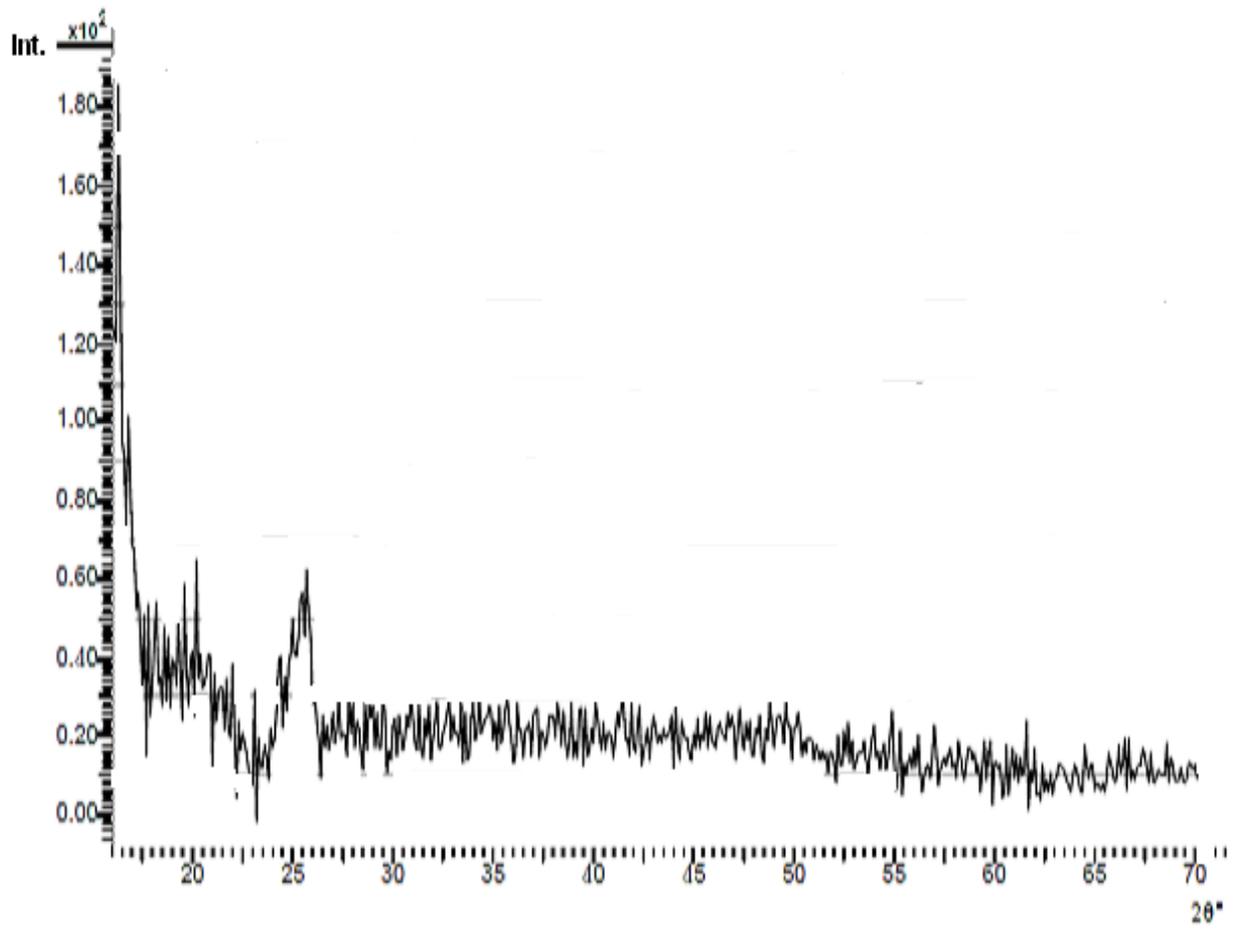
Figure 4.63: X-ray pattern of nanocrystals of PPS
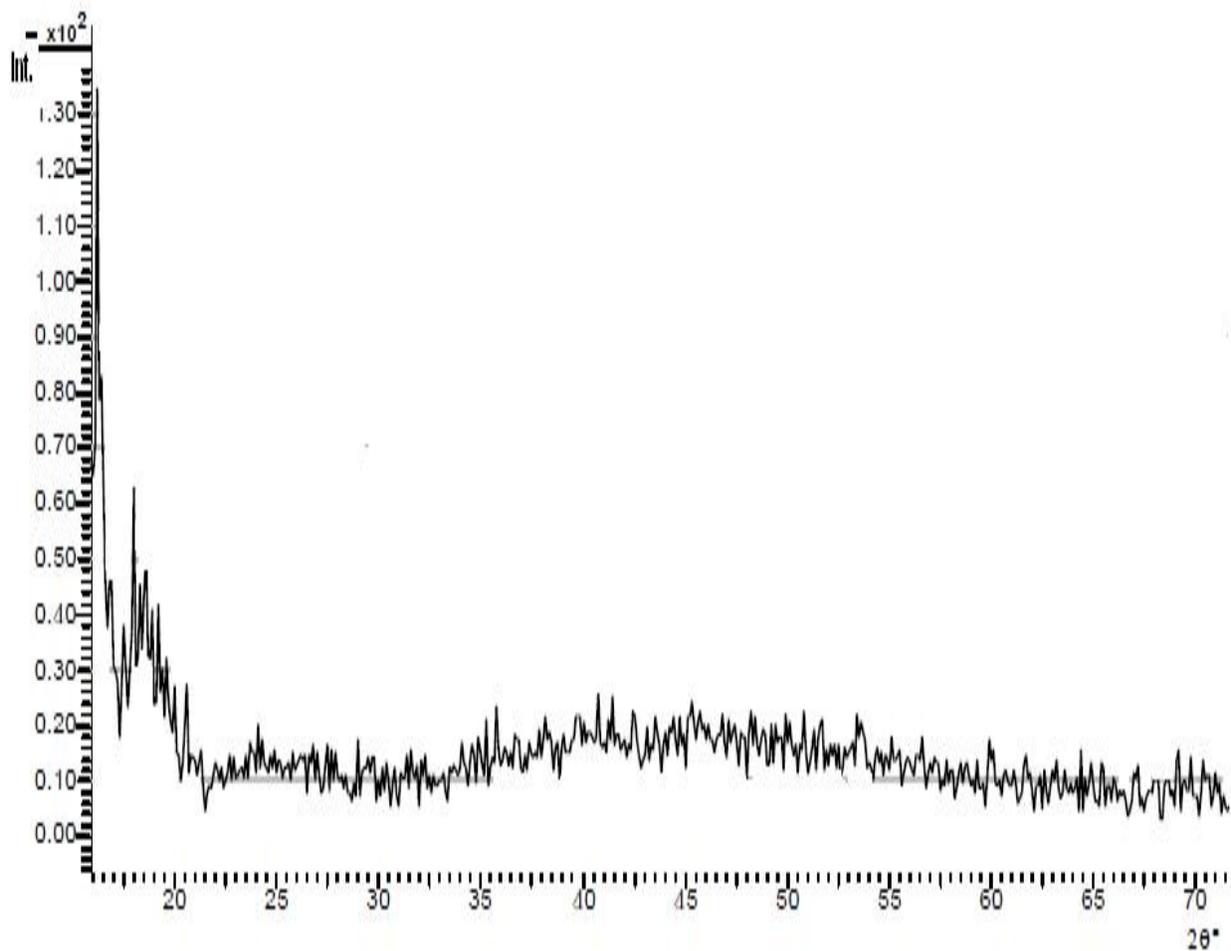
Figure 4.64: X-ray pattern of nanocrystals of LBS
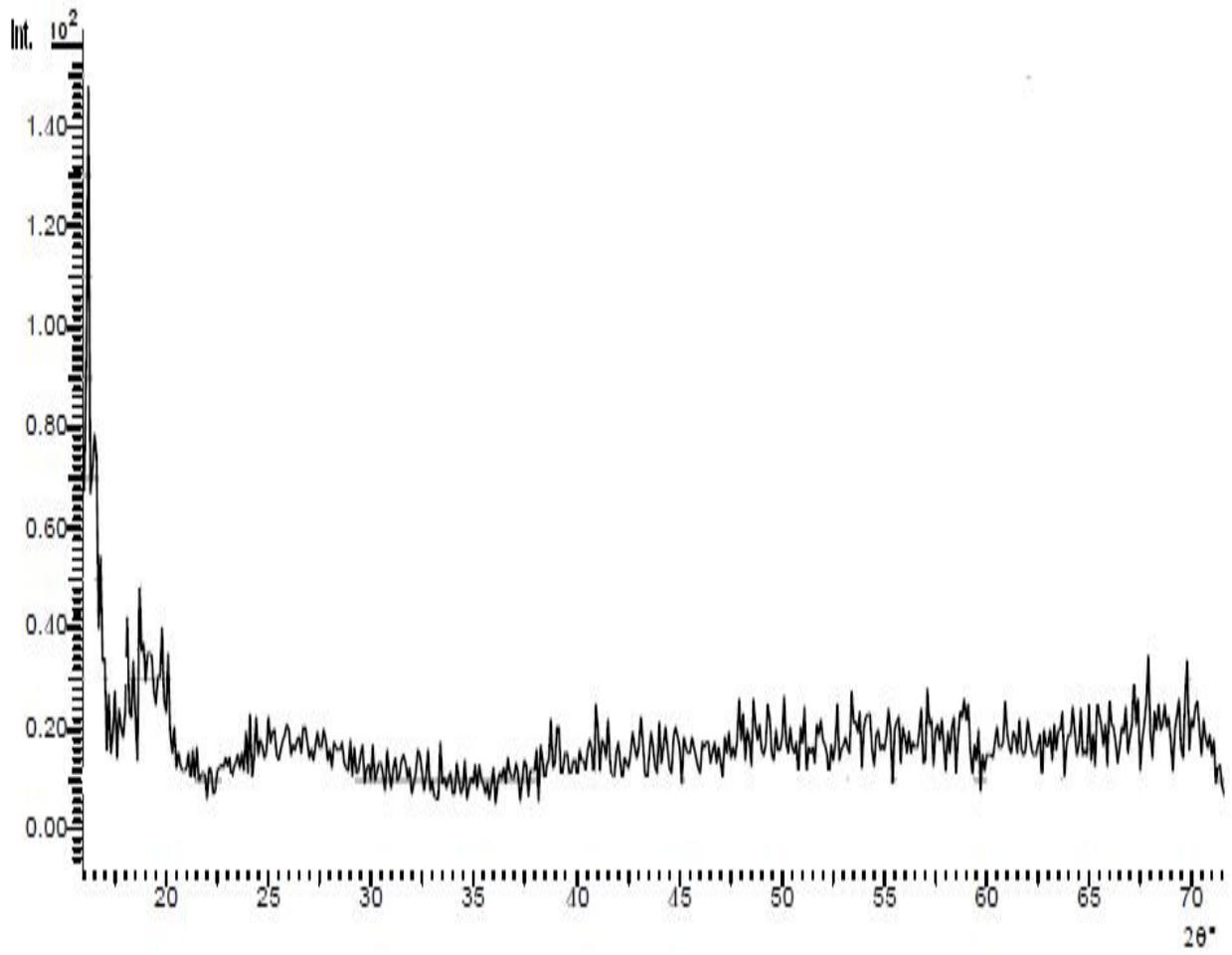
Figure 4.65: X-ray pattern of nanocrystals of JBS
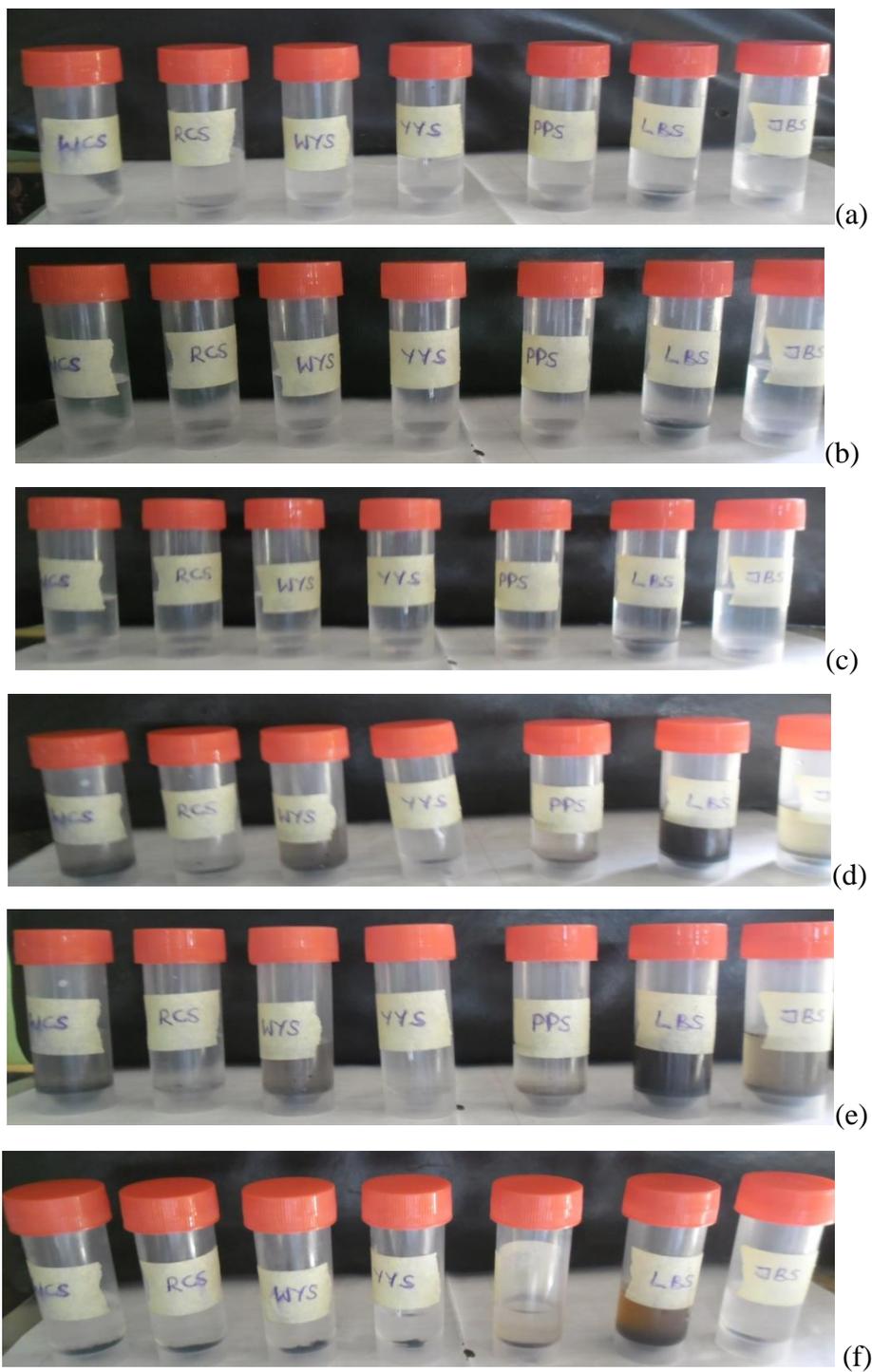
Plate 4.1: Pictures of solubility tests of starch nanocrystals in (a) toluene, (b) xylene, (c) chloroform, (d) acetic acid, (e) ethanol and (f) deionized water (at room temperature)

185

CHAPTER FIVE

5.0   DISCUSSION

5.1   PERCENTAGE YIELD

The percentage yields of the native starches and nanocrystals of starches produced from their native are depicted in Table 4.1. The yields of the native starches were expressed as the percentage of ratio of weight of starch obtained to the weight of the raw sample on a dry weight basis. The yields of nanocrystals of starches were percentage of ratio of weight of nonsolubilized particles, after centrifugation to the initial weight of dry starch. The yields for the native starches were in the order of white cocoyam starch (WCS), 31.70%; red cocoyam starch (RCS), 31.68%; white yam starch (WYS), 42.66%; yellow yam starch (YYS), 41.72%; pigeon pea starch (PPS), 20.57%; lima bean starch (LBS), 20.36% and jack bean starch (JBS), 20.26%. JBS possessed the highest yield (13.51%) of starch nanocrystals prepared via acid hydrolysis after five (5) days. Next in yield was LBS (10.81%) while the least was RCS (5.68%). The starches extracted from tubers were generally low in nanocrystals yield compared to the legume starches used in this research work. The differences in the percentage yields of the native starch and starch nanocrystals could be attributed to the different botanical sources of the starches.

5.2   MOLAR SUBSTITUTION (MS) AND DEGREE OF SUBSTITUTION (DS)

The values of molar substitution and degree of substitution of hydroxypropyl derivatives of the native starches are shown in Table 4.2. Molar substitution is the measure of the average number of hydroxyl units that are derivatized by substituent groups (Karim *et al.*, 2008). The values of molar substitution of the starches increased with increase in the level of substitution, ranging from 0.23 to 0.67. In all cases, the range of value was within the limit of not more than 7% hydroxypropyl group allowed

for the use of hydroxypropylated starch in food application by FDA (US Food and Drug Administration) (Dias *et al.*, 1997). The peak MS (0.67) was obtained for high–substituted YYS while the lowest was for both low-substituted starches of RCS and WYS. YYS equally exhibited the peak molar substitution (0.37) among all the low-substituted starches. Under identical alkaline conditions of substitution, low-substituted WCS had higher MS than low-substituted RCS with the same value at high-substitution level. Irrespective of the level of substitution, YYS possessed higher value of molar substitution than WYS. Among the legume starches, LBS had the peak MS (0.37) for high-substituted starches while PPS (0.27) for low-substituted legume starches. These differences could be adduced to different access of propylene oxide to the interior or subsurface of the starch granules as a result of varying degrees of inter–and intra–molecular forces of the molecules. The degrees of substitution (DS) for all the starches ranged from 0.02 to 0.04, which is below the limit of DS for all commercial food grade starches stipulated at DS$\approx$0.1 to 0.3 (Xu and Seib, 1997). Hydroxypropyl derivatives of these starches could be used as indirect food additives such as thickners in fruit pie fillings, puddings and gravies.

5.3   AMOUNT OF REACTED OZONE

From Table 4.3, there was a general increase in the amount of ozone that reacted with the starch samples as ozone generation time (OGT) increases. This trend was uniform as OGT increased from 5 to 10 min in all the starches while significant deviations were observed in PPS and JBS at 15 min OGT. In other words, all the root and tuber starches (WCS, RCS, WYS and YYS) exhibited consistent increase in the amount of reacted ozone with increase in OGT time while inconsistent increase was observed in the legume starch with the exception of lima bean starch (LBS). This suggests that OGT is the duration of exposure of the molecules of the starch granules to oxidation reaction either at interior or surface level. These observations could be

187

indications of inherent inactiveness of the molecules of the starch granules to a longer time of OGT, especially at 15 min putting the botanical source into consideration. Hence, 10 min could be an optimum OGT for ozone-oxidation of these starches. The consistency in increase in amount of reacted ozone and OGT obtained in this present research work compared favourably with the earlier reports of Chan *et al.* (2009) for starches of corn, sago and tapioca. An and King (2009) have reported that ozonation increases breakdown viscosity of rice starch. At 5 min OGT, the legume starch molecules react more with the generated ozone more than the tuber starch molecules. These differences could mainly be adduced to the variation in botanical source and the availability of natural pores on the surface of the granules. The same trend was observed for these starches at 10 min OGT while an inconsistent trend was exhibited by them at 15 min OGT. At 5 min OGT, the peak amount of reacted ozone (1.46±0.06 mmol) was obtained in LBS while the least (0.03±0.00 mmol) in RCS. At 10 min OGT, the peak amount of reacted ozone (2.10±0.12 mmol) was exhibited by LBS while the least (0.13±0.06 mmol) by WYS. At 15 min OGT, the peak reacted ozone (2.46±0.06 mmol) was obtained in LBS while the least (1.00±0.06 mmol) in RCS. In other words, at both 5 and 15 min OGT, the starch molecules LBS and RCS exhibited highest and lowest affinity for gaseous ozone respectively.

5.4 CARBONYL AND CARBOXYL CONTENTS

The carbonyl and carboxyl contents are paramount to oxidation of starch, because they account for the depolymerization of amylose and amylopectin, and conversion of hydroxyls first to carbonyls ($>$C=O) and then to carboxyls (–COOH). The results of carbonyl and carboxyl contents of the starches are depicted in Table 4.4. There were increases in carbonyl and carboxyl contents of the starches with respect to increase in OGT. The carbonyl contents ranged from 0.232 to 0.711% while carboxyl contents from 0.151 to 0.430%. The range of carboxyl contents obtained in this present

work was less than 1.1% reported by Wurzburg (1986) for most commercial starches oxidized with hypochlorite. The structural and morphological features of these starches could account for their varying carbonyl and carboxyl contents. Wurzburg (1986) has reported the interference on the tendency of amylose to associate and retrograde by the bulkiness of carbonyls and carboxyls. While carbonyls play a minor role in the prevention of retrogradation of starches, carboxyls can result in low retrogradation. The Pearson correlation analysis of the data obtained showed positive relationship between the amounts of ozone reacted with the starches and carboxyl contents (WCS, r = 0.811; RCS, r = 0.934; WYS, r =0.997; YYS, r = 0.913; PPS, r = 0.994; LBS, r = 0.903; JBS, r = 0.953, p< 0.01). A positive relationship existed between the amounts of ozone reacted with the starches and carbonyl contents (WCS, r = 0.996; RCS, r = 0.960; WYS, r =0.921; YYS, r = 0.878; PPS, r = 0.989; LBS, r = 0.989; JBS, r = 0.878, p< 0.01). These observations, invariably, showed that both carboxyl and carbonyl contents of these oxidized starches increased with increase in amounts of ozone that reacted with them. These observations are in agreement with the finding by Kuakpetoon and Wang (2001), who reported that both carboxyl and carbonyl contents of oxidized starch increased as the hypochlorite concentration increased.

5.5   PROXIMATE COMPOSITION

Proximate profiles of the native starches, including moisture, protein, crude fat, crude fibre and ash contents, and carbohydrate by difference, are depicted in Table 4.5. The moisture contents of the starches were in the range of 10.23±0.01 to 10.76±0.01%. High moisture content can lead to microbial damage and subsequent deterioration in quality (Moorthy, 2002). Peak moisture content was observed in RCS and the least in WYS. The range of moisture content obtained in this research work was comparably higher than 8.72 and 9.02% reported for sweet potato and red cocoyam starches by Oladebeye *et al.* (2009). Comparatively, WCS possessed lower moisture content than

RCS, WYS lower than YYS whereas JBS, a legume starch had high moisture content compared to either PPS or LBS.

The values of crude protein were different ($p<0.05$) in all the starches. A range of 1.45 ± 0.01–$7.01\pm0.02\%$ was obtained in this research work. The peak value was obtained for JBS, a legume starch while the least for RCS, a tuber starch. The white cultivars of both cocoyam and yam (WCS and WYS) exhibited higher values of crude protein than the corresponding red and yellow cultivars (RCS and YYS). Notably, PPS, LBS and JBS, which were legume starches, had higher levels of crude protein than the root and tuber starches (WCS, RCS, WYS and YYS). The value of crude protein obtained for RCS ($1.45\pm0.01\%$) is in the same range with the value obtained in the previous work (Oladebeye *et al.*, 2009). The differences in crude protein contents of the starches could be attributed to botanical and cultivar variations as well as the ecological and environmental conditions.

Both the legumes and tubers used in this research work were not good storage organs for excess crude fat in their starch granular network. This was evident in the levels of crude fat, ranging from 1.02 ± 0.01 to $1.16\pm0.01\%$. In other words, these starches were not good sources of fat and oil. LBS appeared as the richest source of fat among all the starches.

Crude fibre of foods has been defined by Amoo (2004) as the washed, dried, organic residue that remains after boiling the defatted food material successively with dilute tetraoxosulphate (vi) acid and dilute sodium hydroxide solutions, which are more preponderant in outer covering of many food than the softer, more edible inner tissues (Pearson, 1976). All the native starches had low levels of crude fibre, ranging between 1.22 ± 0.01 (WCS) and $1.77\pm0.01\%$ (PPS) (Table 4.5). Low crude fibre has been reported to be nutritionally appreciated, because it traps less proteins and carbohydrates (Balogun and Fetuga, 1986).

Ash content, which serves as a preliminary indication of bioavailability of minerals in food, showed peak value (1.26±0.01%) in LBS and lowest value (1.13±0.01%) in RCS. The starches of white cultivars of cocoyam (WCS) and yam (WYS) possessed higher levels of ash contents than the corresponding starches of red cocoyam (RCS) and yellow yam (YYS). These differences could be attributed to the botanical and cultivar variations of the starches. However, the levels of ash contents obtained for these starches are favourably higher than the value (0.31%) reported by Pérez *et al.* (2005) for a cocoyam cultivar.

The carbohydrate levels of the starches were estimated by difference. As expected, the starches isolated from tubers show higher carbohydrate by difference than those isolated from legumes used in this research work. YYS gives the peak carbohydrate by difference (84.28±0.02%) followed by WCS (84.18±0.03%) while the least by JBS (78.61±0.02%).

5.6   MINERAL COMPOSITION

Tables 4.6 shows the mineral profiles of the native starches isolated from tubers and legumes of white (WCS) and red (RCS) cocoyam, white (WYS) and yellow (YYS) yam, pigeon pea (PPS), lima bean (LBS) and jack bean (JBS). High proportions of sodium (Na), calcium (Ca), magnesium (Mg), potassium (K) and phosphorus (P), and low proportions of iron (Fe), zinc (Zn), copper (Cu) and manganese (Mn) were obtained. Heavy metals such as lead (Pb), nickel (Ni), cadmium (Cd) and mercury (Hg), which are detrimental to humans and animals, were undetected within the limits for the other minerals.

Potassium was the most abundant mineral in all the starches, depicting peak value (4332.70±0.14 ppm) for PPS and lowest value (3195.35±0.21 ppm) for JBS. This is in agreement with the report of Olaofe and Sanni (1988) that potassium is the predominant mineral in some Nigerian agricultural products. Comparatively, WCS

191

possessed higher proportion of potassium than RCS. The same trend is observed for WYS and YYS. High K/Na ratio has been reported to serve in maintaining a correct osmotic equilibrium and fluid pH of the body (Lake and Waterworth, 1980).

Phosphorus was equally abundantly available in all the starches. PPS showed the highest proportion of phosphorus (3331.25±0.07 ppm) while JBS the least (1793.45±0.21 ppm). Comparatively, white cultivars of cocoyam (WCS) and yam (WYS) had higher phosphorus proportions than their corresponding red cocoyam (RCS) and yellow yam (YYS) cultivars. High levels of phosphorus has been noted to facilitate increase in swelling power, paste stability, peak viscosity, breakdown, onset and peak gelatinization temperatures of starches (Noda *et al.*, 2007; Karim *et al.*, 2007). These values were higher compared to those reported by Pérez *et al.* (2005) for *Colocasia esculenta* (0.1 ppm), *Xanthosoma sagittifolium* (0.7 ppm) and *Manihot esculenta* (0.5 ppm). Aboubakar *et al.* (2008) have indicated that native starch with high level of phosphorus exhibited low digestibility. A possible explanation is that lower phosphorus content in starch granules generally results in higher resistant starch (Liu *et al.*, 2007). The levels of phosphorous in tuber starches are typically less than 5000 ppm and are usually referred to ash (Thomas and Atwell, 1999).

Sodium proportion was highest in PPS (246.00±0.42 ppm) followed by LBS (224.65±0.21 ppm) and least in RCS (163.50±0.28 ppm). The increasing order of sodium among the starches isolated from tubers used in this research work was RCS<WCS<WYS<YYS while for legume is JBS<LBS<PPS. Calcium proportion was highest in PPS (62.25±0.07%) followed by LBS (56.45±0.21%) and least in JBS (32.30±0.14%). The proportions of calcium in WCS, RCS and WYS were similar (p<0.05). Skeletal abnormalities such as osteopenia, osteomalacia, osteoporosis and rickets have been linked to deficiency in calcium content. In addition, low intake of calcium has been adduced to hypertension, premenstrual cramps and insomania. Although Ca, K and Na have received less attention, unlike phosphorus, they have

been found to have significant influence on some functional properties of potato starch (Zaidul *et al.*, 2007b). According to Zaidul *et al.* (2007a), high calcium content of potato starch is associated with a decrease in peak viscosity and an increase in breakdown, setback viscosity and peak viscosity temperatures, whereas higher potassium content was associated with increasing peak viscosity, breakdown, and setback viscosity and peak viscosity temperature. High sodium content is associated with high peak viscosity and setback viscosity, but low breakdown and peak viscosity temperature (Zaidul *et al.*, 2007a). However, the association of the different mineral elements with functional properties of the starches needs to be established.

Magnesium proportion was highest in JBS (85.55±0.07 ppm) followed by PPS (60.50±0.14 ppm) and least in YYS (54.35±0.07 ppm). Both RCS and WYS were similar in proportion of calcium (p<0.05). The proportions of iron in the starches were low, ranging from 2.15 to 2.35 ppm. There were no significant differences in iron proportions between RCS, LBS and JBS, and YYS and PPS (p<0.05). The ranges 0.15–0.35% and 0.65–1.15% were observed for copper and manganese respectively in all the starches. Copper and manganese were equally in low proportion in these starches. Deficiency in copper may not pose a serious problem as it is widely distributed in other types of foods, but failure to absorb it may lead to chronic diseases (Clifford, 1971).

5.7 PHYSICOCHEMICAL PROPERTIES OF NATIVE STARCH

The colour characteristics, least gelation concentration (LGC), water absorption capacity (WAC) and oil absorption capacity (OAC) of the native starches are shown in Table 4.7. The colour characteristics, in terms of L^* (whiteness), a^* (redness) and b^* (yellowness), were different (p<0.05) for all the starches used in this research work. High value of L^* with correspondingly low values of a^* and b^* suggested high degree of whiteness of the starches. Generally, all the starches had high L^*, ranging from

68.55±0.01 in LBS to 70.45±0.01 in RCS; low a^*, ranging from 5.64±0.02 in LBS to 6.36±0.01 in JBS (or 6.34±0.01 in RCS and WYS) and low b^*, ranging from 12.03±0.01 in JBS to 12.58±0.02 in LBS. The color of starch, due to the presence of polyphenolic compounds, ascorbic acid and carotene, has impact on its quality. Any pigmentation in the starch is carried over to the final product. This reduces the quality, hence acceptability of starch product (Galvez and Resurreccion, 1992). A low value for chroma (red) and a high value for whiteness are desired for the starch to meet the consumer preference. Variation in the b^* values of samples has been attributed to the varying amounts of carbohydrate and protein contents due to their role in developing non-enzymatic browning (Jamin and Flores, 1998).

The least gelation concentrataion (LGC), which is a measure of the minimum concentration at which a gel resists flow, when the container is inverted, was similar (p<0.05) among the starches isolated from tubers and slightly different among the legume starches. The peak LGC (8.00%) occurs simultaneously in PPS and LBS while a value of 6.00% was obtained simultaneously for WCS, RCS, WYS, YYS and JBS. These observations could suggest the rapid tendency of starch granules to swell at an elevated temperature within a short time.

Water absorption capacity (WAC), a measure of degree of engagement of the starch molecules to form hydrogen and covalent bonds between starch chains and the degree of availability of water binding sites among the starches (Hoover and Sosulski, 1986), varied significantly among the starches (Table 4.7). Comparatively, WCS (92.58±0.01%) is lower than RCS (93.36±0.01%). An opposite trend was observed for WYS (95.47±0.01%) and YYS (93.65±0.01%). Both PPS and JBS had similar value (94.47±0.01%) of WAC with LBS exhibiting the peak value (96.23±0.01%) of WAC not only among the legume starches, but the tuber starches also. Previous reports have suggested particle size, amylose/amylopectin ratio and molecular structure as factors influencing differences in the values of WAC (Akalu *et al.*, 1998; Wootton and

Bamunuarachi, 1978). The larger the granular size, the greater the WAC, while the higher the amylose levels, the lower the water binding capacity of starches.

Oil absorption capacity (OAC), a measure of the degree of available oil binding sites, varies significantly among the native starches (Table 4.7). Oil absorption capacity (OAC) is another important functional property, since it plays an important role in enhancing the mouthfeel while retaining the flavor of food products (Kinsella, 1976). The molecules of all the starches showed low affinity for binding with oil molecules. This could suggest a steric interference of the fatty acids of oil on the formation of hydrogen and covalent bonds within the starch chains. The values of OAC of the starches ranged between 4.71±0.01 in YYS and 4.77±0.01% in JBS. The legume starch with least affinity for oil was LBS (4.20±0.01%). These observations are in agreement with the crude fibre contents of the native starches (Table 4.5).

5.8   FUNCTIONAL PROPERTIES OF NATIVE STARCHES AND THEIR DERIVATIVES

5.8.1 SWELLING POWER AND SOLUBILITY

5.8.1.1   Native and Ozone-Oxidized Starches

Swelling power and solubility are measures of the magnitude of the interaction between starch chains within the amorphous and crystalline domains. The extent of this interaction is influenced by the amylose-to-amylopectin ratio and phosphorus content and by the characteristics of the amylose and amylopectin in terms of molecular weight/distribution, degree of branching and branch length, and conformation (Hoover, 2001; Singh and Kaur, 2004). The swelling power and solubility of the native and ozone-oxidized starches are presented in Table 4.8. The swelling power of the ozone-oxidized WCS increased as OGT increased from 5 to 15 mins, but its value was lower than its native at 5 and 10 min OGTs. Increase in swelling power was equally observed for the oxidized RCS starch as OGT increased, but with values less than that of its

native. As OGT increased, swelling powers of the oxidized YYS increased with its native having higher swelling power than the oxidized derivatives at 5 and 10 min OGTs. The oxidized derivatives of WYS appeared to behave like those of LBS and JBS, with higher swelling power than their native starches. Although there was no consistent trend with the increasing order of OGT, the ozone-oxidized derivatives of starches isolated from legumes, PPS, LBS, JBS, exhibited higher swelling power than their corresponding native starches with slight deviation in PPS at 10 min OGT.

The differences in the extent of swelling indicate structural differences among starches. The increase in swelling power of oxidized starch might be due to the introduction of hydrophilic carboxyl groups and the repulsion between negative charges. The reduction in swelling power after oxidation could be attributed to structural disintegration within the starch granule during the process of modification (Lawal, 2004). A similar decrease in the swelling power upon oxidation has been reported for the mucuna bean (Adebowale and Lawal, 2003a). The inconsistency in swelling powers of the starches could be attributed to the different rates of depolymerization of the polymer chain to form a carbonyl group and oxidation of carbonyl group to carboxyl group at different OGTs. The Pearson correlation analysis of swelling powers and carbonyl contents for the oxidized starches was WCS ($r = 0.890$, $p<0.05$), RCS ($r = -0.439$, $p<0.01$), WYS ($r = 0.699$, $p<0.01$), YYS ($r = 0.970$, $p<0.01$), PPS ($r = 0.360$, $p<0.01$), LBS ($r = -0.720$, $p<0.01$) and JBS ($r = -0.756$, $p<0.01$), and swelling powers and carboxyl contents WCS ($r = 0.424$, $p<0.05$), RCS ($r = -0.888$, $p<0.05$), WYS ($r = -0.586$, $p<0.05$), YYS ($r = 0.982$, $p<0.01$), PPS ($r = 0.588$, $p<0.01$), LBS ($r = -0.877$, $p<0.05$) and JBS ($r = -0.863$, $p<0.05$). The swelling power of starches is of great significance in tablet and capsule formulations, as it is believed that disintegrants work through a swelling and wicking action (Adebayo and Itiola, 1998). As a result, starches with higher swelling power would be expected to release the

196

active pharmaceutical ingredient from its compacts at a faster rate, where starch acts as a disintegrant.

Solubility represents the amount of solubilized starch molecules present at a certain temperature. Increase in solubility was obtained for the native starches of white cocoyam (WCS), red cocoyam (RCS), white yam (WYS), yellow yam (YYS), pigeon pea (PPS) and lima bean (LBS) while a decrease was exceptionally obtained for the native starch of jack bean (JBS) upon oxidation with gaseous ozone (Table 4.8). Although the increase in solubility of the starches did not follow a consistent trend with OGT, the increment was most prominent for RCS, WYS, YYS, PPS and LBS at 5 min OGT, and at 15 min OGT for WCS. The increase in solubility after oxidation has been adduced to depolymerization and structural weakening of the starch granules (Hodge and Osman, 1996). That increase in solubility was most prominent at 5 min OGT for some starches used in this present investigation could suggest that depolymerization and structural weakening of the starch granules were initiated at 5 min OGT. Further increment could be as a result of extended depolymerization of the granules, leading to their structural weakening. Increase in the solubility of starches has been reported for normal corn starch (Lim *et al.*, 2008), sago starch (Chan *et al.*, 2009) after oxidation. The decreased solubility after oxidation, as observed for JBS, could be due to the presence of cross-links that prevented the amylopectin molecule from leaching out (Wang and Wang, 2003). Lim *et al.* (2008) have reported lower solubility for waxy corn starch than its native.

5.8.1.2   Native and Hydroxypropylated Starches

The swelling and solubility profiles of the native and hydroxypropylated starches of white cocoyam (WCS), red cocoyam (RCS), white yam (WYS), yellow yam (YYS), pigeon pea (PPS), lima bean (LBS) and jack bean (JBS) are presented in Table 4.9. The swelling power increased for WCS, RCS, WYS, PPS and JBS as molar

substitution (MS) increased. In all these starches, the extent of swelling of the hydroxypropyl derivatives at high-substitution level was more significant than at low-substitution level compared to their corresponding native starches. In addition, the impact of hydroxypropylation on increased swelling was expressed most in high-substituted WCS (21.29 ± 0.10 g/g), followed by high-substituted RCS and least in low-substituted PPS. The increased swelling power of the hydroxypropylated starches is attributed to reduced interactions between glucan chains due to increased hydrophilicity of the starch from the introduction of hydroxypropyl groups, resulting in the disruption of inter- and intra-molecular hydrogen bonds in the glucan chains. Thus, the granular structure of the starch is weakened and perhaps the free motion of the glucan chains in the amorphous regions increases (Singh *et al.*, 2004; Choi and Kerr, 2004). The increases in swelling after hydroxypropylation could be utilized in starch applications such as food thickening and preparation of hydrogels (Lawal, 2011). Conversely, the hydroxypropyl derivatives of YYS and JBS exhibited decrease in swelling power compare to their corresponding native starches. Swelling power has been found to be influenced by a strong bonded micellar network, amylopectin molecular structure and amylose content (Tang *et al.*, 2005; Gujska *et al.*, 1994), which results in crystallite formation by the association between long amylopectin chains, increases granular stability, thereby reducing the extent of granular swelling (Singh *et al.*, 2004).

The solubility profiles of the native WCS, RCS, WYS, PPS and LBS increased upon modification (Table 4.9). As molar substitution increased, solubility profiles of the starches also increased. The impact of hydroxypropylation was mostly expressed in high-substituted RCS ($25.32 \pm 0.06\%$), followed by high-substituted WCS and least in low-substituted WYS. The increment in solubility became significant, when high-substituted starch was compared with the low-substituted. Increase in water absorption after hydroxypropylation enhanced leaching of amylose mainly from the amorphous

198

region of the starches. In addition, inter- and intra- molecular hydrogen bonds in the starch chains were disrupted, the granular structure of the starches were weakened and the motional freedom of starch chains increase as the temperature increases. This resulted in increase in solubility profile. The differences in solubility of the starches could largely be due to structural differences, differences in chain length distributions (Bello-Pérez *et al.*, 2000). Granular size also affects solubility of the starches. The smaller the granule size, the higher the solubility (Tian *et al.*, 1991). Conversely, inconsistent elevation and lowering of solubility profile were observed for the native YYS and JBS upon hydroxypropylation. At low-substitution level, YYS has higher solubility than its native while an opposite trend ws observed for the same starch at low-substitution level. In the same vein, at low-substitution level, JBS had lower solubility than its native while an opposite trend was observed for the same starch at high-substitution level. The decreased solubility could be attributed to incomplete weakening of the granular structure of the starch despite the introduction of hydroxypropyl groups, which disrupted the hydrogen bonds in the starch chains.

5.9   RHEOLOGICAL PROPERTIES

5.9.1 PASTING PROPERTIES

5.9.1.1   Native and Oxidized Starches

The pasting profiles of the native and ozone-oxidized starches analyzed with rapid visco analyzer (RVA) are shown in Table 4.10. There was reduction in the pasting temperature of the oxidized derivatives of the native starches of WCS, RCS, WYS, PPS and JBS upon oxidation with slight deviation at 5 min OGT for PPS. An inconsistent opposite trend of increase in pasting temperature was observed for YYS and LBS with exception at 15 min and 5 min OGTs respectively. The ranges of pasting temperature of the oxidized starches were 82.40–83.25^{o}C (WCS), 82.48–83.29^{o}C (RCS), 80.46–81.67^{o}C (WYS), 84.86–85.77^{o}C (YYS), 86.47–88.14^{o}C (PPS), 86.53–

87.38^{o}C (LBS) and 84.15–84.96^{o}C (JBS) in comparison with the respective values of pasting temperature of native starches (83.89, 83.51, 81.62, 84.92, 86.54, 86.54 and 86.31^{o}C). The reduction of pasting temperature following oxidation is a consequence of structural weakening and disintegration during oxidation (Lawal, 2004).

Peak viscosity values for oxidized cocoyam starches (WCS and RCS) were lower than the corresponding native starches. These differences were more appreciable in terms of their hot paste viscosity and cold paste viscosity. The decrease in peak viscosity, hot paste viscosity and cold paste viscosity could be as a result of partial cleavage of the glycosidic linkage after treatment with gaseous ozone, resulting in a decrease in the molecular weight of starch molecules. This gave rise to a partially degraded network with weak shear resistance and failure to maintain the integrity of the starch granule, thereby resulting in a lower viscosity (Morton and Solarek, 1984). This trend is in agreement with the results reported by Chan *et al.* (2009) for ozone-oxidized corn starches and by Adebowale and Lawal (2003b) for oxidized mucuna bean starch. The oxidized derivatives of native starches isolated from white and yellow cocoyam (WYS and YYS) exhibited the same trend with WCS and RCS with slight exception in term of peak viscosity for WYS at 5 min OGT. Conversely, the oxidized derivatives of the native legume starches (PPS, LBS and JBS) showed increase in the values of peak viscosity, cold paste viscosity and hot paste viscosity upon oxidation in comparison to their corresponding native starches. A slight deviation was observed for LBS in terms of peak viscosity only at 15 min OGT. In addition to the highest values of peak viscosity, hot paste and cold paste viscosity obtained for the ozone-oxidized legume starches at 5 min OGT, gradual decrease of these properties was observed as OGT increased. A slight deviation was, however, observed in PPS at 15 min OGT. These differences were not, in anyway, influenced by the carboxyl contents of the starches as the Pearson correlation analysis of the starches showed negative in some and positive in others (WCS, r = 0.860, p<0.01; RCS = 0.056, p<0.05; WYS, r = -

0.884, p<0.01; YYS, r = -0.715, p<0.05; PPS, r = 0.318, p<0.01; LBS, r = -0.972, p<0.01; JBS, r = -0.995, p<0.01). However, increase in peak viscosity of oxidized starches in comparison to their natives has been reported for oxidized waxy corn starch (Wang and Wang, 2003), periodate-oxidized tapioca starch (Wongsagon, 2005), ozone-oxidized tapioca starch (Chan *et al.*, 2009) and cassava starch (Jyothi *et al.*, 2006) and the increase has been adduced to the effect of chemical crosslinking during oxidation.

Breakdown viscosity is a measure of granule disruption or lesser ability of starch to resist shear force during heating. A gradual increase in breakdown viscosity was observed for oxidized derivatives of WCS and RCS as OGT increased, which were comparatively higher than their corresponding native starches. The increased breakdown viscosity could be attributed to the weakened structure of the granules after treatment with gaseous ozone, which facilitated disruption of the granular structure. Reports have been made of increase in breakdown viscosity after oxidation of native starches with ozone (An and King, 2009; Chan *et al.*, 2009). Invariably, oxidized WYS and YYS showed inconsistent reduction in values of breakdown viscosity with respect to OGT. The same inconsistent trend was observed in pigeon pea (PPS) while LBS and JBS showed higher values at 5 and 10 min OGTs. The reduction in breakdown viscosity has been adduced to the introduction of new substituent groups into the oxidized starches (Adebowale and Lawal, 2003b). The differences have been noticed by Chan *et al.* (2009) as not depending on the carbonyl content of the starches, but could be due to the effect of ozone on the degradation of the amorphous region of the starch granules. In addition, the different responses of these starches to ozone-oxidation could be adduced to variation in their botanical sources.

Setback viscosity is a measure of the degree of retrogradation of starch, mainly amylose (Karim *et al.*, 2000), implying that high setback viscosity value means a high tendency of starch to retrograde. The values of setback viscosity of all the starches

progressively decreased with respect to increase in OGT with a slight deviation observed in JBS at 5 min OGT. During the cooling cycle of hot starch paste, the re-association tendency of the starch granules favoured an increase in viscosity. This phenomenon was largely favoured by the affinity of hydroxyl groups of one molecule for another. Oxidized starches, having been subjected to conformational reordering and rearrangement, through the introduction of carboxyl groups, are less prone to such reassociation. The introduction of carboxyl groups to replace hydroxyl groups inhibits the formation of such binding forces. In other words, the presence of carbonyl and carboxyl groups, caused by oxidation, impedes associations among starch chains, and a true gel structure is not obtained (Adebowale *et al.*, 2002).

The peak time implies a measure of rate of attainment of equilibrium point between swelling and polymer leaching, and rupture and polymer alignment. The peak times for the ozone-oxidized starches were in the ranges of 4.18–4.25 min for WCS, 4.38–4.45 min for RCS, 5.52–5.78 min for WYS, 6.52–6.92 min for YYS, 6.85–6.92 min for PPS, 5.05–5.18 min for LBS and 5.18–5.92 min for JBS. The starches of white cocoyam (WYS), red cocoyam (RCS), white yam (WYS), pigeon pea (PPS) and jack bean (JBS) exhibited lowering in peak time upon oxidation while yellow yam (YYS) and lima bean (LBS) starches exhibited the opposite trend. However, slight deviation was observed for JBS at 15 min OGT. These differences could be due to different responses of starch granules to ozone-oxidation treatments prior analysis and the botanical variations of the starches.

5.9.1.2   Native and Hydroxypropylated Starches

The pasting properties of the native tuber and legume starches and their hydroxypropyl derivatives are shown in Table 4.11. The pasting temperatures of the native starches generally reduced after hydroxypropylation with respect to increase in molar substitution (MS). The decrease in pasting temperature of the starch after

modification could be as a result of the weakening of the starch granules during the modification process. Weakening means disruption of the inter– and intra– molecular bonding such as hydrogen bond existing within the macromolecules and structural re-organisation of mainly the amorphous component and part of the crystalline region particularly under strong alkaline reaction medium used in the preparation of the hydroxypropylated starches (Lawal, 2011). The lowering of pasting temperature of low-molar substituted hydroxypropylated starches (MS≤0.2) has also been reported, decreasing by up to 6 and 14°C for potato starch (Kim *et al.*, 1992; Perera *et al.*, 1997), 22°C for corn starch and 13°C for amaranth starch (Pal *et al.*, 2002).

The values of peak viscosity of the hydroxypropylated starches generally increase with increase in molar substitution (MS) except for the WCS and RCS at all levels of substitution and LBS at high-substitution level. During hydroxypropylation, the starch structure became loose and permitted swelling to a greater extent, creating high viscosity. The reduced peak viscosity could be adduced to compromise in structural integrity of starch granules during hydroxypropylation by disrupting the hydrogen bonds between the starch chains. The lowered pasting temperature and increase in peak viscosity are a reflection of decrease in the strength of the associative bonding forces within the starch granules and could be ascribed to the hydrophilic nature of the substitutes. Incorporated hydroxypropyl groups facilitate the penetration and absorption of water into the starch granules and an increase the initial rate of plasticization of the amorphous regions of modified granules (Seow and Thevamalar, 1993).

Hot paste viscosity reduced upon modification for the native starches of WCS, RCS, WYS, YYS, LBS and JBS with slight deviation observed at low-substitution level for JBS. An opposite trend was observed for PPS. Significantly, cold paste viscosity, also known as final viscosity experiences reduction after hydroxypropylation of native starches isolated from WCS, RCS, WYS and YYS. PPS and JBS showed

distinct increase in cold paste viscosity upon modification whereas LBS showed both elevation and lowering of cold paste viscosity at low- and high- substitution levels respectively.

Breakdown is a measurement of the starch granule stability during the pasting process. Extensive breakdown occurs when the starch granule swells to maximum volume, but lacks the ability to retain its structure and subsequently collapses. Breakdown viscosity is on increase among all the starches as molar substitution increases. A slight deviation was, however, observed for PPS at low-substitution level. It has been suggested that introduction of hydroxypropyl groups reduces associative forces within the starch granule (Hari *et al.*, 1979). This reduction in bond strength affects the hydroxypropyl starch, which cannot withstand heating and shear strain conditions. The observations obtained in this present study indicate the reduced ability of hydroxypropyl starch to retain its swollen structure during the pasting process, resulting in higher breakdown.

Setback value is a measure of retrogradation. Setback viscosity progressively reduces after hydroxypropylation for native starches isolated from WCS, RCS and WYS, and significantly increased for PPS, LBS and JBS with an inconsistent trend for YYS. In other words, the native starches isolated from tubers possessed higher setback viscosity than their hydroxypropyl derivatives while the native starches isolated from legumes possessed lower setback viscosity than their hydroxypropyl derivatives throughout the period of heating and cooling. The reduced setback viscosity was as a result of the prevention of structural realignment of the starch molecules after gelatinization. The bulky hydroxypropyl groups prevented formation of hydrogen bonding among the starch molecules thus minimizing retrogradation. This indicated that the retrogradation determined by associations of the amylose chains was substantially reduced by hydroxypropylation. This phenomenon has been ascribed solely to steric effects imposed by the bulky hydroxypropyl groups, which prevent

proper alignment of starch chains during chain aggregation and crystallization (Perera and Hoover, 1999). In previous works, reduction of setback after hydroxypropylation has been reported for hydroxypropyl starches of wheat, potato and waxy maize starches (Gunaratne and Hoover, 2002). Increased setback viscosity could be ascribed to increased granule fragments or remnants. These fragments would be embedded in the matrix of the associated polymer network, thus enhancing the viscosity of the system (Karim *et al.*, 2008).

The peak times for the hydroxypropyl starches obtained in this present work were lower than those of the native starches isolated from both tubers and legumes. The peak time implies a measure of rate of attainment of equilibrium point between swelling and polymer leaching, and rupture and polymer alignment. These observations are in compliance with the observations expressed for pasting temperature of these starches, but are in invariance with the peak time obtained for the ozone-oxidized derivatives of the same native starches (Table 4.10). The ranges of peak time with increasing molar substitution for the hydroxypropylated starches were 3.38–3.92 min (WCS), 3.45–3.98 min (RCS), 3.40–4.05 min (WYS), 3.78–4.45 min (YYS), 4.52–5.01 min (PPS), 3.87–4.15 min (LBS) and 3.94–4.63 min (JBS). The differences in peak time of the starches could be attributed to difference in intrinsic behaviours and responses of the starch granules to paste formation and botanical variations.

5.9.2 TEXTURAL PROPERTIES

5.9.2.1   Native and Ozone-Oxidized Starches

The textural properties of native and ozone-oxidized starch gels determined, using the texture analyzer are shown in Table 4.12. Gel strength (N), springiness, gumminess (N) and chewiness (Nm) of all the native starch gels from the roots and tubers (WCS, RCS, WYS and YYS) generally decreased following ozone–oxidation with slight deviation at 5 min OGT for RCS in terms of gumminess and chewiness, and

at 5 min OGT for WYS in terms of springiness. Conversely, opposite and inconsistent trends were observed for the starch gels in terms of cohesiveness and resilience. Deviations, in terms of chewiness and resilience, were observed at 5 and 10 min OGT for RCS and 15 min OGT for YYS. Ozone-oxidized starch gel of white cocoyam exhibited the highest gel strength (7.22 N) at 5 min OGT while the lowest (1.60 N) by red cocoyam at 15 min OGT. The native starch gels from the legumes (PPS, LBS and JBS) exhibited general decrease in gel strength, springiness and chewiness upon ozone-oxidation with slight deviations at 5 and 10 min OGT for PPS in terms of chewiness and gel strength respectively. Gumminess behaviour improved upon oxidation in PPS and LBS as OGT increased whereas JBS exhibited a decrease in the characteristics. LBS and JBS exhibited a decrease in cohesiveness upon oxidation with exceptions at 10 min OGT for both starches. Native PPS gel appeared more cohesive upon oxidation. However, the starch gels from the legumes became more resilient after oxidation. Gel firmness was mainly caused by retrogradation of starch gels, which is associated with the syneresis of water and crystallization of amylopectin, leading to harder gels (Miles *et al.*, 1985). These results revealed that the gels of native starches were hard and brittle, and were modified to be softer and more elastic upon the introduction of ozone molecules into the network matrix of the starch granules. This implies that ozone–oxidized starch pastes have higher tendency to flow under an applied stress.

5.9.2.2   Native and Hydroxypropylated Starches

The textural properties of the gels of native and hydroxypropylated starches measured with texture analyzer are shown in Table 4.13. All the native starch gels of both roots and tubers, and legumes were better than their hydroxypropyl derivatives in terms of gel strength, springiness, gumminess and chewiness. A slight deviation observed was for JBS at high-substitution level. Conversely, all the native starch gels

appeared more cohesive and resilient after hydroxypropylation with slight deviation at low-substitution level for both WYS and YYS in terms of cohesiveness. The impact of hydroxypropylation on the cohesiveness of the starch gels was felt most at high-substitution level for WCS, RCS, WYS and YYS (root and tuber starches) and low-substitution level of PPS, LBS and JBS (legume starches) whereas opposite substitution levels were observed for the impact on the resilience of the starch gels.

The initial gel firmness of starch could be attributed to the short-term rapid reassociation of amylose chains within the cold starch paste. The textural and mechanical properties of a starch gel, where swollen gelatinized amylopectin-rich granules are embedded in the continuous amylose gel matrix, would depend on the amylose concentration and rheological characteristics of the amylose gel matrix; rigidity (deformability) of the swollen starch particles; volume fraction of the swollen granules; and interaction between swollen particles and the amylose matrix (Eliasson, 1986; Doublier *et al.*, 1987; Morris, 1990).

It is known that the extent of the amylose gel network is the main factor contributing to starch gel strength. The bulky and hydrophilic nature of the hydroxypropyl groups in hydroxypropylated starch gels make the leached amylose chains difficult to reassociate, and the gel network by amylose chains and the granule remnants could hardly be formed. The action of hydroxypropylation in loosening the starch granule structure would, however, permit more granules to break down, leaving weaker cohesive swollen starch particles in the gel matrix and leading to a weaker starch gel. Hydroxypropyl groups on amylose chains could prevent amylose aggregation and interrupt the formation of junction zones. These observations are consistent with those reported by Chuenkamol *et al.* (2007), Liu *et al.* (1999) and Choi and Kerr (2003), who demonstrated that hydroxypropylation decreased gel hardness. The results obtained from texture analysis revealed a great difference between textures of native and hydroxypropylated starches of both tuber and legume sources, and

thereby confirmed that the retrogradation of starch could be extensively reduced by hydroxypropylation.

5.9.3 FLOW BEHAVIOUR

5.9.3.1   Native and Ozone-Oxidized Starches

The flow behaviour curves obtained for the native and ozone–oxidized starches used in this study are fitted with Herschel-Bulkley Model, $\sigma = \sigma_o + K\gamma^n$, where σ is shear stress (Pa), σ_o is yield stress (Pa), K is consistency coefficient (Pa.s^n), γ is shear rate (s^{-1}) and n is flow behaviour index (dimensionless) at 25°C.The flow behaviour parameters obtained for the starches are presented in Table 4.14. All the starches exhibited a non-Newtonian behaviour, which is evident by $n<1$, and decrease in viscosity as shear rate increased (Figures 4.1–4.7). The values of n were significantly different among the native and hydroxypropylated starches of RCS, WYS, YYS, PPS, LBS, JBS whereas they were similar among oxidized WCS. Within the starch type, both native and oxidized, the peak n values were 0.63 (WCS), 0.66 (RCS), 0.69 (WYS), 0.73 (YYS), 0.86 (PPS), 0.62 (LBS) and 0.76 (JBS). Chan *et al.* (2011) have reported $n<1$ for unmodified (native) and ozone-oxidized starches of corn, tapioca and sago, where peak values of 0.77, 0.46 and 0.61 were respectively reported for the starches. Although there was no consistent order in the impact of ozone–oxidation on the flow behaviour indices, n of the starches as OGT increased, variations in the n values were observed in this study. The flow behaviour index, n was lower in the oxidized starches of WYS, YYS, PPS, LBS and JBS than their native starches. However, flow behaviour index was lower only in the oxidized RCS than the native whereas the oxidized and native starches of WCS appeared significantly similar. High value of flow behaviour index, n could be due to partial depolymerization of amorphous and crystalline lamella during ozone oxidation. According to Kuakpetoon and Wang (2008), oxidation occurred mostly at the amorphous lamellae and more

amylose depolymerisation, from oxidation, occurred at the periphery of common corn starch. The data obtained in this study revealed that the introduction of ozone molecules into the structural network of the starch granules compromised the integrity of the broken amylopectin chains in recrystallizing, thus, resulting in the loss of birefiregence and consequent drop in viscosity as shown in Figures 4.1–4.7.

Yield stress, σ_o represents a finite stress required to achieve flow, and it indicates that there is a cross-linked or other interactive structure in a material, which must be broken down before flow can occur at an appreciable rate (Achayuthakan *et al.*, 2006; Cheng, 1986). Significant differences of yield stresses, σ_o were obtained for WCS, RCS (only at 10 min OGT), WYS and YYS (only at 5 and 10 min OGT) as OGT increased. In the same vein, PPS (only at 10 min OGT), LBS (only at 5 min OGT) and JBS showed significant differences with respect to increase in OGT (Table 4.14). Yield stress increased in WCS, RCS, WYS, YYS, PPS, LBS and JBS at varying OGT. The impact of ozone-oxidation on the yield stresses of the native starches was more pronounced at 5 and 10 min OGT, except for WCS and RCS. The increase in σ_o with OGT could be due to structure formation of the starch paste. This suggests that the pastes of all the ozone-oxidized starches, especially at 5 and/or 10 min OGT, have higher tendency to flow than have their native forms at 25°C. Pearson Correlation analysis for the starch data showed positive and negative relationships between their yield stress and flow behaviour index values (r = -0.137, WCS; r = 0.374, p<0.01, RCS; r = 0.164, p<0.05, WYS; r = -0.684, p<0.05, YYY; r = -0.597, p<0.05, PPS; r = 0.154, LBS; r = -0.597, p<0.05, JBS). The negative and positive relationships might be indications that starches of different sources, though subjected to the same flow process, behave differently. These differences can be attributed to their differences in amylose content, rate and susceptibility of amylose/amylopectin to oxidation, and the rate of oxidation of carbonyl and carboxyl groups at different OGTs (Chan *et al.*, 2011).

Increase in the consistency coefficient (K) was observed for WCS, WYS, YYS, PPS, LBS and JBS upon oxidation with ozone whereas a decrease was observed for RCS. Relative to the level of oxidation (OGT), K seemed to reduce consistently among the oxidized starches with increase in OGT, except in JBS where an increase was observed. An increase in K values upon oxidation suggests that oxidation enhanced the viscous properties of starch. Possibly, the shorter degraded polymers tend to come close to each other to form networks that contribute to the viscous property of the oxidized starches. Pearson Correlation analysis between stress yield, σ_o and consistency coefficient, K gave positive and negative relationship for the starch data (r = 0.693, p<0.05, WCS; r = -0.196, p<0.05, RCS; r = 0.688, p<0.05, WYS; r = 0.826, p<0.05, YYY; r = 0.800, p<0.01, PPS; r = 0.601, p<0.05, LBS and r = 0.571, p<0.05, JBS). This implies that consistency coefficient, which is a measure of pseudoplasticity, increased with increase in stress applied to the starch paste. In addition, the relationship between consistency, K and flow behaviour index, n was analysed using Pearson Correlation (r = -0.561, WCS; r = -0.944, p<0.01, RCS; r = -0.523, WYS; r = -0.922, p<0.01, YYS; r = 0.913, p<0.05, PPS; r = 0.542, LBS and r = -0.904, p<0.01, JBS). Results implied that ozone molecules interacted with the starch molecules to form crosslinks, resulting in high resistance to flow of the starch granules upon the application of stress as OGT increased.

The shear viscosities (0–900 s^{-1}) of the native and ozone-oxidized starches are depicted in Figure 4.8. Oxidation by ozone improved the shear viscosities of all the native starches, except in LBS. However, among the ozone-oxidized starches, shear stress progressively increased as OGT increased from 5 min to 10 min, after which a decrease was obtained at 15 min, except in JBS. This decrease could be as a result of partial depolymerization of the starch network, which could make the network not resistant to shear, coupled with failure to maintain the integrity of the granule, thereby reducing the viscosity of the starch paste. The oxidized starches from WCS, WYS,

YYS and PPS exhibited the highest shear viscosity at 10 min OGT only while the rest had shear viscosities at varying OGTs (Fig. 4.15). Similarly, among the oxidized starches, the peak shear viscosity (28.51 Pa.s) was obtained for WYS at 10 min OGT while the least value (1.113 Pa.s) was obtained for JBS at 10 min OGT. These observations indicate that effect of ozone oxidation on starch properties could not be singularly based on ozone generation time (OGT). Chan *et al.* (2011) have reported differences in amylose content, rate and susceptibility of amylose/amylopectin to oxidation, and the rate of oxidation of carbonyl and carboxyl groups as OGT increased.

5.9.3.2   Native and Hydroxypropylated Starches

The Herschel-Bulkley model is used to fit the flow curves obtained for the native and hydroxypropylated starches. The flow parameters, the consistency coefficients (K), flow behaviour indices (n) and yield stresses (σ_o) for starches are shown in Table 4.15. All the starches exhibited non-Newtonian behaviour, usually called pseudoplastic flow, because their viscosity values decreased with increase in shear rate (Figures 4.9–4.15). This behaviour is defined as shear-thinning and occurs when stress is applied to shear the paste, which caused the structure of the paste to break down, as evidenced by n<1 for all starches. Similar results had been reported for other starch pastes (Zhao *et al.*, 2007; Mohd. Nuru *et al.*, 1999; Nwokocha *et al.*, 2009). The data obtained in this study showed that the native starches possessed higher flow behaviour indices more than the corresponding hydroxypropylated starches of the same source with deviations observed for RCS and LBS (at high-substitution level only). This implies that lower values of flow behaviour indices, *n* obtained for the hydroxypropylated starches made them exhibit less pronounced shear–thinning behaviours than the native, thereby confirming the data obtained for the starches in terms of peak viscosity (Table 4.11). Among the hydroxypropylated starches, flow behaviour index, *n* decreased as the level of substitution increased. This implies that at

high–substitution level, the intra- and inter-molecular forces between the starch molecules reinforce the granular network to prevent breakdown and hence, the paste resists flow. This was evident by the measure of their values of shear viscosities (0–900 s^{-1}), which appeared higher in the low-substituted starches than the high-substituted starches of the same botanical source (Fig. 4.16). These observations support the reasons for obtaining high breakdown value for the hydroxypropylated starches using RVA as substitution level of propylene oxide in the starches increased (Table 4.11).

The yield stresses (σ_o) of the starches were different among the starch types. All the native starches, except RCS and LBS (at high-susbstitution level only), exhibited improved yield stress values after hydroxypropylation. With the exception of RCS and WYS, the hydroxypropyl derivatives of the root and tuber starches possessed higher yield stress (σ_o) values at low-substitution level than the high-substitution level. The same trend was observed for the hydroxypropylated legume starches (PPS, LBS and JBS). High yield stress is an indication of resistance of the starch paste to flow, which could be due to failure of the starch chain to break down upon the introduction of hydroxypropyl groups. Pearson Correlation analysis between the flow behaviour indices (n) and yield stresses (σ_o) of the starches showed that the two parameters are non-linearly related (r = -0.704, p<0.05, WCS; r = -0.915, p<0.01, RCS; r = -0.765, p<0.05, WYS; r = -0.990, p<0.01, YYS; r = -0.846, p<0.01, PPS; r = -0.380, LBS and r = -0.410, p<0.01, JBS).

The consistency coefficients (K) of the native starches favourably increased after hydroxypropylation with the deviation observed for RCS. These could be an indication that hydroxypropylation seemed to enhance the viscous properties of the native starches. A close look at the hydroxypropyl derivatives of the native starches showed that consistency coefficients obtained for WCS, WYS, YYS and JBS increased as the level of substitution increased while an opposite trend was observed for RCS, PPS and

LBS. Increase in consistency coefficient after hydroxypropylation indicates that the introduction of hydroxypropyl groups into the matrix of native starch enhanced the viscosity value of the starch. Conversely, decrease in consistency coefficient after hydroxypropylation indicates that the hydroxypropyl groups introduction into the starch matrix caused partial degradation of the glucan chains, resulting in the fragement being loosely held. This resulted in starch paste with low viscosity property. This shows that the flow behaviours of starches could not be singularly adduced to their botanical sources, but also to their intrinsic properties such as amylose/amylopectin ratio and molecular weight. The Pearson Correlation analysis showed that consistency coefficients (K) and flow behaviour indices (n) of the starches were non–linear as evident by their negative correlation coefficient, r values (r = -0.792, p<0.05, WCS; r = -0.978, p<0.01, RCS, r = -0.933, p<0.01, WYS; r = -0.997, p<0.01, YYS; r = -0.883, p<0.01, PPS; r = -0.725, p<0.05, LBS and r = -0.963, p<0.01, JBS). This implies that there was no corresponding linearity between K and n values of the starches as the level of hydroxypropylation increased. In addition, the Pearson Correlation analysis between yield stresses (σ_o) and consistency coefficient (K) of the starches indicated positive relationship (r = 0.698, p<0.05, WCS; r = 0.868, p<0.01, RCS; r = 0.841, p<0.01, WYS; r = 0.986, p<0.01, YYS; r = 0.972, p<0.01, PPS; r = 0.212, LBS and r = 0.235, p<0.01, JBS). This shows that consistency coefficient, which is a measure of pseudoplasticity, increased with increase in stress applied to the starch paste. Miller *et al.* (1973) have reported that high K and σ_o values are mainly due to the existence of interactions between swollen granules and/or between swollen granules and an extra granular network of exudates. This in turn means that the structural elements formed by molecular interactions that resist the flow are more when the viscosity of one starch pastes is high (Whistler and BeMiller, 1997). The starch paste is regarded as a blend of swollen granules, pieces of disrupted granules and

starch molecules liberated from the granules and then solubilized; the ratio of these different fractions varied.

Shear viscosities (0–900 s^{-1}) of native and hydroxypropylated starches at 25°C are presented in Figure 4.16. All the low-substituted starches showed significant rise in viscosity compared to both the native and high-substituted starches. The increase in viscosity could be adduced to increase in molecular weight of the hydroxypropylated starches as a result of possible reorganization and reinforcement of the glutan chains and its fragment instead of the expected depolymerization of the amylopectin chains. According to Krevelen (1972), bulk properties, such as melt and solution viscosity, are largely determined by the M_w. A study of the rheological properties of the starch pastes also enables the engineering scale up in production (Jackman, 1991), quality control as well as improvement of final products (Race, 1991).

5.10   THERMAL PROPERTIES

5.10.1   GELATINIZATION PROFILE

Gelatinization has been described as a semi cooperative or cooperative process (Marchant and Blanshard, 1978; Donovan, 1979; Evans and Haisman, 1982; French, 1983) in which the amorphous region hydrates and swells to a gel phase, straining the crystalline regions and tearing away molecular chains from the crystallites. This action stresses the crystallites so that they cooperatively melt at a lower temperature than if they were not associated with the gel phase. Structural relationships between the amorphous regions and crystallites within the starch granule are responsible for the sharpness of the transition and the temperature at which it occurs. Size and perfection of crystallites do not have a significant effect on these characteristics during thermal analysis (Donovan and Mapes, 1980).

5.10.1.1 Native and Ozone-Oxidized Starches

The gelatinization temperatures (onset, T_o; peak, T_p; and conclusion, T_c), enthalpies of gelatinization (ΔH_{gel}), temperature range (R) and peak height index (PHI) of the native and ozone-oxidized starches, as measured by DSC, are shown in Table 4.16. From the data obtained, ozone oxidation showed both significant and insignificant differences in the gelatinization parameters of the various starches. The data obtained in this study for both native starches and their oxidized-derivatives of WCS, RCS, WYS, YYS, PPS, LBS and JBS are not in total agreement with the previous findings of Chan *et al.* (2009) for corn, sago and tapioca starches. They reported that the process of gelatinization is not affected by ozone-oxidation treatment of the starches. However, within each starch type used in this study, the highest T_o values were 78.52±0.04^{o}C for WCS (15 min OGT), 75.96±0.07^{o}C for RCS (native), 71.23±0.01^{o}C for WYS (native), 71.55±0.54^{o}C for YYS (native), 76.61±0.06^{o}C for LBS (5 min OGT), 77.22±0.02^{o}C for JBS. However, T_o value remained unchanged among PPS starch type even after oxidation. Likewise, the highest T_p values within each starch type were 80.90±0.12^{o}C for WCS (15 min OGT), 78.66±0.04^{o}C for RCS (native), 74.52±0.06^{o}C for WYS (native), 74.93±0.06^{o}C for YYS (10 min OGT), 79.89±0.11^{o}C and 80.05±0.00^{o}C for LBS (native and 5 min OGT respectively) and 80.93±0.15^{o}C for JBS (native). However, T_p value remained unchanged among PPS starch type even after oxidation. Also, the highest T_c values within each starch type were 89.20±0.13^{o}C for RCS (native), 81.80±1.15^{o}C and 81.27±2.03^{o}C for YYS (native and 5 min OGT respectively) and 88.03±0.04^{o}C for LBS (5 min OGT). However, T_c values remained unchanged among WYS, WYS, PPS and JBS starch types even after oxidation with ozone.

Enthalpy of gelatinization, ΔH_{gel} values were similar among the starch types of WCS and RCS whereas slight differences were observed for other starch types. The highest ΔH_{gel} values within each starch type were 13.94±1.51 J/g and 11.99±0.79 J/g

215

for WYS (native and 5 min OGT respectively), 15.43±2.11 J/g for YYS (5 min OGT), 11.73±2.31 J/g for PPS (15 min OGT), 8.34±0.47 J/g and 7.85±0.83 J/g for LBS (native and 10 min OGT respectively) and 10.51±0.71 J/g for JBS (native). The gelatinization temperature range, R, which is a measure of difference between the conclusion (T_c) and onset (T_o) temperature, showed no significance difference among the starch types of WYS, YYS, PPS and LBS in spite of ozone oxidation treatment. However, the starch types with significant differences showed highest R values of 14.86±1.90^{o}C for WCS (10 min OGT), 13.24±0.21^{o}C for RCS (native) and 14.83±0.14^{o}C for JBS (10 min OGT). The highest PHI values within each starch type were 9.01±0.88 J/g.^{o}C for WCS (10 min OGT), 3.89±0.07 J/g.^{o}C for YYS (5 min OGT), 1.87±0.21 J/g.^{o}C for PPS (15 min OGT), 1.89±0.17 J/g.^{o}C for LBS (native) and 3.10±0.07 J/g.^{o}C for JBS (native). No significant differences were obtained for RCS and WYS. Temperature range of gelatinization and peak height index gave indication of the distribution of starch granules. The more heterogeneous the granules, the broader the temperature range and the lower the PHI (Sasaki, 2005; Yamin *et al.*, 1999; Knutson *et al.*, 1982). Higher amylopectin content can also lead to the narrowing of temperature range of gelatinization (Krueger, 1987).

The differences in gelatinization properties of the starches could, largely, be due to the molecular structure of amylopectin, and granular architecture (Gunaratne and Hoover, 2002). Higher gelatinization temperatures and enthalpy of the starches indicated the presence of strong bonding forces within the granule interior i.e. more orderly arrangement of molecules and thus higher degree of crystallinity (Peroni *et al.*, 2006; Tester and Morrison, 1990). This implies that the lower values of gelatinization temperatures of the starches could affect their crystallinity and crystallite sizes, which depend largely on their amylopectin lamellae. According to Ahmad *et al.* (1999), the gelatinization temperature and enthalpy of starches depend on the microstructure and degree of crystallinity within the granules and also on the granule size and the

amylose-to-amylopectin ratio. This process, according to Miles *et al.* (1985), is a reversible process below 100°C, but amylose retrogradation needs more energy to reverse the crystal formation. The onset temperature is influenced by short amylopectin branch-chains and low gelatinization temperatures are characteristics of starches with larger proportions of short amylopectin branch chains (Jane *et al.*, 1999). Peak temperature is an indication of granular architecture (crystalline quality) and a high peak temperature might be due to a higher proportion of longer chains in the amylopectin as these require higher temperatures to dissociate completely than required for shorter double helices (Karim *et al.*, 2000).

5.10.1.2   Native and Hydroxypropylated Starches

Table 4.17 presents the gelatinization temperatures (onset, T_o; peak, T_p; and conclusion, T_c), enthalpies of gelatinization (ΔH_{gel}), temperature range (R) and peak height index (PHI) of the native and hydroxypropylated starches, as measured by DSC. The gelatinization temperatures (onset, T_o; peak, T_p; and conclusion, T_c) decreased after hydroxypropylation process across the native starches with slight deviations observed for WCS, WYS and LBS at low–substitution level in terms of T_c. This implies that the native starches were more crystalline than their hydroxypropyl derivatives. However, in all cases of substitution levels, the values of gelatinization temperatures decreased as the level of substitution increased. This implies that the starch with higher molar substitution (MS) and degree of substitution (DS) of hydroxypropyl groups has lower gelatinization onset, peak and conclusion temperatures than the low–substituted starch from the same source. These observations are in agreement with previous works (Lawal, 2011; Lee and Loh, 2011). Lowering of gelatinization temperatures as MS and DS increase could be adduced to the addition of hydroxypropyl groups on starch polymer backbone, which allows higher flexibility (Singh *et al.*, 2004), resulting in the disruption of hydrogen bonds between starch

217

chains in the amorphous regions (Chuenkamol *et al.*, 2007; Perera, 1997). This disruption has been described as leading to increase in freedom of motion for starch chains in amorphous regions (Seow andThevamalar 1993; Choi and Kerr 2003). Thus, water accessibility is allowed, which reduces the temperature and gelatinization enthalpy (Liu *et al.*, 2010).

The data obtained in this study showed that starches at high-substitution level lose more crystallinity than the corresponding low-substituted starches of the same source due to rotation of the flexible hydroxypropyl groups, which results in the disruption of the double helices within the amorphous regions (Perera, 1997).

Enthalpy of gelatinization (ΔH_{gel}) values showed significant differences among the starches as the level of substitution increased. Significant differences were obtained for RCS, WYS, YYS, PPS and LBS while insignificant differences for WCS and JBS. In all the cases of significant differences, varying trends were observed for low- and high-substitution levels. Higher values of ΔH_{gel} were obtained for WYS and LBS at low level of substitution than at high level of substitution within the same starch type. An opposite trend was observed for RCS, YYS and PPS. These differences could be an indication that starches from different sources do not behave alike under the same treatment of hydroxypropylation. These observations are at variance with the report of Lawal (2011) for hydroxypropylated pigeon pea starch that enthalpy of gelatinization progressively decreased with increase in MS among the starch derivatives.

Gelatinization temperature range, R significantly and progressively increased as MS increased across the starch types with slight deviation observed for WYS at low level of substitution. This implies that after hydroxypropylation, the widths of gelatinization peaks (T_c–T_o) of the native starches became broader as MS increased. This is an evidence of structural re-organization upon the introduction of hydroxypropyl groups into the starch network, which facilitated the penetration of water as well as granular enlargement as a result of swelling. Peak height index (PHI)

values of the native starches decreased as molar substitution (MS) increased with an exception obtained for WYS at low level of substitution. In other words, the native starches exhibited higher PHI values than the starch derivatives. Temperature range of gelatinization and peak height index gave indication of the distribution of starch granules.

The data obtained in this study showed that, under identical hydroxypropylation process, the gelatinisation profile of starches could be influenced not only by the starch composition (amylose to amylopectin ratio) and botanical sources, but also by others such as the granular architecture (crystalline to amorphous ratio), the molecular structure of amylopectin (extent of branching, unit chain length) (Gunaratne and Hoover, 2002).

5.10.2 RETROGRADATION PROFILE

5.10.2.1 Native and Ozone-Oxidized Starches

The transition temperatures (onset, T_o; peak, T_p; and conclusion, T_c), enthalpies of transition (ΔH_{ret}), temperature range (R) and percentage of retrogradation (%R) of the native and ozone–oxidized starch gels after 7 days of storage at 4^oC, as measured by DSC, are shown in Table 4.18. From the data obtained, ozone oxidation resulted in mixed trends of differences in the retrogradation parameters of the various native starches. Decrease in onset temperature, T_o values of the retrograded starch gels were obtained for WYS and JBS after ozone oxidation. Conversely, T_o values increased upon oxidation for YYS, PPS (except at 10 min OGT) and LBS (except at 10 min OGT). However, no significant differences were obtained for retrograded starch gels of WCS and RCS upon oxidation with ozone at varying OGTs. T_p values of the retrograded native starch gels became higher for WCS and PPS, but lower for RCS, LBS and JBS after ozone oxidation at varying OGTs. However, there were no noticeable changes in T_p values for WYS and YYS in spite of ozone oxidation. The

219

conclusion temperature, T_c values of the retrograded native starch gels decreased for YYS, increased for WYS and LBS and showed insignificant differences for WCS, RCS, PPS and JBS upon oxidation with ozone. The retrogradation enthalpies (ΔH_{ret}) of the retrograded native starch gels increased for WCS, LBS and JBS, reduced for YYS and showed no significant differences for WCS, RCS and PPS upon oxidation with ozone at varying OGTs. The temperature ranges (R) of the retrograded starch gels were similar for WCS, RCS and PPS after ozone-oxidation. However, the temperature ranges of the retrograded gels increased for WYS, LBS (except at 15 min OGT) and JBS, and decreased for YYS upon oxidation with ozone at varying OGTs.

Comparatively, the retrogradation (endothermic) transition temperatures (T_o, T_p, and T_c) and melting enthalpies of retrogradation (ΔH_{ret}) were below the gelatinization temperatures and melting enthalpies of gelatinization (ΔH_{gel}). It has been suggested that the starch fraction responsible for retrogradation, as measured by DSC, is amylopectin (Eliasson, 1985; Eliasson and Ljunger, 1988; Russell, 1983, 1987). Increase in temperatures and enthalpies of retrograded starch gels has been reported for native and oxidized barley and corn starches as being due to the oxidation process, which degraded the amorphous and crystalline lamella and produced dextrins, which might be similar in length to the short chains of amylopectin (Chavez-Murillo *et al.*, 2008). The crystalline region is an ordered arrangement of double helical amylopectin structures. Embedded in the amorphous region, amylose has been proposed to disrupt the crystalline packing of amylopectin (Atichokudomchai *et al.*, 2001). Depolymerization of the amorphous regions by ozone results in a reduced hindrance to double helical chains approaching each other, thus facilitating and promoting crystallization of amylopectin and thereby leading to the increased ΔH_{ret} required to melt the crystalline region (Chan *et al.*, 2009). However, decreasing enthalpy is considered to be due to the decreased proportion of ordered regions (Lui *et al.*, 2010).

Percentage regrogradation (%R) values of the native starch gels varied among the starch sources. No significant differences were observed in the %R values between the native and ozone-oxidized derivatives of RCS and WCS (except at 10 min OGT). Reductions in %R values were observed for YYS and PPS while an increase was observed for WYS (except at 5 min OGT), LBS and JBS after oxidation with ozone. Lui *et al.* (2010) have reported that the final ΔH_{ret} was about 78% of ΔH_{gel} for waxy corn starch. The least ΔH_{ret} observed for the starches used in this study, was about 43% of ΔH_{gel} for WYS (at 5 min OGT) and the highest ΔH_{ret} was about 178% of ΔH_{gel} for LBS (at 5 min OGT).

According to Lewandowicz *et al.* (2002), retrogradation phenomenon is associated with the tendency of amylose to retrograde and amylopectin with low tendency to retrograde. In other words, retrogradation is accompanied by recrystallization of amylopectin chains. High value of ΔH_{ret} could indicate high tendency of recrystallization of amylopectin chains possibly initiated by the assembling of the molecular fragments. Retrogradation of starch has some important consequences in various areas such as a cake not rising well, cream separation, bread hardening (gone stale) without being dry, running pastes and glues (Alais *et al.*, 1999). deMan (1979) has ascribed the staling of bread to retrogradation, which gives the bread its elastic and tender crumb structure. Staling is the hardening of the crumb upon storage. Therefore, the starches, used in this study, with low %R values could be applicable in products where retrogradation is a performance index.

5.10.2.2   Native and Hydroxypropylated Starches

Table 4.19 presents the retrogradation transition temperatures (onset, T_o; peak, T_p; and conclusion, T_c), enthalpies of transition (ΔH_{ret}), temperature range (R) and percentage of retrogradation (%R) of the native and hydroxypropylated starch gels after 7 days of storage at 4^oC, as measured by DSC. From the data obtained in this

study, hydroxypropylation showed mixed trends of significant and insignificant differences in the retrogradation parameters among various native starches. Onset temperatures, T_o showed no significant differences for WCS, YYS and JBS after hydroxypropylation. However, T_o values progressively increased for RCS, WYS, PPS (except at low level of substitution) and LBS as molar substitution increased. Peak temperatures, T_p of the native starches of WCS, RCS and LBS showed no significant differences in the corresponding hydroxypropyl derivatives. Within each starch type, T_p values were higher in the native for WYS, YYS and PPS, and progressively increased for JBS (except at high substitution level). Likewise, T_c values were significantly similar for WCS, RCS, PPS, LBS and JBS, but increased for WYS and decreased for YYS upon hydroxypropylation. Lowering of transition temperatures of retrograded starch gels has been adduced to the rearranged structure of retrograded starch, which is less stable than what had existed in the native starch (Lui*et al.*, 2010; Ward *et al.*, 1994; Fisher and Thompson, 1997). In addition, Tuschhoff (1986) has opined that lowering gelatinization temperature is due mainly to the presence of a substituting group that weakens or strains the internal bond structure holding the granule together.

Transition enthalpy (ΔH_{ret}) values of the retrograded native starch gels remained unchanged after hydroxypropylation for PPS, LBS and JBS. A slight increase was observed for WYS only at high substitution level and a decrease was observed for WCS, RCS and YYS as the molar substitution increased. Decrease in transition enthalpy of retrograded starch has been reported for various starches (Lan *et al.*, 2010; Lui *et al.*, 2010; Butler *et al.*, 1986; Hoover, *et al.*, 1988; Yeh and Yeh, 1993). The hydroxypropyl groups introduced into the starch chains were capable of disrupting intermolecular and intramolecular hydrogen bonds, thereby weakening the granular structure of starch. This would, however, lead to an increase in freedom of motion for

starch chains in amorphous regions (Wootton and Manatsathit, 1983; Seow andThevamalar, 1993; Choi and Kerr, 2003).

The temperature range, R values reduced for WCS, RCS and WYS (except at low substitution level) upon hydroxypropylation. No significant differences were observed for YYS, PPS, LBS and JBS. Within the hydroxypropylated starches, the endothermic temperature range values reduced as more hydroxypropyl groups were introduced into the native starch granular matrix. Retrogradation is an endothermic transition and the reduced temperature range is a possible indication of low cooperative melting due to homogeneous crystalline phase. Thus, high R values of the hydroxypropylated starches suggest the possible presence of crystallite of varying stabilities within the crystalline domains of the starch granules (Hoover *et al.*, 1997).

Comparatively, the retrogradation (endothermic) transition temperatures (T_o, T_p, and T_c), temperature ranges and melting enthalpies (ΔH_{ret}) of retrograded gels were below the gelatinization temperatures and melting enthalpies of gelatinization (ΔH_{gel}). These observations suggest that retrogradation gave rise to reassociation of the gelatinized starch molecules, but in a less ordered and hence less stable way than those existing in the native starch granules (Karim *et al.*, 2000).

Generally, all the hydroxypropyl derivatives showed lower tendency for reassociation of starch molecules than the native starches. These observations were evident by the low %R values obtained after hydroxypropylation for the starches with slight deviations observed for low-substituted YYS and high-substituted JBS. Percentage retrogradation (%R) decreased from 58.99 to 17.27% for WCS, 65.79 to 10.06 for RCS, 50.12 to 37.63 for WYS, 108.37 to 39.69 for YYS, 118.83 to 58.74 for PPS, 58.74 to 37.89 for LBS and 44.99 to 42.84 for JBS. The data obtained in this study reaffirm that hydroxypropylation prevents retrogradation.

5.11   X-RAY DIFFRACTION PATTERNS

5.11.1   Native and Ozone-Oxidized Starches

Table 4.20 shows major characteristics of X-ray diffraction of native and selected ozone-oxidized starches, which are used to both study and classify the crystalline patterns and behaviours of the starches. Ozone-oxidized starches at specific OGTs were analysed, because at these OGTs, the selected ozone-oxidized starches competed favourably, in terms of pasting properties, with oxidized starches prepared by conventional alkaline hypochlorite method. Pasting properties of ozone-oxidized have been reported by An and King (2009) to compare favourably with alkaline hypochlorite oxidized starches. X-ray diffraction characteristics of three strongest peaks were used in this study to investigate the crystallinity of the native starches and ozone-oxidized derivatives.

X-ray diffraction peaks for the native starches appeared at 14.95^{o}, 16.95^{o} and 22.10^{o} 2θ for WCS, corresponding to interplanar d-spacing of 5.95Å, 5.23Å and 3.95Å; 15.25^{o}, 17.30^{o} and 17.40^{o} 2θ for RCS, corresponding to interplanar d-spacing of 5.73Å, 4.90Å and 3.85Å; 5.80^{o}, 15.05^{o} and 17.40^{o} 2θ for WYS, corresponding to interplanar d-spacing of 5.80Å, 5.82Å and 5.04Å; 5.75^{o}, 14.25^{o} and 17.10^{o} 2θ for YYS, corresponding to interplanar d-spacing of 5.75Å, 5.91Å and 5.20Å; 15.25^{o}, 17.10^{o} and $22.80^{o}2\theta$ for PPS, corresponding to interplanar d-spacing of 5.87Å, 5.16Å and 3.85Å; 15.20^{o}, 17.20^{o} and $22.90^{o}2\theta$ for LBS, corresponding to interplanar d-spacing of 5.76Å, 5.15Å and 3.87Å and 15.25^{o}, 17.00^{o} and $22.75^{o}2\theta$ for JBS, corresponding to interplanar d-spacing of 5.80Å, 5.12Å and 3.91Å. The strongest and broadest diffraction peaks appeared at $2\theta = 16.95^{o}$, 17.30^{o}, 17.40^{o} and 17.10^{o} for native starches of WCS, RCS, WYS and YYS respectively. These reflections indicate that these native starches are of B-type crystalline nature. Starches of roots and tubers have been reported to exhibit maximum X-ray diffraction peaks at 17° 2θ (Hoover, 2001). However, other diffraction peaks are observed at 22.10^{o} and 22.11^{o} 2θ for WCS and

RCS, corresponding to 3.95Å and 3.85Å, suggesting the presence of A-polymorph in the root and tuber starches in addition to B-polymorph. Since the relative intensities of B-polymorph of the starch granules (64%, WCS; 68.5%, RCS) were higher than those of A-polymorph (49%, WCS; 64.2%, RCS), crystals of WCS and RCS were better classified as C_B-type. This indicates that the crystals were closer to B chains of amylopectin molecules of the starch matrix (Lopez-Rubio *et al.*, 2008). Likewise, the crystals of PPS, LBS and JBS were mixes of A- and B-polymorphs with B-polymorph more predominant. Hence, they were classified as C_B-type of crystallinity. Morris *et al.* (1998) have reported that C-type pea starch has both the A- and B-polymorphs present in a single granule and the B-polymorph being at the hilum and the A-polymorph at the periphery. These observations are in agreement with previous observations that C-type pattern, which is an intermediate between A and B types, is observed for legume starches (Lopez-Rubio *et al.*, 2008; Karim *et al.,* 2000). Upon oxidation, diffraction peaks appeared at $2\theta = 15.20^o$, 17.30^o and 23.35^o, corresponding to 5.81Å, 5.18Å and 3.80Å interplanar d-spacing (WCS at 10 min OGT); 15.35^o, 17.50^o, 18.30^o and 23.00^o, corresponding to 5.32 Å, 5.12Å, 4.83Å and 3.32Å interplanar d-spacing (RCS at 10 min OGT); 5.85^o, 17.35^o and 23.40^o, corresponding to 15.03Å, 5.17Å and 3.59Å interplanar d-spacing (WYS at 10 min OGT); 5.70^o, 17.25^o and 24.10^o, corresponding to 15.23Å, 5.14Å and 3.60Å interplanar d-spacing (YYS at 10 min OGT); 15.25^o, 17.40^o and 23.05^o, corresponding to 5.92Å, 17.40Å and 3.77Å interplanar d-spacing (PPS at 15 min OGT); 15.15^o, 17.35^o and 23.20^o, corresponding to 5.84Å, 5.12Å and 3.84Å (LBS at 5 min OGT) and 15.20^o, 17.85^o and 23.20^o, corresponding to 5.99Å, 5.07Å and 3.82Å (JBS at 5 min OGT). From these data, there was no significant difference in the X-ray diffraction patterns of the native WCS and RCS upon oxidation with ozone (Figures 4.17–4.18). The same observations were obtained for native PPS, LBS and JBS upon oxidation with ozone, although there were other weak reflections (Fig. 4.21–4.23). However, slight significant differences were observed after ozone–

oxidation for WYS and YYS. Broader peaks were observed at $2\theta = 23.40^{o}$ (WYS) and 24.10^{o} (YYS) in addition to the weaker ones (Fig. 4.19–4.20). The reflections for YYS at 10 min OGT were closely similar to C_A-type reported for sweet potato starch at $2\theta =$ 15.4°, 17.2°, 18.3° and 23.4° (Noda *et al.*, 1995; Osundahunsi *et al.*, 2003).

5.11.2   Native and Hydroxypropylated Starches

Major characteristics of X-ray diffraction of native and selected hydroxypropylated starches used to both study and classify the crystalline patterns and behaviours of the starches, which include intensity (counts), Bragg's angle (2θ degree), interplanar d-spacing (d) and relative intensity (%), are presented in Table 4.21. X-ray diffraction characteristics of three strongest peaks were used in this study to investigate the crystallinity of the native starches and their hydroxypropyl derivatives. From the previous discussion, the natives starches used in this study have been classified to possess mixtures of A- and B-polymorphs, hence, their crystals are C_B-type. It has been shown that A-type and B-type starches are based on the parallel stranded double helices in which the double helices are closely packed in A-type, but loosely packed in B-type, and that starches with short chain length (<20 residues) exhibit A-type crystallinity whereas those with longer average chain length of amylopectin exhibit B-type crystallinity (Hizukuri, 1986; Hizukuri *et al.*, 1983). After hydroxypropylation, X-ray diffraction peaks appeared at $2\theta = 15.30^{o}$, 18.20^{o} and 23.20^{o}, corresponding to 5.79 Å, 4.88Å and 3.83Å interplanar d-spacing (low-substutited WCS); 15.30^{o}, 17.90^{o} and 23.45^{o}, corresponding to 5.79Å, 4.85Å and 3.84Å interplanar d-spacing (low-substutited RCS); 9.80^{o}, 15.10^{o} and 17.25^{o}, corresponding to 7.59 Å, 5.32 Å and 5.11 Å interplanar d-spacing (high-substutited WYS); 5.45^{o}, 17.10^{o} and 23.70^{o}, corresponding to 15.60 Å, 5.19 Å and 3.70 Å interplanar d-spacing (high-substutited YYS); 15.10^{o}, 17.40^{o} and 22.85^{o}, corresponding to 5.60Å, 5.14 Å and 3.85 Å interplanar d–spacing (high–substutited PPS); 15.20^{o}, 17.25^{o} and 23.05^{o}, corresponding

to 5.80 Å, 5.15 Å and 3.79 Å interplanar d-spacing (low-substituted LBS) and 14.90^o, 16.85^o, 17.95^o and 22.65^o, corresponding to 5.94 Å, 5.22 Å, 4.93 Å and 3.86 Å interplanar d-spacing (high-substutited JBS). These observations showed no pronounced pattern differences between the native and hydroxypropylated starches (Figures 4.24–4.30). Therefore, these observations concretize the fact that hydroxypropylation affects the amorphous component of the starch granules being more accessible to the reagents and consequently, the crystalline region is preserved (Lawal, 2011). The data obtained are in agreement with previous works (Liu *et al.*, 2010; Lawal, 2011).

The role of starch in bread staling has been studied, using the X-ray diffraction technique. Starch in freshly baked bread is mostly amorphous, but slowly recrystallizes during storage. Both freshly pasted starch and the starch from fresh bread exhibit amorphous X-ray patterns. However, on storage, each developed crystallinity. This return, from the amorphous to the crystalline state, is called retrogradation (Katz, 1934).

5.11.3   Crystallization Behaviours

Starch is formed by birefringent, semi-crystalline granules that are composed of two different glucose polymers, linear amylose, and highly branched amylopectin. Starch is considered as a two-phase semi-crystalline polymer in which the crystallites are dispersed in a homogeneous amorphous phase (fringed micelle model) (Biliaderis *et al.*, 1986; Jenkins and Donald, 1995; Donova, 1975; Knutson *et al.*, 1982). The development of crystallinity, in an ageing non-waxy starch gel, proceeds in a biphasic manner (Miles *et al*., 1985); crystallization of amylose is completed very much earlier than that of amylopectin (Karim *et al*., 2000). The granule crystallinity is associated with the amylopectin and the single endotherm is attributed to the reorganization of starch crystallites. The crystallization behaviours of starch have strong impact on the

texture of starchy products (anti-staling effect of monoglycerides) and the retention and the controlled release of guest molecules. Processed starches can be semi-crystalline, depending on the conditions used for processing and the ageing history (Buléon *et al.*, 2007).

The degrees of crystallinity of the native and ozone-oxidized starches are depicted in Table 4.22. Among all the starches the native starches exhibit higher crystallinity than their corresponding derivatives oxidized with ozone. The highest crystallinity (31.70%) among the native starches was observed for WCS while the least (21.46%) in JBS. High percentage of crystallinity is an indication of the prepoderance of amylopectin chains in the starch. High crystallinity has been given as the correlation between crystallinity and the amount of amylopectin B1 chains, because amylopectin B1 chains are mainly responsible for the formation of the crystalline lamellae (Hizukuri, 1985). These observations imply that such starches could have less tendency for aging during storage.

Upon oxidation, a decrease in crystallinity (%) was observed in all the starches. Relative to the native starches, drops in crystallinity were 63.06% (WCS), 62.91% (RCS), 71.97% (WYS), 63.29% (YYS), 60.13% (PPS), 77.66% (LBS) and 68.59% (JBS). These observations could imply that oxidation with ozone mostly occur in the amorphous lamellae where amylose molecules are present, thus, resulting in little effect on the crystallinity of the starches. However, the average crystallite sizes (nm) of the native starches increased upon oxidation with ozone. A possible explanation for this is that some of the amylose molecules could have co-crystallized with amylopectin. A partial involvement of amylose in the amylopectin crystallites has been supported by Zobel (1988a). The amylose chains that co-crystallize with the external chains of amylopectin would act as a cross-linker between the crystalline lamellae. In addition, oxidation of these sarches could have brought about crosslinking of the starch molecules, especially amylose, which, when crystallized, appeared as a more giant

network. This would, undoubtedly, increase the size of the crystals as fragments come together to form more huge crystals. This possibility of amylose forming crystalline structure or co-crystallizing with amylopectin besides forming amylase-lipid complex, which is typically V-type diffraction pattern, has been reported by Kuakpetoon and Wang (2006). Relatively, crystallite size, among all the native starches, increased from 0.08 nm to 0.36 nm (WCS), 0.15 nm to 0.26 nm (RCS), 0.14 nm to 0.75 nm (WYS), 0.16 nm to 0.56 nm (YYS), 0.08 nm to 0.44 nm (PPS), 0.11 nm to 1.23 nm (LBS) and 0.11 nm to 0.54 nm (JBS).

Upon hydroxypropylation, there were strong decreases in crystallinity degrees of the starches (Table 4.23). Relatively, the reductions were 79.91% (WCS), 66.71% (RCS), 68.39% (WYS), 43.95% (YYS), 69.16% (PPS), 98.20% (LBS) and 60.71% (JBS). From these data, the least decrease (43.95%) was observed for YYS and the highest (98.20%) for LBS. These observations corroborate the percentage retrogradation values earlier obtained for the hydroxypropylated starches in this study (Table 4.19). The introduction of hydroxypropyl groups into the starch matrix interfered with the retrogradation of starch molecules, thereby inhibiting gelation and syneresis, apparently by sterically interfering with formation of junction zones and double helices in starch (Seib, 1996).

5.12 MOLECULAR MASS DISTRIBUTION

5.12.1 Native and Ozone-Oxidized Starches

The amylose content, amylopectin content, molecular weight, that is, average M_w and number average, M_n, weight average degree of polymerization = DP_w, number average molecular = DP_n and PDI = Polydispersity index (M_w/M_n) of the native starches and selected ozone–oxidized derivatives are presented in Table 4.24. Generally, the amylose contents of the ozone-oxidized derivatives were higher than their corresponding native starches while opposite observations were obtained in terms

of their amylopectin contents. Among all the native starches, the highest (20.75±0.05%) and lowest (19.44±0.10%) amylose contents were obtained for RCS and LBS respectively. Upon oxidation, at various OGTs, there was gradual increase in amylose contents with corresponding decrease in amylopectin contents. Amylose contents of the starches increased from 19.62±0.05 to 25.63±0.05% (WCS), 20.75±0.05 to 24.71±0.05% (RCS), 19.75±0.10 to 25.62±0.05% (WYS), 20.05±0.05 to 25.52±0.10% (YYS), 20.33±0.05 to 25.87±0.10% (PPS), 19.44±0.10 to 24.96±0.11% (LBS) and 20.29±0.20 to 23.93±0.06% (JBS). Conversely, amylopectin contents decreased from 80.39±0.05 to 74.38±0.05% (WCS), 79.26±0.05 to 75.30±0.05% (RCS), 80.28±0.10 to74.38±0.05% (WYS), 79.96±0.05 to 74.48±0.10% (YYS), 79.68±0.05 to 74.13±0.10% (PPS), 80.56±0.10 to 75.05±0.11% (LBS) and 79.71±0.20 to 76.07±0.06% (JBS). This could imply that oxidation with ozone mostly occured in the amorphous lamellae where amylose molecules are present, thus, resulting in little effect on the crystallinity of the starches. In other words, ozone-oxidation of the starches results in partial depolymerization of portion of the crystalline lamellae, which mainly consist of amylopectin chains. These observations might substantiate the lowering of crystallinity of the native starch upon oxidation. Kuakpetoon and Wang (2006) have proposed that the degradation of amylose and amylopectin is not proportional to the concentration of the oxidizing agent, and that starch granules might have two locations with different accessibility and susceptibility to oxidation.

The values of M_w (g/mol) of the oxidized starches increased significantly compared to the native starches. Opposite trend of general decrease in the values of M_n (g/mol) was observed for the native starches following oxidation at various OGTs with slight deviation observed for LBS at 5 min OGT. The relative increase in M_w of the oxidized starches to the native starches were 78.72%, 69.64%, 63.91%, 79.25%, 96.18%, 12.42% and 4.08% for WCS, RCS, WYS, YYS, PPS, LBS and JBS respectively. In the same vein, the relative decrease in M_n of the oxidized starches to

the native starches were 47.66%, 46.36%, 50.94%, 50.91%, 45.28% and 1.85% for WCS, RCS, WYS, YYS, PPS and JBS respectively. M_n values increased for LBS by 1.94%. Higher values of weight average, M_w of the oxidized starches could be indicative of formation of intermolecular cross-links (Wang and Wang, 2003) between ozone gas and the amylose molecules, which is accompanied by partial depolymerization of portion of amylopectin chains as evident by their increased proportion of amylose. These observations show that amylose content and amylopectin content are linearly proportional to M_w and M_n respectively. Mizukami *et al.* (1999) have reported that molecular weight is associated with starch solubility, meaning that small amylopectin molecules dissolve more easily in hot water than the large molecules. For easy release of the active ingredients in the pharmaceuticals and in the food industry such as baby food, yoghurt and dessert like products, where high solubility is associated with good cooking and eating qualities, starch with small amylopectin molecules are more suitable than those with large amylopectin molecules (Moorthy, 2002). These observations are supported by the data obtained for the starches used in this present study as their solubility values upon ozone-oxidation as OGT increased from 5 to 15 min (Table 4.8). Amylopectin molecular weight has also been reported to influence the pasting viscosity of starch (Bultosa *et al.*, 2008). Larger molecular weight amylopectin molecules have capability of inter- and intra-molecular interactions, thus making them more difficult to dissolve in hot water which may affect starch pasting properties (Mufumbo *et al.*, 2011).

Degrees of polymerization (weight and number) are expressed according to the method of Chen and Bergman (2007). They hypothesized that amylose is predominantly located in the amorphous growth rings, and that the interaction between amylose and amylopectin in these amorphous regions may be the cause of decreased crystallinity. The degree of interaction between amylose and amylopectin could depend on the botanical source of the starch (Oates, 1997), with amylose and amylopectin

more closely associated in potato starch than in corn starch (Hoover and Vasanthan, 1994; Saibene *et al.*, 2008; Zobel, 1988b). The DP_w values of the native starches increased upon oxidation with ozone while DP_n values decreased upon oxidation with slight exception at 5 min OGT for LBS. Relative increases in DP_w values upon oxidation were 78.82%, 69.37%, 63.84%, 79.59%, 95.88%, 12.17% and 4.27% for WCS, RCS, WYS, YYS, PPS, LBS and JBS respectively. Likewise, decrease in DP_n values were 47.58%, 46.39%, 59.92%, 50.96%, 45.26% and 1.95% for WCS, RCS, WYS, YYS, PPS and JBS respectively. However, increase in DP_n by 2.93% was observed for LBS. The data obtained in terms of DP_w and DP_n are true reflections of the varying values of M_w and M_n respectively in the various starches.

Polydispersity index, M_w/M_n is an indication of broadness of molecular weight distribution (Gowariker *et al.*, 1986). Polydispersity indices of the oxidized starches were higher than the corresponding native starches. This is an indication that, upon oxidation, M_n decreased faster than M_w. The ranges of polydispersity indices 2.91–3.44 and 10.59–11.56 were observed for native and oxidized starches respectively. These observations imply that the oxidized derivatives possess broader range of molecular weights than the native starches.

Table 4.25 shows the classification of amylopectin branched chains into chain types and corresponding degree of polymerization (DP) according to Hanashiro *et al.* (1996) as A chain (DP <12), B1 chain (DP 13–24), B2 chain (DP 25–36) and B3[†]chain (DP≥37). According to the revised cluster model of amylopectin branching proposed by Hizukuri (1986), A and B1 chains are located withina single cluster in which they form double helices, which corresponds to one crystalline lamella, whereas B2 andB3[†] chains extend through two or more clusters. Therefore, B2 and longer chains are present in both the crystalline and amorphous lamellae. Based on this model, the degradation of each chain type after oxidation could indirectly suggest the site of oxidation. From the data, percentage distribution of amylopectin in A chain reduced

upon oxidation while that of B1 chain increased with slight deviation observed for WYS. Upon oxidation of the native starches, the percentage distribution of amylopectin in B2 chain increased, with deviation observed for RCS, and that of B3[†] chain increased with deviation observed for YYS. With reduction in the crystallinity of the native starch upon oxidation, as earlier explained, the depolymerization of amylopectin directly occurs in the branched A chain located within a single cluster in which it forms double helices, which corresponds to one crystalline lamella (Kuakpetoon and Wang, 2006). It is surprising that B1 chain, which is in the same location with A chain, showed increase in amylopectin chain distribution upon oxidation. These observations may substantiate the reason for higher crystallite sizes of the oxidized derivatives than the native starches with corresponding lower values of percentage crystallinity (Table 4.22). Of all the chain lengths, B1 chain wass most abundant and the least was B3[†]. The peak percentage chain length distribution of B1 chain (DP 13–24) was 35.50±0.71 obtained for ozone-oxidized LBS while the lowest percentage chain length distribution of B1 chain (DP 13–24) was 31.50±0.71 obtained for native WCS, RCS, PPS and oxidized WYS (at 10 min OGT). It is worthy of note that, from the data displayed in Table 4.22, LBS possessed the least crystallinity (3.93%) and the peak crystallite size (1.23 nm) at 10 min OGT (Table 4.22). These may imply that as A chain, which is in the same cluster with B1 chain, undergoes depolymerization, the other chain, B1 chain undergoes cross-linking with ozone molecules simultaneously. This insight has been earlier divulged with the classification of both native and oxidized derivatives of PPS, LBS and JBS (legume starches) as C_B-type crystals, as mixture of A- and B-polymorphs (Lopez-Rubio *et al.*, 2008).

5.12.2 Native and Hydroxypropylated Starches

The amylose and amylopectin contents, molecular weight, that is, average weight, M_w and number average, M_n, weight average degree of polymerization = DP_w,

number average molecular $= DP_n$ and PDI = Polydispersity index (M_w/M_n) of the native and selected hydroxypropylated starches are presented in Table 4.26. The selection is with the view to exploring more information on the mixed integrity of the starch pastes as earlier discussed for data obtained in paste viscosity analysis (Table 4.11). From Table 4.26, the amylose contents of the native starches generally increased after hydroxypropylation and corresponding decrease was obtained for them in terms of amylopectin contents. These observations justify the decrease in percentage retrogradation of the native starches upon hydroxypropylation (Table 4.19). Retrogradation, which is associated with crystallization of amylopectin molecules (Karim *et al.*, 2000), is prevented by hydroxypropylation.

The values of M_w of the native starches significantly increase after hydroxypropylation while M_n decreased with exception observed for RCS and LBS. M_w values increased relative to the native starches by 10.33% (WCS), 82.17% (RCS), 77.41% (WYS), 84.28% (YYS), 98.73% (PPS), 16.67% (LBS) and 85.42% (JBS). M_n values decreased relative to the native starches by 3.74% (WCS), 46.23% (WYS), 41.82% (YYS), 45.28% (PPS) and 43.52% (JBS). However, 8.74% decrease in M_n value was observed for (LBS). The increase in M_w upon hydroxypropylation could suggest the reinforcement of the granule structure rather than the expected depolymerization of the amylopectin chains in the starch granules. This structural reinforcement instead of depolymerization could be responsible for the increased values of peak viscosity, cold paste viscosity, breakdown and setback hydroxypropylated starches. Chen *et al.* (2010) have reported that molecular weight appeared to be an important factor affecting the pasting properties. Amylopectin molecules with higher molecular weight have more branched chains and more densely packed molecules (Yoo and Jane, 2002). The decrease in amylopectin molecular weight obtained in this study is favourable, because high molecular amylopectin molecular weight has been reported to decrease the amount of long–branch chain

length as well as branching degree of amylopectin, resulting into an increased peak and breakdown viscosity, decrease in setback and final viscosity (Takeda *et al.*, 1989), thus making such starch unsuitable in textile and paper industries, where high final viscosities are desired (Mufumbo, 2011).

Degrees of polymerization (weight and number) are expressed according to the method of Chen and Bergan (2007). They hypothesized that amylose is predominantly located in the amorphous growth rings, and that the interaction between amylose and amylopectin in these amorphous regions may be the cause of decreased crystallinity. The degree of interaction between amylose and amylopectin may depend on the botanical source of the starch (Oates, 1997), with amylose and amylopectin more closely associated in potato starch than in corn starch (Hoover and Vasanthan, 1994; Saibene*et al.*, 2008; Zobel, 1988a). The DP_w values of the native starches increased upon hydroxypropylation while DP_n values decreased except for RCS and LBS. DP_w values increased by 10.34% (WCS), 96.85% (RCS), 77.68% (WYS), 84.69% (YYS), 98.45% (PPS), 16.40% (LBS) and 86.26% (JBS).

Likewise, DP_n values decreased by 3.64% (WCS), 46.82% (WYS), 41.83% (YYS), 45.26% (PPS) and 43.48% (JBS). However, DP_n values increased by 101.77% (RCS) and 2.93% (LBS). The data obtained in terms of DP_w and DP_n are true reflections of the varying values of M_w and M_n respectively in the various starches, meaning that they are linearly related.

Polydispersity index, M_w/M_n is an indication of broadness of molecular weight distribution (Gowariker *et al.*, 1986). Polydispersity indices (PDI) of the hydroxypropyl derivatives are higher than the corresponding native starches. This is an indication that, upon hydroxypropylation, M_n decreased faster than M_w. Comparatively, the high-substituted starches showed higher PDI values than the low-substituted starches. This discrepancy could be adduced to increase in interaction between the

hydroxypropyl groups and the starch molecules as molar substitution and/or degree of substitution increases.

The classification of amylopectin branched chains into chain types and corresponding degree of polymerization (DP), according to Hanashiro *et al.* (1996) as A chain (DP <12), B1 chain (DP 13–24), B2 chain (DP 25–36) and B3[†]chain (DP ≥37) is shown in Table 4.27. From the data, percentage chain length distribution of amylopectin in the A chain reduced after hydroxypropylation while that of B1 chain increased with deviations observed for RCS and WYS. The introduction of hydroxypropyl group into the matrix of the native starch network could have been on B1 chain rather than A chain due to decrease in chain length distribution of the A chain. The short branched chains (A and B1), which do not easily reassociate on cooling, are known to inhibit retrogradation (Kalichevsky *et al.*, 1990; Wursch and Gumy, 1994). B1 chain length distribution increased after hydroxypropylation with deviations observed for RCS and WYS. As earlier expressed, it is surprising that B1 chain, which is in the same location with A chain, showed increase in amylopectin chain distribution upon hydroxypropylation. These observations may substantiate the reason for higher crystallite sizes of the hydroxypropyl derivatives than the native starches with corresponding lower values of percentage crystallinity (Table 4.23). B2 chain length distribution virtually remains constant, except for RCS and WYS. This may account for tendency of cluster cleavage between the locations of short chains (A and B1) and (B2 and B3[†]) in the starch granules. Of all the chain lengths, B1 chain was most abundant and the least was B3[†]. The peak percentage chain length distribution of B1 chain (DP 13–24) was 36.00±1.41 obtained for low-substituted WCS and the lowest percentage chain length distribution of B1 chain (DP 13–24) was 25.00±1.41 obtained for high-substituted WYS.

Mufumbo *et al.* (2011) have reported correlation of pasting properties of starches, such as final viscosity and temperature with the short and long chains of

amylopectin with the view to ascertaining the participation of the amylopectin molecules in determining the pasting behaviours of the starches. It is interesting to know the actual chains involved in determining the pasting behaviours of the starches. Pearson Correlation analysis of relationship between pasting temperature and the chains is A Chain ($r = 0.969$, $p<0.05$, WCS; $r = 0.951$, $p<0.05$, RCS; $r = 0.931$, WYS; $r = 0.622$, YYS; $r = 0.976$, $p<0.05$, PPS; $r = -0.033$, LBS and $r = 0.974$, $p<0.05$, JBS), B1 Chain ($r = -0.943$, WCS; $r = 0.915$, RCS; $r = -0.969$, $p<0.05$, WYS; $r = -0.543$, YYS; $r = -0.934$, PPS; $r = -0.057$, LBS and $r = -0.887$, JBS), B2 Chain ($r = 0.704$, WCS; $r = -0.097$, RCS; $r = 0.049$, WYS; $r = -0.839$, YYS; $r = -0.778$, PPS; $r = 0.417$, LBS and $r = -0.015$, JBS), B3† Chain ($r = -0.584$, WCS; $r = -0.990$, $p<0.01$, RCS; $r = -0.902$, WYS; $r = -0.177$, YYS; $r = -0.999$, $p<0.01$, PPS; $r = -0.476$, LBS and $r = -0.901$, JBS). Positive and negative values of coefficient, r could imply the participation and indifference of the various chains to the determination of pasting temperatures of the starches upon hydroxypropylation. A chain has positive correlation with pasting temperatures of all the starches except LBS while B1 chain has negative correlation for all the starches except PPS, LBS and JBS. B2 chain had positive correlation for only WCS, WYS and LBS while B3† chain had negative correlation for all the starches. From the analysis, it can be inferred that the interaction between hydroxypropyl groups and amylopectin molecules of the starches depend largely on their chain type, crystallinity and botanical source. Negative correlation between short chains (A and B1) and pasting temperature has been adduced to the inability of short chains to contribute to a high crystalline quality and hence, less energy would be required to melt the starch crystallinity, resulting in a low pasting temperature (Jane *et al.*, 1999).

Pearson Correlation analysis of relationship between peak viscosity and the chains was A Chain ($r = 0.933$, WCS; $r = 0.915$, RCS; $r = 0.944$, WYS; $r = -0.978$, $p<0.05$, YYS; $r = -0.962$, $p<0.05$, PPS; $r = 0.141$, LBS and $r = -0.705$, JBS), B1 Chain ($r = -0.937$, WCS; $r = 0.980$, $p<0.05$, RCS; $r = 0.979$, $p<0.05$, WYS; $r = -0.889$, YYS; $r

= 0.903, PPS; r = -0.284, LBS and r = 0.603, JBS), B2 Chain (r = 0.682, WCS; r = -0.112, RCS; r = 0.021, WYS; r = 0.012, YYS; r = 0.685, PPS; r = 0.563, LBS and r = -0.435, JBS), B3[†] Chain (r = -0.713, WCS; r = 0.9965 $p<0.05$, RCS; r = 0.907, WYS; r = 0.952, $p<0.05$, YYS; r = 0.978, $p<0.05$, PPS; r = -0.312, LBS and r = 0.897, JBS). Negative correlation between the short chains and peak viscosity could be attributed to the weak interactions of the short branch chains, which did not hold the integrity of the swollen granules resulting into granule disruption during heating and leading to a reduced final viscosity (Stevenson, 2003). A higher proportion of long chains have been reported to contribute to high viscosity because long chains increase the gyration radius of amylopectin molecules (Whistler and BeMiller, 1997).

5.13 FTIR SPECTROSCOPY

FTIR spectra of the native and ozone-oxidized starches, obtained by Attenuated Total Reflectance Fourier-Transform Infrared Spectrophotometer, are shown in Figure 4.31–4.37. The transmittances (%) at 1000.98 cm^{-1}(WCS), 1000.79 cm^{-1} (RCS), 996.15 cm^{-1} (WYS), 995.94 cm^{-1} (YYS), 996.14 cm^{-1} (PPS), 996.77 cm^{-1} (LBS) and 996.55 cm^{-1} (JBS) were indicative of hydrogen bonding of the hydroxyl group at C6 (Van Soest *et al.*, 1995). These bands shifted after oxidation with ozone, although within the limit of the original value. Nevertheless, the intensities of spectral peaks changed by being broader with mixed increase and decrease in intensity upon oxidation. Spectral peaks between 2925.11 and 2927.14 cm^{-1} can be adduced to CH_2 asymmetric stretching. Upon oxidation with ozone, there were no new peaks observed. These could be adduced to the low ability of ozone molecules in forming crosslinks between the starch molecules. In addition, the interactive site for ozone molecules in the starch granules could be predominantly in the amorphous regions and infinitesimally in the crystalline regions of the starch lamella.

Comparison between the FTIR spectra of the native starches and their hydroxypropyl derivatives are shown in Figure 4.38–4.44. The native starches exhibited infrared bands of 1000.98cm^{-1} (WCS), 1000.79 cm^{-1} (RCS), 996.15 cm^{-1} (WYS), 995.95 cm^{-1} (YYS), 996.14 cm^{-1} (PPS), 996.77 cm^{-1} (LBS) and 996.55 cm^{-1} (JBS), which were related to hydrogen bonding of the hydroxyl group at C6. The native starches, upon hydroxypropylation, shifted from bands within the limit of the native starches. Possibility of shift of band from 1022 cm^{-1} to 1015 cm^{-1} and band 994 cm^{-1} to 991 cm^{-1} for amorphous starches with water content above 10% has been reported by Van Soest *et al.* (1995). Though the bands shift that occured as a result of hydroxypropylation was within the limit of the bands obtained for native starches, bands became intense upon hydroxypropylation. Garcia *et al.* (2009) have suggested that starch with low intensity possesses large fraction of regions of local order. The structural organization of amylopectin within the semi-crystalline part of the granules involves double helix structures linked to each other by chains to form clusters. All hydrogen atoms are located inside the double helix, whereas hydroxyl groups are found outside. Upon hydroxypropylation, new hydrogen bonds were formed and these links were located between the double helices. Thus, formation of links between the hydroxyl groups and hydrogen bonds was facilitated, resulting in greater local order (Garcia *et al.*, 2009; Capron *et al.*, 2007).

From the FTIR spectra, broad bands at 3200–3400 cm^{-1} were shown by native starches, indicating the presence of hydrogen-bonded hydroxyl groups that contribute to the vibrational stretches associated with inter- and intra-molecular bound hydroxyl group having polymeric association, which make up the gross structure of starch. These bands became intense upon hydroxypropylation due to addition of hydroxyl groups to the original hydroxyl groups that made up the native starch structure. This, without doubt, would make the introduction of hydroxypropyl groups into the starch matrix to produce both steric and bulky effects, which ensured high solubility of the

starch, but low retrogradation profile. In addition, the FTIR spectra of the native starch showed medium strong band at 2850–3000 cm^{-1}, indicating C–H stretch Leo of alkyl groups. Apart from hydroxyl groups introduced into the starch matrix from hydroxypropyl groups, propyl groups were simultaneously introduced. Originally, the native starch is composed of C–H groups, but the addition of more C–H groups after hydroxypropylation was evident in the shapes and peaks obtained for their hydroxypropyl derivatives. After hydroxypropylation, the bands became broader and more intense. Peaks at 1350–1475cm^{-1} (C–H deformation) have been reported for hydroxypropylated starches, where absorbance phenomena specific to the methyl group are known to occur (Forrest and Cove, 1992). In this study, peaks within the range 1337.29–1416.70 cm^{-1} were obtained. Weak new peaks were observed at 2347.16 cm^{-1} (low-substituted WCS), 2343. 47cm^{-1} (high-substituted WCS), 2346.43 cm^{-1} (low-substituted WYS) and 2360.40cm^{-1} (low-substituted JBS), which could be attributed to CH$_2$ assymetric stretching from the hydroxypropyl groups.

5.14   MORPHOLOGICAL PROPERTIES

5.14.1   Scanning Electron Microscopy of Native Starches

The starch granules of the native starches observed with scanning electron microscope vary in shapes (Figure 4.45–4.51). The mean granular sizes of the native starches, measured with the aid of Scanning Electron Microscope (FESEM Leo Supra 50VP, Carl-Zeiss SMT, Oberkochen, Germany) were 11.54 μm, 9.87 μm, 18.20 μm, 21.77 μm, 18.67 μm, 23.08 μm and 26.23 μm for WCS, RCS, WYS, YYS, PPS, LBS and JBS respectively. WCS granules were spherical granules mixed with truncated spherical granules. RCS granules were regular spherical granules co-existing with truncated spherical granules. Irregular polygonal shapes were observed for WYS. YYS granules, unlike WYS, were oval, ellipsoidal granules mixed with spherical granules. The granular shapes of PPS granules were oblong co-existing with oval and ellipsoidal

granules. The granules of LBS were mainly spherical and oval. JBS granules were mixtures of oval, ellipsoidal and bean-like granules. Pérez *et al.* (2005) have reported small rounded, medium ellipsoidal-truncated and large polyhedral shaped starch granules for cocoyam starch. Lawal (2011) has reported oval or elliptical granular shapes for pigeon pea starch. The surfaces of the starches were smooth for WCS and RCS and minimal rough for other starches. The roughness was not adduced to damages, but the presence of surface proteins, which could be removed by intensive purification process of the starch samples. However, this suggests that the processes of extraction and drying had no damaging effect on the starches. Observations on the unaltered shapes and surface characteristics of starch granules have been reported (Chuenkamol *et al.*, 2007; Lawal, 2011).

5.14.2 Transmission Electron Microscopy of Starch Nanocrystals

Nanocrystals prepared from the native starches, after five (5) days of mild acid hydrolysis, are examined with Transmission Electron Microscope (Philips CM 12 microscope, FEI Company, Eindhoven, Netherlands) and the micrographs obtained are shown in Figure 4.52–4.58. Evidences of nanocrystals of starches through acid hydrolysis have been reported (Angellier *et al.*, 2006a; Putaux *et al.*, 2003). Figure 4.52 shows the views of platelets formed by crystallization of the amylopectin of WCS in aggregates. This compares favourably with report by Angellier *et al.* (2006a) that granules of nanocrystals do not have discreet shapes, but they exist as aggregates. YYS nanocrystals appeared as aggregate of fibres (Fig. 4.55). This may suggest the possible plasticization of YYS granules by mild acid hydrolysis after five (5) days. LBS nanocrystals are observed to be aggregate of spherical parallel piped blocks (Fig. 4.57). JBS nanocrystals equally appeared as aggregate of lamellar fragments stacked together (Fig. 4.58). Putaux *et al.* (2003) have reported Transmission Electron Microscopy (TEM) observations for waxy maize in terms of: (a) a longitudinal viewof lamellar

fragments, consisting of stack of elongated elements, with a thickness of 5–7 nm, and (b) a planar view of individualized platelets after hydrolysis. Shapes and lateral dimensions are derived from observation of individual platelets in planar view and marked 60–65° acute angles for parallel piped blocks with a length of 20–40 nm and a width of 15–30 nm. However, more recent publications reported bigger starch nanocrystals (Chen *et al*., 2008; Namazi and Dadkhah, 2010), with round edges (Wang and Zhang, 2008) and found as grape-like aggregates of 1–5 μm.

The heterogeneity in particle size could be explained by the differences in starch botanical origin, as recently presented (LeCorre *et al.*, 2009) and also by the difficulty to obtain well-defined pictures of non-aggregated nanocrystals. The aggregate nature of starch nanocrystals has been adduced to hydrogen bond interaction via the surface hydroxyl groups (Xu *et al.*, 2010). This implies that the particle sizes of the individual platelets are not altered by the platelet-like, as aggregate, of the nanocrystals. Irrespective of the shape of the nanocrystals, all nanocrystals can be considered as potential fillers in nanocomposites (LeCorre *et al*., 2011). This, therefore, suggests that all the starch nanocrystals prepared in this study could be potential fillers in nanocomposites. Starch nanocrystals obtained by acid hydrolysis of potato and waxy maize starch granules have been used as filler in asynthetic polymeric matrix and appeared to be an interesting reinforcing agent in natural rubber (Angellier *et al.*, 2005; Song *et al.*, 2008), polylacticacid, and polycaprolactone for getting nanocomposites with unique properties (Song *et al.*, 2008) and pharmaceuticals. Starch nanocrystals could, henceforth, serve as replacement for the use of petrochemicals in the food and non–food applications.

5.15   X–RAY DIFFRACTION PATTERN OF NANOCRYSTALS

The X–ray patterns of the starch nanocrystals prepared from the native starches are presented in Figure 4.58–4.64. In all, there were no significant peaks. However,

weak peaks appear at $2\theta \approx 18.0^o$ (WCS), 17° (RCS), 17° (WYS), 26° (PPS), 16° (LBS) and $17^o/20^o$ (JBS). The possibility from these observations could be that mild acid hydrolysis, by which starch nanocrystals are produced, resulted in the formation of amylose–lipids complex in the amorphous lamella. This could make the amorphous regions larger than the crystalline region.The V-pattern is relatively amorphous with a few weak lines that show crystallinity (Willhoft, 1973).

It is opined that the relative amorphosity of the starch nanocrystals is not as a result of its high water content. This assertion is true, based on the fact that X-ray powder diffraction is usually done on hydrated starch samples (Karim *et al.*, 2000). Hydration is accomplished by equilibrating the sample in a desiccator maintained at a certain relative humidity and temperature. Hydration is known to influence X-ray patterns (Buléon *et al.*, 1987), and a certain amount of water is necessary to maintain structural ordering as detected by X-ray diffraction. Hydration has been found to improve resolution of the profiles, that is, the patterns become sharper and more pronounced without the true patterns being affected (Sievert *et al.*, 1991).

5.16   SOLUBILITY TEST OF STARCH NANOCRYSTALS

The results of solubility test of starch nanocrystals with six different solvents (both organic and inorganic), namely toluene, xylene, trichloromethane (chloroform), acetic acid, ethanol and de-ionized water are presented in Table 4.28. The starch nanocrystals were practically insoluble in toluene and xylene. Their dispersion in trichloromethane resulted in the formation of precipitates, and appeared less dense than the solvent (Plate 4.1). In WCS, RCS and LBS, the precipitates floated and appeared as large aggregate (black blocs) whereas in WYS, YYS, PPS and JBS, they floated and appeared as aggregate in fragments. In acetic acid and ethanol, the starch nanocrystals were insoluble, except LBS nanocrystals, which appeared sparingly soluble with cloudy supernatant.

The starch nanocrystals were insoluble in deionized (DI) water, except PPS, LBS and JBS nanocrystals. PPS nanocrystals form suspension, which remained unsettled after stirring with larger portion of the particles floating on the supernatant. LBS nanocrystals appeared soluble upon stirring, but only sparingly soluble, when left to settle. JBS nanocrystals appeared as insoluble suspension. However, upon stirring, nanocrystals of WCS, RCS, WYS and YYS formed false suspensions, which settled fast, when left to settle, resulting in sediments at the bottom of the containers (Plate4.1). The nonpolarity of chloroform coupled with its linear chemical structure could be adduced to its precipitating ability, when used to disperse starch nanocrystals. DI water has better performance as inorganic and polar solvent due to its low concentration of ions. Xu *et al.* (2010) have reported insoluble dispersion for starch nanocrystals of waxy corn with some organic solvents, except dimethylsulphoxide. Dispersion of starch nanocrystals as aqueous suspensions prior to their incorporation into nanocomposite matrix has been a challenge (Xu *et al.,* 2010). This is due to its poor solubility in organic solvents, and this singular obstacle, has limited the application of starch nanocrystals as a reinforcing phase in a wide variety of polymers. The use of surfactant to disperse starch nanocrystals in a nonpolar solvent for cellulose whiskers has been proposed (Bonini *et al.*, 2002; Heux *et al.,* 2000), but this ends up with large volume of the surfactant being used to maintain the stability of the suspension (Xu *et al.*, 2010). From this study, although large volume of the surfactant could be used, DI exhibited the highest tendency, among other solvents used for nanocrystals solubility, to stabilize nanocrystals suspensions of PPS and JBS (Table 4.28).

CHAPTER SIX

6.0 CONCLUSION AND RECOMMENDATION

6.1 CONCLUSION

The native starches isolated from white and red cocoyam (*Colocasia esculenta*), white yam (*Dioscorea rotundata*) and yellow yam (*Dioscorea cayenensis*), and seeds of pigeon pea (*Cajanus cajan*), lima bean (*Phaseolus lunatus*) and jack bean (*Canavalia ensiformis*) were successfully modified through ozone-oxidation and hydroxypropylation processes. Ozone-oxidation of starches competed favourably with the conventional alkaline hypochlorite process, and was preferred to the latter due to its environmental friendliness. The introduction of ozone molecules and hydroxypropyl groups into the starch matrix gave significant changes in the intrinsic characteristics of these native starches.

From the study, the molar substitutions of the starches were within the limit allowed for the use of hydroxypropylated starch in food application by FDA (US Food and Drug Administration). The amount of reacted ozone showed linear relationship with both carbonyl and carboxyl content of the starches as ozone generation time (OGT) increased.

The results obtained for the proximate compositions of the native starches showed that crude protein was predominantly available in jack bean starch, which is surprisingly considered as a wild crop in the tropics. Lima bean starch appeared as having biggest storage organ for oil, indicating highest affinity for oil, among other starches, which was evident in its high oil absorption capacity (OAC) compared to other starches. White yam starch possessed low moisture content, indicating less tendency to microbial attack and deterioration upon storage.

The most abundant mineral in all the starch samples is potassium followed by phosphorus, which were predominantly available in pigeon pea starch. Pigeon pea starch was distinct among other starches studied, because of comparatively high

bioavailability of sodium and calcium it possessed. Harmful heavy metals such as lead, nickel, cadmium and mercury were not detected within the limit of analysis.

This study has revealed that the whitest starch of all the starches, under the same purification and isolation processes, was red cocoyam starch. Starches isolated from pigeon pea and lima bean had the same peak least gelation concentration (LGC) while lima bean starch exhibited the highest values of WAC and OAC.

Based on consistent and significant differences upon oxidation, the swelling powers of the native starches improved for the legume starches as OGT increased. The native starch of lima bean possessed the highest value of swelling power compared to others upon oxidation with ozone. Ozone-oxidized lima bean starches had appreciable high swelling power, which is a factor for the release the active pharmaceutical ingredient from its compacts at a faster rate, where starch acts as a disintegrant. The granules of the ozone-oxidized starch of jack bean were least soluble among all the starches studied. The introduction of hydroxypropyl groups into the starch matrix improved their swelling power and solubility. These impacts were felt most at high substitution level of propylene glycol.

The results obtained for the pasting behaviours of the starches have revealed that pasting temperatures of the native starches were lowered upon oxidation with ozone. White yam starch at 5 min OGT exhibited the least pasting temperature. Pigeon pea starch at 5 min OGT possessed least ability to withstand shear force during heating. Apparently, hydroxypropylation lowered the tendencies of the tuber starches (white and red cocoyam, white and yellow yam cultivars) to retrograde whereas it elevated those of the legume starches (pigeon pea, lima bean and jack bean). Nevertheless, the pasting temperatures of all the starches were lowered upon hydroxypropylation.

The strongest starch gel obtained was for white cocoyam and its oxidized derivative at 10 min OGT was stronger than all other native starches and their derivatives at different OGTs. All the oxidized starches were more resilient than their

native with white cocoyam at 15 min OGT being most resilient. The most resilient hydroxypropylated starch gel was low-substituted white yam starch, which happened to be the least gummy and cohesive gel.

From the results of flow behaviours, all the starches (native, ozone-oxidized and hydroxypropylated) were pseudoplastic, and their viscosities reduced with increase in shear rate.

The thermal properties of the native starches showed that their gelatinization profiles after oxidation and hydroxypropylation were lower than the retrogradation profiles after seven (7) days of storage at 4°C. White yam starch (at 5 min OGT) and red cocoyam starch (at high-substitution) possessed the least tendencies to retrograde after storage for 7 days at 4°C.

The X-ray diffraction studies revealed that all the starches from both tubers and legumes exhibited C_B-type patterns, indicating the mix of A- and B-polymorphs, and B-polymorphs more predominant than A-polymorphs in the starch helical chains. These patterns remained unchanged after oxidation and hydroxypropylation. Crystallinity decreased after oxidation with ozone and this decrease was more pronounced after hydroxypropylation. Both the ozone-oxidized and hydroxypropylated starches had less tendency for aging during storage.

On modification, the starches underwent partial degradation, rendering them more soluble for applications in baby food, yoghurt and dessert-like products. The interaction between the substituents introduced into the original native matrix, in terms of ozone molecules and hydroxypropyl groups, and amylopectin molecules of the starches depended largely on their chain type, crystallinity and botanical source.

Peaks of hydroxyl group, CH_2 asymmetric stretching, C–H stretch of alkyl groups and C–H deformation were identified on the spectra obtained with ATR-FTIR spectroscope. Though there were no new peaks observed after oxidation and

hydroxypropylated, the bands of spectral peaks changed by being broader with varying intensities upon oxidation.

The morphological studies of the starches revealed that the granular sizes of the native starches were in the range 11.54–26.23 μm. The micrographs obtained through SEM showed that there was no native starch with single type of shape. Mixtures of shapes obtained were oval, ellipsoidal, irregular polygon, bean–like and spherical. The TEM micrographs of the starch nanocrystals prepared by mild acid hydrolysis for five (5) days showed that nanocrystals of the starches appeared as platelets, which were not discrete in shape, but existed as aggregates. It is opined that, irrespective of the shape the nanocrystals, all the nanocrystals could be potential fillers in nanocomposites.

Furthermore, X-ray diffraction of the starch nanocrystals revealed that they were V-type patterns. This showed that the amylose molecules existing in the original native network, after mild acid hydrolysis for 5 days, did not recrystallize or reassociate with amylopectin molecules rather they interacted with lipid to form amylase-lipid complex, which characterized the V-type pattern.

The solubility test of the starch nanocrystals is vital for the incorporation of nanocrystals of starches in aqueous form into nanocomposite matrix. Of all the solvents used in testing the solubility tendency of starch nanocrystals, trichloromethane (chloroform) showed the tendency of forming light precipitates (black blocs) with all the nanocrystals while LBS nanocrystals were sparingly soluble in acetic acid, ethanol and deionized (DI) water. Evidence of the nanocrystals is a step towards meeting the quest for nanotechnology in all fields.

The modification of the starches, which were, hitherto, regarded as staple crops and underutilized crops could serve as relief for the ever-increasing demands for starch in food and non–food industries such as pharmaceuticals, cosmetics, paints, pulp and paper, textiles, adhesives, tissue engineering, polymers and other polymer matrixes.

The evidence of their nanocrystals could be the emergence and meeting the quest for replacement of petrochemicals in product manufacture.

6.2   RECOMMENDATION

From the foregoing, the following recommendations can be drawn to add more insights to the coverage of this study:

a) Modification of the starch nanocrystals can be carried out to extend their industrial usage;

b) Characterization of the modified starch nanocrystals should be carried out; and

c) Product manufacture of these nanocrystals can be attempted.

REFERENCES

Aboubakar, Njintang, Y.N., Scher, J. and Mbofung, C.M.F. (2008). Physicochemical, thermal properties and microstructure of six varieties of taro (*Colocasia esculenta L. Schott*) flours and starches. Journal of Food Engineering, 86, 294–305.

Achayuthakan, P., Suphantharika, M. and Rao, M.A. (2006). Yield stress components of waxy corn starch–xanthan mixtures: Effect of xanthan concentration and different starches. Carbohydrate Polymers, 65, 469–478.

Adebayo, A.S. and Itiola, O.A. (1998). Evaluation of breadfruit and cocoyam starches as exodisintegrants in a paracetamol tablet formulation. Pharmacy Pharmacology Commununications, 4, 385–389.

Adebowale, K.O. and Lawal, O.S. (2002). Effect of annealing and heat moisture conditioning on the physicochemical characteristics of babarra groundnut (*Voandzeia subterranean*) starch. Nahrung/Food, 46, 311–316.

Adebowale, K.O., Afolabi, T.A. and Lawal, O.S. (2002). Isolation, chemical modification and physicochemical characterization of bambarra groundnut (*Voandzeia subterranean*) starch and flour. Food Chemistry, 78, 305–311.

Adebowale, K.O. and Lawal, O.S. (2003a). Functional properties and retrogradation behaviour of native and chemically modified starch of mucuna bean (*Mucuna pruriens*). Journal of the Science of Food and Agriculture, 83, 1541–1546.

Adebowale, K.O. and Lawal, O.S. (2003b). Microstructure, physicochemical properties and retrogradation behaviour of mucuna bean (Mucuna pruriens) starch on heat moisture treatment. Food Hydrocolloids, 17, 265–272.

Adebowale, K.O. and Lawal, O.S. (2004). Comparative study of the functional properties of bambara groundnut (*Voandzeia subterranean*), jack bean (*Canavalia ensiformins*) and mucuna bean (*Mucuna pruriens*) flours. Food Research International, 37(4), 355–365.

Adebowale, K.O., Olu-Owolabi, B.I., Olayinka, O.O. and Lawal, O.S. (2005). Effect of heat moisture treatment and annealing on physicochemical properties of red sorghum starch. African Journal of Biotechnology, 4(9), 928–933.

Afolabi, T.A., Olu-Owolabi, B.I. and Adebowale, K.O. (2010). Effect of heat moisture treatment on the functional and tabletting properties of corn starch. African Journal of Pharmacy and Pharmacology, 4(7), 498–510.

Ahmad, F.B., Williams, P.A., Doublier, J.-L., Durand, S., and Buleon, A. (1999). Physicochemical characterization of sago starch. Carbohydrate Polymers, 38, 361–370.

Akalu, G., Tufvesson, F., Jonsson, C. and Nair, B.M. (1998). Physicochemical characteristics and functional properties of starch and dietary fibre in grass pea seeds. Starch/Stärke, 50, 374–382.

Alais, C., Liden, G., Morton, I., and Whitehead, A. (1999). Food Biochemistry. Aspen Publ., Inc., Gaithersburg. pp. 38–40

Al-Assaf, S., Phillips, G.O. and Williams, P.A. (2005). Studies on acacia exudates gums. Part I: the molecular weight of Acacia senegal gum exudates. Food Hydrocolloids, 19, 647-660.

Amanze, N.J., Agbo, N.J., Eke-Okoro, O.N. and Njoku, D.N. (2011). Selection of yam seeds from open pollination for adoption in yam (*Dioscorea rotundata Poir*) production zones in Nigeria. Journal of Plant Breeding and Crop Science, 3(4), 68–73.

Amoo, I.A. (2004). Lecture Note on Food Chemistry. Chemistry Department, Federal University of Technology, Akure. (Unpublished).

An, H.J. and King, J.M. (2009). Using ozonation and amino acids to change pasting properties of rice starch. Journal Food Science, 74(3), C278–C283.

Anderson, K.A. (1996). Micro-digestion and ICP-AES analysis for the determination of macro and micro elements in plant tissues. Atomic Spectroscopy, 17, 30–33.

Angellier, H., Dufresne, A., Molina-Boisseau, S. and Lebrun, L. (2005a). Processing and structural properties of waxy maize starch nanocrystals reinforced natural rubber. Macromolecules, 3, 3783–3793.

Angellier, H., Molina-Boisseau, S. and Dufresne, L. (2005b). Mechanical properties of waxy maize starch nanocrystal reinforced natural rubber. Macromolecules, 38, 9161–9170.

Angellier, H., Molina-Boisseau, S., Lebrun, L. and Dufresne, L. (2005c). Processing and structural properties of waxy maize starch nanocrystals reinforced natural rubber Macromolecules, 38, 3783–3792.

Angellier, H., Molina-Boisseau, S. and Dufresne, A. (2006a). Waxy maize starch nanocrystals as filler in natural rubber. Macromolecular Symposia, 233, 132–136.

Angellier, H., Molina-Boisseau, S., Dole, P. and Dufresne, A. (2006b). Thermoplastic starch–waxy maize starch nanocrystals nanocomposite. Biomacromolecules, 7, 531–539.

Angellier-Coussy, H., Putaux, J., Molina-Boisseau, S. and Dufresne, A. (2009). The molecular structure of waxy maize starch nanocrystals. Carbohydrate Research, 344, 1558–1566.

AOAC, Association of Official Analytical Chemists (1975). Official Methods of Analysis (8th Ed.). Association of Official Analytical Chemists, Washington D.C.

AOAC, Association of Official Analytical Chemists (1990). Official Methods of Analysis of the Association of Official Analytical Chemists. (18th ed.) Washington D.C.

Apata, D.F. and Ologhobo, A.D. (1997). Trypsin inhibitor and the other anti-nutritional factors in tropical legume seeds. Tropical Science, 37, 52–59.

Asiedu, J.J. (1989). Processing Tropical Crops. Macmillan Edu. Ltd., London. pp. 1–22.

Atichokudomchai, N., Shobsngob, C. and Padvaravinit, S. (2001). A study of some physicochemical properties of high-crystalline tapioca starch.Starch/Stärke, 53, 577–581.

Atwell, W.A., Hood, L.F., Lineback, D.R., Varriano-Marston, E. and Zobel, H.F. (1988). The terminology and methodology associated with basic starch. Cereal Foods World, 33, 306.

Azemi, B.M.N.M. and Wootton, M. (1984). In vitro digestibility of hydroxypropyl maize, waxy maize and high amylose maize starches. Starch, 36, 273–275.

Baik, M.Y., Kim, K.J., Cheon, K.C., Ha, Y.C. and Kim, W.S. (1997). Recrystallization kinetics and glass transition of rice starch gel system. Journal of Agricultural Food Chemistry, 45, 4242–4248.

Bailey, L.H. (1963). The standard cyclopedia of horticulture. The Macmillan Company: New York.

Baker, A.A., Miles, M.J. and Helbert, W. (2001). Internal structure of the starch granule revealed by AFM. Carbohydrate Research, 330, 249–256.

Bakker, J. and Arnold, G.M. (1993). Analysis of sensory and chemical data for a range of red port wines. *American* Journal of Enology and Viticulture, 44, 27–34.

Baldev, B. (1988). Origin, distribution, taxonomy, and morphology. In pulse crops, Baldev, B., Ramanujam, S. and Jain, H.K. (Eds.). Oxford and IBH Publishing Co.: India. pp 3–51.

Baldwin, P.M., Davies, M.C. and Melia, C.D. (1997). Starch granule surface imaging using low-voltage scanning electron microscopy and atomic force microscopy. International Journal of Biological Macromolecules, 21, 103–107.

Balogun, A.M. and Fetuga, B.L. (1986). Chemical composition of some under exploited leguminous crop seeds in Nigeria. Journal of Agriculture and Food Chemistry, 34, 189–192.

Baudoin, J.P. (1988). Genetic resources, domestication and evolutionof lima bean (*Phaseolus lunatus*). In Genetic resources of *Phaseolus* Beans, Gepts P (Ed.).Kluwer Academic Publishers: Dordrecht. pp 393–407.

Bello-Pérez, L.A., Roger, P., Baud, B. and Colonna, P. (1998). Macromolecular features of starches determined by aqueous high-performance size exclusion chromatography. Journal of Cereal Science, 27, 267-278.

Bello-Pérez, L.A., Contreras-Ramos, S.M., Jimenez-Aparicio, A., and Paredes-Lopez , O. (2000). Acetylation and characterization of banana (*Musa paradisiaca*) starch. Acta Cientifica Venezuela, 51, 143–149.

Bello-Pérez, L.A., De Francisco, A., Agama-Acevedo,E., Gutierrez-Meraz, F. and Garcia-Suarez, F.J.L. (2005). Morphological and molecular studies of banana starch. Food Science and Technology International, 11(5), 367–372.

Betancur-Ancona, D., Lopez-Luna, J. and Chel-Guerrero, L. (2003). Comparison of the chemical composition andfunctional properties of *Phaseolus lunatus* prime andtailing starches. Food Chemistry, 82, 217–225.

Beuchat, L.R. (1977). Functional and electrophoretic characteristics of succiylated peanut flour proteins. Journal of Agriculture and Food Chemistry, 25, 258–262.

Biliaderis, C.G., Page, C.M., Maurice, T.J. and Juliano, B.O. (1986). Thermal characterization of rice starches: A polymericapproach to phase transitions of granular starch. J. Agric. Food Chemistry, 34, 6–14.

Björck, L., Gunnarsson, A. and Østergard, K. (1989). A study of native and chemically modified potato starch. Part II. Digestibility in the rat intestinal tract. Starch, 41, 128–134.

Blanshard, J.M.V. (1987). Starch granule structure and function: a physicochemical approach, In: Starch: Properties and Potential, Galliard, T. (Ed.) John Wiley and Sons: Chichester. pp. 17–54.

Bonini, C., Heux, L., Vavailler, J.-Y., Linder, P., Dewhurst, C. and Terech, P. (2002). Rodlike cellulose whiskers coated with surfactant: A small-angle neutron scattering characterization. Langmuir, 18(8), 3311–3314.

Bourne, M.C. (1978). Texture profile analysis. Food Technology, 32(7), 62–66, 72.

Bulèon, A., Bizot, H., Delage, M.M. and Pontoire, B. (1986). Comparison of X-ray diffraction patterns and sorption properties of the hydrolysed starches of potato, wrinkled and smooth pea, broad bean and wheat. Carbohydrate Polymers, 7, 461.

Buléon, A., Colonna, P., Planchot, V. and Ball, S. (1998a). Starch granules: structure and biosynthesis. International Journal of Biological Macromolecules, 23, 85–112.

Buléon, A., Gerard, C., Riekel, R., Vuong, R. and Chanzy, H. (1998b). Details of the crystalline ultrastructure of C-starch granulesrevealed by synchrotron microfocus mapping. Macromolecules, 31, 6605–6610.

Bulèon, A. and Colonna, P. (2007). Physicochemical behaviour of starch in food applications. In: The Chemical Physics of Food, P.S. Belton (ed.), Blackwell Publishing Ltd., Oxford, pp 20–26.

Buléon, A., Véronèse, G. and Putaux, J-L. (2007). Self-Association and Crystallization of Amylose. Australian Journal of Chemistry, 60, 706–718.

Bultosa, G., Hamaker, B.R. and Bemiller, J.N. (2008). An SEC-MALLS study of molecular features of water soluble amylopectin and amylose of Tef (*Eragrostis tef* Zucc.) Trotter starches. Starch/Stärke, 60, 8–22.

Butler, L.E., Christianson, D.D., Scheerens, J.C. and Berry, J.W. (1986). Buffalo gourd root starch. Part 4. Properties of hydroxypropylderivatives. Starch/Stärke, 38, 156–159.

Cable, W.J. (*1984*). The spread of taro (*Colocasia spp*) in the Pacific. In: *Chandra*, *S.* (ed.) *Edible Aroids*. *Clarendon* Press, *Oxford*, *UK*, pp. 28–33.

Cameron, R.E., Durrani, C.M.and Donald, A.M. (1994). Gelation of amylopectin biopolymer. Colloids and Surfaces B: Biointerfaces, 78, 30–35.

Capron, L., Robert, P., Colonna, P., Brogly, M. and Planchot, V. (2007). Starch in rubbery and glassy states by FTIR spectroscopy. Carbohydrate Polymers, 68, 249–259.

Ceirwyn, S.J. (1995). Analytical Chemistry of Foods. Blackie Academic and Professional, London. pp 84–85.

Chan, H.T., Bhat, R. and Karim, A.A. (2009). Physicochemical and functional properties of ozone-oxidized starch. Journal of Agriculture and Food Chemistry, 57, 5965–5970.

Chan, H.T., Leh, C.P., Bhat, R., Senan, C., Williams, P.A. and Karim, A.A. (2011). Molecular structure, rheological and thermal characteristics of ozone–oxidized starch. Food Chemistry, 126, 1019–1024.

Chattopadhyay, S., Singhal, R.S. and Kulkarni, P.R. (1997). Optimization of conditions of synthesis of oxidized starch from corn and amaranth for use in film forming applications. Carbohydrate Polymers, 34, 203–212.

Chavez-Murillo, C.E., Wang, Y.-J. and Bello-Perez, L.A. (2008). Morphological, physicochemical and structural characteristics of oxidized barley and corn starches.Starch/Stärke, 60, 634–645.

Chel-Guerrero, L., Perez-Flores, V., Betancur-Ancona, D. and Davila-Ortiz, G. (2002). Functional properties of flours and protein concentrates from *Phaseolus lunatus* and *Canavalia ensiformis* seeds. Journal of Agricultural and Food Chemistry, 50, 578–583.

Chen, C.-J., Shen, Y.-C. and Yeh, A.-I. (2010). Physicochemical characteristics of media-milled corn starch. Journal of Agriculture and Food Chemistry, 8 (16), 9083–9091.

Chen, G., Wei, M., Chen, J., Huang, J., Dufresne, A. and Chang, P.R. (2008). Simultaneous reinforcing and toughening: new nanocomposites of waterborne polyurethane filled with low loading level of starch nanocrystals.Polymer, 49, 1860–1870.

Chen, H, Weiss, J. and Shahidi, F. (2006). Nanotechnology in nutraceuticals and functional foods. Food Technology, 60(3), 30–36.

Chen, M.-H. and Bergman, C.J. (2007). Method for determining the amylose content, molecular weight and weight– and molar–based distribution of degree of polymerization of amylose and fine–structure of amylopectin. Carbohydrate Polymers, 69, 562–578.

Chen, Y., Cao, X., Chang, P.R. and Huneault, M.A. (2008). Comparative study on the films of poly(vinyl alcohol)/pea starch nanocrystals and poly(vinyl alcohol)/native pea starch. Carbohydrate Polymers, 73, 8–17.

Chen, Z., Schols, H.A., and Voragen, A.G.J. (2003). Physicochemical properties of starches obtained from three varieties of Chinese sweet potatoes. Journal of Food Science, 68, 431-437.

Cheng, D.C.-H. (1986). Yield stress: A time-dependent property and how to measure it. Rheologica Acta, 25, 542–554.

Choi, S.G. and Kerr, W.L. (2003). Water mobility and textural properties of native and hydroxypropylated wheat starch gels. Carbohydrate Polymers, 51(1), 1–8.

Chou, D.H. and Morr, C.V. (1979). Protein-water interactions and functional properties. Journal of the American Oil Chemists' Society, 56, 534.

Chuenkamol, B., Puttanlek, C., Rungsardthong, V. and Uttapap, D. (2007). Characterization of the low-substituted hydroxypropylated cannna starch. Food Hydrocolloids, 21, 1123–1132.

Clifford, R.A. (1971). Your Guide to Health, Chapter 3 (2nd ed.). Oriental Watchman Publishing House, India, pp 47-66.

Coffman, C.W. and Garcia, W. (1977). Functional properties and amino acid content of a protein isolate from bean flour. Journal of Food Technology, 12, 473–484.

Colonna, J.T. and Mercier, C. (1989). Extrusion cooking of starch and starchy products. In: C. Mercier and J.M. Harper, eds. Extrusion Cooking. St. Paul, MN: American Association of Cereal Chemists, Inc., 247–320.

Cooke, D. and Gidley, M.J. (1992). Loss of crystalline and molecular order during cross-linked rice starch. Cereal Chemistry, 70(5), 596–601.

Cui, S.W. (2005). Structural analysis of polysaccharides. In Food carbohydrates: chemistry, physical properties and applications, Cui, S.W. (Ed.). CRC Press: New York. pp. 309–355.

Curá, J.A., Jansson, P-E and Krisman, C.R. (1995). Amylose is not strictly linear. Starch/Stärke, 47, 207-209.

Deffenbaugh, L.B. and Walker, C.E. (1989). Comparison of starch pasting properties in the Brabender Viscograph and the Rapid Visco-Analyzer. Cereal Chemistry, 66, 493–499.

deMan, J.M. (1976). Principles of Food Chemistry. The AVI Publi. Co., Westport, pp. 155–159.

Dengate, H.N. (1984). Swelling, pasting, and gelling of wheat starch. In Y. Pomeranz, Advances in cereal science and technology, Vol. 6, American Association of Cereal Chemists, Minnesota, pp 49–82.

Dias, F.F., Tekchandani, H.K. and Mehta, D. (1997). Modified starches and their uses by food industries. Indian Food Industry, 16, 33–39.

Dillon, D., Combes, R., McConville, M. and Zeiger, E. (1992). Ozone is mutagenic in Salmonella. Environmental and Molecular Mutagen, 19, 331–337.

Donovan, J.W. (1979). Phase transitions of the starch-water system. Biopolymers, 18, 263.

Donovan, J.W. and Mapes, C.J. (1980). Multiple phase transitions of starches and Nageli amylodextrins. Starch/Stärke, 32, 190.

Doublier, J.L., Llamas, G. and Le Meur, M. (1987). A rheological investigation of cereal starch pastes and gels. Effects of pasting procedures. Carbohydrate Polymers, 7, 251–275.

Doublier, J.L. and Choplin, L. (1989). A rheological description of amylose gelation. Carbohydrate Research, 193, 215–222.

Duan, B., Sun, P., Wang, X. and Yang, C. (2011). Preparation and properties of starch nanocrystals/carboxymethyl chitosan nanocomposite films Starch/Stärke, 63, 528–535.

Durrani, C.M. and Donald, A.M. (1995). Physical characterisation of amylopectin gels. Polymer Gels and Networks, 3, 1–27.

Eidam, D., Kulicke, W.M., Kuhn, K. and Stute, R. (1995). Formation of maize starch gels selectively regulated by the addition of hydrocolloids. Starch/Stärke, 47, 378–384.

Eke, C.N.U. Asoegwu, S.N. and Nwandikom, G.I. (2007). Physical properties of jackbean (*Canavalia ensiformis*), Agricultural Engineering International: the CIGR Ejournal Manuscript FP 07 014, 9, 1–11.

Eliasson, A.-C. (1985). Retrogradation of starch as measured by differential scanning calorimetry. In R. D. Hill and L. Munck (Eds.), New approaches to research on cereal carbohydrates. Amsterdam, Netherlands: Elsevier Science Publishers. pp. 93–98.

Eliasson, A.-C. (1986). Viscoelastic behavior during the gelatinization of starch. I. Comparison of wheat, maize, potato, and waxy-barley starches. Journal of Texture Studies, 17, 253–265.

Eliasson, A.-C. and Ljunger, G. (1988). Interactions between amylopectin and lipid additives during retrogradation in a model system. Journal of the Science of Food and Agriculture, 44, 353–361.

Ellis, H.S. and Ring, S.G. (1985). A study of some factors influencing amylose gelation. Carbohydrate Polymers, 5, 201–213.

Ellis, R.P., Cochrane, M.P., Dale, M.F.B., Duffus, C.M. Lynn, A., Morrison, I.M., Prentice, R.D.M, Swanston, J.S., and Tiller, S.A. (1998). Starch production and industrial use. Journal of the Science and Food Agriculture, 77, 289–311.

Evans, I.D. and Haisman, D.R. (1982). The effect of solutes on the gelatinization temperature range of potato starch. Starch/Stärke, 34, 224.

Evans, R.B., Kruger, L.H. and Szymanski, C.D. (1969). Inhibited starch products. U.S. Patent 3, 463, 668.

Fanon, J.E., Hauber, R.J., and BeMiller, J.N. (1992). Surface pores of starch granules. Cereal Chemistry 69, 284–288.

FAO, Food and Agriculture Organization of the United Nations (1998). Roots and Tuber. Quarterly Bulletin of Statistics 11(1/2), 35.

FAO/WHO (1990). Protein Quality Evaluation. Report of a Joint FAO/WHO Expert Consultation Held in Bethesda, USA. FAO. Rome.

Fisher, D.K. and Thompson, D.B. (1997). Retrogradation of maize starch after thermal treatment within and above the gelatinization temperature range. Cereal Chemistry, 74, 344–351.

Food and Agriculture Organization (FAO) (2000). Functional properties of starches. http://www.fao.org/ag/ags/Agsi/agsi.htm.

Forrest, B. and Cove, L. (1992). Identification and quantification of hydroxypropylation of starch by FTIR. Starch/Stärke, 5,179–183.

French, D. (1983). Organization of the starch granule. In Starch: Chemistry and Technology, R.L. Whistler, J.N. BeMiller and E.F. Paschall (Eds.). Academic Press: Orlando. p 183.

Gallant, D.J., Bouchet, B., Buléon, A., and Pérez, S. (1992). Physical characteristics of starch granules and susceptibility to enzymatic degradation. European Journal of Clinical Nutrition, 46, S3–S16.

Gallant, D.J., Bouchet, B. and Baldwin, P.M. (1997). Microscopy of starch: Evidence of a new level of granule organization. Carbohydrate Polymers, 32, 177–191.

Galvez, F.C.F. and Resurreccion, A.V.A. (1992). The effects of decortication and method of extraction on the physical and chemical properties of starch from mung bean (*Vigna radiate (L.) wilczec*). Journal of Food Processing and Preservation, 17, 93–107.

Garcia, N.L., Famá, L., Dufresne, A., Aranguren, M. and Goyanes, S. (2009). A comparison between the physicochemical properties of tuber and cereal tubers. Food Research International, 42, 976–982.

Giami, S.Y. (2006). In the nutritive value of three new lima bean (*Phaseolus lunatus L.*) breeding lines. Legume Resources, 29(1), 25–31.

Gidley, M.J. and Bociek, S.M. (1985). Molecular organization in starches: a 13C CP/MAS NMR study. Journal of the American Chemical Society, 107(24), 7040–7044.

Gidley, M.J. (1989). Molecular mechanisms underlying amylose aggregation and gelation. Macromolecules, 22(1), 351–358.

Goering, K.J., and DeHaas, B. (1972). New starches. VIII. Properties of the small granule-starch from *Colocasia esculenta. AACC*, 712-719.

Gomand, S.V., Lamberts, L., Visser, R.G.F. and Delcour, J.A. (2010a). Physicochemical properties of potato and cassava starches and their mutants in relation to their structural properties. Food Hydrocolloids, 24, 424–433.

Gomand, S.V., Lamberts, L., Derde, L.J., Goesaert, H., Vandeputte, G.E., Goderis, B., Visser, R.G.F. and Delcour, J.A. (2010b). Structural properties and gelatinization characteristics of potato and cassava starches and mutants thereof. Food Hydrocolloids, 24, 307–317.

Goodfellow, B.J. and Wilson, R.H. (1990). A Fourier Transform IR study of the gelation of amylose and amylopectin. Biopolymers, 30, 1183–1189.

Gowariker, V.R., Viswanathan, N.V. and Sreedhar, J. (1986). Polymer science. New Delhi: Wiley Eastern Limited, (Chapter 12).

Grundschober, F. and Prey, V. (1963). Acetylation in aqueous solution. Starch/Stärke, 15, 225–227.

Gujska, E., Reinhard, W.D. and Khan, R. (1994). Physicochemical properties of field pea, pinto and navy bean starches. Journal of Food Science, 59, 634–636.

Gunaratne, A. and Hoover, R. (2002). Effect of heat-moisture treatment on the structure and physicochemical properties of tuber and root starches. Carbohydrate Polymers, 49, 425–437.

Gunaratne, A. and Corke, H. (2007). Functional properties of hydroxypropylated, cross-linked, and hydroxypropylated cross-linked tuber and root starches. Cereal Chemistry, 84(1), 30–37.

Hanashiro, I., Abe, J. and Hizukuri, S. (1996). A periodic distribution of the chain length of amylopectin as revealed by high performance anion–exchange chromatography. Carbohydrate Research, 283, 151–159.

Hanashiro, I., Tagawa, M., Shibahara, S., Iwata, K. and Takeda, Y. (2002). Examination of molar-based distribution of A, B and C chains of amylopectin by fluorescent labeling with 2-aminopyridine. Carbohydrate Research, 337, 1211–1215.

Hari, P.K., Garg, S. and Garg, S.K. (1979). Gelatinization of starch and modified starch. Starch/Stärke, 41, 88–91.

Heux, L., Chauver, G. and Bonini, C. (2000). Nonflocculating and chira-nematic self-ordering of cellulose microcrystals suspensions in nonpolar solvents. Langmuir, 16(21), 8210–8212.

Hizukuri, S., Kanebo, T. and Takeda, Y. (1983). Measurement of the chain length of amylopectin and its relevance of the origin of crystalline polymorphism of starch granules. Biochimica et Biophysical Acta, 760, 188–191.

Hizukuri, S. (1985). Relationship between the distribution of the chain length of amylopectin and the crystalline structure of starch granules. Carbohydrate Research, 141, 295–306.

Hizukuri, S. (1986). Polymodal distribution of the chain lengths of amylopectin and its significance. Carbohydrate Research, 147, 342–347.

Hodge, J.E. and Osman, E.M. (1996). Carbohydrates. In O. R. Fennema (Ed.), Food chemistry. New York: Marcel Dekker, p. 47.

Hoover, R. and F. Sosulski. (1986). Effect of cross linking on functional properties of legume starches. Starch/Stärke, 38, 149–155.

Hoover, R., Hannouz, D. and Sosulski, F.W. (1988). Effect of hydroxypropylation on thermal properties, starch digestibility and freeze-thaw stability of field pea (*Pisum sativum cv trapper*) starch. Starch/Stärke, 40, 383–387.

Hoover, R. and Vasanthan, T. (1994). Effect of heat-moisture treatment on the structure and physicochemical properties of cereal, legume, and tuber starches. Carbohydrate Research, 252, 33–53.

Hoover, R., Swamidas, G., Kok, L.S. and Vasanthan, T. (1995). Composition and physicochemical properties of starch from pearl millet grains. Food Chemistry, 56(4), 355–367.

Hoover, R. and Manuel, H. (1996). The effect of heat-moisture treatment on the structure and physicochemical properties of normal maize, waxy maize, dull waxy maize and amylomaize V starches. Journal of Cereal Sciences, 23, 153–162.

Hoover, R. (2001). Composition, molecular structure, and physicochemical properties of tuber and root starches: A review. Carbohydrate Polymers, 45: 253-267.

Huaiguo, T., Qing, Q., Youping, W. Guohua, L, Liqun, Z. and Jun, M. (2006). Reinforcement of polymer by starch. Macromolecular Materials and Engineering, 291, 629–639.

Hudson, R.F. and Moss, G. (1962). The mechanism of hydrolysis of phosphorochloridates and related compounds. Part IV. Phosphoryl chloride. Journal of Chemistry Society, 703, 3599–3604.

Hullinger, C.H. and Whistler, R.L. (1951). Oxidation of amylose with hypochlorite and hypochlorus acid. Cereal Chemistry, 28, 153–157.

Hung, P.V. and Morita, N. (2005). Effects of granule sizes on physicochemical properties of cross-linked and acetylated wheat starches. Starch/Stärke, 57, 413–420.

Hussain, M, Norton, G. and Neale, R.J. (1984). Composition and nutritive value of cormels of *Colocasia esculenta* (L) Schott. Journal of Science, Food and Agriculture, 35, 1112–1119.

Ihekoronye, A.I. and Ngoddy, P.O. (1985). Integrated food science and technology for the tropics. Macmillan Publ. Ltd., London. pp 11-27, 284.

Imberty, A., Chanzy, H., Pérez, S., Buléon, A. and Tran, V. (1987). New three dimensional structure for A-type starch. Macromolecules, 20, 2634–2636.

Imberty, A. and Pérez, S. (1988). A revisit to the three-dimensional structure of β-amylose. Biopolymers, 27, 1205–1221

Imberty, A., Chanzy, H., Pérez, S., Buléon, A. and Tran, V. (1988). The double helical nature of the crystalline part of A-starch. Journal of Molecular Biology, 201, 365–378.

Imberty, A., Buléon, A., Tran, V. and Péerez, S. (1991). Recent advances in knowledge of starch structure. Starch/Stärke, 43(10), 375–384.

Jackman, M. (1991). In-line viscometers help achieve perfect products. Food Technology, 45, 90–91.

Jacobs, H. and Delcour, J.A. (1998). Hydrothermal modifications of granular starch, with retention of the granular structure: A review. Journal of Agricultural and Food Chemistry, 468, 2895–1905.

Jacobson, M.R., Obanni, M. and BeMiller, J.N. (1997). Retrogradation of starches from different botanical sources. Cereal Chemistry, 74, 571–578.

264

Jamin, F.F. and Flores, R.A. (1998). Effect of additional separation and grinding on the chemical and physical properties of selected corn dry-milled streams. Cereal Chemistry 75, 166–170.

Jane, J. and Chen, J. (1992). Effect of amylose molecular size and amylopectin branch chain length on paste properties of starch. Cereal Chemistry, 69: 60-65.

Jane, J., Chen, Y.Y., Lee, L.F., McPherson, A.E., Wong K.S., Radosavjevic M. and Kasemsuwan, T. (1999). Effects of amylopectin branch chain length and amylose content on the gelatinization and pasting properties of starch. Cereal Chemistry, 76, 629–637.

Jane, J. (2003). Starch: Structure and properties. In: Chemical and functional properties of food saccharides. P. Tomasik (Ed.). CRC Press, Taylor Francis Group: New York. pp 81–84.

Jane, J.L. and Robyt, J.F. (1984). Structure studies of amylose V complexes and retrograded amylose by action of alpha amylase, a new method for preparing amylodextrins. Carbohydrate Research, 132, 105–110.

Jarowenko, W. (1986). Acetylated starch and miscellaneous organic esters. In: O.B. Wurzburg, ed. Modified Starches: Properties and Uses. Boca Raton, FL: CRC Press, 55–78.

Jayakody, L., Hoover, R., Liu, Q. and Donner, E. (2007). Studies on tuber starches. II. Molecular structure, composition and physicochemical properties of yam (*Dioscorea spp*) starches grown in Sri Lanka. Carbohydrate Polymers, 69:148–163.

Jenkins, P.J., Comerson, R.E., and Donald, A.M. (1994). In situ simultaneous small and wide angle X-ray scattering: a new technique to study starch gelatinization. Journal of Polymer Science B, 32(8), 1579–1583.

Jenkins, P.J. and Donald, A.M. (1995). The influence of amylose on starch granule structure. International Journal of Biological Macromolecules, 17(6), 315–321.

Jenkins, P.J. and Donald, A.M. (1997). The effect of acid hydrolysis on native starch granule structure. Starch/Stärke, 49(7-8), 262–267.

Ji, Y., Wong, K., Hasjim, J., Pollak, L.M., Duvick, S. and Jane, J. (2003). Structure and function of starch from advanced generations of new corn lines. Carbohydrate Polymers, 54, 305–319.

Jobling, S.A., Schwall, G.P., Westcott, R.J., Sidebottom, C.M., Debet, M., Gidley, M.J., Jeffcoat, R., and Safford, R. (1999). A minor form of starch branching enzyme in potato (*Solanum tuberosum L.*) tubers has a major effect on starch structure: cloning and characterisation of multiple forms of SBE A. Plant Journal, 18,163–171.

Jobling, S. (2004). Improving starch for food and industrial applications. Current Opinion in Plant Biology, 7, 210–218.

Joint FAO/WHO Expert committee on Food Additives. (2001). Compendium of food additive specifications. Hydroxypropyl starch. FAO Food and Nutrition Paper, 52 (Add. 9). INS No. 1440. Geneva.

Juszczak, L., Fortuna, T. and Krok, F. (2003a). Non-contact Atomic Force Microscopy of starch granules surface. Part I. Potato and tapioca starches. Starch/Stärke, 55, 1–7.

Juszczak, L., Fortuna, T. and Krok, F. (2003b). Non-contact Atomic Force Microscopy of starch granules surface. Part II. Selected cereal starches. Starch/Stärke, 55, 8–18.

Jyothi, A.N. Moorthy, S.N. and Rajasekharan, K.N. (2006). Effect of cross-linking with epichlorohydrin on the properties of cassava (*Manihot esculenta Crantz*) starch. Starch/Stärke, 58, 292–299.

Jyothi, A.N., Moorthy, S.N. and Rajasekharan, K.N. (2007). Studies on the synthesis and hydroxypropyl derivatives of cassava (*Manihot esculenta* Crantz) starch. Journal of the Science of Food and Agriculture, 87, 1964–1972.

Kalichevsky, M.T., Orford, P.D. and Ring, S.G. (1990). The retrogradation and gelation of amylopectins from various botanical sources. Carbohydrate Research, 198, 49–55.

Karim, A.A., Norziah, M.H. and Seow, C.C. (2000). Methods for the study of starch retrogradation: A review. Food Chemistry, 71, 9–36.

Karim, A.A., Toon, L.C., Lee, V.P., Ong, W.Y., Fazilah, A. and Noda, T. (2007). Effects of phosphorus contents on the gelatinization and retrogradation of potato starch. Journal of Food Science, 72(2), 132–138.

Karim, A.A., Sufha, E.H. and Zaidul, I.S.M. (2008). Dual modification of starch via partial enzymatic hydrolysis in the granular state and subsequent hydroxypropylation. Journal of Agricultural and Food Chemistry, 56, 10901–10907.

Katcher, J.H. and Ackilli, J.A. (1980). Process for preparing an odor-free acetylated starch. U.S. Patent 4, 238, 604.

Katz, J.R. (1934). The physical chemistry of starch and bread baking XX. Z. Physical Chemistry, A169, 321.

Kay, D.E. (1979). Crop and Product. Food Legumes Tropical Products, Institute, London, 3, 217–228.

Kay, D.E. (1987). Root Crops. Tropical Development and Research Institute: London.

Keetels, C.J.A.M., van Vliet, T. and Walstra, P. (1996a). Gelation and retrogradation of concentrated starch systems: 2. Retrogradation. Food Hydrocolloids, 10, 355–362.

Keetels, C.J.A.M., van Vliet, T. and Walstra, P. (1996b). Gelation and retrogradation of concentrated starch systems: 3. Effect of concentration and heating temperature. Food Hydrocolloids, 10, 363–368.

Kesselmans, R.P.W. and Bleeker, I.P. (1997). Method for oxidizing dry starch using ozone. World Intellectual Property Organization, WO/1997/032902.

Kim, H.R., Hermansson, A.M. and Eriksson, C.E. (1992). Structural characteristics of hydroxypropyl potato starch granules depending on their molar substitution. Starch/Stärke, 44, 111–116.

Kim, H.R. and Eliasson, A.C. (1993). Influence of molar substitution onthe thermal transition properties of hydroxypropyl potato starches. Carbohydrate Polymers, 22(1), 31–35.

Kinsella, J.E. (1976). Functional properties of proteins in foods: A Survey. Journal of Food Science, 37, 219–280.

Kittipongpatana, O.S. and Kittipongpatana, N. (2011). Preparation and physicochemical properties of modified jackfruit starches. LWT - Food Science and Technology 44, 1766–1773.

Knutson, C.A., Khoo, U., Cluskey, J.E. and Inglett, G.E. (1982). Variation in enzyme digestibility and gelatinization behavior of corn starch granule fractions. Cereal Chem. 1982, 59, 512–515.

Konoo, S., Ogawa, H., Mizuno, H. and Iso, N.J. (1996). Japanese Society of Food Science and Technology, 43, 880–886.

Koo, S.H., Lee, K.Y. and Lee, H.G. (2010). Effect of cross-linking on the physicochemical and physiological properties of corn starch. Food Hydrocolloids, 24, 619–625.

Kouakou, D.J.E.M., Dabonne, S., Guehi, S.T., Kouame, L.P. (2010). Effects of post-harvest storage on some biochemical parameters of different parts of two yams species (*Dioscorea spp*). African Journal of Food Science and Technology, 1(1), 001–009.

Krevelen, D.W.V. (1972). Properties of polymer: Correlations with chemical structure, Elsevier Publishing Company, Amsterdam. pp. 9–25.

Krok, F., Szymońska, J., Tomasik, P. and Szymoński, M. (2000). Non-contact AFM investigation of influence of freezing process on the surface structure of potato starch granule. Applied Surface Science, 157, 382–386.

Krueger, B.R., Knutson, C.A., Inglett, G.E. and Walker, C.E. (1987). A differential scanning calorimetry study on the effect of annealing on gelatinization behaviour of corn starch. Journal of Food Science, 52, 715–718.

Kuakpetoon, D. and Wang, Y.J. (2001). Characterization of different starches oxidized by hypochlorite. Starch/Stärke, 53, 211–218.

Kuakpetoon, D. and Wang, Y.J. (2006). Structural characteristics and physicochemical properties of oxidized corn starches varying in amylose content. Carbohydrate Research, 341, 1896–1915.

Kuakpetoon, D. and Wang, Y.J. (2008). Locations of hypochlorite oxidation in cornstarches varying in amylase content. Carbohydrate Research, 343, 90–100.

Kulkarni, K.D., Kerure, Y.E., Kulkarni D.N. (1988). Evaluation of potato cultivars for flour production. Beverage and Food World, 8, 214.

Lai, H.M. (2001). Effect of hydrothermal treatment of the physicochemical properties of pregelatinized rice flour, Food Chemistry, 72, 455–463.

Lake, B. and Waterworth, M. (1980). Foods and Nutrition. London: .Mill and Boon, Ltd.

Lan, C., Liu, H., Chen, P., Yu, L., Chen, L., Li, X. and Zhang, X. (2010). Gelatinization and Retrogradation of Hydroxypropylated Cornstarch," International Journal of Food Engineering, 6(4), Article 11. DOI: 10.2202/1556-3758.1905.

Laovachirasuwan, P., Peerapattana, J., Srijesdaruk, V., Chitropas, P. and Otsuka, M. (2010). The physicochemical properties of a spray dried glutinous rice starch biopolymer. Colloids Surfaces B: Biointerfaces, 78, 30–35.

Launay, B., Doublier, J. L. and Cuvelier, G. (1986). Flow properties of aqueous solutions and dispersions of polysaccharides. In J.R. Mitchell, and D.A. Ledward (Eds.), Functional properties of food macromolecules, Elsevier: London. pp. 1–78

Lawal, O.S. (2004). Composition, physicochemical properties and retrogradation characteristics of native, oxidized, acetylated and acid-thin new cocoyam (*Xanthosoma sagittifolium*) starch. Food Chemistry, 87, 205–218.

Lawal, O.S. and Adebowale, K.O. (2005). Physicochemical characteristics and thermal properties of chemically modified jack bean (*Canavalia ensiformis*) starch. Carbohydrate Polymers, 60, 331–341.

Lawal, O.S. (2011). Hydroxypropylation of pigeon pea (*Cajanus cajan*) starch: Preparation, functional characterizations and enzymatic digestibility. LWT - Food Science and Technology, 44, 771–778.

Lawton Jr, J.W. (2004). Native starch. Encyclopaedia of Grain Science, 1-3, 195–202.

Leach, H.W., McCowen, L.D. and Schoch, T.J. (1959). Structure of the starch granule I. Swelling and solubility patterns of various starches. Cereal Chemistry, 36, 534–544.

LeCorre, D., Bras, J. and Dufresne, A. (2009). In Starch Nanoparticles for Eco-Efficient Packaging: Influence of Botanic Origin. 2nd InternationalConference on Biodegradable Polymers and Sustainable Composites (BIOPOL 2009); Jimenez, A., Ed.; Alicante, Spain.

LeCorre, D., Bras, J. and Dufresne, A. (2011). Evidence of micro- and nanoscaled particles during starch nanocrystals preparation and their isolation. Biomacromolecules, 12, 3039–3046.

LeCorre, D., Bras, J. and Dufresne, A. (2012). Influence of native starch's properties on starch nanocrystals thermal properties. Carbohydrate Polymers, 87, 658–666.

Lee, J. and Loh, P.C. (2011). Hydroxypropylation of saba banana starch. 3rd International Conference on Chemical, Biological and Environmental Engineering, vol. 20, IACSIT Press, Singapore.

Lee, J.-S., Kumar, R.N., Rozman, H.D., Azemi, B.M.N. (2004). Flow behaviour of sago starch-g-poly(acrylic acid) in distilled water and NaOH–effect of photografting. Carbohydrate Polymers, 56, 347–354.

Lee, Y.E. and Osman, E.M. (1991). Correlation of morphological changes of rice starch granules with rheological properties during heating in excess water. Journal of Korean Agricultural and Chemical Society, 34, 379–389.

Lewandowicz, G., Fornal, J., Soral-Emietana, M. and Walkoski, A. (2002). Microwave modified starch-structure, properties and resistant starch formation. Nutritional Starch and Chemical Co., Poland.

Li, L., Blanco, M. and Jane, J.-I. (2007). Physicochemical properties of endosperm and pericarp starches during maize development. Carbohydrate Polymers, 67, 630–639.

Lim, S., Sandhu, K.S., Kaur, M. and Singh, N. (2008). A comparison of native and oxidized normal and waxy corn starches: Physicochemical, thermal, morphological and pasting properties. LWT, 41, 1000 – 1010.

Liu, H., Ramsden, L. and Corke, H. (1997). Physical properties and enzymatic digestibility of acetylated ae, wx, and normal maize starch. Carbohydrate Polymers, 34, 283–289.

Liu, H., Ramsden, L. and Corke, H., (1999). Physical properties of cross-linked and acetylated normal and waxy rice starch, Starch/Stärke, 51, 249–252.

Liu, Q., Tarn, R., Lynch, D. and Skjodt, N.M. (2007). Physicochemical properties of dry matter and starch from potatoes grown in Canada. Food Chemistry, 105, 897–907.

Liu, H., Li, M., Chen, P., Yu, L., Chen, L. and Tong, Z. and (2010). Morphologies and thermal properties of hydroxypropylated high–amylose corn starch. Cereal Chemistry, 87(2), 144–149.

Lopez-Rubio, A., Flanagan, B.M., Gilbert, E.P. and Gidley, M.J. (2008). A novel approach for calculating starch crystallinity and its correlation with double helix content: A combined XRD and NMR study. Biopolymers, 89(9), 761–768.

Lu, T.J., Chen, J.C., Lin, C.L. and Chang, Y.H. (2005). Properties of starches from cocoyam (*Xanthosoma sagittifolium*) tubers planted in different seasons. Food Chemistry, 91, 69–77.

Lui, H., Yu, L., Tong, Z. and Chen, L. (2010). Retrogradation of waxy corn starch studied by DSC. Starch/Stärke, 62, 524–529.

Malcolm, P.S. (1990). Polymer Chemistry: An Introduction (2nd Ed.). Oxford University Press, New York. pp 537–69.

Marchant, J.L. and Blanshard, J.M.V. (1978). Studies of the dynamics of the gelatinization of starch granules employing a small angle light scattering system. Starch/Stärke, 30, 257.

Marotta, N.C. and Trubiano, P.C. (1969). Pulpy textured food systems containing inhibited starches. U.S. Patent 3, 443, 964.

Mazur, P.Y., Stolyarova, L.I., Muraschkina, L.V. and Dyatiov, V.A. (1989). Modified starches as dough conditioners for bread. Emaehrung, 13, 155–156.

McPherson, A.E. and Jane, J. (1999). Comparison of waxy potato with other root and tuber starches. Carbohydrate Polymers, 40, 57–70.

Mellon, E.F., Korn, A.H. and Hoover, S. (1947). Water absorption of proteins: The effect of free amino groups in casein. Journal of American Oil Chemical Society, 69, 827.

Mercier, C., Charbonniere, R., Gallant, D., and Delagueriviere, J.F. (1980). Formation of amylose-lipid complexes by twin-screw extrusion cooking of manioc starch. Cereal Chemistry, 57, 4–9.

Miles, M.J., Morris, V.J., Orford, P.D. and Ring, S.G. (1985). The roles of amylose and amylopectin in the gelation and retrogradation of starch. Carbohydrate Research, 135, 271–278.

Millan-Testa, C.E., Mendez-Montealvo, M.G., Ottenhof, M.A., Farhat, I.A. and Bello-Pérez, L.A. (2005). Determination of the molecular and structural characteristics of okenia, mango, and banana starches. Journal of Agricultural and Food Chemistry, 53, 495–401.

Miller, B.S., Derby, R.I. and Trimbo, H.B.A. (1973). A pictorial explanation for the increase in viscosity of a heated wheat starch–water suspension. Cereal Chemistry, 50, 271–280.

Mishra, S., and Rai, T. (2006). Morphological and functional properties of corn, potato and tapioca starches. Food Hydrocolloids, 20, 557–566.

Mitsunaga, T. and Kawamura, Y. (2004). Relationship between functionality and structure in barley starches. Carbohydrate Polymers, 57,145–152.

Mizukami, H., Takeda, Y. and Hizikuri, S. (1999). The structure of the hot water soluble components in the starch granules of new Japanese rice cultivars. Carbohydrate Polymers, 38, 329–335.

Mohd. Nuru, I., Mohd. Azemi, B.M.N. and Manan, D.M.A. (1999). Rheological behaviour of sago (*Metroxylon sagu*) starch paste. Food Chemistry, 64(4), 501–505.

Moorthy, S.N. (2002). Physicochemical and functional properties of tropical tuber starches: A review. Starch/Stärke, 54, 559–592.

Morris, M.J. (1990). Starch gelation and retrogradation. Trends in Food Science and Technology, 1, 2–6.

Morton, M .W. and Solarek, D. (1984). Starch derivatives: Production and uses. In R. L. Whistler, J. N. BeMiller & E. F. Paschall (Eds.), Starch chemistry and technology, New York: Academic Press, pp. 311–366.

Mua, J.P. and Jackson, D.S. (1997). Relationships between functional attributes and molecular structures of amylose and amylopectin fractions from corn starch. Journal Agriculture and Food Chemistry, 45(10), 3848–3854.

Mufumbo, R., Baguma, Y., Kashub, S., Nuwamanya, E., Rubaihayo, P., Mukasa, S., Hamaker, B. and Kyamanya, S. (2011). Amylopectin molecular structure and functional properties of starch from three Uganda cassava. Journal of Plant Breeding and Crop Science, 3(9), 195–202.

Munro, H.N. and Fleck, A. (1969). Analysis of Tissues and Body Fluids for Nitrogenous Constituents, In H.N. Munro, (Ed.), Mammalian Protein Metabolism, vol. III, Academic Press: New York. pp. 423–525.

Namazi, H. and Dadkhah, A. (2010). Convenient method for preparation ofhydrophobically modified starch nanocrystals with using fatty acids. Carbohydrate Polymers, 79, 731–737.

Noda, T., Takahata, Y., Sato, T., Hisamatsu, M. and Yamada, T. (1995). Physicochemical properties of starches extracted from sweet potato roots differing in physiological age. Journal of Agricultural and Food Chemistry,43, 3016–3020.

Noda, T., Tsuda, S., Mori, M., Takigawa, S., Matsuura-Endo, C., Saito, K., Mangalika, W.H.A., Hanaoka, A., Suzuki, Y. and Yamauchi, H. (2004). The effect of harvest dates on the starch properties of various potato cultivars. Food Chemistry, 86, 119–125.

Noda, T., Kottearachchi, N.S., Tsuda, S., Mori, M., Takigawa, S., Watsuura-Endo, C., Kim, S-J., Hashimoto, N. and Yamauchi, H. (2007). Starch phosphorus content in potato (*Solanum tuberosum L.*) cultivars and its effect on starch properties. Carbohydrate Polymers, 68(4), 793–796.

Numfor, I.A., Walter, W.W. and Schwark, S.J. (1995). Physicochemical changes in cassava starch and flour associated with fermentation: Effect on textural properties. Starch/Stärke, 47(3), 86–91.

Nwokocha, L.M., Aviara, N.A., Senan, C. and Williams, P.A. (2009). A comparative study of some properties of cassava (*Manihot esculenta*, Crantz) and cocoyam *(Colocasia esculenta, Linn)* starches. Carbohydrate Polymers, 76 (3), 362–367.

O'Sullivan, O.C. and Perez, S. (1999). The relationship between internal chain length of amylopectin and crystallinity in starch. Biopolymers, 50(4), 381–390.

Oates, C.G. (1997). Towards an understanding of starch granule structure and hydrolysis. Trends in Food Science and Technology, 8, 375–382.

Odetokun, S.M. (2000): Effect of fermentation on physiochemical properties, anti-nutrient and in-vitro multi-enzyme digestibility of selected legumes. Ph.D Dissertation, Chemistry Department, Federal University ofTechnology, Akure, Nigeria.

Ohtani, T., Yoshino, T., Hagiwara, S. and Maekawa, T. (2000). High-resolution imagingof starch granule structure using Atomic Force Microscopy. Starch/Stärke, 52(5), 150–153.

Oladebeye, A.O. (2003). Proximate compositions and physicochemical properties of starches of the corms and cormels of white and red varieties of cocoyam (*Colocasia esculenta*) and Cassava (*Manihot esculenta*), PGD Research Dissertation Submitted to Department of Chemistry, Federal University of Technology, Akure.

Oladebeye A.O., Oshodi A.A. and Oladebeye A.A. (2009). Physicohemical properties of starches of sweet potato (*Ipomea batata*) and red cocoyam (*Colocasia esculenta*) cormels. Pakistan Journal of Nutrition, 8(4), 313–315.

Oladebeye, A.O., Oshodi, A.A., Oladebeye, A.A. and Amoo, I.A. (2011). Pasting properties of heat-moisture treated starches of white and yellow yam (*Dioscorae species*) Cultivars. Nature and Science, 9(1), 29–33.

Olaofe, O., Oladeji, F.O. and Ayodeji, O.I. (1987). Metal content of cocoa bean produced in Ondo State. Nigerian Journal of Science, Food and Agriculture, 141, 241–244.

Olaofe, O. and Sanni, C.O. (1988). Mineral content of agricultural products. Food Chemistry, 30(1), 73–77.

Onwueme, I.C. (1978). The Tropical Tuber Crops, Yams, Cassava, Sweet Potato and Cocoyam. John Wiley, Inc., Chichester. pp. 199-234.

Oshodi, A.A. and Ekperigin, M.M. (1989). Functional properties of pigeon pea flour. Food Chemistry, 34, 187–191.

Osundahunsi, O.F., Fagbemi, T.N., Kesselman, E. and Shimoni, E. (2003). Comparison of the physicochemical properties and pasting characteristics of flour from red and white sweet potato cultivars. Journal of Agricultural and Food Chemistry, 51(8), 2232–2236.

Othman, Z., Al-Assaf, S. and Hassansains, O. (2010). Molecular characterisation of sago starch using gel permeation chromatography multi-angle laser light scattering. Sains Malaysiana, 39(6), 969–973.

Pal, J., Singhal, R.S. and Kulkarni, P.R. (2002). Physicochemical properties of hydroxypropyl derivative from corn and amaranth starch. Carbohydrate Polymers, 48(1), 49–53.

Paris, M., Bizot, H., Emery, J., Buzaré, J.Y. and Buléon, A. (1999). Crystallinity and structuring role of water in native and recrystallized starches by ^{13}C CP-MAS NMR spectroscopy. 1: spectral decomposition. Carbohydrate Polymers, 39(4), 327–339.

Parker, R. and Ring, S.G. (2001). Aspects of the physical chemistry of starch. Journal of Cereal Science, 34, 1–17.

Parovuori, P., Hamunen, A., Forssell, P., Autio, K. and Poutanen, K. (1995). Oxidation of potato starch by hydrogen peroxide. Starch/Stärke, 47, 19–23.

Pearson, D. (1976). The Chemical Analysis of Foods (7th Ed.), Longman Group Ltd, London. pp 6-19, 126–127.

Pearson, D., Egan, H., Kirk, R.S. and Sawyer, R. (1981). Pearson's Chemical Analysis of Food. Churchill Livingston: Edinburgh.

Perera, C., Hoover, R. and Martin, A.M. (1997). The effect of hydroxypropylation on the structure and physicochemical properties of native, defatted and heat-moisture treated potato starches. Food Research International, 30(3–4), 235–247.

Perera, C. and Hoover, R. (1999). Influence of hydroxypropylation on retrogradation properties of native, defatted and heat-moisture treated potato starches. Food Chemistry, 64(3), 361–375.

Pérez, E.E., Borneo, R., Melito, C.G. and Tovar, J. (1999). Chemical, physical and motphometric properties of Peruvian carrot (*Arracacia xanthorrhiza* B.). Acta Cientifica Venezolana, 50, 240-244.

Pérez, E.E, Schultz, F.S. and de Delahaye, E.P. (2005). Characterization of some properties of starches isolated from *Xanthosoma sagittifolium* (tannia) and *Colocasia esculenta* (taro). Carbohydrate Polymers, 60, 139-145.

Perez, S., Baldwin, P. and Gallant, D.J. (2009). Structural features of starch granules I, In Starch: Chemistry and Technology, R. Whistler and J. BeMiller (Eds.), pp. 149–192, Academic Press, New York, NY, USA, 3rd edition.

Peroni, F.H.G., Rocha, T.S. and Franco, C.M.L. (2006). Some structural and physicochemical characteristics of tuber and root starches. Food Science Technology International, 12(6), 505–513.

Peterson, M.S. and Johnson, A.H. (1978). Encyclopedia of Food Science. AVI Publishing Co. Inc., Wesport. pp 707–710

Pitchon, E., O'Rourke, J.D., and Joseph, T.H. (1981). Process for cooking or gelatinizing materials. U.S. Patent 4, 280, 851.

Plucknett, D.L. (1983). Taxonomy of the Genus Colocasia In Taro, A Review of *Colocasia esculenta* and Its Potentials (Wang, J.K. ed.). Honolulu: University of Hawaii Press, pp 14-19.

Politz, M.L., Timpa, J.D., White, A.R. and Wasserman, B.P. (1994). Non-aqueous gel permeation chromatography of wheat starch in dimethylacetamide (DMAC) and LiCl: extrusion-induced fragmentation. Carbohydrate Polymers, 24, 91–99.

Pomeranz, Y. (1985). Functional Properties of Food Components. Academic Press, Inc., Orlando, FL.

Purshottam, L.S., Harshwardhan, S., Harish, C.S. and Mahendrasinh, M.G. (1990). Physiological properties of *Canna edulis* starch-Comparison with maize starch. Starch/Stärke 42, 460–464.

Putaux, J.L., Buléon, A. and Chanzy, H. (2000). Network formation in dilute amylose and amylopectin studied by TEM. Macromolecules, 33(17), 6416–6422.

Putaux, J.L., Molina-Boisseau, S., Momaur, T. and Dufresne, A. (2003). Platelet nanocrystals resulting from the disruption of waxy maize starch granules by acid hydrolysis. Biomacromolecules, 4, 1198–1202.

Race, S.W. (1991). Improved product quality through viscosity measurement. Food Technology, 45, 86–88.

Radley, J.A. (1968). The starch esters and ethers. In: Radley, J.A (ed.) Starch and its derivatives. 4th Edition, London, pp 396–399.

Radley, J.A. (1976). The manufacture of sweet potato starch. In: Radley, J.A (ed.) Starch Production Technology. Applied Science Pub Ltd., London. pp 222–225.

Rao, M.K.V. and Rao, R.G. (1974). Gibberellins like substance in developing and germinating seeds of pigeon pea. Indian Journal of Plant Physiology, 17(1, 2), 65–72.

Rasper, V. (1980). Theoretical aspects of amplographology, In W.C. Shuey, and K.E. Triples (Eds.). The amylograph handbook. St. Paul, MN: American Association of Cereal Chemists, pp 1–6.

Ratnayake, W.S. and Jackson, D.S. (2009). Starch gelatinization. Advances in Food and Nutrition Research, 55, 221–268.

Ridout, M.J., Gunning, A.P., Parker, M.L., Wilson, R.H. and Morris, V.J. (2002). Using AFM to image the internal structure of starch granules. Carbohydrate Polymers, 50(2), 123–132.

Ridout, M.J., Parker, M.L., Hedley, C.L., Bogracheva, T.Y. and Morris, V.J. (2003). Atomic force microscopy of pea starch granules: Granule architecture of wild-type parent, r and rb single mutants, and the double mutant. Carbohydrate Research, 338, 2135–2147.

Ring, S.G., Collona, P., Panson, K.J., Kalicheversky, M.T., Miles, M.J. and Morris, V.J. (1987). The gelation and crystallization of amylopectin. Carbohydrate Research, 162, 277–293.

Riva, M., Schiraldi, A., and Piazza, L. (1994). Characterization of rice cooking: Isothermic differential calorimetry investigations. Thermochimica Acta, 246, 317–328.

Robyt, J.F. (2008). Starch: Structure, properties, chemistry and enzymology. In: Glycoscience. B. Fraser-Reid, K. Tatsuta and J. Thiem (Eds.). Springer-Verlag Berlin Heidelberg, USA, pp. 1437–1472.

Ross, A.S., Walker, C.E., Booth, R.I., Orth, R.A. and Wrigley, C.W.(1987). The Rapid Visco Analyser: a new technique for the evaluation of sprout damage. Cereal Foods World, 32, 827–829.

Russell, P.L. (1983). A kinetic study of bread staling by differential scanning calorimetry and compressibility measurements. The effect of added monoglyceride. Journal of Cereal Science, 1, 297–303.

Russell, P.L. (1987). The ageing of gels from starches of different amylose/amylopectin content studied by differential scanning calorimetry. Journal of Cereal Science, 6, 147–158.

Rutenberg, M.W., Tessler, M.M. and Kruger, L. (1975). Inhibited starch products containing labile and non-labile cross-links. U.S. Patent 3, 899, 602.

Rutenberg, M.W. and Solarek, D. (1984). Starch derivatives: Production and uses. In: R. Whistler, J.N. BeMiller and E.F. Paschall, eds. Starch: Chemistry and Technology. New York: Academic Press, Inc., 314–388.

Sablani, S.S. (2009). Gelatinization of starch. In Food properties handbook, M.S. Rahman (Ed.), CRC Press: USA. pp. 287–321.

Sahle-Demessie, E. and Devulapelli, V.G. (2008). Vapor phase oxidation of dimethyl sulfide with ozone over V_2O_5/TiO_2 catalyst. Appl. Catal., B, 84, 408–419.

Saibene, D., Zobel, H.F., Thompson, D.B. and Seetharaman, K. (2008). Iodine binding by granular corn and potato starch: Evidence for differential location of amylose. Starch/Stärke, 60, 165–173.

Sanchez-Rivera, M.M., Mendez-Montealvo, G., Nunez-Santiago, C., Rosa-Millan, J.D.L., Wang, Y.J. and Bello-Perez, L.A. (2009). Physicochemical properties of banana starch oxidized under different conditions. Starch/Stärke, 61, 206–213.

Sanderson, G.R. (1981). Polysaccharides in Foods. Food Technology, 315, 50–57.

Sandhu, K.S. and Singh, N. (2007). Some properties of corn starches II: Physicochemical, gelatinization, retrogradation, pasting and gel textural properties. Food Chemistry, 101, 1499–1507.

Sasaki, T. (2005). Effect of wheat starch characteristics on the gelatinization, retrogradation and gelation properties. JARQ, 39(4), 253–260.

Sasaki, T. and Matsuki, J. (1998). Effect of wheat starch structure on swelling power. Cereal Chemistry, 75, 525–529.

Scallet, B.L. and Sowell, E.A. (1967). Production and use of hypochlorite-oxidized starches by In Starch Chemistry and Technology; Whistler, R.L., Paschall, E.F., Eds.; Academic Press: New York, Vol. 2, pp 237–251.

Scott, G.J., Rosegrant, M.W. and Ringler, C. (2000). Global projections of root and tuber crops to the year 2020. Food Policy, 25, 561–597.

Seetharaman, K., Tziotis, A., Borras, F., White, P.J., Ferrer, M. and Robutti, J. (2001). Thermal and functional characterization of starch from Argentinean corn. Cereal Chemistry, 78, 379–386.

Segura, M.E.M. and Sira, E.E.P (2003). Characterization of native and modified cassava starches by scanning electron microscopy and X-ray diffraction techniques. Cereal Foods World, 48, 78–81.

Seib, P.A. (1996). Starch Chemistry and Technology, Syllabus. Kansas State University, Manhattan, KS.

Seow, C.C. and Thevamalar, K. (1993). Internal plasticization of granular rice starch by hydroxypropylation: Effects on phase transitions associated with gelatinization. Starch/Stärke, 45, 85–88.

Sharma, D. and Green, J.M. (1980). Pigeon pea. In hybridization of crop plants, Fehr, W.R. and Henry, H. (Eds.). American Society of Agronomy and Crop Science: Madison. pp 471–181.

Shibanuma, Y., Takeda, Y., and Hizukuri,S. (1996). Molecular and pasting properties of some wheat starches. Carbohydrate Polymers, 29, 253–261.

Sievert, D., Czuchajowska, Z. and Pomeranz, Y. (1991). Enzyme-resistant starch. III. X-ray diffraction of autoclaved amylomaize VIIstarch and enzyme-resistant starch residues. Cereal Chemistry,68(1), 86–91.

Silverio, J., Svensson, E., Eliasson, A.C. and Olofsson, G. (1996). Isothermal microcalorimetric studies on starch retrogradation. Journal of Thermal Analysis, 47, 1179–1200.

Singh, N. and Kaur, L. (2004). Morphological, thermal, rheological and retrogradation properties of starch fractions varying in granule size. Journal of Science, Food and Agriculture, 84, 1241–1252.

Singh, N., Singh, J., Kaur, L., Sodhi, N.S. and Gill, B.S. (2003). Morphological, thermal and rheological properties of starches from different botanical sources. Food Chemistry, 81, 219–231.

Singh, N., Singh, J. and Kaur, L. (2004). Factors influencing the properties of hydroxypropylated potato starches. Carbohydrate Polymers, 55, 211–223.

Singh, N., Inouchi, N. and Nishinari, K. (2006). Structural, thermal and viscoelastic characteristics of starches separated from normal, sugary and waxy maize. Food Hydrocolloids, 20, 923–935.

Sivak, N.M., and Preiss, J. (1997). Physicochemical structure of the starch granule. Advances in Food and Nutrition Research, 41, 13–32.

Slade, L. and Levine, H. (1986). Recent advances in starch retrogradation. In Industrial polysaccharides, Stivala, S.S., Crescenzi, V.and Dea, I.C.M. (Eds.) Gordon and Breach: New York. pp. 387–430.

Slade, L. and Levine, H. (1989). A food polymer science approach to selected aspects of starch gelatinization and retrogradation. In Frontiers in carbohydrate research, Millane, R.P., BeMiller, J.N. and Chandrasekaran, R. (Eds.). Elsevier Applied: London.pp. 215–270.

Slade, L., and Levine, H. (1993). Water relationship in starch transitions. Carbohydrate Polymers, 21, 105–131.

Smith, R.J. (1967). Production and uses of hypochlorite oxidized starches. In R.L. Whistler, & E.F. Paschall (Eds.), Starch chemistry and technology, Vol. II (pp. 620–625). New York: Academic Press.

Smits, A.L.M., Ruhnau, F.C., Vliegenthart, J.F.G. and van Soest, J.J.G. (1998). Ageing of starch based systems as observed with FTIR and solid state NMR spectroscopy. Starch/Stärke, 50, 478–483.

Solorza-Feria, J., Jime´nez-Aparicio, A., Arenas-Ocampo, M.L. and Bello-Pe´rez, L.A. (2002). Rheology of Okenia hypogaea starch dispersions in aqueous solution of DMSO. Starch/Stärke, 54, 198–202.

Song, S., Wang, C., Pan, Z. and Wang, X. (2008). Preparation and characterization of amphiphilic starch nanocrystals. Journal of Applied Polymer Science, 107, 418–422.

Spigno, G. and De Faveri, D.M. (2004). Gelatinization kinetics of rice starch studied by non-isothermal calorimetric technique: influence of extraction method, water concentration and heating rate. Journal of Food Engineering, 62, 337–344.

Srivastava, H.C. and Patel, M.M. (1973). Viscosity stabilization of tapioca starch. Starch/Stärke, 25, 17–21.

Stevens, D.J. and Elton, G.A.H. (1971). Thermal properties of the Starch water system. Part I. Measurement of heat of gelatinization by differential scanning calorimetry. Starch/Stärke, 23, 8.

Stevenson, D.G. (2003). Role of starch structure in texture of winter squash (*Cucurbita maxima D.*) fruit and starch functional properties. Ph.D. Dissertation. Iowa State University. Ames. Iowa. U.S.A.

Stevenson, D.G., Domoto, P.A. and Jane, J.L. (2006). Structures and functional properties of apple (*Malus domestica Borkh*). Carbohydrate Polymers, 63, 432– 441.

Sugimoto, Y., Yamamoto, M., Abe, K. and Fuwa, H. (1987). Developmental changes in starch properties of the Chinese yam. Journal of Japan Society of Starch Science, 34, 11- 20.

Suzuki, T., Chiba, A. and Yano, T. (1998). Interpretation of small angle X-ray scattering from starch on the basis of fractals. Carbohydrate Polymers, 34(4), 357–363.

Szymonska, J. and Krok, F. (2003). Potato starch granule nanostructure studied by high resolution non-contact AFM. International Journal of Biological Macromolecules, 33, 1–7.

Takahata, Y. Noda, T. and Sato, T. (1995). Changes in carbohydrates and enzyme activities of sweet potato lines during storage. Journal of Agricultural and Food Chemistry 43(7), 1923–1928.

Takeda, Y. (1993). Structure of rice, maize and other plant starches. Denpun Kagaku, 40, 61–71.

Tang, H., Ando, H., Watanabe, K., Takeda, Y. and Mitsunaga, T. (2001a). Fine granule revealed by AFM. Carbohydrate Research, 330, 249–256.

Tang, H., Ando, H., Watanabe, K., Takeda, Y. and Mitsunaga, T. (2001b). Physicochemical properties and structures of large, medium, and small granule starches in fractions of normal barley endosperm. Carbohydrate Research, 330, 241– 248.

Tang, H., Mitsunaga, T. and Kawamura, Y. (2005). Functionality of starch granules in milling fractions of normal wheat grain. Carbohydrate Polymers, 59, 11-17.

Tang, H., Watanabe, K., and Mitsunaga, T. (2002). Characterization of storage starches from quinoa, barley and adzuki seeds. Carbohydrate Polymers, 49, 13–22.

Tang, H., Mitsunaga, T. and Kawamura, Y. (2006). Molecular arrangement in blocklets and starch granule architecture. Carbohydrate Polymers, 63, 555–560.

Tester, R.F. and Morrison, W.R. (1990). Swelling and gelatinization of cereal starches I: Effects of amylopectin, amylose and lipids. Cereal Chemistry, 60, 551–557.

Tester, R.F. and Karkalas, J. (1996). Swelling and gelatinization of oat starches. Cereal Chemistry, 78, 271–273.

Tester, R.F., Debon, S.J.J. and Karkalas, J.J. (1998). Annealing of wheat starch. Journal of Cereal Science, 28, 259–272.

Tester, R.F. and Debon, S.J.J. (2000). Annealing of starch – A review. International Journal of Biological Macromolecules, 27, 1–12.

Tester, R.F., Karkalas, J. and Qi, X. (2004). Starch-composition, fine structure and architecture. Journal of Cereal Science, 39, 151–165.

Thomas, D.J. and Atwell, W.A. (1999). Starch modifications. In: D.J. Thomas and W.A. Atwell, eds. Starch Chemistry and Technology. St. Paul, MN: American Association of Cereal Chemists, 43–48.

Tian, S.J., Rickard, J.E. and Blanshard, J.M. (1991). Physicochemical properties of sweet potato starch. Journal of the Science of Food and Agriculture, 57, 451–491.

Tomasik P, Wiejak S, Palasinski M. (1989). The thermal decomposition of carbohydrates. Part II. The decomposition of starch. Advances in Carbohydrate Chemistry and Biochemistry, 47, 279–343.

Trubiano, P.C. and Marotta, N.C. (1971). Pulpy textured food systems containing inhibited starches. U.S. Patent 3, 579, 341.

Tuschhoff, J.V. (1986). Hydroxypropylated starches. In: O.B. Wurzburg, ed. Modified Starches: Properties and Uses. Boca Raton, FL: CRC Press, 89–96.

Uzoechina, O.B. (2009). Nutrient and anti-nutrients potentials of brown pigeon pea (*Cajanus cajan var* bicolor) seed flours. Nigerian Food Journal, 27, 10–16.

Vaclavik, V.A., and Christian, E.W. (2008). Starches in food. In: Essentials of Food Science. D. R. Heldman (Ed.). Springerlink, New York, USA, pp. 49–67.

Van der Maesen, L.J.G. (1980). India is the native home of the pigeon pea. In Libergratulatorius in honorem H.C.D. de Wit. Landbouwhogeschool, Arends, J.C., Boelema, G., de Groot, C.T. and Leeuwenberg, A.J.M. (Eds.). Miscellaneous Paper, 19, 257–262.

Van Soest, J.J.C., Tournois, V.H., De Wit, D. and Vliegenthart, J.F.C. (1995). Short–range structure in (partially) crystalline potato starch determined with attenuated total reflectance Fourier-Transform IR spectroscopy. Carbohydrate Research, 279, 201–214.

Van Soest, J.J.G., de Wit, D., Tournois, H. and Vliegenthart, J.F.G. (1994a). Retrogradation of potato starch as studied by Fourier Transform Infrared spectroscopy. Starch/Stärke, 12, 453–457.

Van Soest, J.J.G., de Wit, D., Tournois, H. and Vliegenthart, J.F.G. (1994b). The influence of glycerol on structural changes in waxy maize starch as studied by Fourier transform infra-red spectroscopy. Polymer, 35(22), 4722–4727.

Visavarungroj, N. and Remon, J.P. (1990). Crosslinked starch as a disintegrating agent. International Journal of Pharmaceutics, 62, 125–131.

Waigh, T.A., Hopkinson, I., Donald, A.M., Butler, M.F., Heidelbach, F. and Riekel, C. (1997). Analysis of the native structure of starch granules with X-ray microfocus diffraction. Macromolecules, 30(13) 13, 3813–3820.

Waigh, T.A., Donald, A.M., Heidelbach, F., Riekel, C. and Gidley, M.J. (1999). Analysis of the native structure of starch granules with small angle X-ray microfocus scattering. Biopolymers, 49(1), 91–105.

Waigh, T.A., Gidley, M.J., Komanshek, B.U. and Donald, A.M. (2000). The phase transformations in starch during gelation: A liquid crystalline approach. Carbohydrate Research, 328, 165–176.

Waliszewski, K.N., Aparicio, M.A., Bello, L.A. and Monroy, J.A. (2003). Changes of banana starch by chemical and physical modification. Carbohydrate Polymers, 52, 237–242.

Walker, C.E., Ross, A.S., Wrigley, C.W. and McMaster, G.J. (1988). Accelerated starch-paste characterization with the Rapid Visco-Analyzer. Cereal Foods World, 33, 491–494.

Walter, W.M., Truong, V.D., Wiesenborn, D.P. and Carvajal, P. (2000). Rheological and physicochemical properties of starches from moist- and dry-type sweet potatoes, Journal of Agriculture and Food Chemistry, 48, 2937–2942.

Wang, J.K. (1983). Taro: A Review of *Colocasia esculenta* and Its Potentials. University of Hawaii Press, Honolulu. pg. 400.

Wang, T.L., Bogracheva, T. Y. and Hedley, C.L. (1998). Starch: As simple as A, B, C. Journal of Experimental Botany, 49(320), 481–502.

Wang, Y.J. and Wang, L. (2003). Physicochemical properties of common and waxy corn starches oxidized by different levels of sodium hypochlorite. Carbohydrate Polymers, 52: 207–217.

Wang, Y.J and Zhang, L. (2008). High-strength waterborne polyurethane reinforced with waxy maize starch nanocrystals. Journal of Nanoscience and Nanotechnology, 8, 5831–5838.

Ward, K.E.J., Hoseney, R. C. and Seib, P.A. (1994). Retrogradation of amylopectin from maize and wheat starches. Cereal Chemistry, 71, 150–155.

Weslen, K.B. and Weslen, B. (2002). Synthesis of amphiphilic amylose and starch derivatives. Carbohydrate Polymers, 47, 303–311.

Whistler, R.L. and Paschall, E.F. (1965 and 1967). Starch: Chemistry and Technology (2nd Ed.). Academic Press, Inc., New York.

Whistler, L. and BeMiller, J.N. (1997). Carbohydrates chemistry for food scientists. Eagan Press: Minnesota, pp. 142–143.

Wickramasinghe, H.A.M., Takigawa, S., Matsuura-Endo, C., Yamauchi, H. and Noda, T. (2009). Comparative analysis of starch properties of different root and tuber crops of Sri Lanka. Food Chemistry, 112, 98–103.

Willhoft, E.M.A. (1973). Mechanism and theory of staling of bread and baked goods, and associated changes in textural properties.Journal of Texture Studies, 4, 292–322.

Williams, P.C., Kuzina, F.D. and Hlynka, I. (1970). A rapid calorimetric procedure for estimating the amylose content of starches and flours. Cereal Chemistry, 47, 411–420.

Wilson, R.H. and Belton, P.S. (1988). A Fourier Transform Infra-red study of wheat starch gels. Carbohydrate Research, 180, 339–344.

Wilson, R.H., Kalichevski, M.T., Ring, S.G. and Belton, P.S. (1987). A Fourier Transform IR study of the gelation and retrogradation of waxy maize starch. Carbohydrate Research, 166, 182.

Wilson, R.H., Goodfellow, B.J., Belton, P.S., Osborne, B.G., Oliver, G. and Russell, P.L. (1991). Comparison of Fourier Transform MID Infrared Spectroscopy and Near Infrared Spectroscopy with Differential Scanning Calorimetry for the study of staling of bread. Journal of Science of Food and Agriculture, 54, 471–483.

Wongsagon, R. Shobsngob, S. and Varavinit, S. (2005). Preparation and physicochemical properties of dialdehyde tapioca starch. Starch/Stärke, 57, 166–172.

Wootton, M. and Bamunuarachi, A. (1978). Water binding capacity of commercial produced and modified starches. Starch/Stärke, 33, 159–161.

Wootton, M. and Manatsathit, A. (1983). The influence of molar substitution on the water binding capacity of hydroxypropyl maize starches. Starch/Stärke, 35, 92–94.

Wu, H.C.H. and Sarko, A. (1978a). The double-helical molecular structure of crystalline B-amylose. Carbohydrate Research, 61, 7.

Wu, H.C.H. and Sarko, A. (1978b). The double-helical molecular structure of crystalline A-amylose. Carbohydrate Research, 61, 27.

Wursch, P. and Gumy, D. (1994). Inhibition of amylopectin retrogradation by partial beta-amylolysis. Carbohydrate Resources, 256(1), 129–137.

Wurzburg, O.B. (1986). Converted starches. In: Wurzburg, O.B. (Ed.), modified starches: properties and uses. Boca Raton: CRC Press. pp. 17–41.

Xu, A. and Seib, P.A. (1997). Determination of the level and position of substitution in hydroxypropylated starch by high-resolution ^{1}H-NMR spectroscopy of alpha limit dextrins. Journal of Cereal Science, 25, 17–26.

Xu, Y., Ding, W., Liu, J., Li, Y., Kennedy, J.F., Gu, Q. and Shao, S. (2010). Preparation and characterization of organic-soluble acetylated starch nanocrystals. Carbohydrate Polymers, 80, 1078–1084.

Yamin, F.F., Lee, M., Pollak, L. M. and White, P.J. (1999). Thermal properties of starch in corn variants isolated after chemical mutagenesis of inbred line B73. Cereal Chemistry, 76, 175–181.

Yeh, A.-I. and Yeh, S.-L. (1993). Some characteristics of hydroxypropylated and Cross-Linked Rice Starch. Cereal Chemistry, 70, 596–601.

Yoo, S. and Jane, J. (2002). Structural and physical characteristics of waxy and other wheat starches. Carbohydrate Polymers, 49, 297–305.

Yu, J., Ai, F., Dufresne, A., Gao, S., Huang, J. and Chang, P.R. (2008). Structure and mechanical properties of poly(lactic acid) filled with (starch nanocrystal)-graft-poly(ε-caprolactone). Macromolecule Material Engineering, 293, 763–770.

Yuan, Y., Zhang, L., Dai, Y. and Yu, J. (2007). Physicochemical properties of starch obtained from *Dioscorea nipponica Makino* comparison with other tuber starches. Journal of Food Engineering, 82, 436–442.

Zaidul, I.S.M., Norulaini, N., Omar, M.O.K., Yaauchi, H. and Noda, T. (2007a). Correlations of the composition, minerals, and RVA pasting properties of various potato starches. Starch/Stärke, 59, 269–276.

Zaidul, I.S.M., Yamauchi, H., Takigawa, S., Matsura-Endo, C., Suzuki, T. and Noda, T. (2007b). Correlation between the compositional and pasting properties of various potato starches. Food Chemistry, 105, 164-172.

Zannou, A., Agbicodo, E., Zoundjihékpon, J., Struik, P.C., Ahanchédé, A. and Kossou, D.K. (2009). Genetic variability in yam cultivars from the Guinea Sudan zone of Benin assessed by random amplified polymorphic DNA, African Journal of Biotechnology, 8(1), 26–36.

Zasypkin, D.V., Braudo, E.E. and Tolstoguzov, V.B. (1997). Multicomponent biopolymergels. Food Hydrocolloids, 11, 159–170.

Zhao, S-M., Qiu, C-G., Xiong, S-B. and Liu, Y-M. (2007). Rheological properties of amylopectins from different rice type during storage. Journal of Central South University of Technology, 14(1), 510–513.

Zhou, M., Robards, K., Glennie-Holmes, M. and Helliwell, S. (1998). Structure and pasting properties of oat starch. Cereal Chemistry,75(3), 273–281.

Zobel, H.F (1988a). Starch crystal transformations and their industrial importance. Starch/Stärke, 40(2), 1–7.

Zobel, H.F. (1988b). Molecules to granules: A comprehensive starch review. Starch/Stärke, 40(2), 44–50.

Zobel, H.F., Young, S.N. and Rocca, L.A. (1988). Starch gelatinization: An X-ray diffraction study. Cereal Chemistry, 65(6), 443–446.

APPENDIX

PROXIMATE COMPOSITION

DESCRIPTIVES

Parameter	Starch	N	Mean	Std. Deviation	Std. Error	95% Confidence Interval for Mean		Minimum	Maximum
						Lower Bound	Upper Bound		
Moisture Content	WCS	3	10.2800	.01000	.00577	10.2552	10.3048	10.27	10.29
	RCS	3	10.7600	.01000	.00577	10.7352	10.7848	10.75	10.77
	WYS	3	10.2300	.01000	.00577	10.2052	10.2548	10.22	10.24
	YYS	3	10.4500	.01000	.00577	10.4252	10.4748	10.44	10.46
	PPS	3	10.5500	.01000	.00577	10.5252	10.5748	10.54	10.56
	LBS	3	10.3533	.00577	.00333	10.3390	10.3677	10.35	10.36
	JBS	3	10.6700	.01000	.00577	10.6452	10.6948	10.66	10.68
	Total	21	10.4705	.18920	.04129	10.3844	10.5566	10.22	10.77
Protein Content	WCS	3	2.1000	.01000	.00577	2.0752	2.1248	2.09	2.11
	RCS	3	1.4500	.01000	.00577	1.4252	1.4748	1.44	1.46
	WYS	3	2.2400	.01000	.00577	2.2152	2.2648	2.23	2.25
	YYS	3	1.7967	.00577	.00333	1.7823	1.8110	1.79	1.80
	PPS	3	5.6400	.01000	.00577	5.6152	5.6648	5.63	5.65
	LBS	3	6.5800	.01000	.00577	6.5552	6.6048	6.57	6.59
	JBS	3	7.0067	.01528	.00882	6.9687	7.0446	6.99	7.02
	Total	21	3.8305	2.33185	.50885	2.7690	4.8919	1.44	7.02
Crude Fat	WCS	3	1.0200	.01000	.00577	.9952	1.0448	1.01	1.03
	RCS	3	1.0700	.01000	.00577	1.0452	1.0948	1.06	1.08
	WYS	3	1.0600	.01000	.00577	1.0352	1.0848	1.05	1.07
	YYS	3	1.0900	.01000	.00577	1.0652	1.1148	1.08	1.10
	PPS	3	1.0367	.00577	.00333	1.0223	1.0510	1.03	1.04
	LBS	3	1.1633	.00577	.00333	1.1490	1.1777	1.16	1.17
	JBS	3	1.0400	.01000	.00577	1.0152	1.0648	1.03	1.05
	Total	21	1.0686	.04597	.01003	1.0476	1.0895	1.01	1.17
Crude Fibre	WCS	3	1.2200	.01000	.00577	1.1952	1.2448	1.21	1.23
	RCS	3	1.4700	.01000	.00577	1.4452	1.4948	1.46	1.48
	WYS	3	1.2600	.01000	.00577	1.2352	1.2848	1.25	1.27
	YYS	3	1.2333	.00577	.00333	1.2190	1.2477	1.23	1.24
	PPS	3	1.7700	.01000	.00577	1.7452	1.7948	1.76	1.78
	LBS	3	1.6300	.01000	.00577	1.6052	1.6548	1.62	1.64
	JBS	3	1.5233	.00577	.00333	1.5090	1.5377	1.52	1.53
	Total	21	1.4438	.20370	.04445	1.3511	1.5365	1.21	1.78
Ash Content	WCS	3	1.1967	.00577	.00333	1.1823	1.2110	1.19	1.20
	RCS	3	1.1300	.01000	.00577	1.1052	1.1548	1.12	1.14
	WYS	3	1.1700	.01000	.00577	1.1452	1.1948	1.16	1.18
	YYS	3	1.1500	.01000	.00577	1.1252	1.1748	1.14	1.16
	PPS	3	1.1967	.00577	.00333	1.1823	1.2110	1.19	1.20
	LBS	3	1.2633	.00577	.00333	1.2490	1.2777	1.26	1.27
	JBS	3	1.1533	.00577	.00333	1.1390	1.1677	1.15	1.16

	Total	21	1.1800	.04243	.00926	1.1607	1.1993	1.12	1.27
CHO	WCS	3	84.1833	.02517	.01453	84.1208	84.2458	84.16	84.21
by	RCS	3	84.1200	.01732	.01000	84.0770	84.1630	84.11	84.14
Difference	WYS	3	84.0400	.01000	.00577	84.0152	84.0648	84.03	84.05
	YYS	3	84.2800	.01732	.01000	84.2370	84.3230	84.27	84.30
	PPS	3	79.8067	.01155	.00667	79.7780	79.8354	79.80	79.82
	LBS	3	79.0100	.02646	.01528	78.9443	79.0757	78.99	79.04
	JBS	3	78.6067	.02082	.01202	78.5550	78.6584	78.59	78.63
	Total	21	82.0067	2.56578	.55990	80.8387	83.1746	78.59	84.30

ANOVA

Parameter		Sum of Squares	df	Mean Square	F	Sig.
Moisture Content	Between Groups	.715	6	.119	1316.421	.000
	Within Groups	.001	14	.000		
	Total	.716	20			
Protein Content	Between Groups	108.749	6	18.125	165487.551	.000
	Within Groups	.002	14	.000		
	Total	108.750	20			
Crude Fat	Between Groups	.041	6	.007	84.667	.000
	Within Groups	.001	14	.000		
	Total	.042	20			
Crude Fibre	Between Groups	.829	6	.138	1706.275	.000
	Within Groups	.001	14	.000		
	Total	.830	20			
Ash Content	Between Groups	.035	6	.006	94.590	.000
	Within Groups	.001	14	.000		
	Total	.036	20			
Carbohydrate By Difference	Between Groups	131.660	6	21.943	59078.056	.000
	Within Groups	.005	14	.000		
	Total	131.665	20			

HOMOGENEOUS SUBSETS
Moisture Content

	Starch	N	Subset for alpha = .05						
			a	b	c	d	e	f	g
Duncan(a)	WYS	3	10.2300						
	WCS	3		10.2800					
	LBS	3			10.3533				
	YYS	3				10.4500			
	PPS	3					10.5500		
	JBS	3						10.6700	
	RCS	3							10.7600
	Sig.		1.000	1.000	1.000	1.000	1.000	1.000	1.000

Means for groups in homogeneous subsets are displayed.
a Uses Harmonic Mean Sample Size = 3.000.

Protein Content

| | Starch | N | Subset for alpha = .05 |
			a	b	c	d	e	f	g
Duncan(a)	RCS	3	1.4500						
	YYS	3		1.7967					
	WCS	3			2.1000				
	WYS	3				2.2400			
	PPS	3					5.6400		
	LBS	3						6.5800	
	JBS	3							7.0067
	Sig.		1.000	1.000	1.000	1.000	1.000	1.000	1.000

Means for groups in homogeneous subsets are displayed.
a Uses Harmonic Mean Sample Size = 3.000.

Crude Fat

| | Starch | N | Subset for alpha = .05 |
			a	b	c	d	e
Duncan(a)	WCS	3	1.0200				
	PPS	3		1.0367			
	JBS	3		1.0400			
	WYS	3			1.0600		
	RCS	3			1.0700		
	YYS	3				1.0900	
	LBS	3					1.1633
	Sig.		1.000	.657	.195	1.000	1.000

Means for groups in homogeneous subsets are displayed.
a Uses Harmonic Mean Sample Size = 3.000.

Crude Fibre

| | Starch | N | Subset for alpha = .05 |
			a	b	c	d	e	f
Duncan(a)	WCS	3	1.2200					
	YYS	3	1.2333					
	WYS	3		1.2600				
	RCS	3			1.4700			
	JBS	3				1.5233		
	LBS	3					1.6300	
	PPS	3						1.7700
	Sig.		.091	1.000	1.000	1.000	1.000	1.000

Means for groups in homogeneous subsets are displayed.
a Uses Harmonic Mean Sample Size = 3.000.

Ash Content

	Starch	N	Subset for alpha = .05				
			a	b	c	d	e
Duncan(a)	RCS	3	1.1300				
	YYS	3		1.1500			
	JBS	3		1.1533			
	WYS	3			1.1700		
	WCS	3				1.1967	
	PPS	3				1.1967	
	LBS	3					1.2633
	Sig.		1.000	.612	1.000	1.000	1.000

Means for groups in homogeneous subsets are displayed.
a Uses Harmonic Mean Sample Size = 3.000.

Carbohydrate By Difference

	Starch	N	Subset for alpha = .05						
			a	b	c	d	e	f	g
Duncan(a)	JBS	3	78.6067						
	LBS	3		79.0100					
	PPS	3			79.8067				
	WYS	3				84.0400			
	RCS	3					84.1200		
	WCS	3						84.1833	
	YYS	3							84.2800
	Sig.		1.000	1.000	1.000	1.000	1.000	1.000	1.000

Means for groups in homogeneous subsets are displayed.
a Uses Harmonic Mean Sample Size = 3.000.

MINERAL ANALYSIS

DESCRIPTIVES

Parameter	Starch	N	Mean	Std. Deviation	Std. Error	95% Confidence Interval for Mean		Minimum	Maximum
						Lower Bound	Upper Bound		
Na	WCS	2	182.3000	.14142	.10000	181.0294	183.5706	182.20	182.40
	RCS	2	163.5000	.28284	.20000	160.9588	166.0412	163.30	163.70
	WYS	2	201.2500	.07071	.05000	200.6147	201.8853	201.20	201.30
	YYS	2	214.4000	.28284	.20000	211.8588	216.9412	214.20	214.60
	PPS	2	246.0000	.42426	.30000	242.1881	249.8119	245.70	246.30
	LBS	2	224.6500	.21213	.15000	222.7441	226.5559	224.50	224.80
	JBS	2	171.2500	.07071	.05000	170.6147	171.8853	171.20	171.30
	Total	14	200.4786	28.83174	7.70561	183.8316	217.1255	163.30	246.30
Ca	WCS	2	36.4000	.14142	.10000	35.1294	37.6706	36.30	36.50
	RCS	2	36.3500	.07071	.05000	35.7147	36.9853	36.30	36.40
	WYS	2	36.5000	.14142	.10000	35.2294	37.7706	36.40	36.60
	YYS	2	37.4500	.07071	.05000	36.8147	38.0853	37.40	37.50
	PPS	2	62.2500	.07071	.05000	61.6147	62.8853	62.20	62.30

		N	Mean	Std. Deviation	Std. Error	Lower Bound	Upper Bound	Minimum	Maximum
	LBS	2	56.4500	.21213	.15000	54.5441	58.3559	56.30	56.60
	JBS	2	32.3000	.14142	.10000	31.0294	33.5706	32.20	32.40
	Total	14	42.5286	11.26802	3.01151	36.0226	49.0345	32.20	62.30
Mg	WCS	2	59.4500	.21213	.15000	57.5441	61.3559	59.30	59.60
	RCS	2	77.7000	.14142	.10000	76.4294	78.9706	77.60	77.80
	WYS	2	65.6500	.21213	.15000	63.7441	67.5559	65.50	65.80
	YYS	2	54.3500	.07071	.05000	53.7147	54.9853	54.30	54.40
	PPS	2	60.5000	.14142	.10000	59.2294	61.7706	60.40	60.60
	LBS	2	55.2500	.07071	.05000	54.6147	55.8853	55.20	55.30
	JBS	2	85.5500	.07071	.05000	84.9147	86.1853	85.50	85.60
	Total	14	65.4929	11.38099	3.04170	58.9217	72.0640	54.30	85.60
K	WCS	2	3482.3500	.21213	.15000	3480.4441	3484.2559	3482.20	3482.50
	RCS	2	3262.6500	.21213	.15000	3260.7441	3264.5559	3262.50	3262.80
	WYS	2	3582.2500	.07071	.05000	3581.6147	3582.8853	3582.20	3582.30
	YYS	2	3366.4500	.21213	.15000	3364.5441	3368.3559	3366.30	3366.60
	PPS	2	4332.7000	.14142	.10000	4331.4294	4333.9706	4332.60	4332.80
	LBS	2	4201.0500	.21213	.15000	4199.1441	4202.9559	4200.90	4201.20
	JBS	2	3195.3500	.21213	.15000	3193.4441	3197.2559	3195.20	3195.50
	Total	14	3631.8286	436.28994	116.60339	3379.9223	3883.7349	3195.20	4332.80
P	WCS	2	2362.3500	.21213	.15000	2360.4441	2364.2559	2362.20	2362.50
	RCS	2	1925.4000	89.37830	63.20000	1122.3679	2728.4321	1862.20	1988.60
	WYS	2	2660.3500	6.85894	4.85000	2598.7249	2721.9751	2655.50	2665.20
	YYS	2	2481.1500	.07071	.05000	2480.5147	2481.7853	2481.10	2481.20
	PPS	2	3331.2500	.07071	.05000	3330.6147	3331.8853	3331.20	3331.30
	LBS	2	3221.4500	.35355	.25000	3218.2734	3224.6266	3221.20	3221.70
	JBS	2	1793.4500	.21213	.15000	1791.5441	1795.3559	1793.30	1793.60
	Total	14	2539.3429	565.55521	151.15099	2212.8010	2865.8847	1793.30	3331.30
Fe	WCS	2	2.1500	.07071	.05000	1.5147	2.7853	2.10	2.20
	RCS	2	2.2500	.07071	.05000	1.6147	2.8853	2.20	2.30
	WYS	2	2.5500	.07071	.05000	1.9147	3.1853	2.50	2.60
	YYS	2	2.3500	.07071	.05000	1.7147	2.9853	2.30	2.40
	PPS	2	2.3500	.07071	.05000	1.7147	2.9853	2.30	2.40
	LBS	2	2.2500	.07071	.05000	1.6147	2.8853	2.20	2.30
	JBS	2	2.2500	.07071	.05000	1.6147	2.8853	2.20	2.30
	Total	14	2.3071	.13281	.03549	2.2305	2.3838	2.10	2.60
Zn	WCS	2	2.3500	.07071	.05000	1.7147	2.9853	2.30	2.40
	RCS	2	2.3500	.07071	.05000	1.7147	2.9853	2.30	2.40
	WYS	2	2.5500	.07071	.05000	1.9147	3.1853	2.50	2.60
	YYS	2	2.3500	.07071	.05000	1.7147	2.9853	2.30	2.40
	PPS	2	2.2500	.07071	.05000	1.6147	2.8853	2.20	2.30
	LBS	2	2.5500	.07071	.05000	1.9147	3.1853	2.50	2.60
	JBS	2	2.1500	.07071	.05000	1.5147	2.7853	2.10	2.20
	Total	14	2.3643	.14991	.04006	2.2777	2.4508	2.10	2.60
Cu	WCS	2	.3500	.07071	.05000	-.2853	.9853	.30	.40
	RCS	2	.1500	.07071	.05000	-.4853	.7853	.10	.20
	WYS	2	.3000	.00000	.00000	.3000	.3000	.30	.30
	YYS	2	.3500	.07071	.05000	-.2853	.9853	.30	.40

	PPS	2	.2000	.00000	.00000	.2000	.2000	.20	.20
	LBS	2	.2500	.07071	.05000	-.3853	.8853	.20	.30
	JBS	2	.2500	.07071	.05000	-.3853	.8853	.20	.30
	Total	14	.2643	.08419	.02250	.2157	.3129	.10	.40
Mn	WCS	2	.7500	.07071	.05000	.1147	1.3853	.70	.80
	RCS	2	.9500	.07071	.05000	.3147	1.5853	.90	1.00
	WYS	2	.8500	.07071	.05000	.2147	1.4853	.80	.90
	YYS	2	.9500	.07071	.05000	.3147	1.5853	.90	1.00
	PPS	2	.6500	.07071	.05000	.0147	1.2853	.60	.70
	LBS	2	.8500	.07071	.05000	.2147	1.4853	.80	.90
	JBS	2	1.1500	.07071	.05000	.5147	1.7853	1.10	1.20
	Total	14	.8786	.16257	.04345	.7847	.9724	.60	1.20

ANOVA

Parameter		Sum of Squares	df	Mean Square	F	Sig.
Na	Between Groups	10806.089	6	1801.015	30378.562	.000
	Within Groups	.415	7	.059		
	Total	10806.504	13			
Ca	Between Groups	1650.469	6	275.078	16046.222	.000
	Within Groups	.120	7	.017		
	Total	1650.589	13			
Mg	Between Groups	1683.704	6	280.617	13547.046	.000
	Within Groups	.145	7	.021		
	Total	1683.849	13			
K	Between Groups	2474535.639	6	412422.606	11547832.980	.000
	Within Groups	.250	7	.036		
	Total	2474535.889	13			
P	Between Groups	4150049.344	6	691674.891	602.523	.000
	Within Groups	8035.750	7	1147.964		
	Total	4158085.094	13			
Fe	Between Groups	.194	6	.032	6.476	.013
	Within Groups	.035	7	.005		
	Total	.229	13			
Zn	Between Groups	.257	6	.043	8.571	.006
	Within Groups	.035	7	.005		
	Total	.292	13			
Cu	Between Groups	.067	6	.011	3.133	.080
	Within Groups	.025	7	.004		
	Total	.092	13			
Mn	Between Groups	.309	6	.051	10.286	.004
	Within Groups	.035	7	.005		
	Total	.344	13			

HOMOGENEOUS SUBSETS

Na

	Starch	N	Subset for alpha = .05						
			a	b	c	d	e	f	g
Duncan(a)	RCS	2	163.5000						
	JBS	2		171.2500					
	WCS	2			182.3000				
	WYS	2				201.2500			
	YYS	2					214.4000		
	LBS	2						224.6500	
	PPS	2							246.0000
	Sig.		1.000	1.000	1.000	1.000	1.000	1.000	1.000

Means for groups in homogeneous subsets are displayed.
a Uses Harmonic Mean Sample Size = 2.000

Ca

	Starch	N	Subset for alpha = .05				
			a	b	c	d	e
Duncan(a)	JBS	2	32.3000				
	RCS	2		36.3500			
	WCS	2		36.4000			
	WYS	2		36.5000			
	YYS	2			37.4500		
	LBS	2				56.4500	
	PPS	2					62.2500
	Sig.		1.000	.306	1.000	1.000	1.000

Means for groups in homogeneous subsets are displayed.
a Uses Harmonic Mean Sample Size = 2.000

Mg

	Starch	N	Subset for alpha = .05						
			a	b	c	d	e	f	g
Duncan(a)	YYS	2	54.3500						
	LBS	2		55.2500					
	WCS	2			59.4500				
	PPS	2				60.5000			
	WYS	2					65.6500		
	RCS	2						77.7000	
	JBS	2							85.5500
	Sig.		1.000	1.000	1.000	1.000	1.000	1.000	1.000

Means for groups in homogeneous subsets are displayed.
a Uses Harmonic Mean Sample Size = 2.000

K

	Starch	N	Subset for alpha = .05
			a	b	c	d	e	f	g
Duncan(a)	JBS	2	3195.35						
	RCS	2		3262.65					
	YYS	2			3366.45				
	WCS	2				3482.35			
	WYS	2					3582.25		
	LBS	2						4201.05	
	PPS	2							4332.70
	Sig.		1.000	1.000	1.000	1.000	1.000	1.000	1.000

Means for groups in homogeneous subsets are displayed.
a Uses Harmonic Mean Sample Size = 2.000

P

	Starch	N	Subset for alpha = .05
			a	b	c	d	e	f	g
Duncan(a)	JBS	2	1793.45						
	RCS	2		1925.40					
	WCS	2			2362.35				
	YYS	2				2481.15			
	WYS	2					2660.35		
	LBS	2						3221.45	
	PPS	2							3331.25
	Sig.		1.000	1.000	1.000	1.000	1.000	1.000	1.000

Means for groups in homogeneous subsets are displayed.
a Uses Harmonic Mean Sample Size = 2.000

Fe

	Starch	N	Subset for alpha = .05
			a	b	c
Duncan(a)	WCS	2	2.1500		
	RCS	2	2.2500	2.2500	
	LBS	2	2.2500	2.2500	
	JBS	2	2.2500	2.2500	
	YYS	2		2.3500	
	PPS	2		2.3500	
	WYS	2			2.5500
	Sig.		.222	.225	1.000

Means for groups in homogeneous subsets are displayed.
a Uses Harmonic Mean Sample Size = 2.000

Zn

	Starch	N	Subset for alpha = .05		
			a	b	c
Duncan(a)	JBS	2	2.1500		
	PPS	2	2.2500	2.2500	
	WCS	2		2.3500	
	RCS	2		2.3500	
	YYS	2		2.3500	
	WYS	2			2.5500
	LBS	2			2.5500
	Sig.		.200	.222	1.000

Means for groups in homogeneous subsets are displayed.
a Uses Harmonic Mean Sample Size = 2.000

Cu

	Starch	N	Subset for alpha = .05	
			a	b
Duncan(a)	RCS	2	.1500	
	PPS	2	.2000	.2000
	LBS	2	.2500	.2500
	JBS	2	.2500	.2500
	WYS	2	.3000	.3000
	WCS	2		.3500
	YYS	2		.3500
	Sig.		.052	.053

Means for groups in homogeneous subsets are displayed.
a Uses Harmonic Mean Sample Size = 2.000.

Mn

	Starch	N	Subset for alpha = .05			
			a	b	C	d
Duncan(a)	PPS	2	.6500			
	WCS	2	.7500	.7500		
	WYS	2		.8500	.8500	
	LBS	2		.8500	.8500	
	RCS	2			.9500	
	YYS	2			.9500	
	JBS	2				1.1500
	Sig.		.200	.216	.222	1.000

Means for groups in homogeneous subsets are displayed.
a Uses Harmonic Mean Sample Size = 2.000

AMOUNT OF REACTED OZONE WITH SAMPLES

DESCRIPTIVES

Starch	OGT	N	Mean	Std. Deviation	Std. Error	95% Confidence Interval for Mean		Minimum	Maximum
						Lower Bound	Upper Bound		
WCS	5	3	.5967	.05774	.03333	.4532	.7401	.53	.63
	10	3	1.3967	.75056	.43333	-.4678	3.2611	.53	1.83
	15	3	1.8300	.00000	.00000	1.8300	1.8300	1.83	1.83
	Total	9	1.2744	.65976	.21992	.7673	1.7816	.53	1.83
RCS	5	3	.0300	.00000	.00000	.0300	.0300	.03	.03
	10	3	.1300	.00000	.00000	.1300	.1300	.13	.13
	15	3	.9967	.05774	.03333	.8532	1.1401	.93	1.03
	Total	9	.3856	.46128	.15376	.0310	.7401	.03	1.03
WYS	5	3	.4967	.05774	.03333	.3532	.6401	.43	.53
	10	3	1.2967	.05774	.03333	1.1532	1.4401	1.23	1.33
	15	3	1.5300	.00000	.00000	1.5300	1.5300	1.53	1.53
	Total	9	1.1078	.47111	.15704	.7457	1.4699	.43	1.53
YYS	5	3	.3300	.00000	.00000	.3300	.3300	.33	.33
	10	3	.4967	.05774	.03333	.3532	.6401	.43	.53
	15	3	1.1300	.20000	.11547	.6332	1.6268	.93	1.33
	Total	9	.6522	.38006	.12669	.3601	.9444	.33	1.33
PPS	5	3	1.1300	.00000	.00000	1.1300	1.1300	1.13	1.13
	10	3	1.8967	.05774	.03333	1.7532	2.0401	1.83	1.93
	15	3	1.4633	.23094	.13333	.8896	2.0370	1.33	1.73
	Total	9	1.4967	.35355	.11785	1.2249	1.7684	1.13	1.93
LBS	5	3	1.4633	.05774	.03333	1.3199	1.6068	1.43	1.53
	10	3	2.0967	.11547	.06667	1.8098	2.3835	2.03	2.23
	15	3	2.4633	.05774	.03333	2.3199	2.6068	2.43	2.53
	Total	9	2.0078	.44378	.14793	1.6667	2.3489	1.43	2.53
JBS	5	3	.8300	.00000	.00000	.8300	.8300	.83	.83
	10	3	1.4300	.00000	.00000	1.4300	1.4300	1.43	1.43
	15	3	1.2467	.02887	.01667	1.1750	1.3184	1.23	1.28
	Total	9	1.1689	.26667	.08889	.9639	1.3739	.83	1.43

ANOVA

		Sum of Squares	df	Mean Square	F	Sig.
WCS	Between Groups	2.349	2	1.174	6.218	.034
	Within Groups	1.133	6	.189		
	Total	3.482	8			
RCS	Between Groups	1.696	2	.848	763.000	.000
	Within Groups	.007	6	.001		
	Total	1.702	8			
WYS	Between Groups	1.762	2	.881	396.500	.000
	Within Groups	.013	6	.002		
	Total	1.776	8			

YYS	Between Groups	1.069	2	.534	37.000	.000
	Within Groups	.087	6	.014		
	Total	1.156	8			
PPS	Between Groups	.887	2	.443	23.471	.001
	Within Groups	.113	6	.019		
	Total	1.000	8			
LBS	Between Groups	1.536	2	.768	115.167	.000
	Within Groups	.040	6	.007		
	Total	1.576	8			
JBS	Between Groups	.567	2	.284	1021.000	.000
	Within Groups	.002	6	.000		
	Total	.569	8			

Post Hoc Tests
Homogeneous Subsets

WCS

	group	N	Subset for alpha = .05	
			a	b
Duncan(a)	5	3	.5967	
	10	3	1.3967	1.3967
	15	3		1.8300
	Sig.		.065	.268

Means for groups in homogeneous subsets are displayed.
a Uses Harmonic Mean Sample Size = 3.000.

RCS

	group	N	Subset for alpha = .05		
			a	b	c
Duncan(a)	5	3	.0300		
	10	3		.1300	
	15	3			.9967
	Sig.		1.000	1.000	1.000

Means for groups in homogeneous subsets are displayed.
a Uses Harmonic Mean Sample Size = 3.000.

WYS

	group	N	Subset for alpha = .05		
			a	b	c
Duncan(a)	5	3	.4967		
	10	3		1.2967	
	15	3			1.5300
	Sig.		1.000	1.000	1.000

Means for groups in homogeneous subsets are displayed.
a Uses Harmonic Mean Sample Size = 3.000.

YYS

	OGT	N	Subset for alpha = .05	
			a	b
Duncan(a)	5	3	.3300	
	10	3	.4967	
	15	3		1.1300
	Sig.		.140	1.000

Means for groups in homogeneous subsets are displayed.
a Uses Harmonic Mean Sample Size = 3.000.

PPS

	OGT	N	Subset for alpha = .05		
			a	b	c
Duncan(a)	5	3	1.1300		
	15	3		1.4633	
	10	3			1.8967
	Sig.		1.000	1.000	1.000

Means for groups in homogeneous subsets are displayed.
a Uses Harmonic Mean Sample Size = 3.000.

LBS

	OGT	N	Subset for alpha = .05		
			a	b	c
Duncan(a)	5	3	1.4633		
	10	3		2.0967	
	15	3			2.4633
	Sig.		1.000	1.000	1.000

Means for groups in homogeneous subsets are displayed.
a Uses Harmonic Mean Sample Size = 3.000.

JBS

	group	N	Subset for alpha = .05		
			a	b	c
Duncan(a)	5	3	.8300		
	15	3		1.2467	
	10	3			1.4300
	Sig.		1.000	1.000	1.000

Means for groups in homogeneous subsets are displayed.
a Uses Harmonic Mean Sample Size = 3.000.